NASA Contractor Report 3472

Experimental Investigation of Elastic Mode Control on a Model of a Transport Aircraft

Staff of Douglas Aircraft Company

CONTRACT NAS1-15327
NOVEMBER 1981

NASA

NASA Contractor Report 3472

Experimental Investigation of Elastic Mode Control on a Model of a Transport Aircraft

Staff of Douglas Aircraft Company
McDonnell Douglas Corporation
Long Beach, California

Prepared for
Langley Research Center
under Contract NAS1-15327

National Aeronautics
and Space Administration

Scientific and Technical
Information Branch

1981

FOREWORD

The work reported on in this document was conducted under Contract NAS1-15327 by the Douglas Aircraft Company. It was part of the Energy Efficient Transport (EET) project of the Aircraft Energy Efficient (ACEE) program.

The NASA Project Manager was R. V. Hood of the EET Project Office at the Langley Research Center. His technical monitor was T. G. Gainer. The NASA on-site representative was J. R. Tulinius. Special acknowledgment and appreciation is given to the following of the Multi-Disciplinary Analysis and Optimization Branch at Langley who have been directly involved in analytical support and wind tunnel test activities:

I. Abel
J. R. Newsom
B. Perry III

The following Douglas personnel contributed to this program and were authors of this report:

M. Abramovitz	Avionics Engineering
R. M. Heimbaugh	Dynamics Engineering
J. K. Nomura	Dynamics Engineering
R. M. Pearson	Dynamics Engineering
W. A. Shirley	Task Manager
R. H. Stringham	Dynamics Engineering
E. L. Tescher	Dynamics Engineering
I. E. Zoock	Avionics Engineering

Other Douglas personnel who have contributed significantly to this effort were:

W. J. Chades	Wind Tunnel Model Group
W. A. Fowles	Wind Tunnel Model Group
J. B. Gaddy	Wind Tunnel Model Group
G. E. Hinote	Dynamics Engineering
B. S. Hite	Wind Tunnel Model Group
M. Klotzsche	ACEE Program Manager
N. Mayo	Wind Tunnel Model Design
J. D. McDonnell	Avionics Engineering
C. H. Meyer	Wind Tunnel Model Group
J. B. Miller	Wind Tunnel Model Group
R. W. Scofield	Wind Tunnel Model Group
J. T. Slama	Avionics Engineering
A. B. Taylor	EET Project Manager
J. Tong	Dynamics Engineering
T. G. Weathermon	Laboratory Programs
F. L. Wilson	Dynamics Engineering
B. A. Winther	Dynamics Engineering
G. Ziegler	Secretary

CONTENTS

ILLUSTRATIONS

ILLUSTRATIONS

ILLUSTRATIONS

ILLUSTRATIONS

TABLES

SUMMARY

The ability to control aircraft elastic modes with actively controlled surfaces has been successfully demonstrated with a wind tunnel model of a DC-10 derivative. The 4.5-percent scale aeroelastic model of the DC-10 had actuators and servo-system components to activate the control surfaces. The model was analyzed and tested in both semispan and complete model configurations. The semispan model was tested in the Douglas low-speed wind tunnel (three test periods), and the full-span complete model was tested in the Northrop Aircraft Company 7- x 10-foot low-speed wind tunnel.

Using classical methods, control laws were developed which suppressed flutter and reduced wing bending loads due to gusts. Alternative control laws were developed by NASA personnel which were based on aerodynamic energy and optimal control methods. These were also successfully tested. Flutter tests with the various control laws showed 15- to 25-percent increase in the critical flutter speed and substantial reduction in wing bending response in turbulence with the active system on.

In general, good correlation was obtained between test and analytical predictions; however, certain areas were identified which require further investigation and development.

INTRODUCTION

Owing to the rapid rise of the cost of fuel, energy efficiency has become a crucial factor in the design of new and derivative transport aircraft. The use of active controls to improve aircraft efficiency has been receiving increased attention. Considerable study and development has provided confidence that reduced drag and lower structural weight can be realized by using control surfaces for static stabilization and elastic mode suppression. Once the aircraft control surfaces are designed for multiple use and high response, as they must be for stability augmentation and wing load alleviation, it becomes possible to extend the concept to flutter margin augmentation, which offers additional weight savings for many aircraft. Such augmentation could also make it easier to incorporate other advanced technologies such as winglets and high-aspect-ratio supercritical wings which offer further improvements in aerodynamic efficiency. Analysis has shown that applying these technologies could result in a flutter-critical design, which means the designer would have to consider adding either heavy structural reinforcement or an augmentation system to stabilize the flutter modes.

The purpose of the present study was to investigate the use of active controls to suppress flutter and alleviate gust loads on a DC-10 derivative. The derivative investigated was a "stretch" version having a 4.3-m (14-foot) longer span and an 8.1-m (26.7-foot) longer fuselage than the DC-10-30 aircraft. Specific objectives of the investigation were to:

- Confirm the effectiveness of active controls to suppress critical flutter modes at speeds above passive flutter.

- Assess the accuracy of dynamic analysis methods applied to the active control functions of flutter suppression and gust load alleviation.

- Obtain engineering experience in the design, fabrication, and testing of actively controlled flexible models.

Two aeroelastic models of the DC-10 derivative were tested — a semispan model tested in three different tunnel entries in the Douglas-Long Beach low-speed wind tunnel, and a full-span model tested in the Northrop 7- by 10-foot low-speed wind tunnel. The design of both models included development of a small hydraulic actuator to use in controlling the outboard ailerons and elevators, and this development work is described in some detail in this report.

Several different control laws were investigated including laws developed by Douglas based on classical methods and laws developed by the NASA Langley Research Center based on aerodynamic energy and optimal control methods. The tests were made for a range of fuel-loading conditions and tunnel velocities. For gust-alleviation tests, a canvas banner was stretched across the tunnel upstream of the test section to provide the necessary turbulence.

To assess the accuracy of flutter analysis methods, the modes of vibration, frequencies, transfer functions, and damping characteristics measured in the tests were compared with analytical predictions. Gust-load-alleviation methods were evaluated by comparing measured transfer functions and the RMS model response to turbulence with analytical predictions.

Use of trade names or names of manufacturers in this report does not constitute an official endorsement of such products or manufacturers, either expressed or implied, by the National Aeronautics and Space Administration.

SYMBOLS AND NOTATIONS

Principal measurements and calculations were in customary units and were converted to International (SI) units for this document.

a, b, c	Coefficients of aerodynamic approximation
ACEE	Aircraft energy efficiency
ACS	Active control system
AIC	Aerodynamic influence coefficients
A7, A8	Designation of aileron control law
BM	Bending moment
c	Damping
c_c	Critical damping
c_t	Wing tip chord
cg	Center of gravity
C	Eigenvalue matrix
CL	Designation for control law
dB	Decibel
DAC CL 2.5	Designation for Douglas Aircraft Company control law 2.5
DLBWT	Douglas-Long Beach wind tunnel
E3, E4, E5	Designation of elevator control law
E	Modulus of elasticity in tension
EET	Energy efficient transport
EMC	Elastic mode control
EMS	Elastic mode suppression
f	Frequency
f_f	Flutter frequency
FS	Fuselage sensor
FUS	Fuselage
f_α	Pitch frequency
f_θ	Roll frequency
f_ψ	Yaw frequency
g	Gravitational constant, 9.81 m/sec^2
g	Structural damping
G	Transfer function of actuator-servo
G_s	Transfer function of valve/actuator
GLA	Gust load alleviation
GEL	Elevator control law filter
h	Vertical displacement in vertical direction, positive down
h_{WS}	Wing sensor accelerometer output in vertical direction, positive down
h_{FS}	Fuselage sensor accelerometer output in vertical direction, positive down
I_{xx}, I_{yy}, I_{zz}	Bending moments of inertia for pitch, roll, and yaw, respectively
I_{xy}, I_{yz}, I_{xz}	Cross products of inertia
$I_{\beta\beta}$	Control surface bay moment of inertia
J	Torsional moment of inertia
K_A	Gain multiplier of aileron control law
K_E	Gain multiplier of elevator control law

SYMBOLS AND NOTATIONS

KEAS	Knots equivalent airspeed
ℓ	Lateral displacement in Y direction, positive outboard
$\ddot{\ell}$	Lateral acceleration in Y direction, positive outboard
M, D, K	Matrices used to describe generalized inertia, damping, and stiffness forces
MLC	Maneuver load control
N	Newton
$N_{W_g}^{BM_x}$	Open loop numerator of BM_x/W_g transfer function
$N_{W_g}^{BM_x} \ddot{h}_{\delta_a}^{WS}$	Example of a coupling numerator
NASA CL1, etc.	Designation of alternate control laws
PSD	Power spectral density
RMS	Root mean square
Rxx	Run number xx
s	Laplacian operator
SIC	Structural influence coefficient
TF	Transfer function
V	Velocity
v	Volts
V_f	Flutter speed
W_g	Wind gust
wg	Wing
WS	Wing sensor
X_{EA}	Distance along the wing elastic axis
X_F, Y_F, Z_F	Right-hand fuselage coordinate system — lateral, longitudinal, and vertical, respectively
X_w, Y_w, Z_w	Right-hand wing coordinate system — lateral, longitudinal, and vertical, respectively
α	Pitch angle
δ_a	Aileron deflection, positive trailing edge down
$\delta_{a_{cmd}}$	Input to aileron actuator
δ_e	Elevator deflection, positive trailing edge down
$\delta_{e_{cmd}}$	Input to elevator actuator
δ_{WLA_a}	Output of aileron control law filter
δ_{WLA_e}	Output of elevator control law filter
Δ	Open loop denominator
θ	Roll angle
$\phi_{12\,Hz}$	Phase angle at 12 Hz
ψ	Yaw angle
τ	Time constant

METHODOLOGY

ANALYSES

Analytical Flutter Methods

The modal vibration analyses were based upon a "lumped" mass representation in which the model was sectioned into bays. The motions of each bay were represented by six degrees of freedom plus a control surface rotation where applicable. The inertial properties of each bay were described by calculating 10 mass items (mass, three static unbalances, three moments of inertia, and three products of inertia referenced to an elastic axis system).

Structural influence coefficients (SICs), relating control-point static deflections to applied forces, were generated using beam equations that contained the stiffness distribution and geometry data of each component. The SIC and mass distribution matrices are given in Appendix A. Component mode shapes and frequencies of the different configurations were then calculated, assuming the component to be cantilevered at a selected point. The rotational rigidity values used for the ailerons and elevator were taken from bench tests of the actuator assembly. For the semispan model, the only components considered were the wing, aileron, and nacelle-pylon arrangement; for the full-span model, rigid-body modes for the fuselage, elevator, and tail were added to generate free-flight modes. The full-span analysis assumed symmetric mass and stiffness distributions about the centerline, simplifying the analysis to half the model.

Since the usual "required damping versus velocity," or v-g, method of flutter analysis was impractical to use with feedback systems, an alternate iterative procedure was used in which the control law equations, which were frequency-dependent instead of reduced-frequency-dependent, could be easily included.

The essentials of the method, which was a variation on the p-k method, were as follows: the velocity was fixed and a desired range of solution frequencies was specified. The reduced frequency of the initial trial was based on flight velocity and the first frequency in the desired frequency range. Generalized aerodynamic influence coefficients were calculated for this trial's reduced frequency and the control laws evaluated for the corresponding trial frequency. The eigenvalues and corresponding solution frequencies, damping, and velocities were then obtained for the closed-loop system. Based on an automated inspection of the solution, a new trial reduced frequency and corresponding trial frequency were estimated, aerodynamics and control law evaluation were updated, and new eigensolutions obtained. This process was repeated until convergence was achieved, in turn, for each aeroelastic mode. Convergence was defined by agreement of the modal solution frequency and reduced frequency with the current trial values.

Generalized aerodynamic updates in the above process were found by interpolation among a directly generated set for six values of reduced frequency. The process was more computationally efficient and much easier to use than the v-g method when active feedback paths were included. The procedure is incorporated into the Douglas production computer program C4EZ, Flutter and Dynamic Response Analysis, Douglas Report MDC-J6469.

Aerodynamics for the flutter analyses were based upon aerodynamic influence coefficients (AICs) using the method of Reference 1. All analyses used AICs generated for Mach number 0.2. Structural damping for selected modes were taken from the model vibration test results. For modes not measured, a value of g = 0.02 was used. Geometric data, mass and inertia data, stiffness data, and aerodynamic data are presented in Appendix A.

Analytical Gust Methods

Transfer functions (TFs) were obtained by computing the model's response to a unit-amplitude sinusoidal gust input. These transfer functions were then used to compute the model's response to any specified turbulence spectrum. The analysis was done in terms of the RMS values, obtained by power spectral density (PSD) analysis methods.

The basic model transfer functions were obtained by linear analysis using the same structural and aerodynamic representations used in the flutter analysis. These basic transfer functions were modified by adding the control law transfer functions: transfer functions relating the output of a given sensor to control surface movement. It should be noted that in determining transfer functions for the semispan model control system, the transfer function for the servo-actuator was represented by third-order fit to the measured transfer function; for the full-span model the measured transfer function was used directly, in tabular form, and not approximated.

The tunnel turbulence distributions used in the gust loads analysis included both one- and two-dimensional models of turbulence. Although control law synthesis was based on a one-dimensional single-transfer-function model, later comparisons showed that a two-dimensional multiple-transfer-function model would be more accurate. The frequency domain analysis was then based on the two-dimensional as well as the one-dimensional model of turbulence.

The one-dimensional turbulence distributions for both the semispan and full-span models were based on the turbulence measured at the tunnel centerline. The two-dimensional distributions were based on the turbulence distributions measured across the tunnel span. For the two-dimensional distributions, the distributions at the different spanwise stations were assumed to be statistically independent of each other.

The unsteady AICs for use in the flutter and gust load analyses were generated by Douglas procedures which use the doublet lattice method, Reference 1, and surface spline interpolation. The wing lift distribution was weighted to agree with steady wind tunnel data. The weighting factors relating test data to theoretical data are included in Appendix A.

Control Law Synthesis

The methods used in control law synthesis are described in detail in the section on control law development. Included here is a brief summary of the sequential steps performed. First, a control law transfer function which minimized the wing bending moment due to a gust disturbance was plotted as a Bode diagram. A simple filter was designed to approximate this shape. This resulting control law was then tested for stability using the root locus and Nyquist features. Adjustments were made to assure adequate stability margins and still achieve the desired bending

moment reductions. The high-frequency portion of the control law was then shaped to provide flutter suppression. Finally, adjustments to the control law were made to provide the desired performance and stability over the entire test speed range.

Three different control laws were tested on the semispan model. The Douglas control law (DAC CL 2.5) was developed by classical techniques. Alternate control law No. 1 (NASA CL 1) was developed at NASA Langley Research Center and employed aerodynamic energy methods. Alternate control law No. 2 (NASA CL 2) was also developed at NASA Langley by using optimal control theory. New control laws, A7/E4 and A8/E5, were developed for the full-span model.

MODEL DESCRIPTION

The semispan model was a 4.5 percent scale model representative of a DC-10 stretch derivative airplane with an actively controlled outboard aileron. The full-span model included actively controlled inboard elevators and outboard ailerons.

Figure 1 is a photograph of the semispan wing showing its general construction. The wing was cantilevered from a rigid base located outside the tunnel wall. The base could be rotated to operate the wing at minimum lift. The stiffness of the wing was represented by a single aluminum spar. The aerodynamic shape of the wing was simulated by balsa-wood segments. The mass and inertia properties were represented by ballasting these segments with lead weights. Various fuel configurations were simulated by additional lead weights. A flow-through nacelle with mass and inertia properties simulating the engine pod was mounted to the wing by means of a single aluminum beam whose stiffness represented that of the supporting pylon.

The full-span model was a modification of an existing DC-10 flutter model. The fuselage was extended to represent the stretched DC-10 derivative and changes were made to accommodate the required control components. The left wing was the same as used for the semispan model. The right wing was designed and built to match the mass and stiffness properties of the left side. The vertical stabilizer and rudders did not require modification. The horizontal stabilizer was modified to accommodate active inboard elevators. The elevators were made of balsa wood and covered with aluminum skin for strength and stiffness. A three-view sketch of the model is shown in Figure 2. All primary structural stiffnesses were represented by equivalent single beams. Aerodynamic simulation was achieved with segmented fairings made of balsa wood or fiberglass. These were ballasted to simulate the desired mass distribution. The model could be modified to simulate variations in wing fuel, pylon stiffness, and fuselage payload. Various wing tip weights could also be added. Figure 3 is a diagram of the wing-aileron construction showing the locations of the aileron hinge points. Both inboard elevators were driven by a single hydraulically operated rotary vane actuator, as shown in Figure 4. The left and right outboard ailerons were driven individually by hydraulically operated rotary vane actuators. The geometric, mass, and stiffness properties of the semispan and full-span model are presented in Appendix A.

After the second wind tunnel test of the semispan model, the actuators were further developed to improve performance and reliability. Minor geometry changes, the use of a softer elastomer for the vane, and substituting Teflon for brass bearings made the actuator performance more consistent. Actuator development is discussed later.

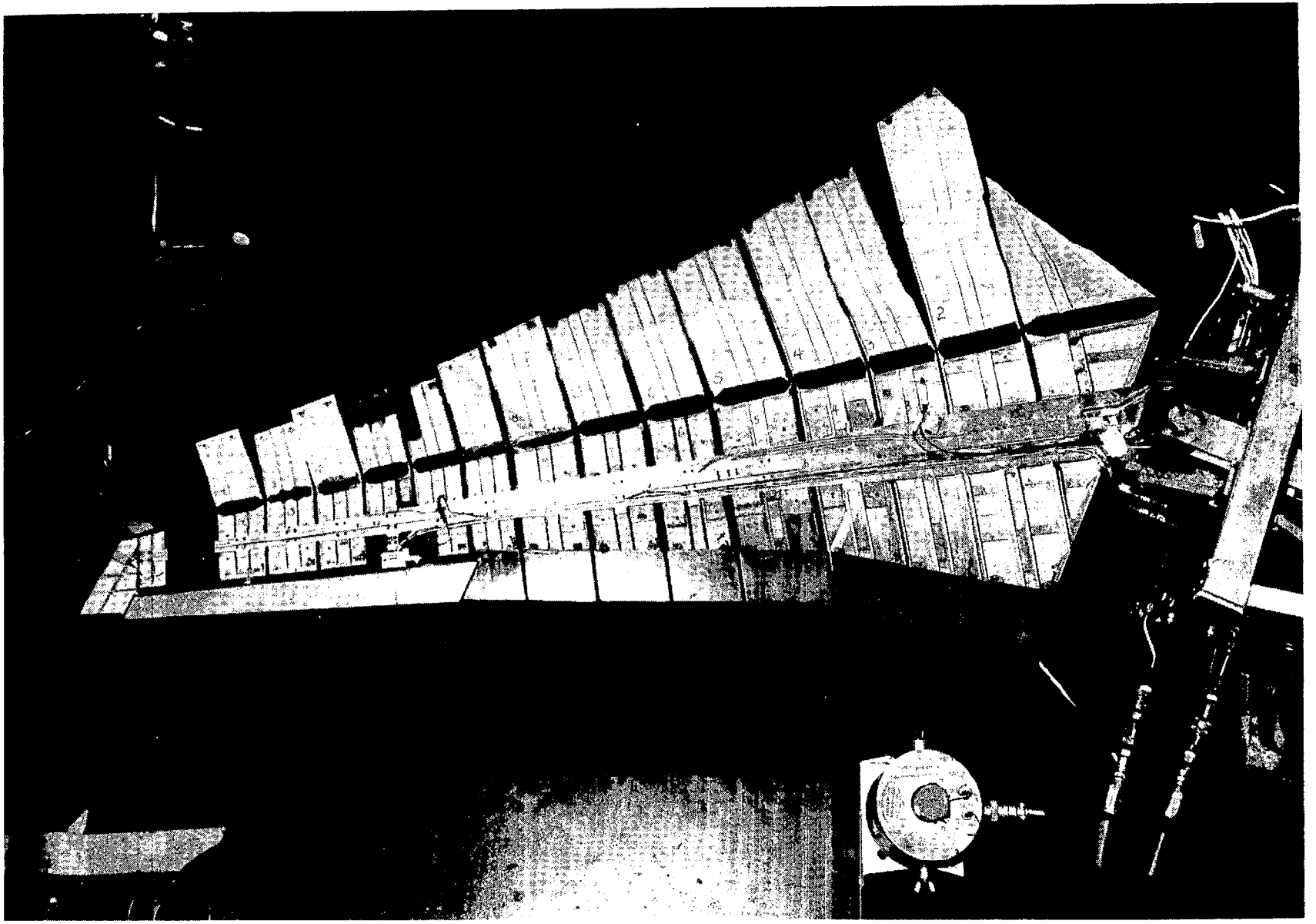

FIGURE 1. SEMISPAN AEROELASTIC MODEL – WING BAYS OPEN

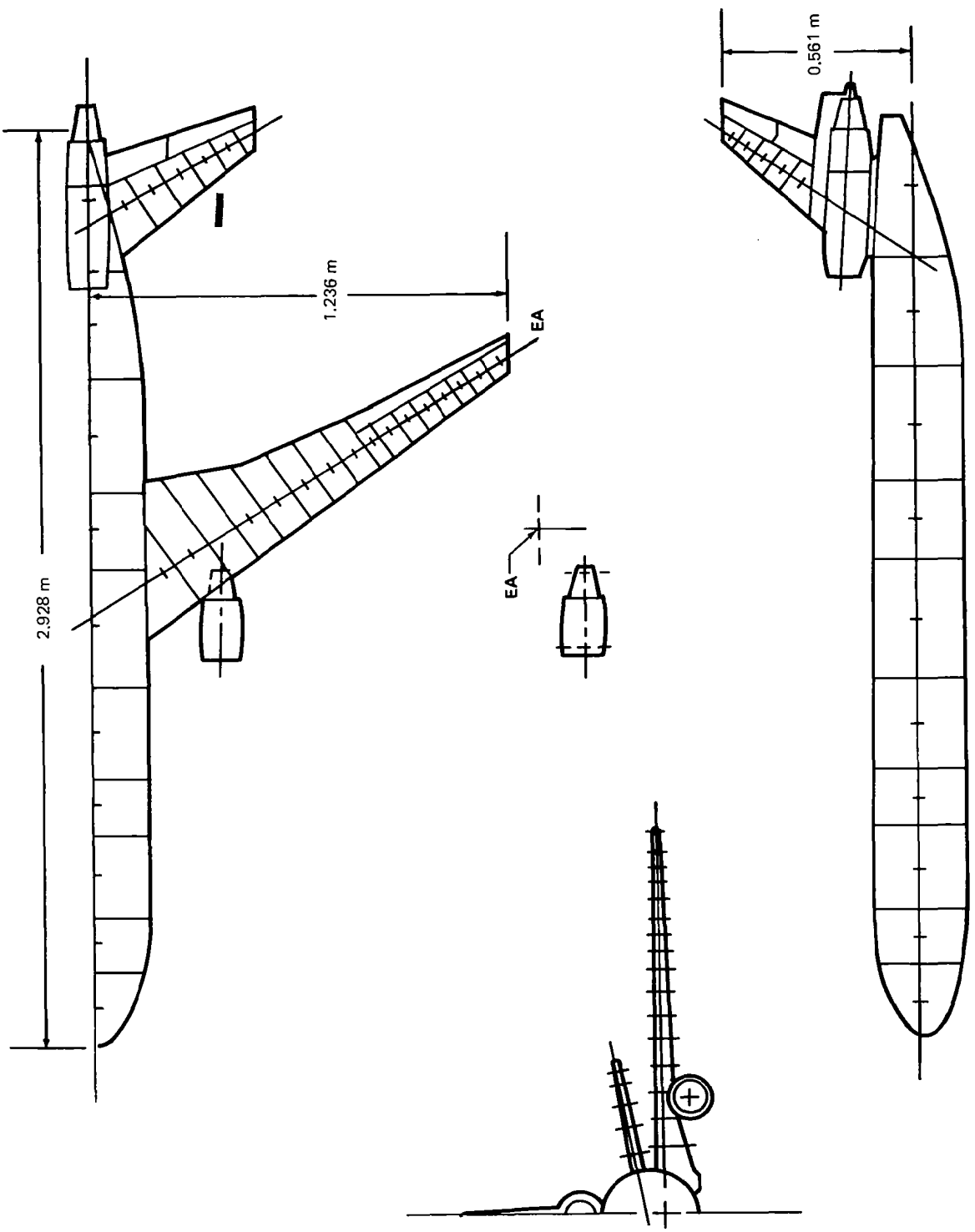

FIGURE 2. FULL SPAN ACTIVE-CONTROLLED FLUTTER MODEL

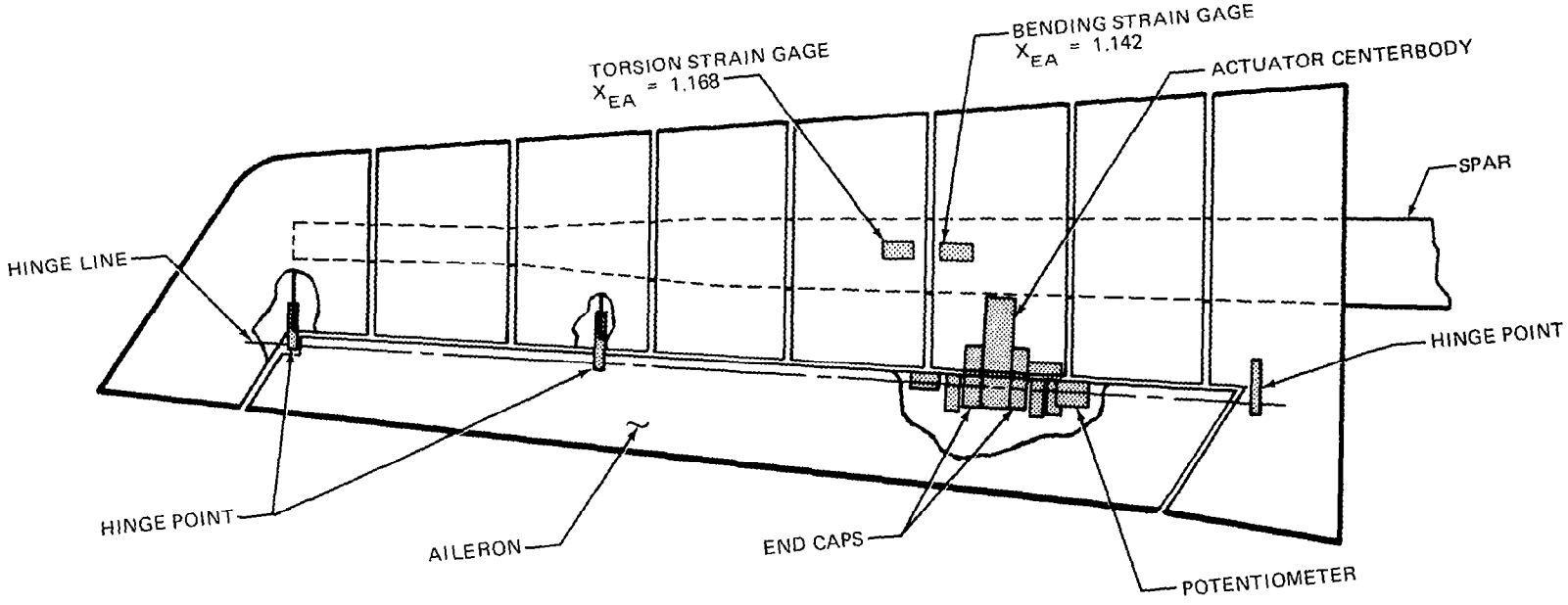

FIGURE 3. WING/AILERON FEATURES

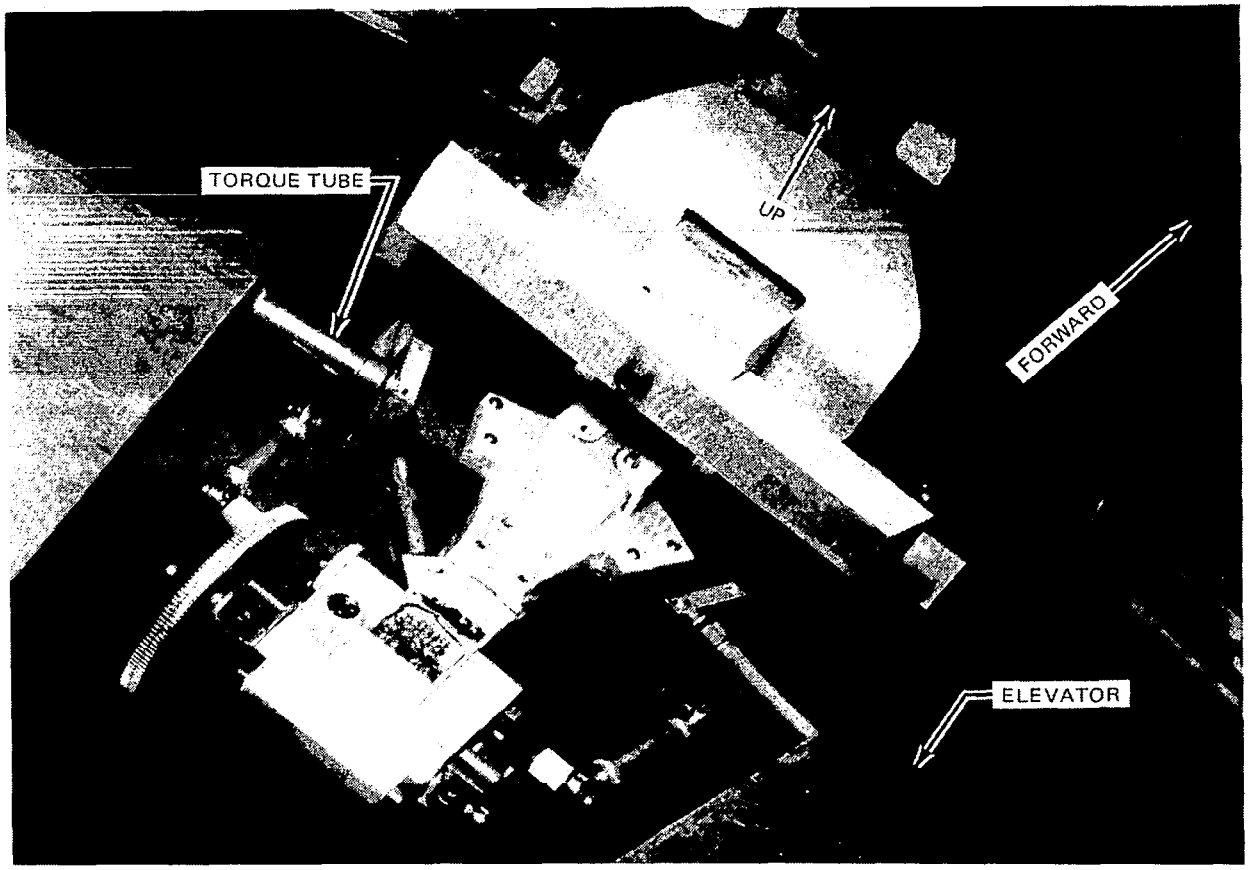

FIGURE 4. INSTALLATION OF ELEVATOR ACTUATOR

The actuator servo-system was designed to operate with position feedback as shown by the block diagram in Figure 5. The actuator design used in the full-span model was the same as the actuator used in the semispan model. Figure 6 is an illustration of the rotary vane actuator. Control surface position was sensed by a potentiometer coupled to the shaft of the hydraulic actuator. For the full-span model all three servo-valves were supplied with hydraulic fluid from a common supply manifold.

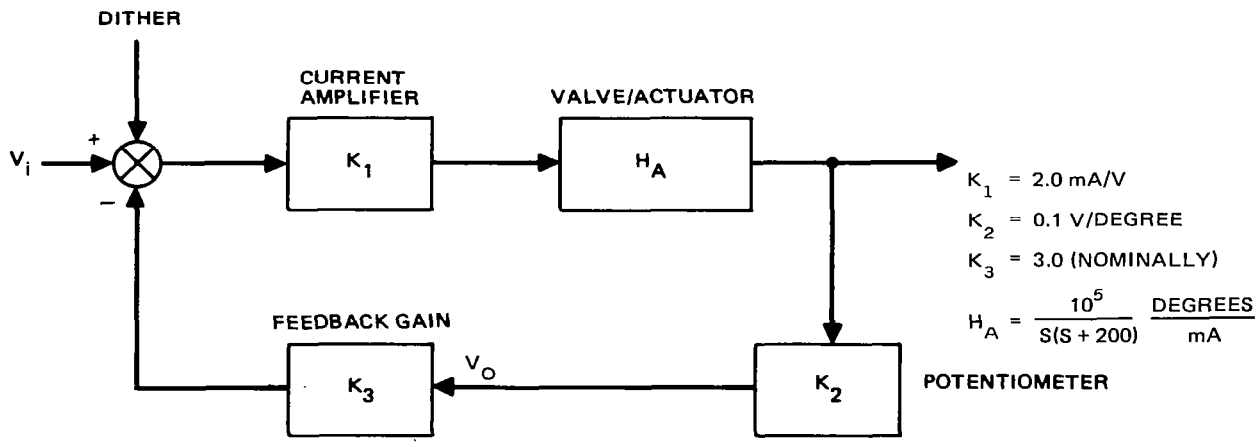

FIGURE 5. ACTUATOR SERVO LOOP

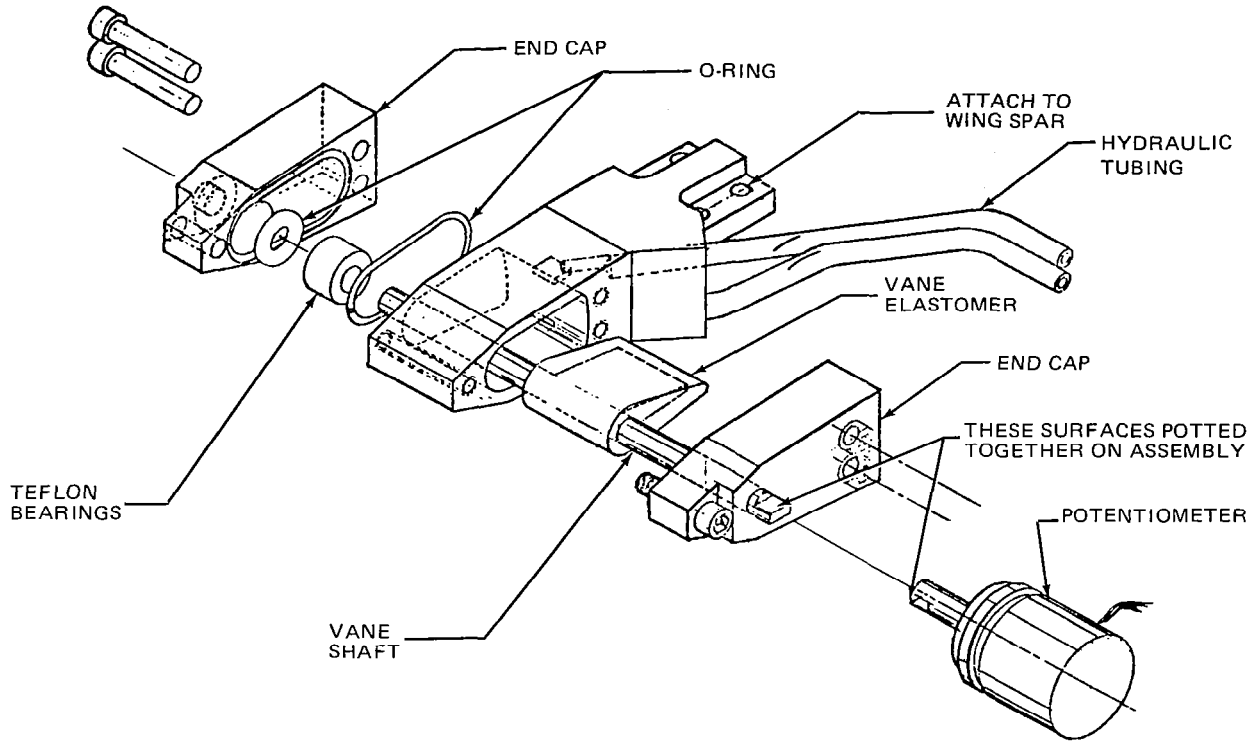

FIGURE 6. ROTARY VANE HYDRAULIC ACTUATOR

The servo-controlled hydraulic valve was a MOOG Type No. 30 valve rated at a flow rate of 49.2 cc/s (3 in^3/s) at 6.895 x 10^6 N/m^2 (1000 psi) supply pressure. At a frequency of 20 Hz, a flow rate of about 9.8 cc/s (0.6 in^3/s) is required for full throw of the actuator. The maximum flow rate capability of the actuator was approximately 32.8 cc/s (2 in^3/s) assuming 1.379 x 10^6 N/m^2 (200 psi) at the actuator. To reduce the effect of friction in the servo-valve, a dither signal of 400 Hz was supplied to the current amplifier.

Figure 7 is a system block diagram of the model and instrumentation. The control laws derived for the semispan and full-span models were programmed on a COMCOR 175 analog computer. The analog computer programming included servo-actuator loop stabilization, the capability to vary gain and phase independently of each other, and logic circuits for the hydraulic dump system. Because of current limitations of the analog computer, independent current drivers for each servo-valve were fabricated for use in the full-span model. Schematic diagrams of the analog computer circuits are in Appendix B.

The aileron control system for the semispan model was based on the use of a single accelerometer located near the wing tip (X_{EA} = 1.4376 meters) or at X_{EA} = 1.308 meters. The full-span aileron control accelerometer sensors were located on each wing at X_{EA} = 1.308 meters. The left and right accelerometer signals were averaged so that both ailerons received the same command signal. The feedback arrangement was based on the assumption that there would be no requirement for asymmetric control.

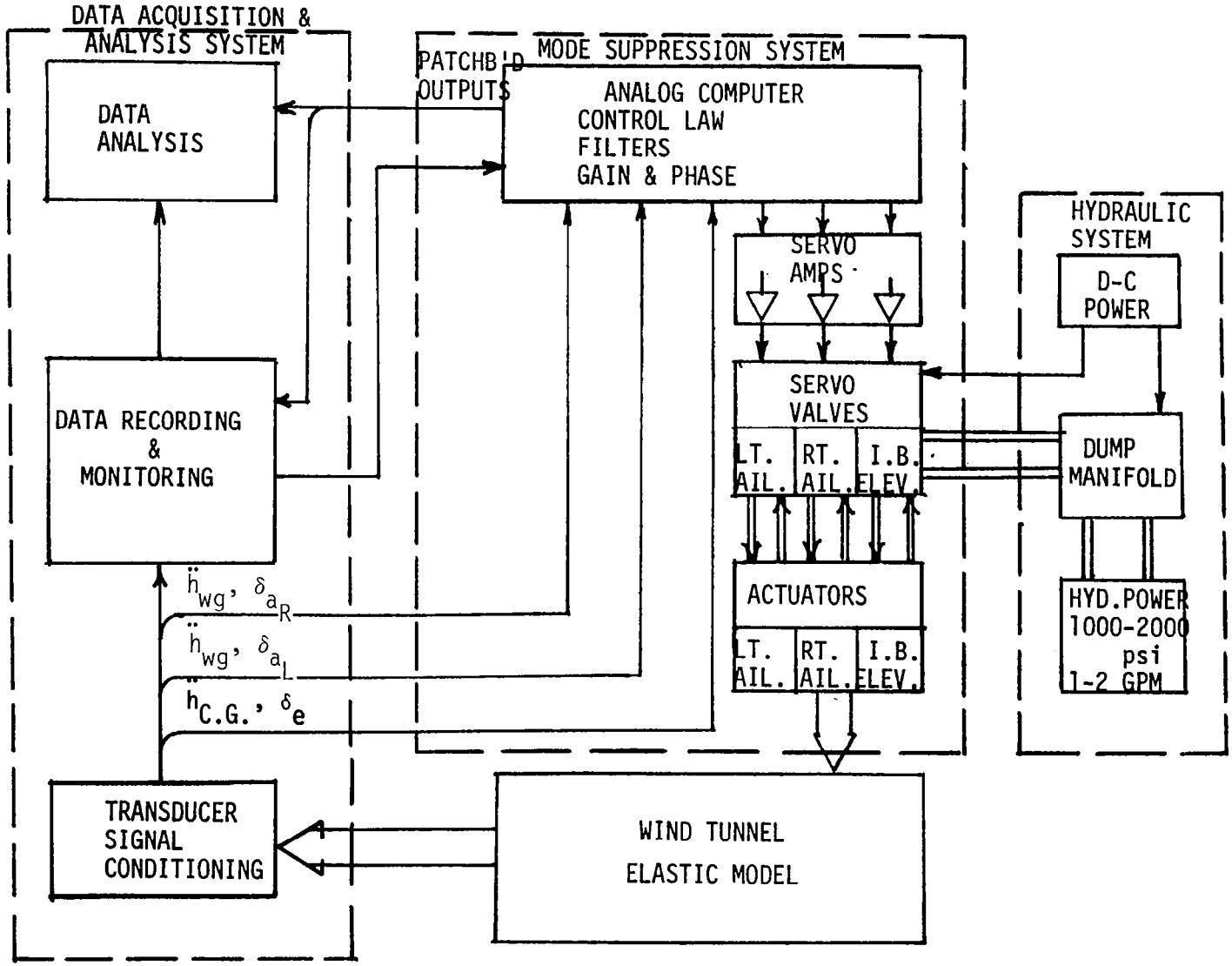

FIGURE 7. ACTIVE-CONTROLLED FLUTTER MODEL TEST BLOCK DIAGRAM

The instrumentation used to measure structural and control system responses during the tests is shown in Figures 8 and 9. The instrumentation consisted of strain gages to measure bending and torsional response on the wing spars, vertical and lateral sensing accelerometers in the wing engine nacelles, and vertical sensing accelerometers located at three wing spanwise stations which could be used for feedback to the aileron control system. A vertical sensing accelerometer was located at the model cg which provided the feedback signal for the elevator control system. A pendulum-type potentiometer was installed on the forward fuselage spar to measure the fuselage angle-of-attack. Control surface positions were measured by the potentiometers located on each actuator.

The signal-conditioning equipment used during the semispan and full-span tests were essentially identical. The equipment consisted of CYBER Systems bridge amplifiers and Endevco 4470 system charge amplifiers. The data acquisition system consisted of a Bell and Howell 4-channel FM tape recorder, a Honeywell 36-channel direct-write oscillograph, a Spectral Dynamics SD 1003-D Mechanical Impedance System (for transfer functions), a Spectral Dynamics Model SD 335 Real Time Analyzer, an EMR 1410 Analyzer, and two X-Y plotters. Significant data acquisition equipment is summarized in Table 1.

Hydraulic actuator systems for the semispan and full-span models were powered by a portable hydraulic power cart capable of 2.068×10^7 N/m^2 (3000 psi) pressure. A pressure regulator maintained the required working pressure at 6.89×10^6 N/m^2 (1000 psi). Bypass valves in the hydraulic lines were relay-operated and controlled by logic in the analog computer which could "dump" the hydraulic pressure quickly in the event of malfunctions. The hydraulic fluid used in the system was MIL-5606.

TUNNEL DESCRIPTIONS AND MODEL INSTALLATIONS

Tunnel Descriptions

The semispan model test was conducted in the Douglas-Long Beach subsonic wind tunnel. This is a low-speed tunnel with a test section 0.965 m x 1.3716 m x 3.048 m (3.17 ft x 4.5 ft x 10 ft). The facility is an atmospheric continuous-flow recirculating type capable of speeds of 70 to 72 m/s (135 to 140 KEAS) depending on blockage.

For the turbulence tests a 0.305-m (1.0-ft) wide banner was stretched across the center of the stilling chamber 6.4 m (21 ft) upstream of the model. The turbulence spectrum had been measured for the clear tunnel using hot wire anemometry techniques. Results for a tunnel speed of 38.6 m/sec (75 KEAS) with the turbulence banner installed are shown in terms of the power spectral density, Figure 10, and the RMS gust velocity distribution, Figure 11.

Full-span model tests were conducted in the Northrop 7- x 10-foot subsonic wind tunnel. This tunnel is a one-atmosphere recirculating type capable of speeds up to 123 m/s (240 KEAS) depending upon blockage. As with the DLBWT, modifications for turbulence tests were made by inserting a 0.305-m wide banner horizontally in the center of the stilling chamber 6.1 m (20 ft) upstream of the test section. Figure 12 shows the installation. Characteristics of the generated turbulence are shown by the power spectrum, Figure 13, and the RMS velocity distribution, Figure 14. As indicated by these figures, the turbulence level distribution is not uniform.

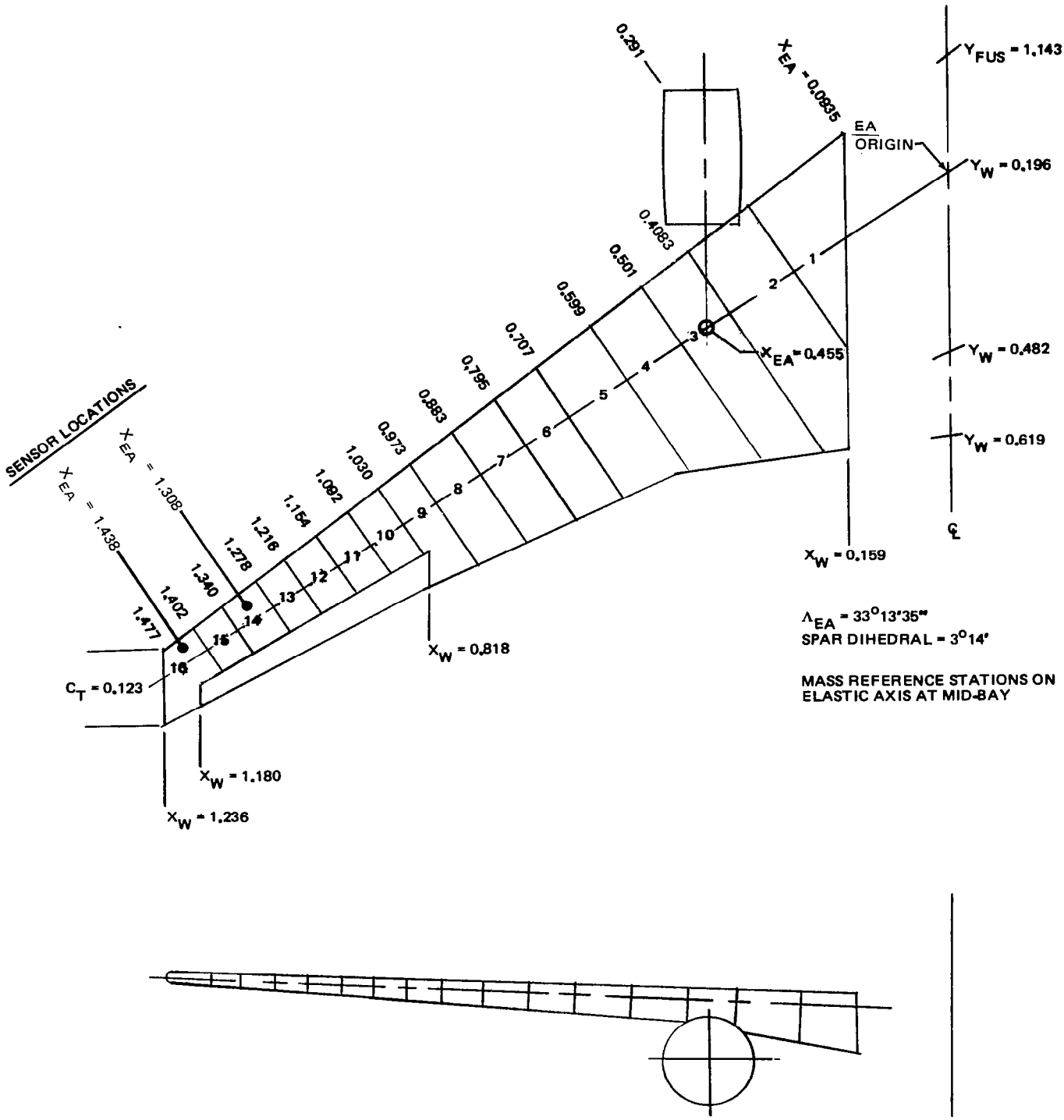

FIGURE 8. SEMISPAN LOW SPEED FLUTTER MODEL GEOMETRY

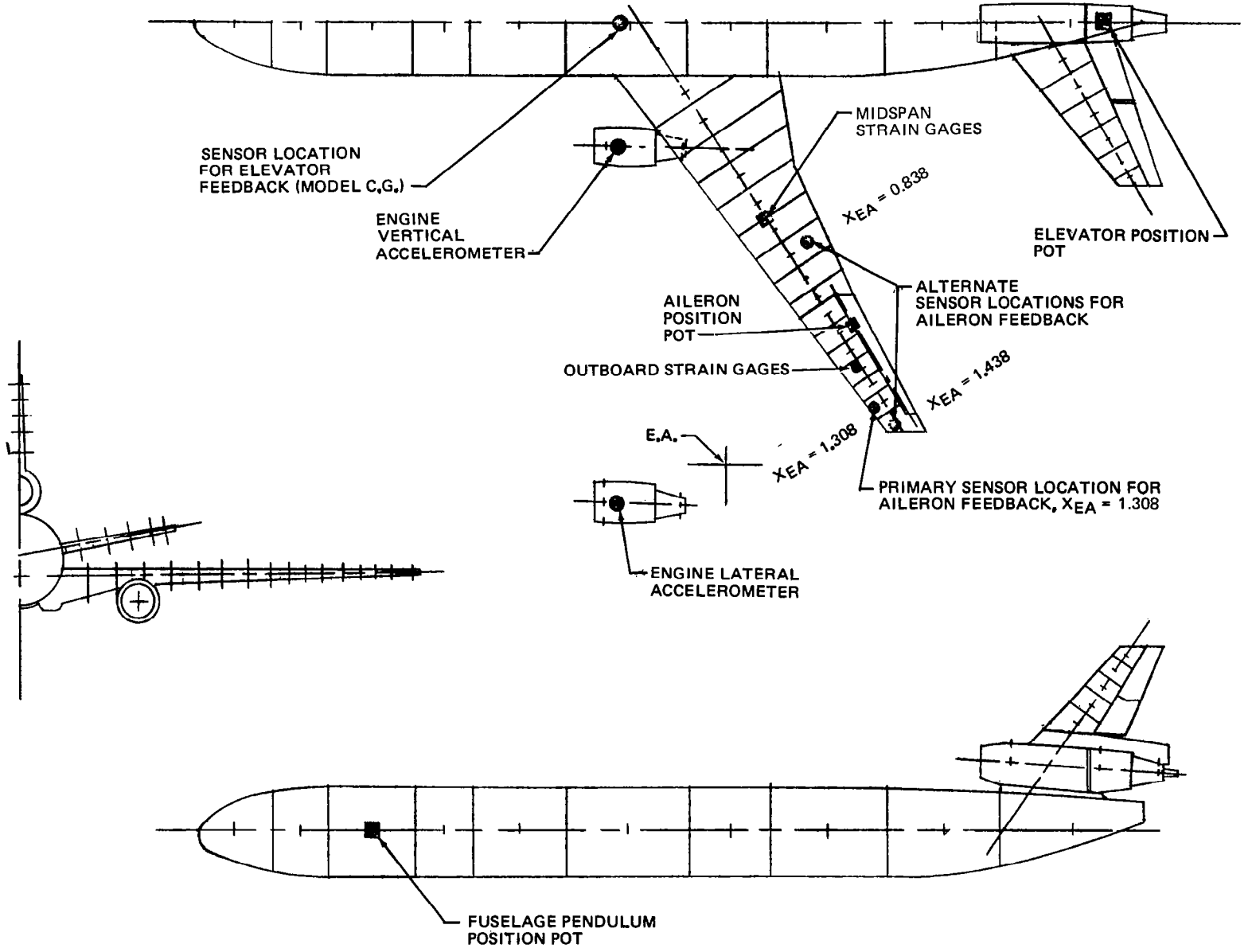

FIGURE 9. SENSOR LOCATIONS ON FULL SPAN FLUTTER MODEL

TABLE 1

DATA ACQUISITION SYSTEM

EQUIPMENT	FUNCTION
14 Channel FM Tape Deck	Record maximum of test data with voice ID for playback to analyze for frequency response data
36 Channel Direct Write Oscillograph	Visual on-line record for monitoring and to provide manual means for data reduction as backup
Real Time Analyzer SD 335A	Spectral response of model to random gust
Impedance Analyzer	Frequency response data of selected channels
EMR 1410 Analyzer	Discrete point data for Bode plots
X-Y Plotter	Plot transfer functions
Dual Beam Oscilloscope	Visual monitoring of selected channels
Rem-Tech Vibration System	Vibrate model and obtain frequencies and mode shapes

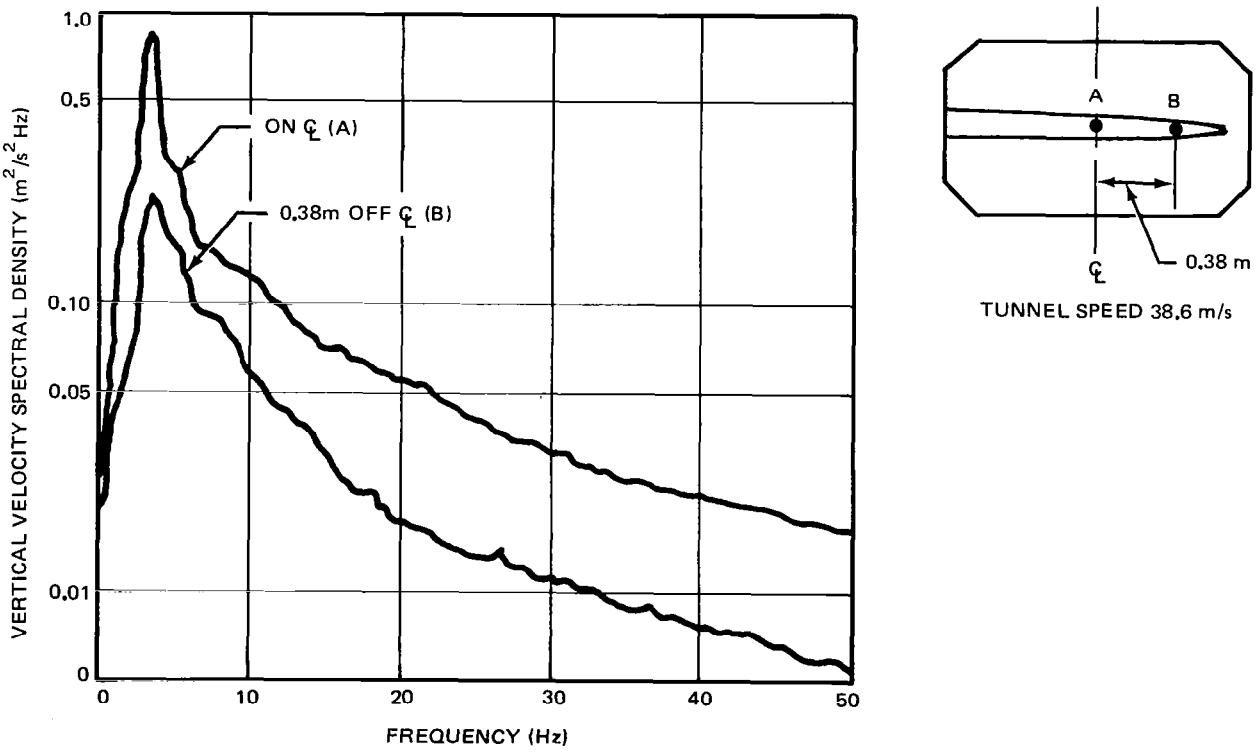

FIGURE 10. MEASURED POWER SPECTRAL DENSITIES OF VERTICAL VELOCITY WITH THE TURBULENCE BANNER INSTALLED IN THE DOUGLAS WIND TUNNEL

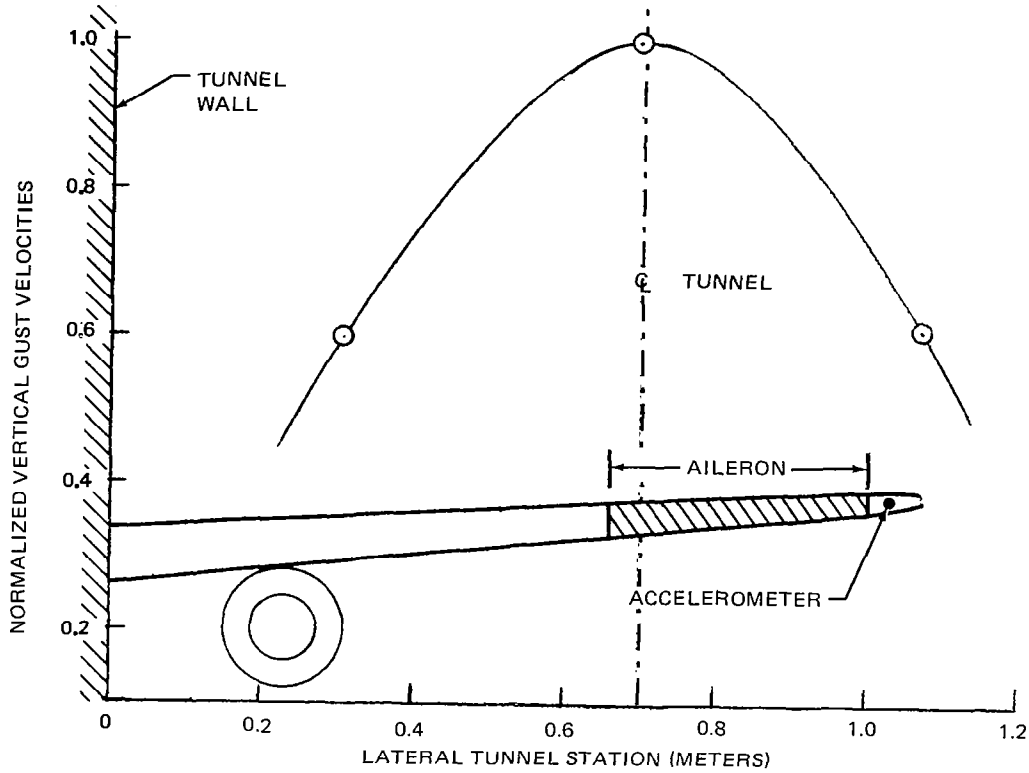

FIGURE 11. RMS VERTICAL VELOCITY DISTRIBUTION WITH THE TURBULENCE BANNER INSTALLED IN THE DOUGLAS WIND TUNNEL

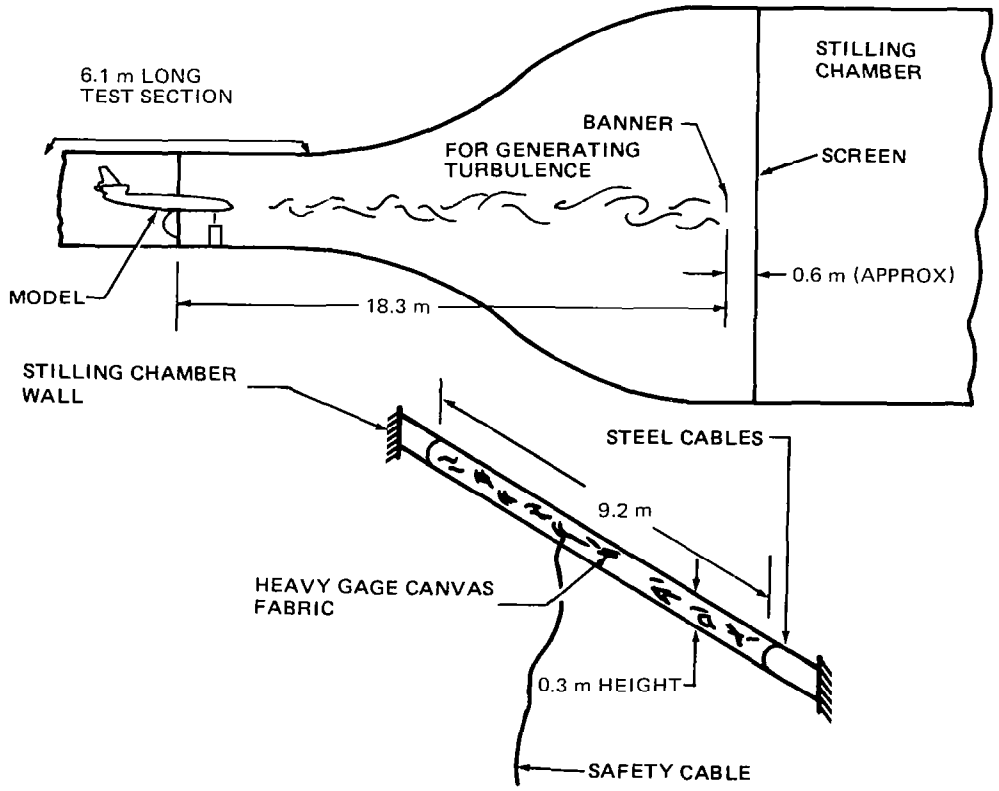

FIGURE 12. METHOD FOR GENERATING TURBULENCE IN THE NORTHROP 7 X 10 FOOT WIND TUNNEL

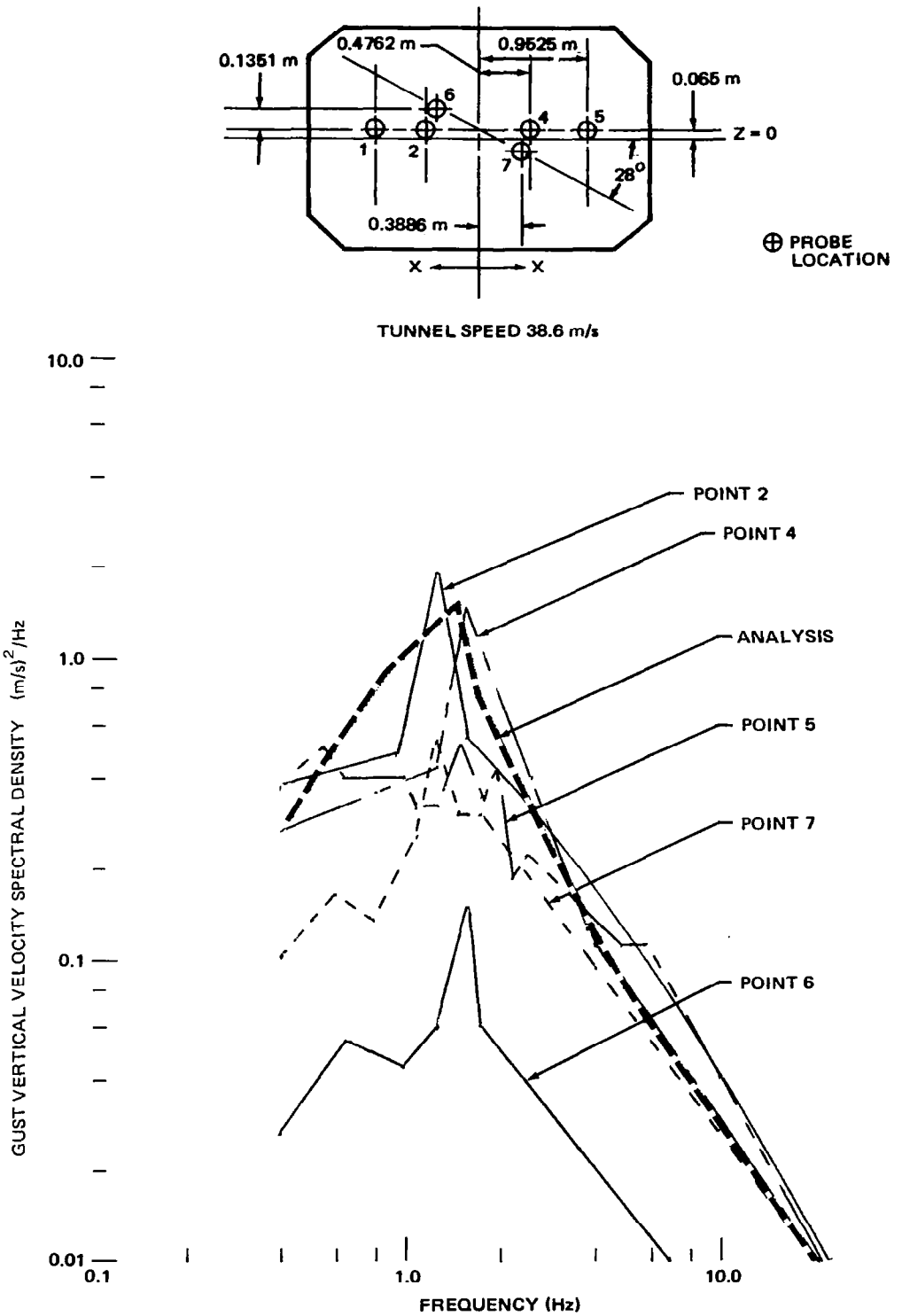

FIGURE 13. POWER SPECTRAL DENSITIES OF VERTICAL VELOCITY WITH THE TURBULENCE BANNER INSTALLED IN THE NORTHROP 7- BY 10-FOOT WIND TUNNEL

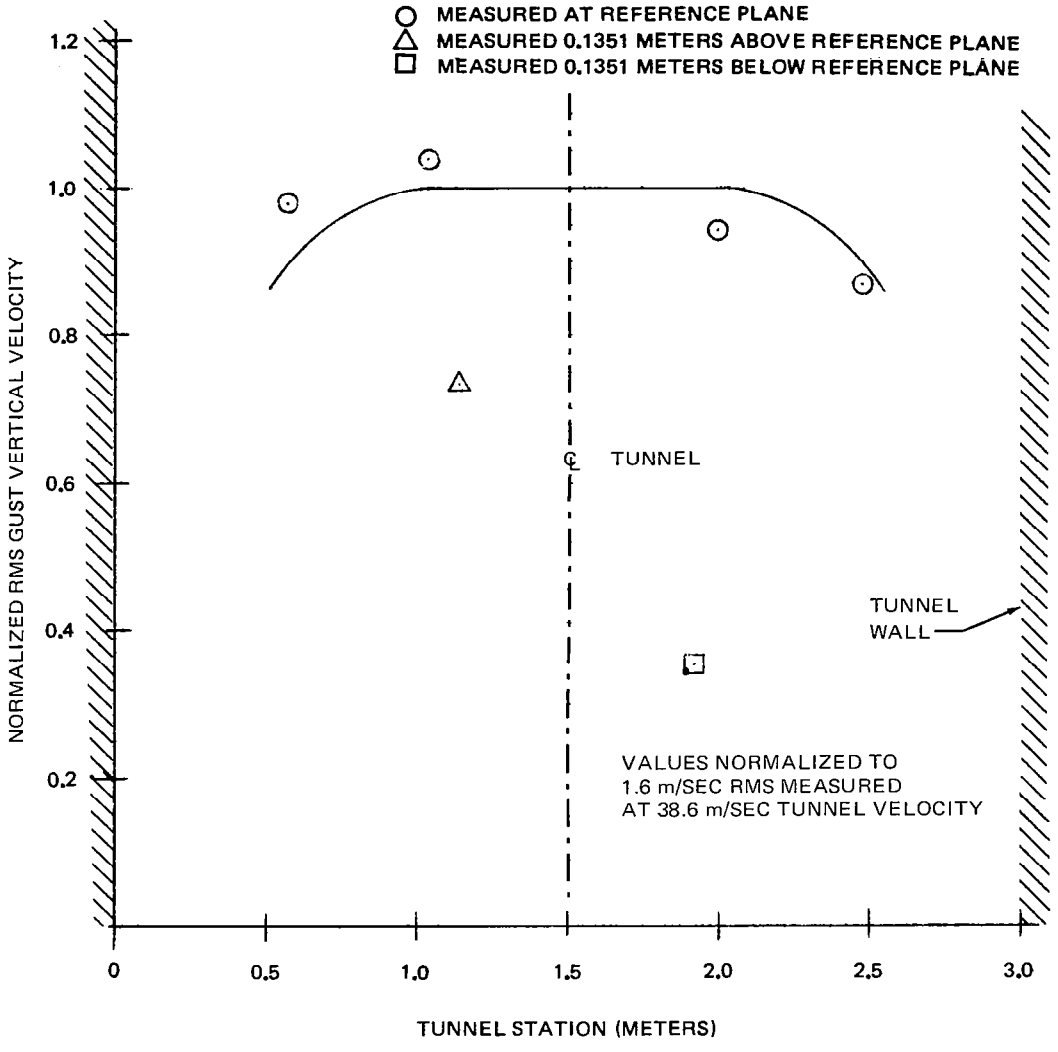

FIGURE 14. RMS VERTICAL VELOCITY DISTRIBUTION IN THE NORTHROP WIND TUNNEL WITH THE TURBULENCE BANNER INSTALLED

Model Installations

The semispan wing root was supported by brackets to a rigid dummy fuselage spar which in turn was attached to a machine vise. In this way the model could be trimmed to a desired angle of attack. Small-diameter cables attached to the nacelle and wing tip were used to pulse the model and to snub any instabilities. Figure 15 is a photograph of the semispan installation.

The full-span model was installed in the wind tunnel by using a vertical rod tensioned between the ceiling and the floor. A gimbal mount system allowed freedom in pitch, plunge, roll, and yaw. Small-diameter cables attached to the nacelles and wing tips were used to pulse the model and to snub any instabilities. A larger cable was attached to the forward fuselage spar for a vertical snubber. Figure 16 is a photograph of this installation.

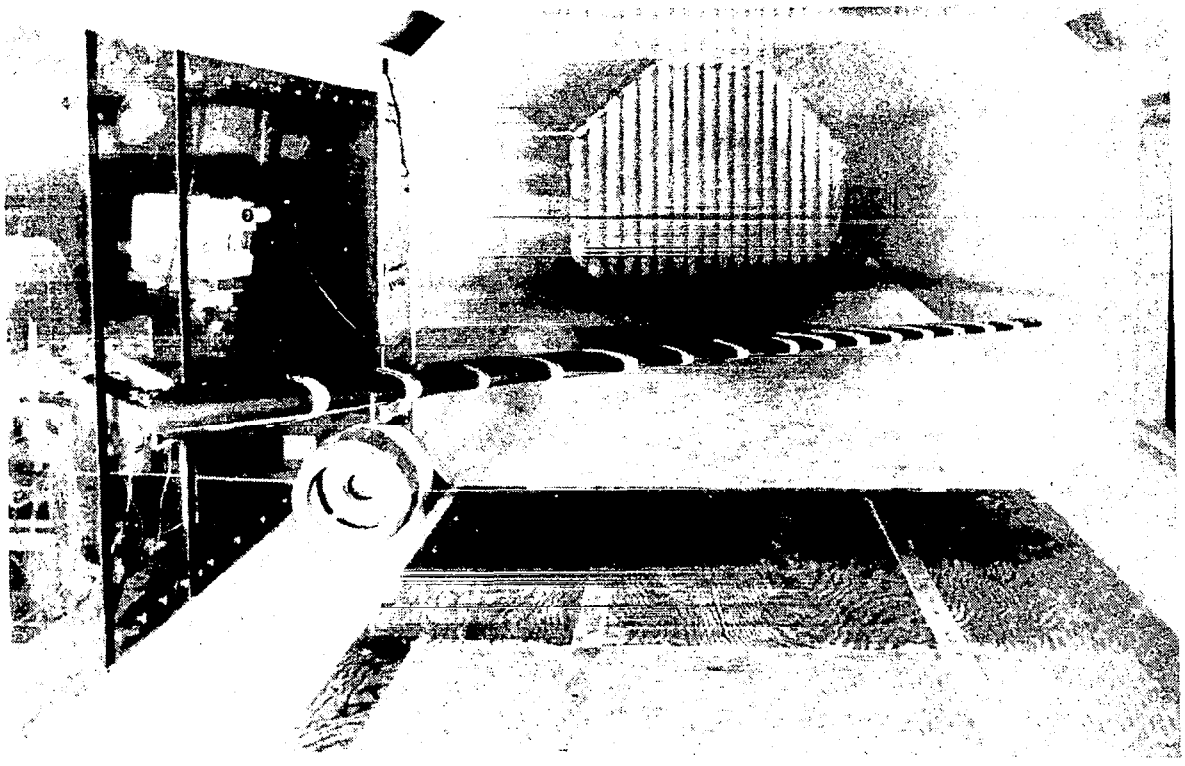

FIGURE 15. SEMISPAN MODEL INSTALLATION IN DOUGLAS LONG BEACH WIND TUNNEL

TEST PROCEDURES AND MEASUREMENTS

Bench Test

The hydraulic actuator used in the model was designed, fabricated, and developed at Douglas. The initial configuration was bench tested and the design modified before installation in the wing. Subsequent semispan wind tunnel tests revealed need for further development prior to full-span tests.

Before actuators were assembled, all parts were cleaned with a degreasing solvent to minimize particle contamination of the hydraulic fluid. Hydraulic lines and the MOOG servo-valve were flushed. The assembled system was bled at a pressure of 6.894×10^5 N/m^2 (100 psi). The position feedback potentiometers were verified by polarity before mounting to the actuator shaft. A calibration adjustment followed to obtain desired sensitivity.

Prior to measuring actuator characteristics, the vane was cycled for a break-in period of 30 minutes. Static friction was measured by hanging weights on an arm clamped to the actuator shaft. Internal leakage (across the vane) was measured with the actuator vane blocked in the middle position and pressurized on one side; leakage was measured in terms of the rate fluid drained from the unpressurized side through a bleed orifice. Bench tests established the position feedback signal gain and the dither frequency and amplitude.

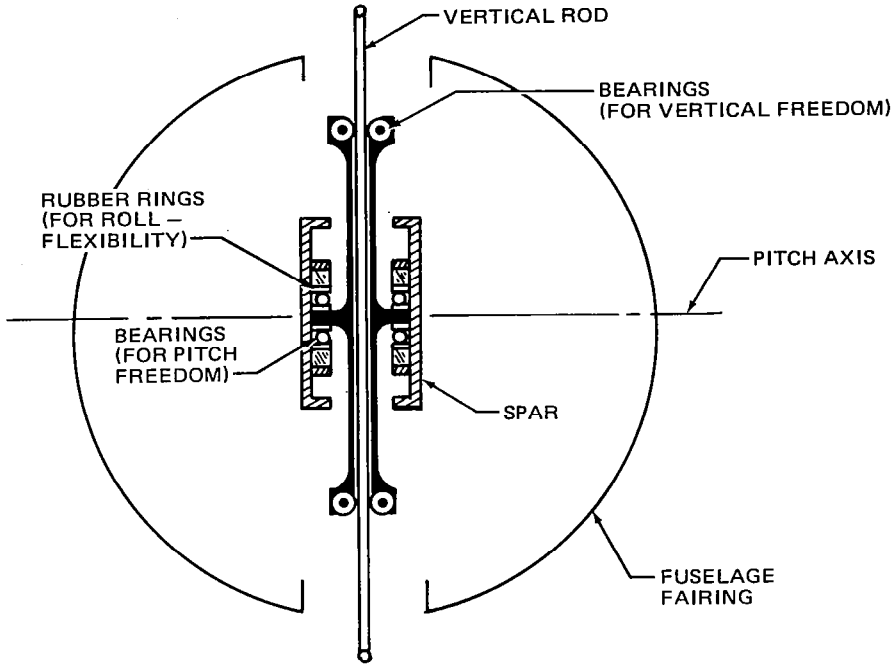

VIEW LOOKING FORE AND AFT

MODEL MOUNT SYSTEM

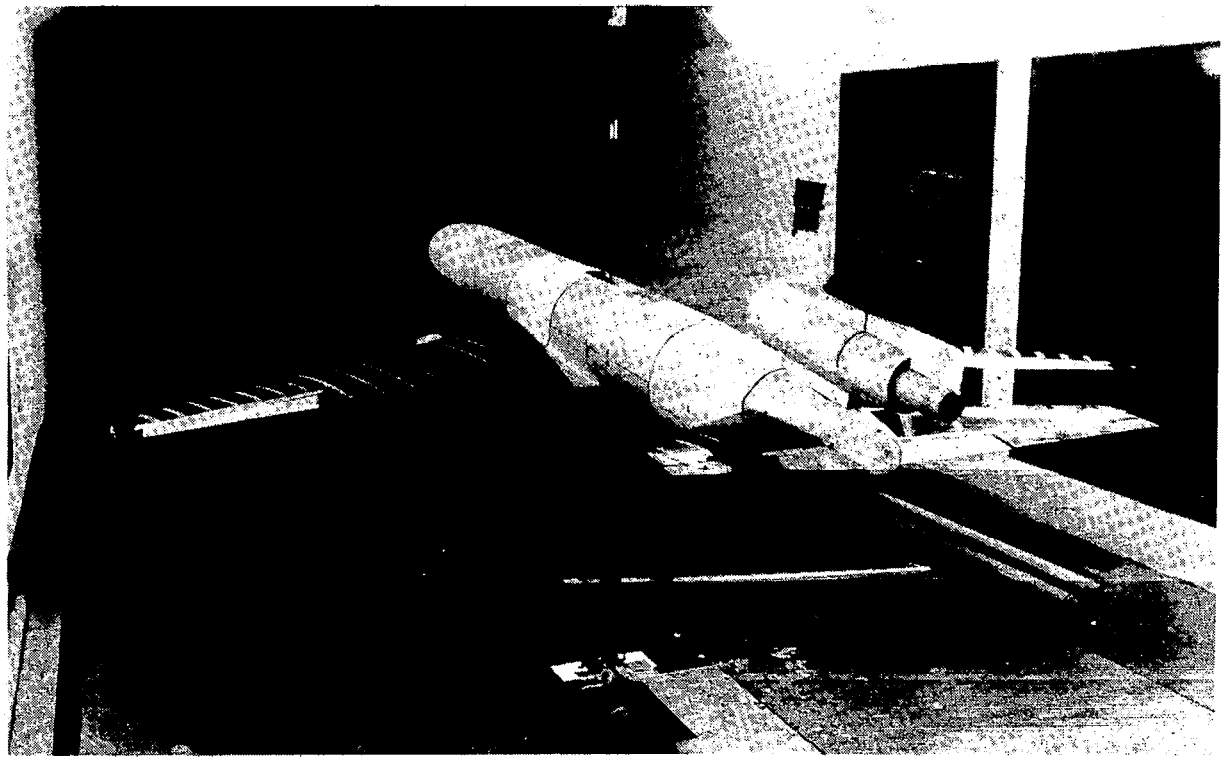

FIGURE 16. FULL SPAN MODEL INSTALLATION IN NORTHROP WIND TUNNEL

Dynamic performance evaluation consisted of transfer function measurements, response wave shape fidelity checks, and analysis of low-frequency hysteresis plots of position versus command signals. Actuator tests were run with and without inertia and spring loading. A mass represented control surface rotational inertia and a spring load simulated aerodynamic hinge moment.

Transfer function measurements were made using either an EMR Model 1400 frequency analyzer or a Spectral Dynamics Model SD 1002 impedance analyzer system. The EMR analyzer was a manually operated unit requiring the recording of test values by hand. The SD 1002 system had an automatic frequency sweep capability enabling the use of two-axis plotters but a minimum frequency limit of 2 Hz. The EMR unit was occasionally used for frequencies below 2 Hz. Amplitude and phase responses of the servo-actuator system were measured for various command levels from 2 Hz to 50 Hz.

Photographs of wave shapes were obtained with a Polaroid camera mounted on an oscilloscope. The X-Y plotter was used to measure hysteresis at low frequencies. A direct-write oscillograph was frequently used to record time histories of the input and response signals.

Since a common supply manifold was used for the three servo-valves of the full-span model, after performance was checked on each of the three actuator systems individually, the complete system was checked for "cross-talk" between channels. During random on-off switching of the channels, response signals were monitored to see if "cross-talk" was evident. This testing included driving the elevator system at one frequency and the ailerons at another. Command levels used were ±10 degrees to ensure a high demand on the supply pressure. Following actuator bench test verification, the components were installed in the model.

Vibration Tests

The normal modes of vibration of the models were measured prior to and during the wind tunnel tests. Structural properties of the model were obtained through a conventional sinusoidal vibration test using a multiple shaker system. One shaker was used to excite the semispan model and two shakers were used to excite the full-span model. Normal modes of vibration were detected by adjusting the excitation frequency such that the response velocity at all points on the model, as observed on an oscilloscope, were either in or out of phase with the driving force. Descriptions of the modal shapes and comparisons with the analytical results are presented in Appendix C. During the vibration test, the control system closed-loop gain was adjusted to obtain 6-dB gain margin.

Wind Tunnel Tests

The wind tunnel test procedure was basically the same for both the semispan and full-span models. The structural damping of the least-stable mode was measured at selected increments of velocity by measuring the structural decay response to a sharp input pulse on the wing tips or engine pods. Measurements were made with the system in both the passive and active states. Flutter characteristics were evaluated by plotting subcritical damping and frequency as a function of wind tunnel velocity. Passive and active flutter characteristics were determined for several wing-fuel configurations.

Phase and gain variations of the aileron control law were made independently of each other. A description of the configurations tested is presented in Table 2. The full-span model was tested with and without weights that were added aft of the wing tips to reduce flutter speed and modify the flutter mode.

TABLE 2

TEST CONFIGURATIONS

MODEL	% FUEL	PYLON FREQUENCY	WING TIP WEIGHT	FUSELAGE PAYLOAD	REMARKS
		f_α/f_ψ-Hz	(GMS)	(Kg)	
Semispan	0	15.3/6.2	0	-	Flutter and turbulence testing performed
Semispan	10	15.3/6.2	0	-	Flutter and turbulence testing performed
Semispan	21.5	15.3/6.2	0	-	Flutter testing only performed
Semispan	40	15.3/6.2	0	-	Flutter and turbulence testing performed
Semispan	60	15.3/6.2	0	-	Flutter testing only performed
Semispan	80	15.3/6.2	0	-	Flutter testing only performed
Semispan	100	15.3/6.2	0	-	Flutter and turbulence testing performed
Full Span	10	15.3/6.2	0	0	Flutter and turbulence testing performed
Full Span	10	15.3/6.2	0	4.54	Flutter testing only performed
Full Span	10	15.3/6.2	0	9.07	Flutter testing only performed
Full Span	10	20.6/8.89	0,10,20	0	Flutter testing only performed
Full Span	100	15.3/6.2	0	0	Turbulence testing only performed

For the gust alleviation tests, the canvas banner was installed horizontally across the stilling chamber to generate a near-random gust field. The aeroelastic response of the model was measured in terms of wing bending and torsional moments, vertical and lateral engine accelerations, aileron position, and wing vertical acceleration. Aeroelastic response characteristics to the random gust field were defined in terms of overall RMS amplitude response of the wing. These response measurements were made with the elastic mode suppression (EMS) system on and off. Gust response tests were performed at several speeds below the passive flutter speeds during which the loop gain and phase were varied. Phase variations were obtained by inserting a filter,

$$G_p = \pm \frac{1 - \tau S}{1 + \tau S}$$

in the control loop. With the EMS system in the open-loop configuration and the banner removed, a sine sweep was input to the servo-actuator. The transfer function of model response of aileron deflection was then measured at various wind tunnel velocities.

Test Measurements

The following experimental data were obtained:

1. Model vibration frequencies and mode shapes.

2. Open-loop control system transfer functions, i.e., Bode plots, presented as amplitude and phase versus frequency as a function of input.

3. Frequency-velocity and damping-velocity data: These measurements were recorded and plotted for all configurations tested. The damping of the model was calculated using the logarithmic decrement

$$g/2 = \frac{1}{2n\pi} \ln \frac{A_1}{A_2}$$

where n = number of cycles
A_1 = initial amplitude
A_2 = amplitude of n^{th} cycle

4. Model RMS reponse to turbulence. These data were obtained with the system turned on and off. Turbulence response data were obtained for the 0 percent and the 100-percent fuel configurations for both semispan and full-span models.

RESULTS AND DISCUSSION

BENCH TESTS

The initial bench tests of the actuator resulted in several modifications before it was installed in the wing for the first semispan test:

1. The end caps were machined to accept "O" ring seals of 90 Duro Buna N material.

2. The vane seal material was changed from a commercially molded Adiprene (chloroprene) to Flexane 94, a urethane elastomer which could be cast in-house.

3. The molded vane seal width was narrowed to reduce vane preload and the wiping radius was increased to prevent failures which had occurred due to direct impingement of the hydraulic jets.

The performance characteristics of this first working version (Mod I) of the actuator were measured and the results were:

1. Stall torque of 0.184 kg-m (15.97 lb-in.)

2. Breakaway torque of 0.028 to 0.034 kg-m (2.5 to 3.0 lb-in.)

3. Travel limits of ±17 degrees

4. Acceptable frequency response (transfer functions discussed below)

The bench test transfer function measurements of the Mod I actuator are presented in Figures 17 through 19 for control surface amplitudes from ±1/2 degree to ±10 degrees. These response functions were made with the actuator under an inertia load of 0.175×10^{-4} kg-m-sec^2 (0.0152 lb-in.-sec^2) and a spring load of 0.0794 kg-m/rad (6.9 lb-in./rad) that represented design conditions. The amplitude responses were normalized to the static gain value of 0 dB equal to 1 degree response for a 1 degree command. Later studies, discussed below, showed the response to be within ±2 dB due to nonlinear behavior of the actuator.

Figure 20 is a zero-speed transfer function of the aileron position versus command with the servo-actuator system installed in the semispan model and shows that the installed transfer function was similar to the bench test results. The command was ±5 degrees and this Bode plot was used for later comparison to monitor the system performance.

The Mod I actuator performed reliably during the first semispan test. The same actuator was used for the second semispan test and performed well initially; then a degradation occurred and test results could not be repeated. A thorough checkout of the servo-system failed to isolate the problem. During these checkout procedures the following observations were made:

1. A repeatable Bode plot of the actuator system was not necessarily an indication that flutter speed results would be repeatable.

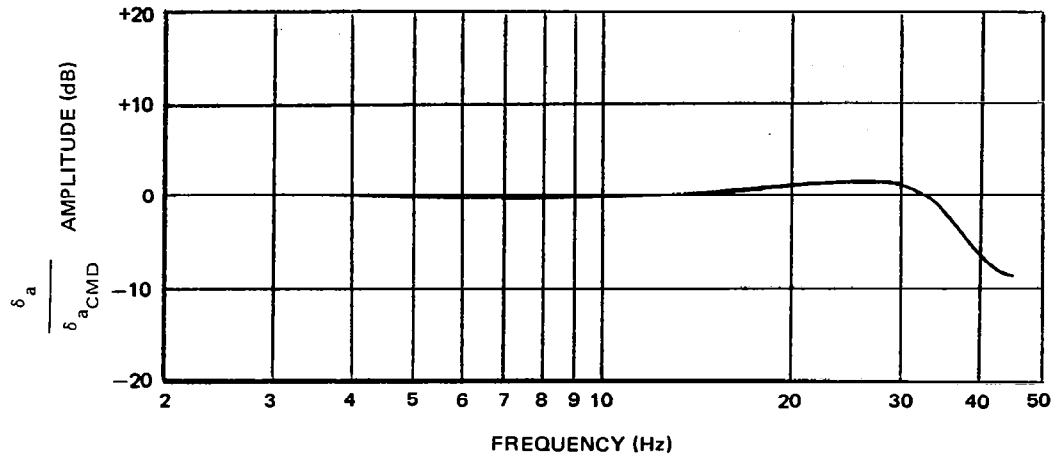

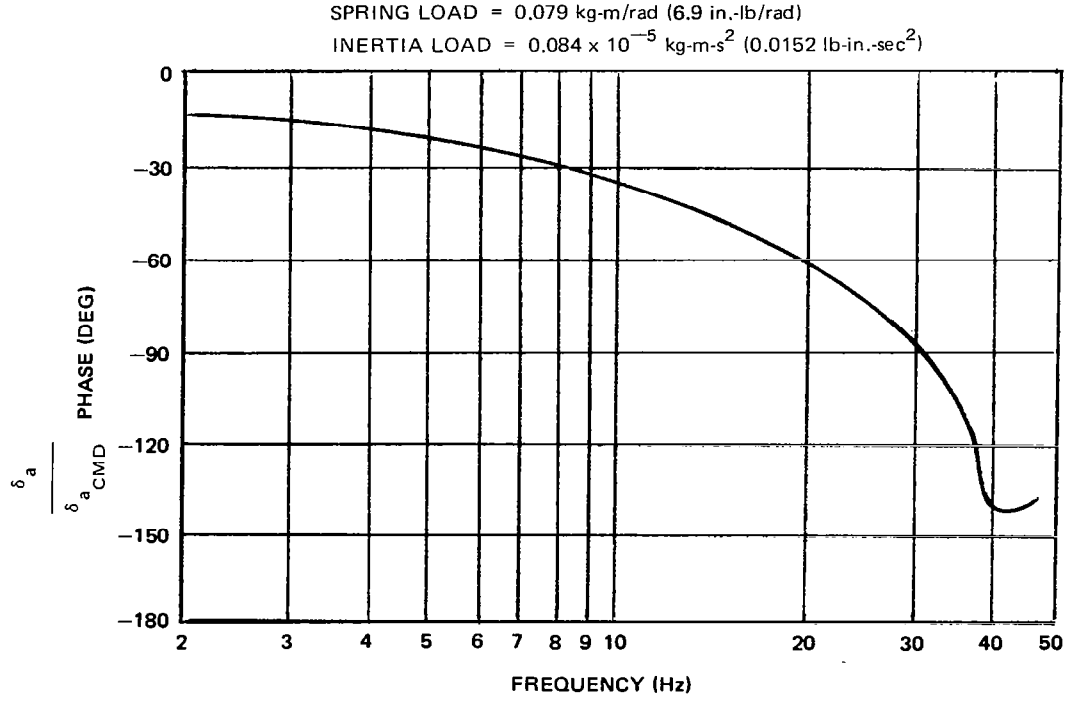

FIGURE 17. TRANSFER FUNCTION OF MOD I SERVO-ACTUATOR POSITION FEEDBACK VERSUS COMMAND SIGNAL – COMMAND = ± 1/2 DEGREE

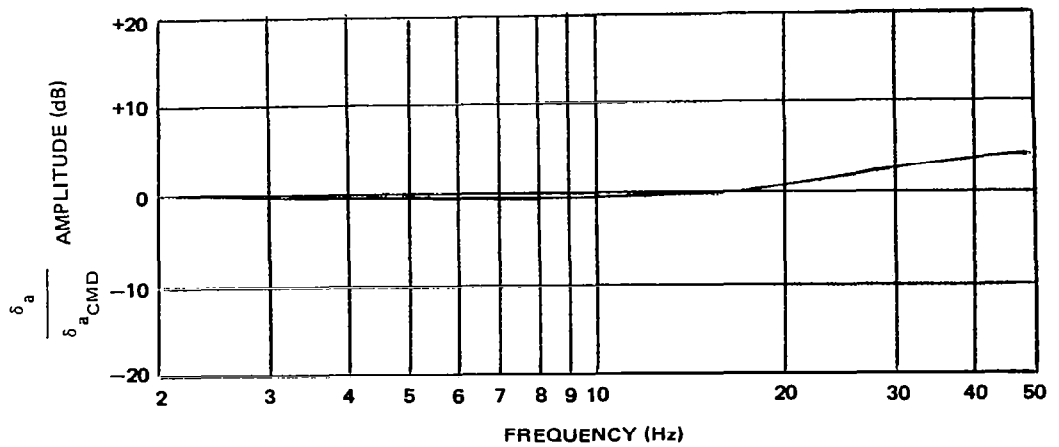

SPRING LOAD = 0.079 kg-m/rad (6.9 lb-in./rad)
INERTIA = 0.084×10^{-5} kg-m-s^2 (0.0152 lb-in.-sec^2)

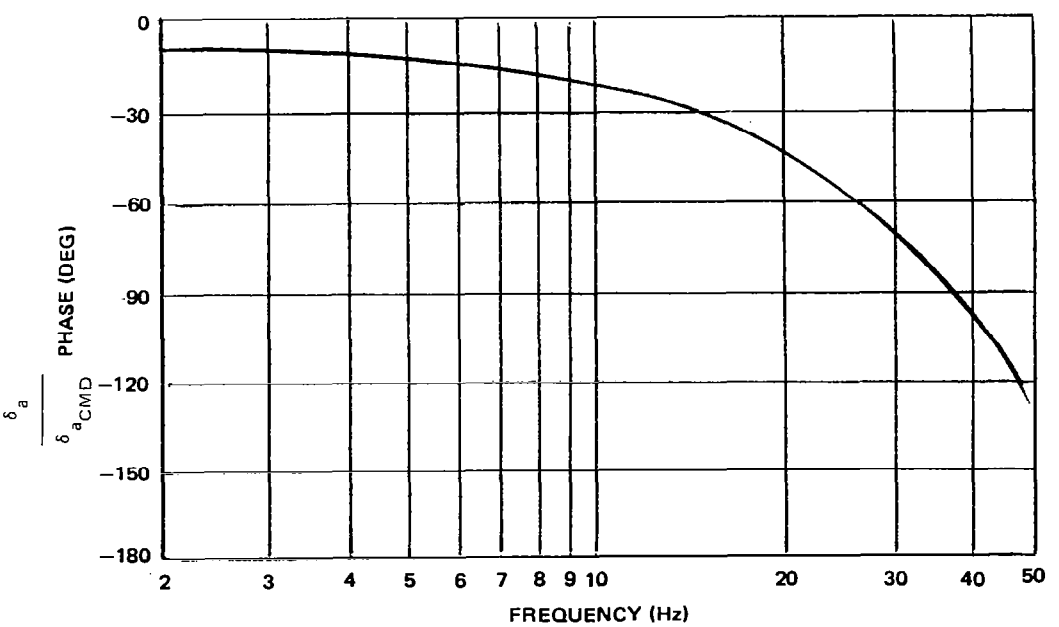

FIGURE 18. TRANSFER FUNCTION OF MOD I SERVO-ACTUATOR POSITION FEEDBACK VERSUS COMMAND SIGNAL – COMMAND = ± 1 DEGREE

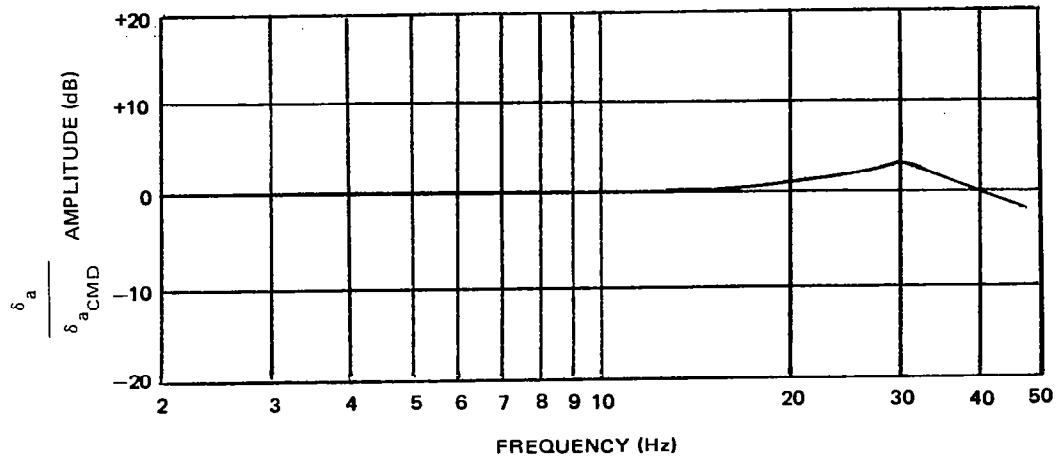

SPRING LOAD = 0.079 kg-m/rad (6.9 lb-in./rad)
INERTIA LOAD = 0.084×10^{-5} kg-m-s^2 (0.0152 lb-in.-sec^2)

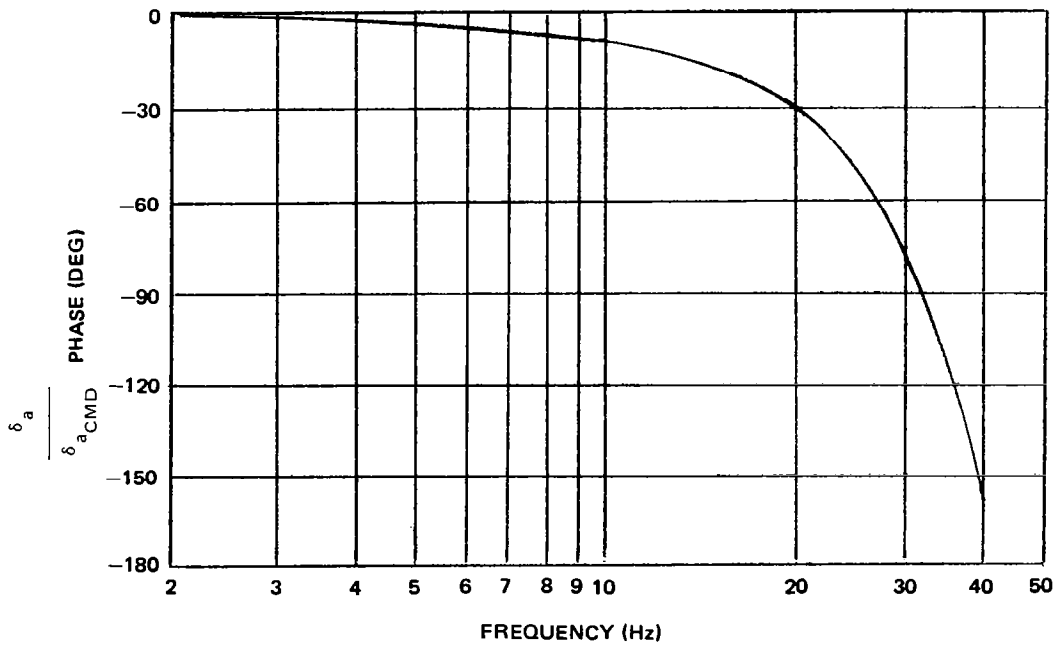

FIGURE 19. TRANSFER FUNCTION OF MOD I SERVO-ACTUATOR POSITION FEEDBACK VERSUS COMMAND SIGNAL – COMMAND = ± 10 DEGREES

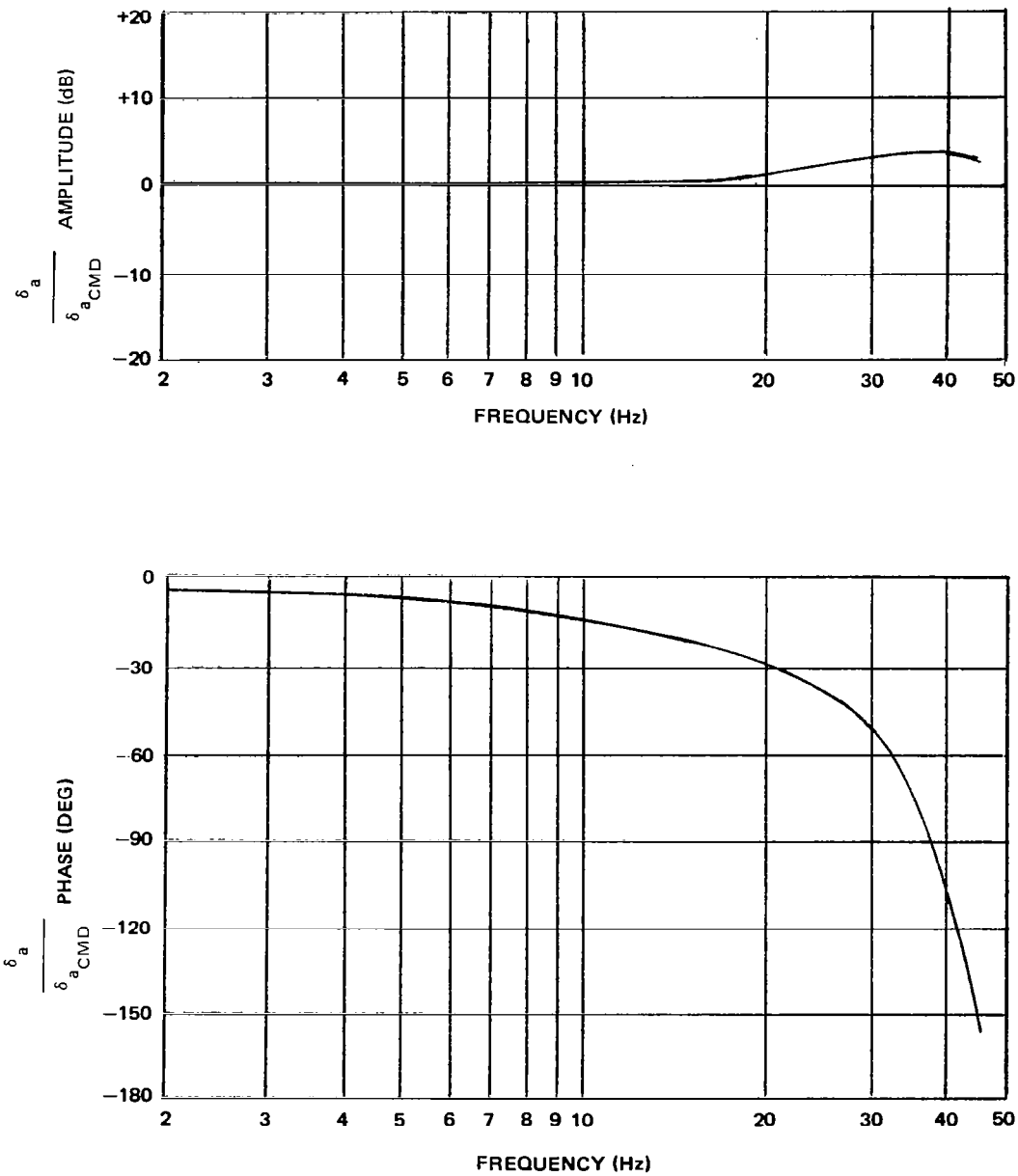

FIGURE 20. TRANSFER FUNCTION OF AILERON VERSUS COMMAND SIGNAL AT ZERO WIND SPEED – MOD I ACTUATOR, COMMAND = ±5 DEGREES

2. Harmonic distortion in the position feedback signal (e.g., square waving) was a good indicator but amplitude sensitivity of the distortion required judgment and experience to evaluate acceptability of the actuator.

3. Low-frequency hysteresis plots of response versus command were also good indicators but actual performance was not consistent with acceptable hysteresis characteristics.

Figure 21 shows examples of the left aileron position feedback signal. Sample A is an acceptable wave shape, while B and C exhibit wave distortions indicating an unacceptable actuator.

A development program followed the second semispan test. Each modification of the actuator was evaluated by wave shape reproduction (position feedback) of sinusoidal command signals. The product of these studies was a Mod II actuator with improved reliability and consistency of performance. Physical changes to the actuator were:

1. The listed hardness of the vane elastomer was reduced from 90 to 80 durometers (manufacturer's designation) on a Shore A hardness scale. However, the actual measured hardness values after cast averaged 60 to 65.

2. The vane shaft brass bearings were replaced with Teflon bearings.

3. Both the leading edge and trailing edge radii of the vane were increased by 0.0001 m to ensure good wiping contact between the housing and the vane's edges.

4. The large radius edge of the vane was reworked by hand to reduce surface contact between the vane and housing to minimize friction. Static friction was eventually reduced from an average of 0.0403 kg-m (3.5 lb-in.) down to 0.00403 kg-m (0.35 lb-in.) of torque.

Figure 22 shows sample wave shapes of all three control surfaces of the full-span model (Mod II actuator with acceptable performance). The kink in the right-hand aileron actuator shape was not objectionable in terms of subsequent performance, and was found to be due to a shaft concentricity problem.

Acceptable leakage rate of hydraulic fluid across the vane averaged 1.5×10^{-6} m^3/s (0.09 $in.^3/s$). The Mod II actual stall torque was about 0.098 kg-m (8.5 lb-in.) as compared with 0.20 kg-m (17.35 lb-in.) of the Mod I actuator. The Mod II actuator performed acceptably under simulated load conditions. Figures 23 and 24 are sample Bode diagrams for the full-span model installation.

The linear behavior of the actuator system was measured by varying command levels at several frequencies. Figure 25 shows the change in gain and phase as functions of amplitudes of surface rotation for several frequencies. The improvements of the Mod II actuator were confirmed by an additional semispan wind tunnel entry. The additional phase lag in the servo system due to the changes in the actuator did produce slightly different wind tunnel test results than previously with the same control laws. These differences are discussed later.

The full-span bench test was primarily to check for inter-channel interference since all three servo-valves were mounted on a common supply manifold. While observing the three separate

A

δ_a = ±2 DEG AT 12 Hz

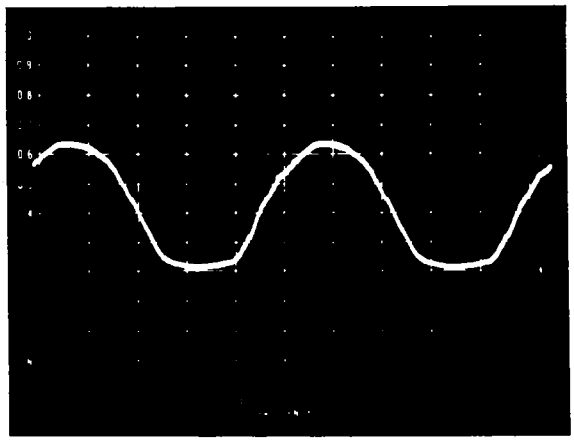

δ

HEALTHY ACTUATOR

TIME

B

δ_a = ±1.5 DEG AT 12 Hz

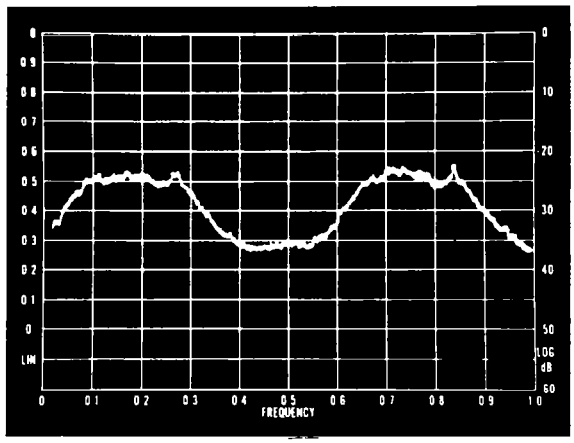

δ

UNACCEPTABLE RESPONSE

TIME

C

δ_a = ±2 DEG AT 10 Hz

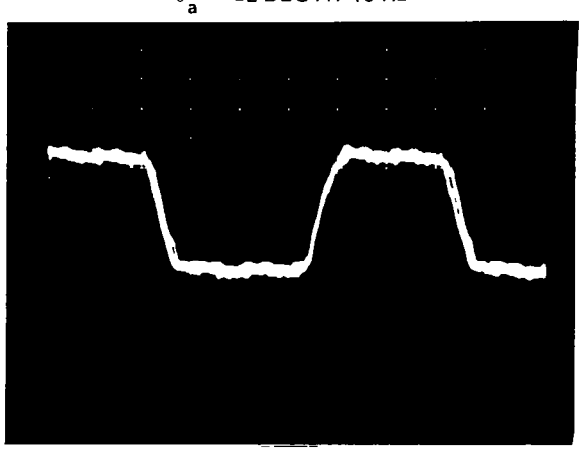

δ

UNACCEPTABLE RESPONSE

TIME

FIGURE 21. LEFT AILERON WAVE SHAPE CHARACTERISTICS COMPARING NORMAL AND DEGRADED OPERATION

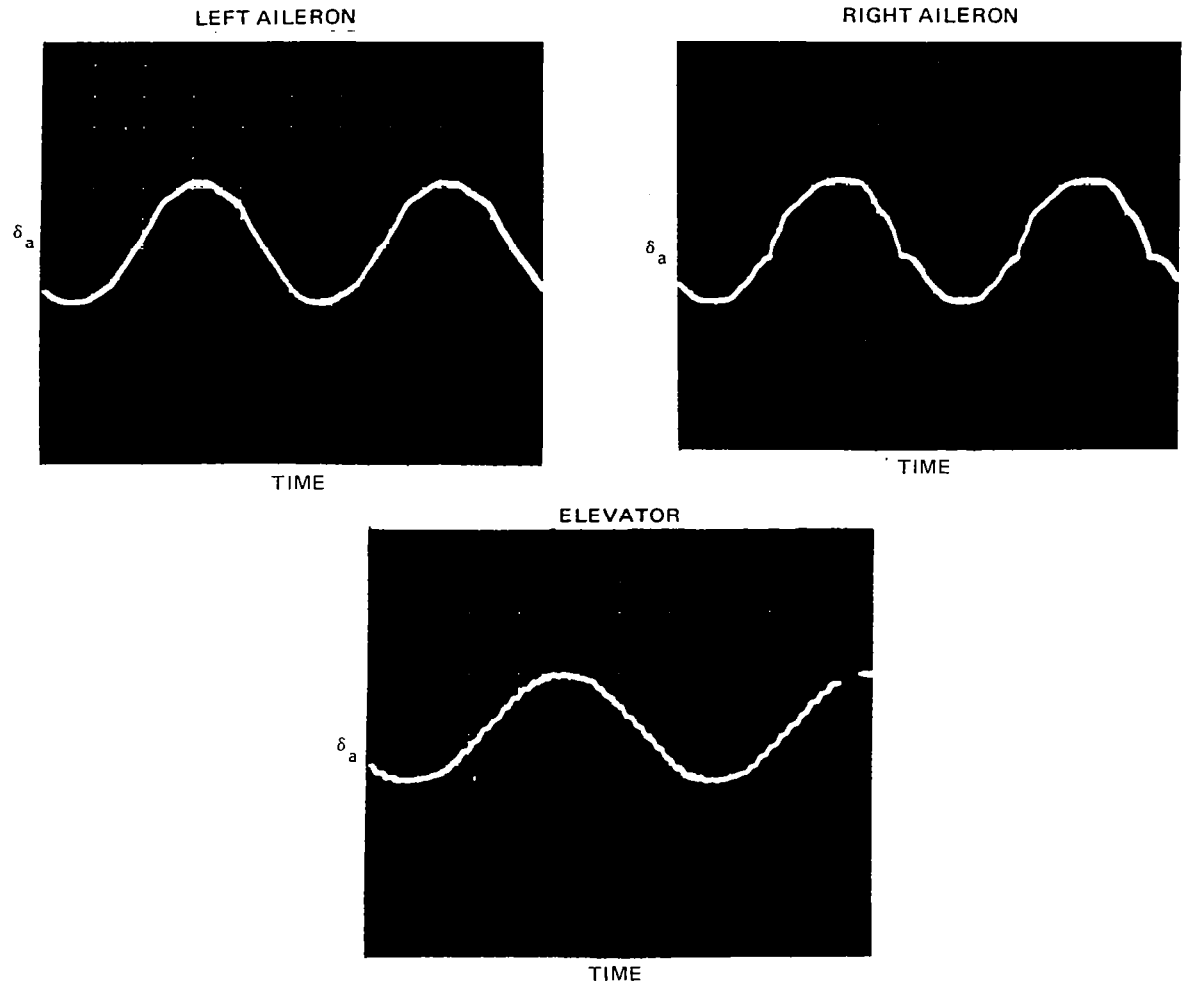

FIGURE 22. FULL SPAN MODEL AILERONS AND ELEVATOR WAVE SHAPE CHARACTERISTICS WITH MOD II ACTUATORS

position feedback signals on an oscilloscope, the left and right ailerons and elevator systems were individually switched on and off. This was done at various frequencies and amplitudes, and in some cases the elevator was driven at a different frequency than the ailerons. No effects of "cross-talk" were observed.

VIBRATION TESTS

Measured frequencies and mode shapes of both the semispan and full-span models are presented in Appendix C. The experimental mode shapes and frequencies are compared to analytical predictions. Experimental data and analytical results closely agree for the basic DC-10 configuration.

The important flutter modes for the semispan and full-span models are symmetric first wing bending and inner panel torsion. The control law filters for flutter suppression were designed for the inner panel torsion mode. The gust load alleviation control law filter was designed for the reduction of bending moment in the wing first bending mode.

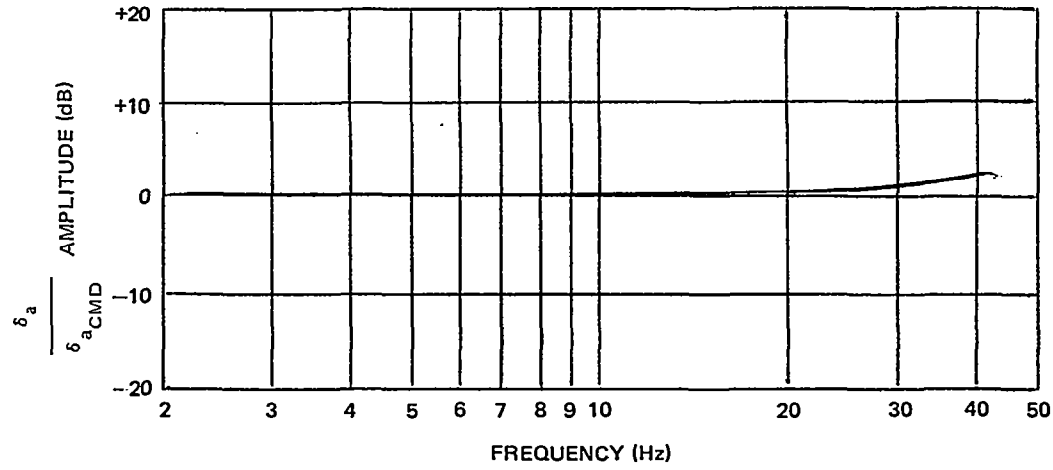

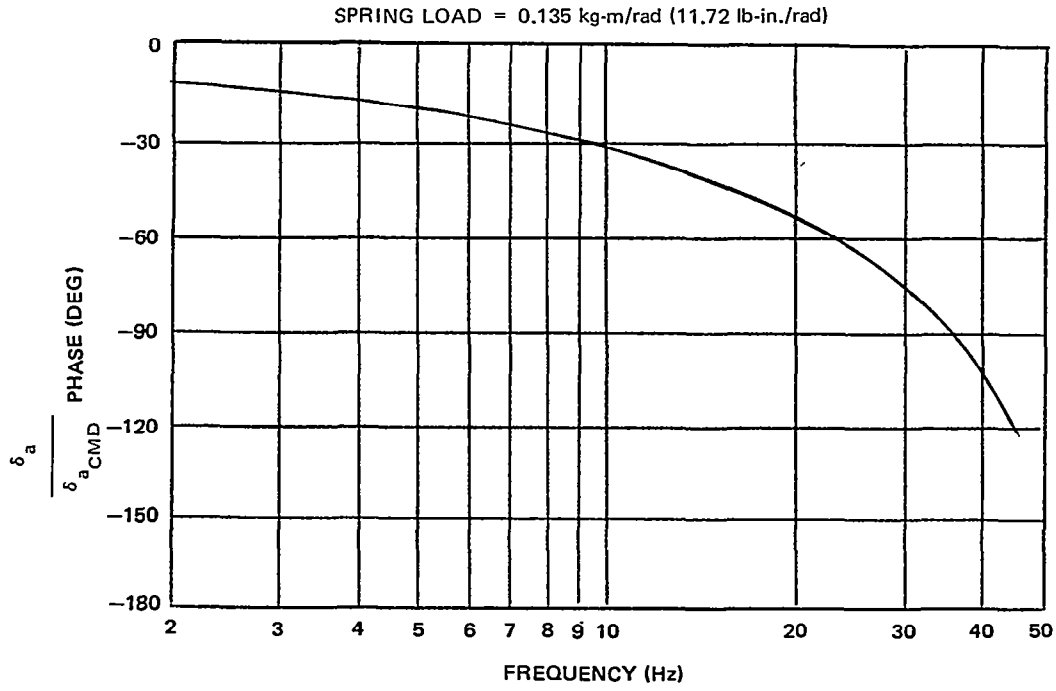

FIGURE 23. TRANSFER FUNCTION OF ELEVATOR POSITION VERSUS COMMAND SIGNAL — MOD II ACTUATOR — COMMAND = ± 2 DEGREES

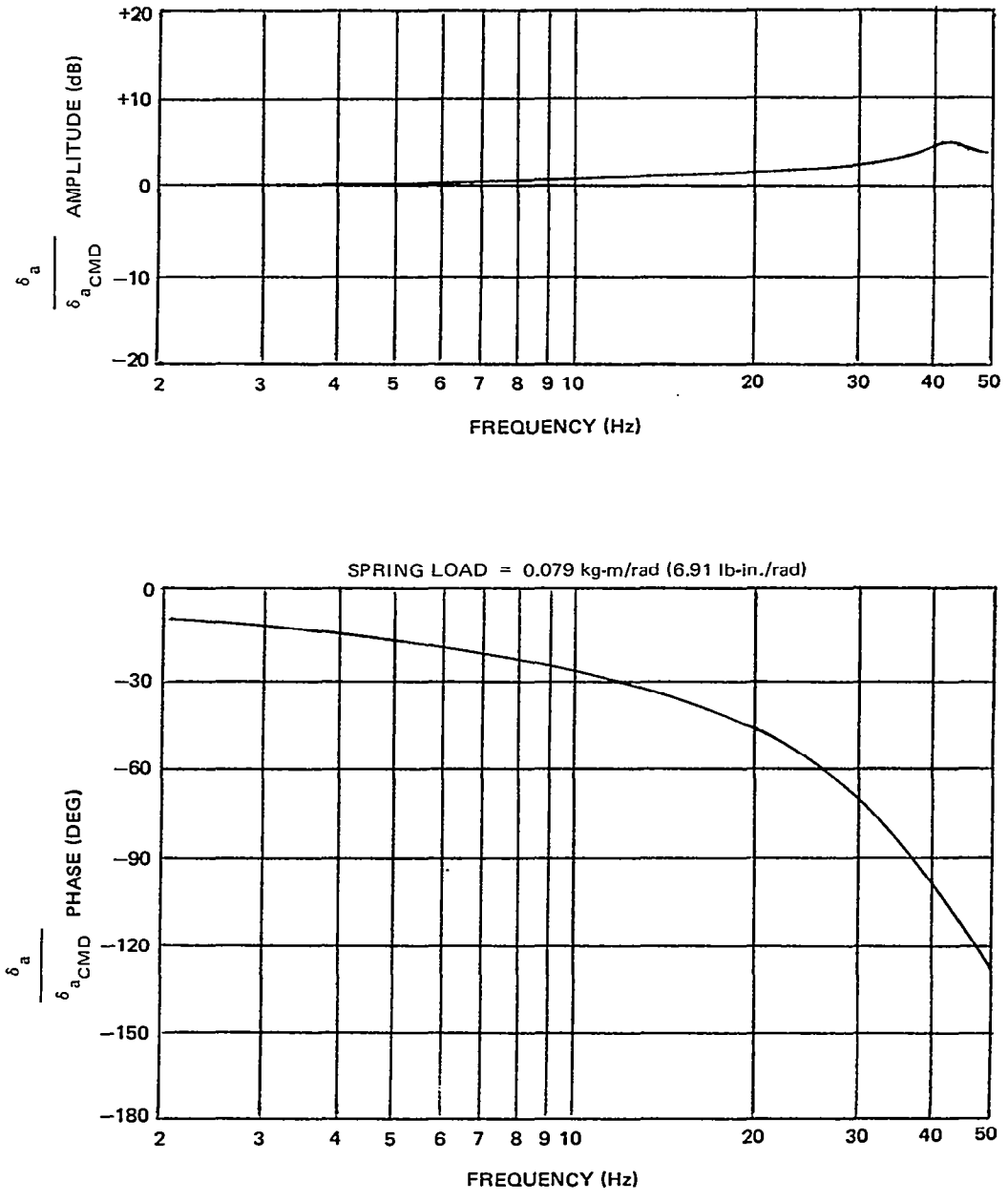

FIGURE 24. TRANSFER FUNCTION OF LEFT AILERON POSITION VERSUS COMMAND SIGNAL — MOD II ACTUATOR — COMMAND = ± 2 DEGREES

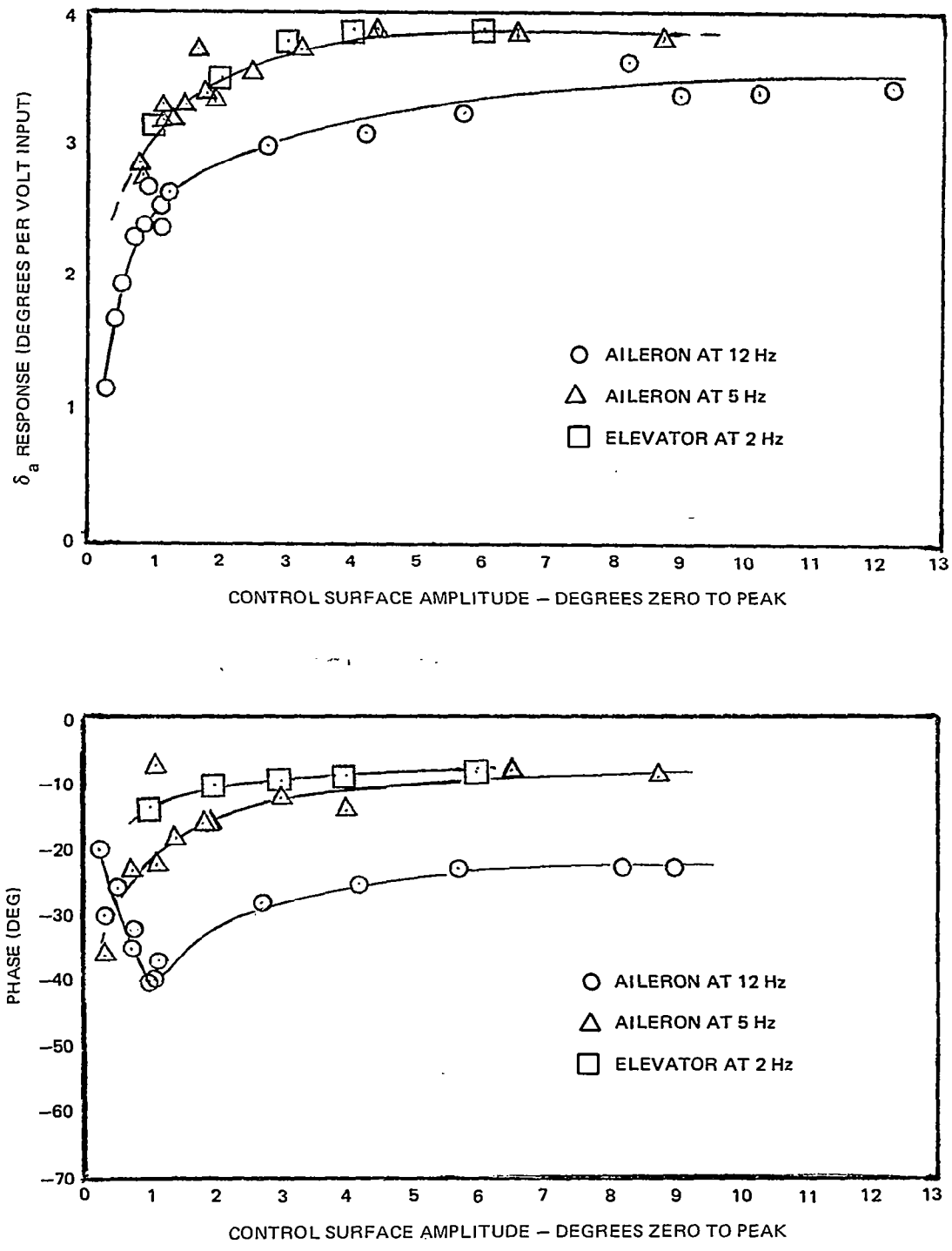

FIGURE 25. LINEARITY OF SERVO ACTUATOR SYSTEM AT THREE FREQUENCIES – MOD II ACTUATOR

CONTROL LAW DEVELOPMENT

Synthesis Methods

For control system synthesis it was necessary to directly obtain aeroelastic transfer functions in an explicit form. To meet this requirement, equations of motion were simplified by introducing a time-domain approximation of the aerodynamic coefficients A(k) in the form:

$$A(k)\, q(t) = aq(t) + b\dot{q}(t) + c\ddot{q}(t)$$

where a, b and c are real coefficients dependent upon the fit reduced frequency k. The approximation was made piecemeal by use of the functional values of A(k) at k = 0 and a k-value in the neighborhood of a chosen reduced frequency k_1. The coefficients used to approximate the aerodynamic forces were combined with the generalized forces due to structural mass, damping, and stiffness into a set of equations that is expressed in matrix form by:

$$M\ddot{q} + D\dot{q} + Kq = F(t)$$

The eigenvalues and eigenvectors of the homogeneous equation were computed in an iterative manner by letting k_1 assume the reduced frequency value k_n obtained in the preceding iteration for root number n. Using the resulting eigenvectors, the generalized coordinates q were transformed into a new set of generalized coordinates associated with uncoupled equations of motion. With the eigenvalues known, the transformed equations were reduced to a first order form similar to the equation

$$\dot{p} = Cp + G(t)$$

where C is an eigenvalue matrix. This equation was now in a form compatible with existing control system analysis routines. By transforming the equation into the Laplace domain, the required transfer functions could be obtained.

The control system analysis considered 12 to 19 generalized degrees of freedom, depending on the number of higher frequency modes required. This size reduction was achieved by truncating the original structural degrees of freedom in a manner that retained the residual effects of higher-order modes. To simplify the control law design process further, the equations of motion described above were developed for a limited number of configurations and flight conditions.

The methods used to synthesize the control laws were originally developed during design studies of a derivative version of the DC-10 with active controls for gust load alleviation, maneuver load control, and flutter mode augmentation. The methods employed classical control system analysis techniques for which several computer programs were available and well tested.

The gust load alleviation (GLA) control law was determined first, assuming an accelerometer feedback sensor located near the wingtip (with output h_{WS}) and the outboard ailerons (δ_a)deflected symmetrically as the controls.

The objective was to minimize the bending moment at the critical outboard wing station (BM_{OB}) resulting from wind gusts. The open-loop transfer function, calculated from the linearized and truncated equations of motion, is represented as

$$\frac{BM_{OB}}{W_g} = \frac{N_{W_g}^{BM_{OB}}}{\Delta}$$

With the GLA loop closed, the transfer function becomes

$$\left(\frac{BM_{OB}}{W_g}\right)_{\text{CLOSED LOOP}} = \frac{N_{W_g}^{BM_{OB}} + (GLA)\, N_{W_g}^{BM_{OB}} \ddot{h}_{\delta_a}^{WS}}{\Delta + (GLA)\, N_{\delta_a}^{\ddot{h}WS}}$$

To minimize the bending moment, then

$$GLA = - \frac{N_{W_g}^{BM_{OB}}}{N_{W_g}^{BM_{OB}} \ddot{h}_{\delta_a}^{WS}}$$

Figure 26 is a Bode plot of this relationship for one of the gust critical configurations of the full-span model. The predominant mode of this transfer function near 3 Hz was unstable with a very low damping ratio. In comparison, the corresponding theoretical control law derived earlier for the DC-10 derivative aircraft was similar in shape although the low damped mode was stable. The characteristics of either GLA filter could be approximated by a stable second-order low-pass filter with a low damping ratio. This resulted in the feedback of wingtip acceleration in the low-frequency region, at the short period and below (which is very similar to aircraft cg acceleration at these frequencies), and wingtip deflection at higher frequencies including the important first wing bending mode. Because the semispan model did not have rigid body degrees of freedom, the GLA characteristic determined in this manner resulted in the feedback of wingtip deflection over the whole frequency range. To keep the low frequency gain in terms of wingtip acceleration at reasonable levels, a low-pass filter shape was also used for the semispan model. The break-point was taken at the highest usable frequency that did not interfere with the bending moment reduction at the first wing bending frequency.

The low damping ratio required to match the theoretical shape resulted in a low damped closed-loop filter mode. For this reason, the bending moment reduction was compromised by a small amount to assure good closed-loop response according to classical analysis standards. In addition, control surface magnitudes resulting from the wind tunnel gust spectra were analyzed and the control system gains were adjusted to prevent saturation. The semispan model tests resulted in lower surface deflections than predicted, so that surface saturation did not actually impose any compromise to the control laws and was not considered a critical factor for the full span model control law development.

For flutter suppression, the GLA control law was analyzed at the critical speed and fuel load conditions for flutter. The high frequency portion of the GLA control law was shaped to add damping and alter the phase characteristics to provide the desired gain and phase margins and

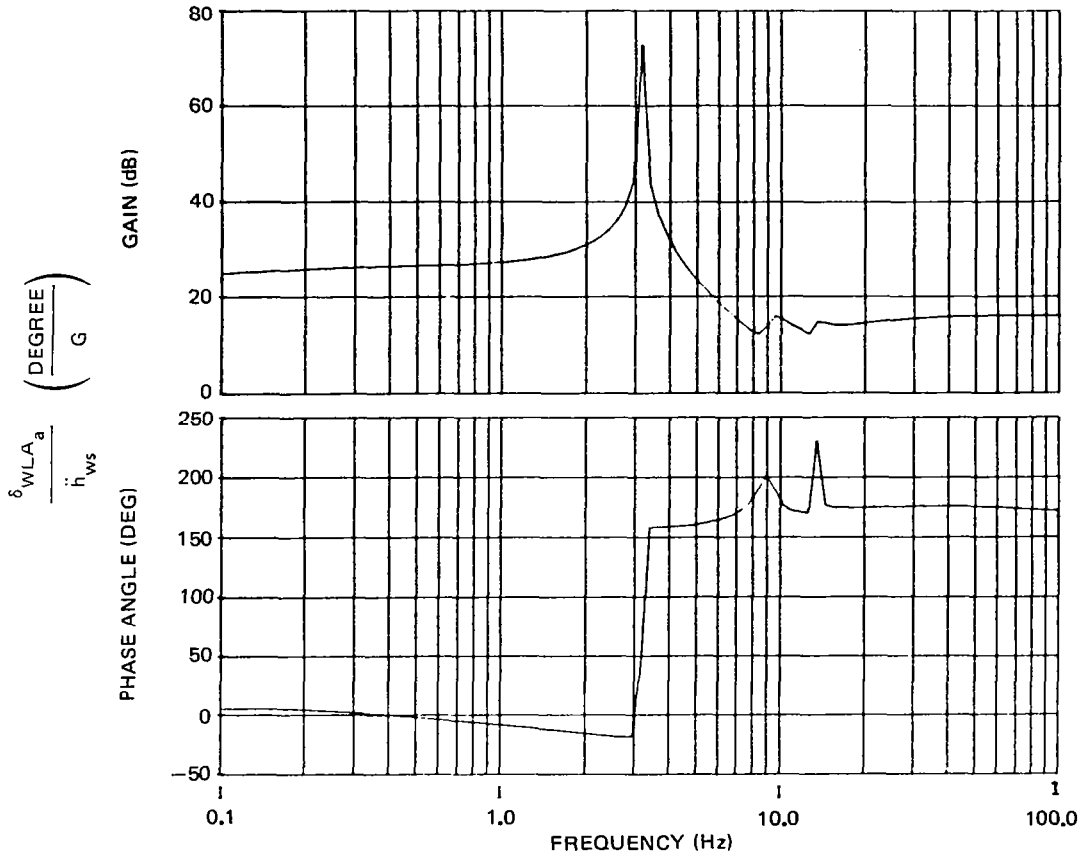

FIGURE 26. BODE PLOT OF IDEALIZED GLA FILTER

flutter mode damping. Classical synthesis techniques were applied using root-locus and Nyquist analyses. The resulting control law was rechecked with the gust critical condition to assure that the GLA performance was not adversely affected.

The elevator control law was designed to add damping to the low frequency modes. In providing gust load alleviation at low frequencies the aileron control law could destabilize the short-period mode and introduce a poorly damped filter mode, depending on the gain required. The elevator control law was adjusted to compensate for these effects at low frequencies and to provide some additional damping to the flutter mode at high frequency. Since the adjustment was compensating for the aileron control law effects, it became desirable to adjust the elevator loop when aileron control law gain changes were made.

Gust Modes

For the semispan model tests, measurements of the power spectral density of the gusts produced by the banner gust generator were made over a range of speeds and at various locations in the test section. Some of the measured data are shown in Figure 27 with two different curve fits that were used in the analysis. The Dryden form curve fit attempted to approximate the higher frequency data points and the average standard deviation of the gust intensity over the tunnel width. A non-Dryden curve fit approximated the maximum gust levels in the mid-frequency

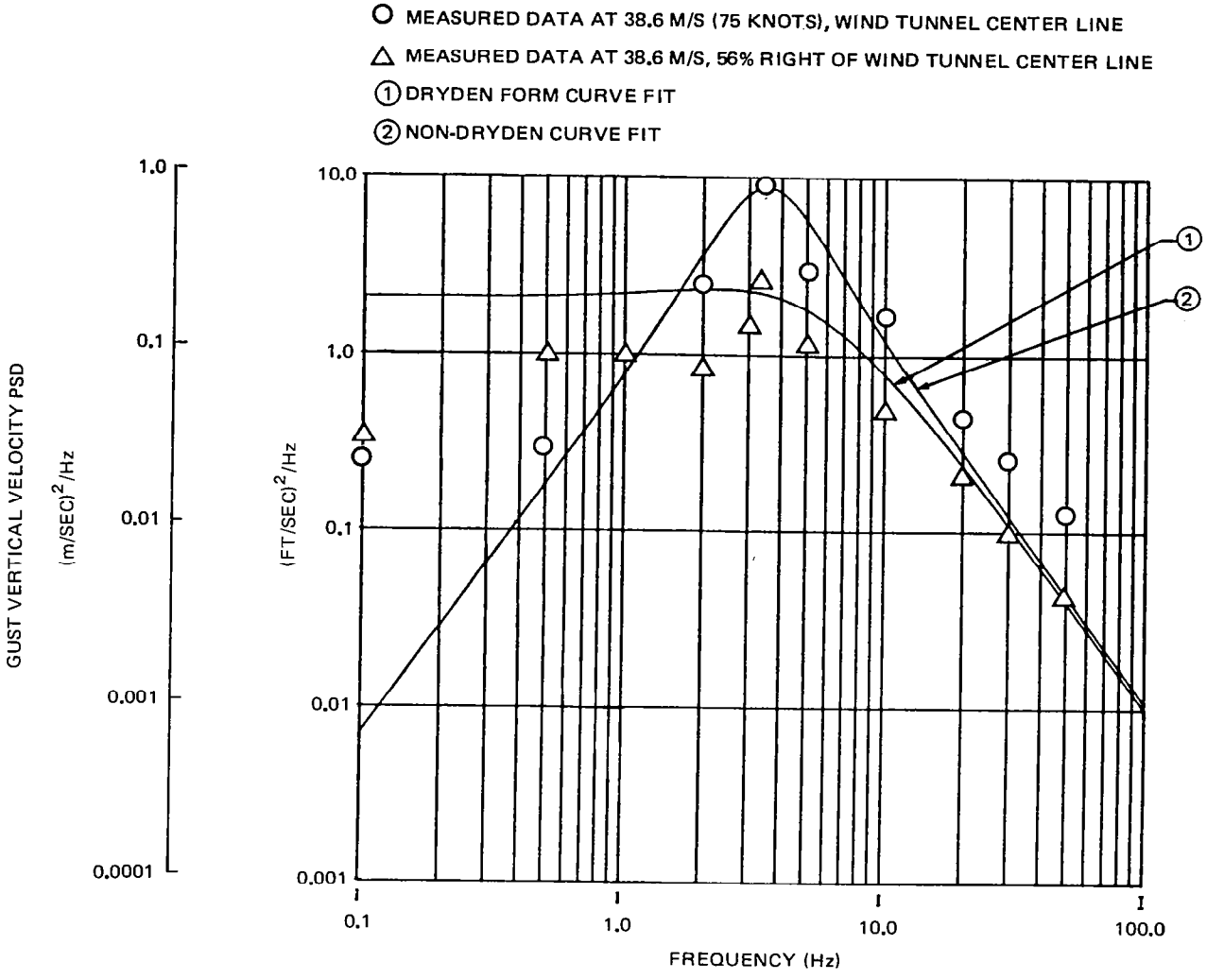

FIGURE 27. VERTICAL VELOCITY PSD WITH THE TURBULENCE BANNER INSTALLED IN THE DOUGLAS WIND TUNNEL

range and the larger standard deviation for the centerline measurements, and was used in the gust analysis. In this way, more accurate comparisons were made of the results obtained by the linearized, truncated equations and the non-linear, frequency domain equations containing additional higher frequency modes.

For the full span tests in the Northrop wind tunnel, several measured gust spectra were available from previous DC-10 tests. The control system analysis program was modified to accept a plot of such discrete point data. Figure 28 shows two of these measured spectra together with the analytical curve fit.

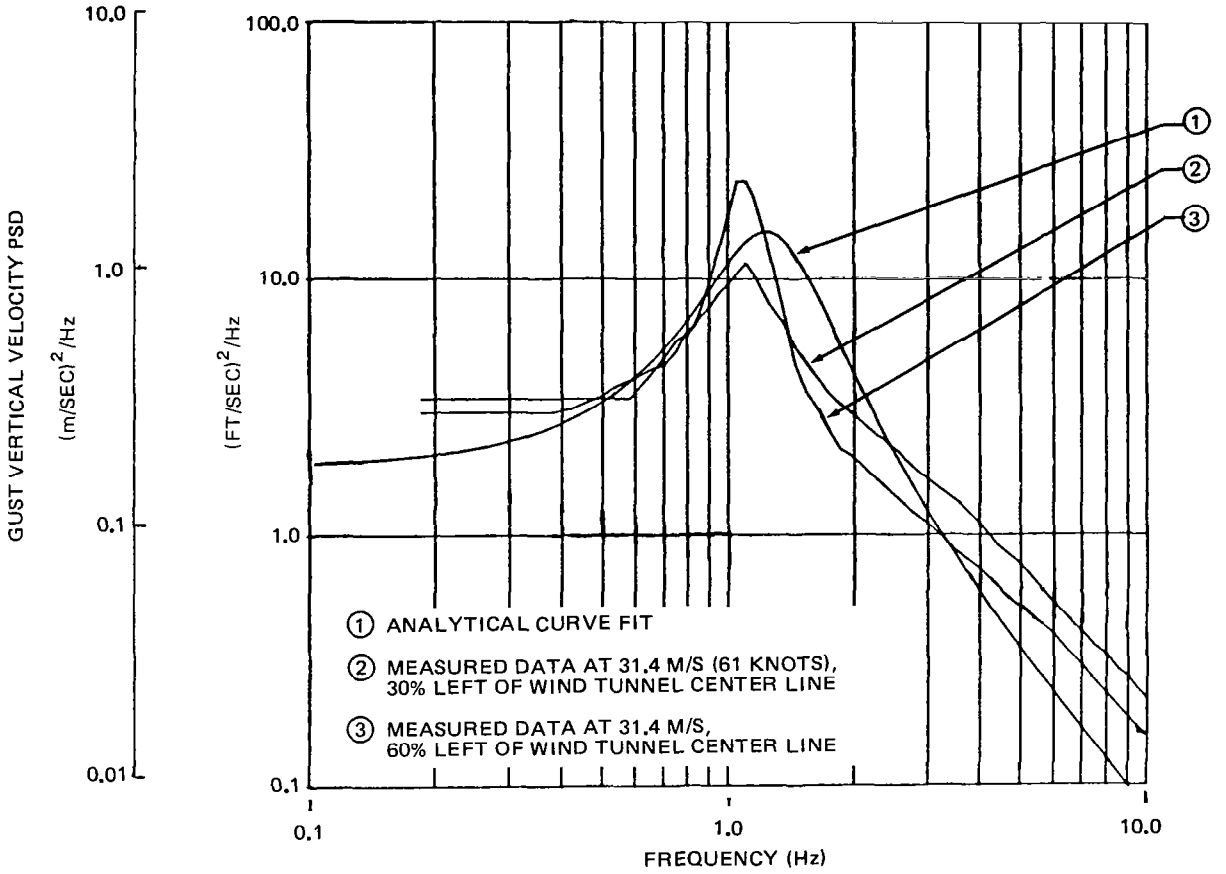

FIGURE 28. VERTICAL VELOCITY PSD WITH THE TURBULENCE INSTALLED IN THE NORTHROP WIND TUNNEL

Actuator Models

A frequency response of the actuator to sine wave commands was measured prior to the semispan tests. An analytical curve fit of the measured data used to model the actuator characteristics for the control law analysis is shown in Figure 29. This model fit the measured characteristics for large (±5 degrees) commands. Subsequent actuator measurements showed considerably larger phase lags at low frequency (2 Hz) for small command inputs. A non-linear actuator model was developed with a hysteresis loop in the forward path to match these measured characteristics (see Figure 30). However, the linear model was used for most of the control law synthesis since linear techniques were employed. An attempt was made to allow adequate phase margins to cover the non-linear effects.

Control Laws

Figures 31 through 34 are Bode plots and block diagrams that summarize the control laws developed for this task using the methods discussed above. For clarity, washout filters are not included in the Bode plots. The aileron control law for the semispan model involved several adjustments from theoretically derived parameters. The gain was reduced because large surface deflections were predicted in gusts. The lead time constant was increased because of lower than

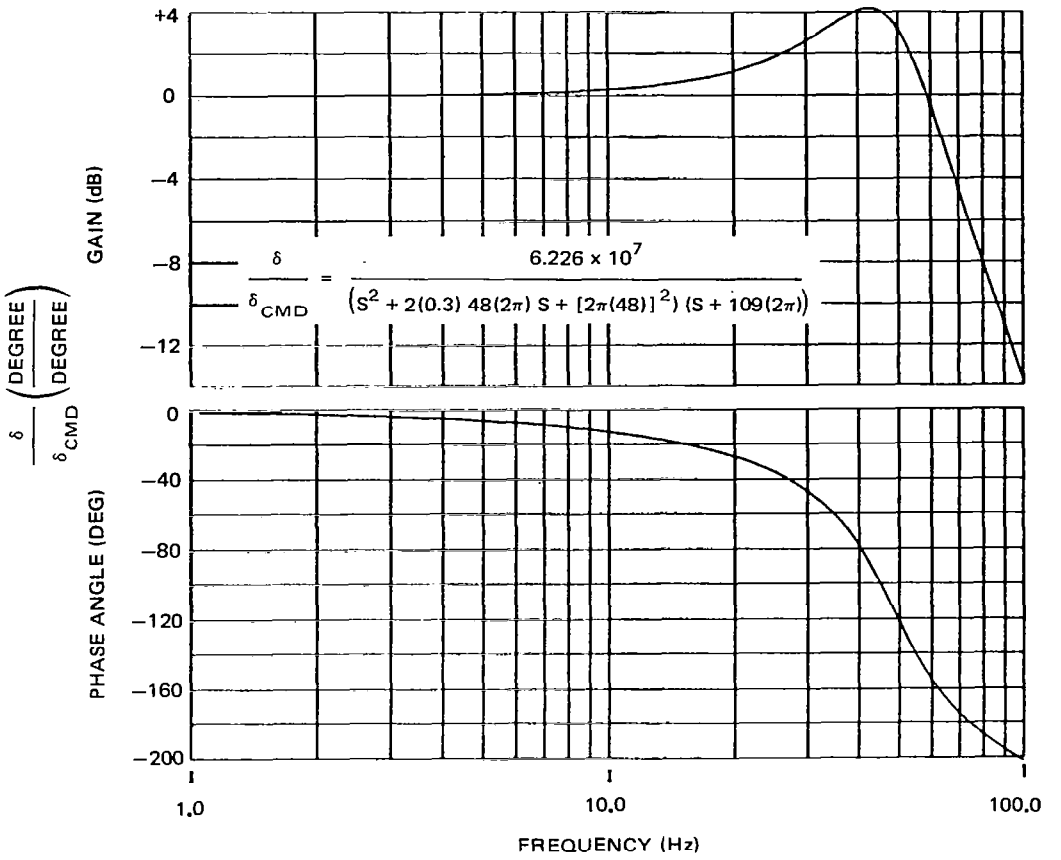

FIGURE 29. ACTUATOR RESPONSE APPROXIMATION WITH LINEAR CURVE FIT

predicted damping for the primary 12 Hz flutter mode. An additional gain reduction adjustment was made experimentally because of inadequate high-frequency margins. The calculated gust PSD response for this control law is shown in Figure 35 and indicates a 26 percent reduction of the outboard bending moment PSD. A 20 percent increase in the flutter speed was provided by this control law. Increasing the flutter margin beyond this was complicated by a secondary flutter mode with a frequency near 25 Hz.

Alternative control laws for the semispan model, generated by NASA personnel using aerodynamic energy (NASA CL 1) and optimal control methods (NASA CL 2), are presented in Bode and block diagram form in Figures 36 and 37. These methods are described in Reference 2. A discussion of these control laws and wind tunnel results can be found in References 3 and 4.

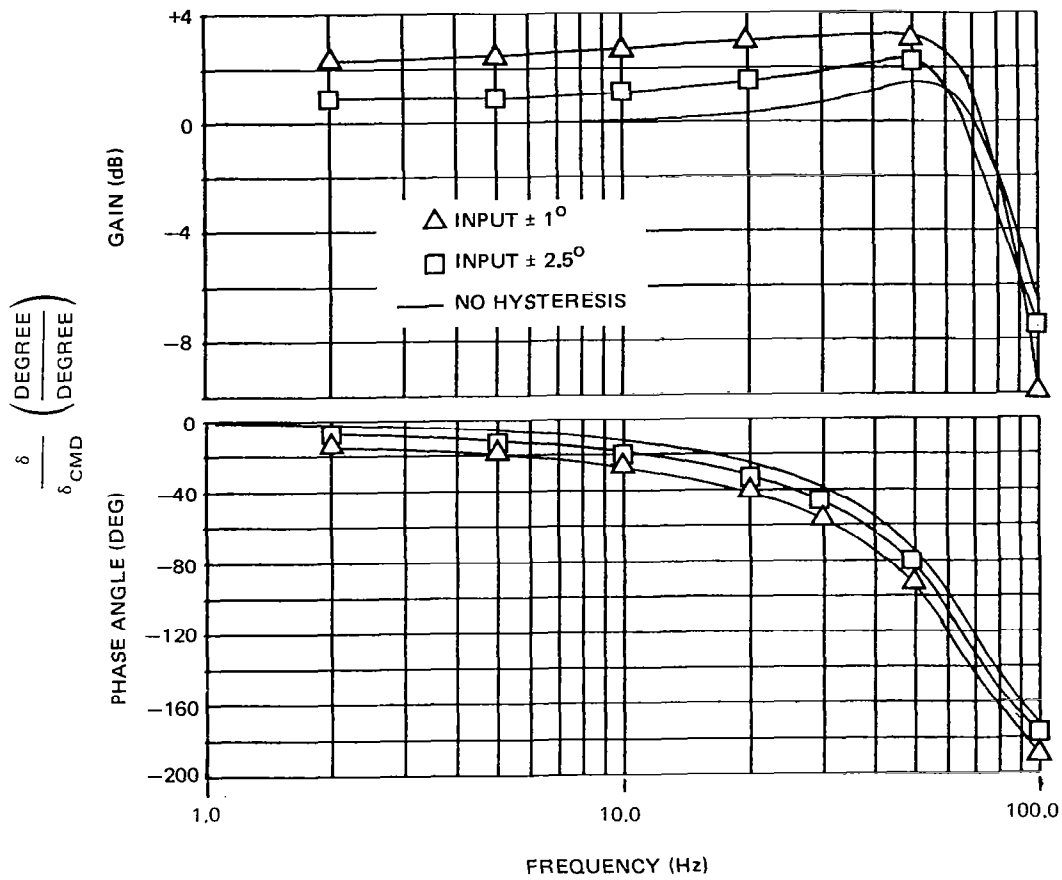

FIGURE 30. ACTUATOR RESPONSE APPROXIMATION WITH NONLINEAR CURVE FIT

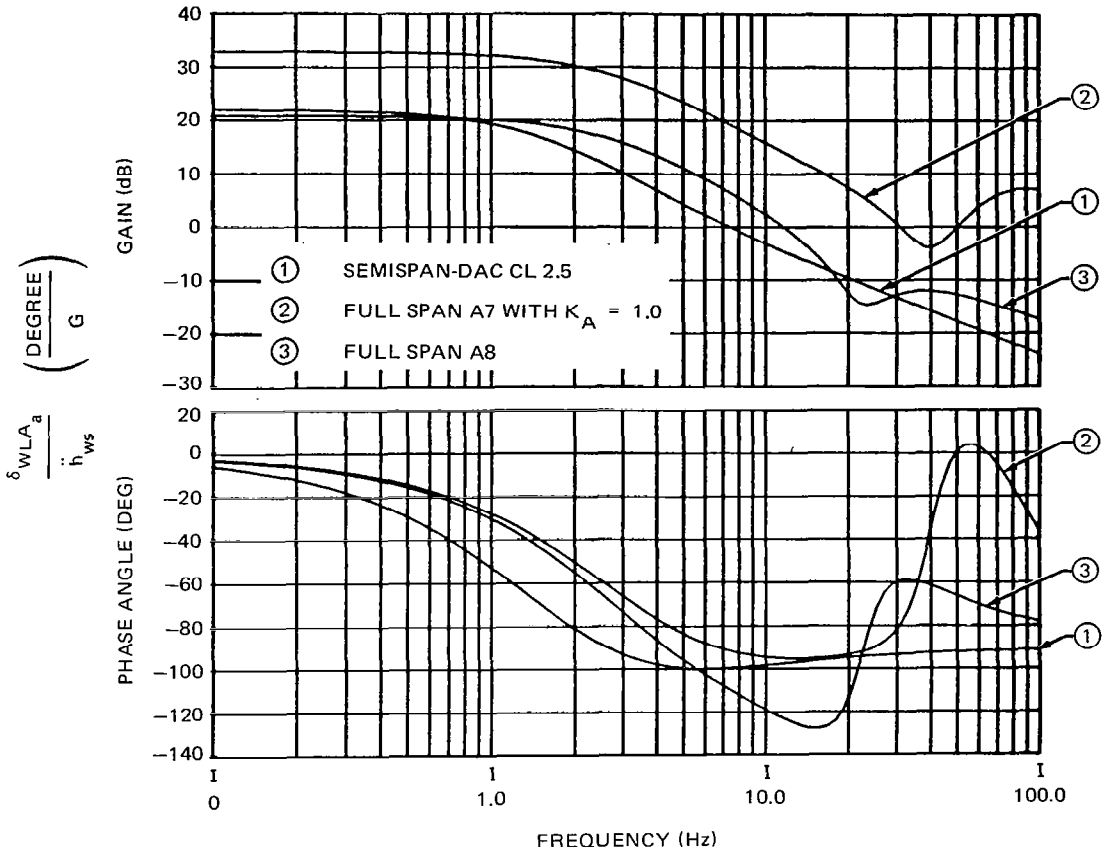

FIGURE 31. BODE DIAGRAM OF AILERON CONTROL LAW FILTERS

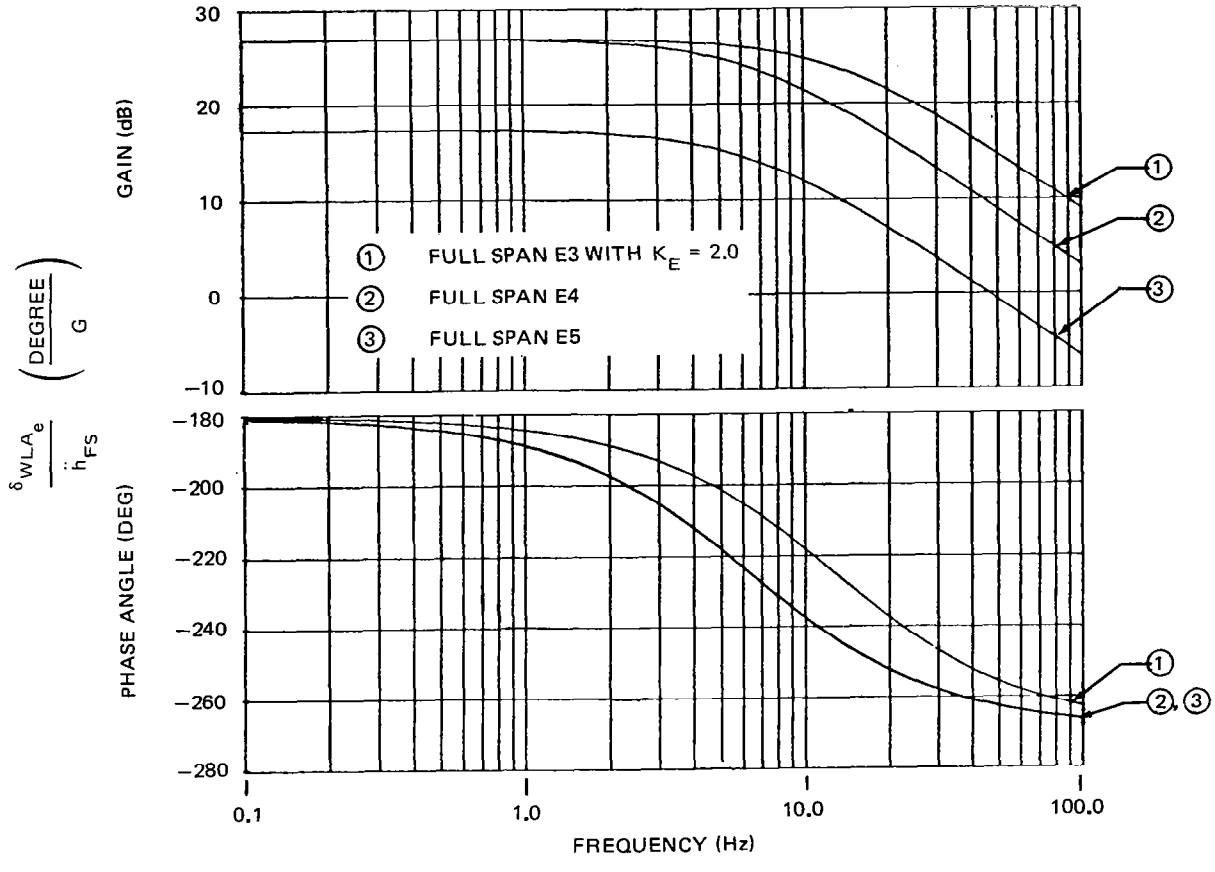

FIGURE 32. BODE DIAGRAM OF ELEVATOR CONTROL LAW FILTERS

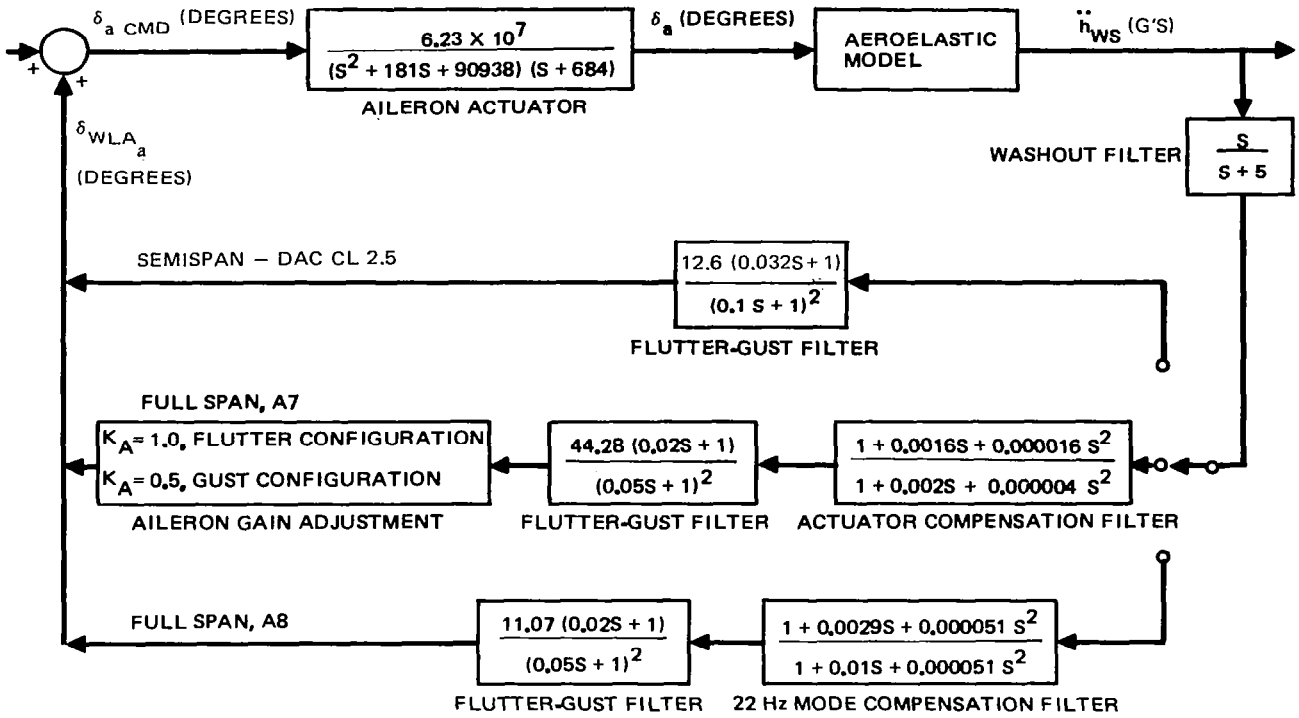

FIGURE 33. BLOCK DIAGRAM OF AILERON CONTROL LAWS

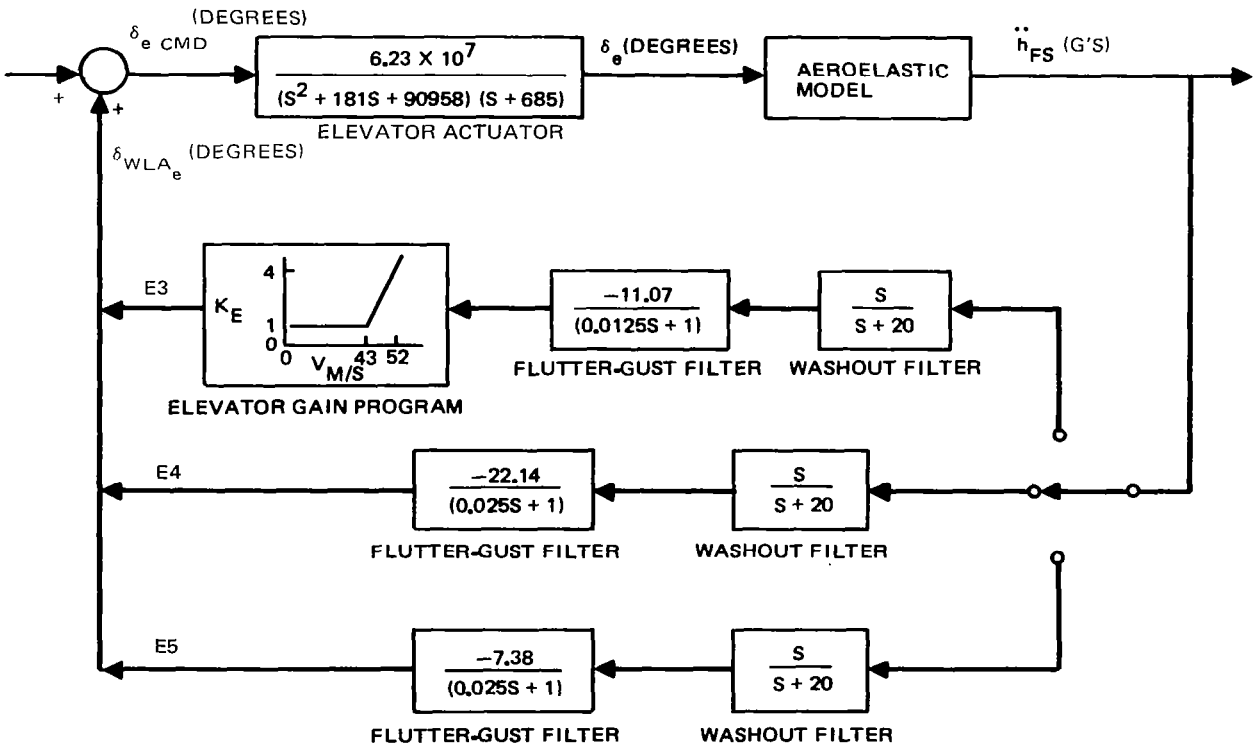

FIGURE 34. BLOCK DIAGRAM OF ELEVATOR CONTROL LAWS

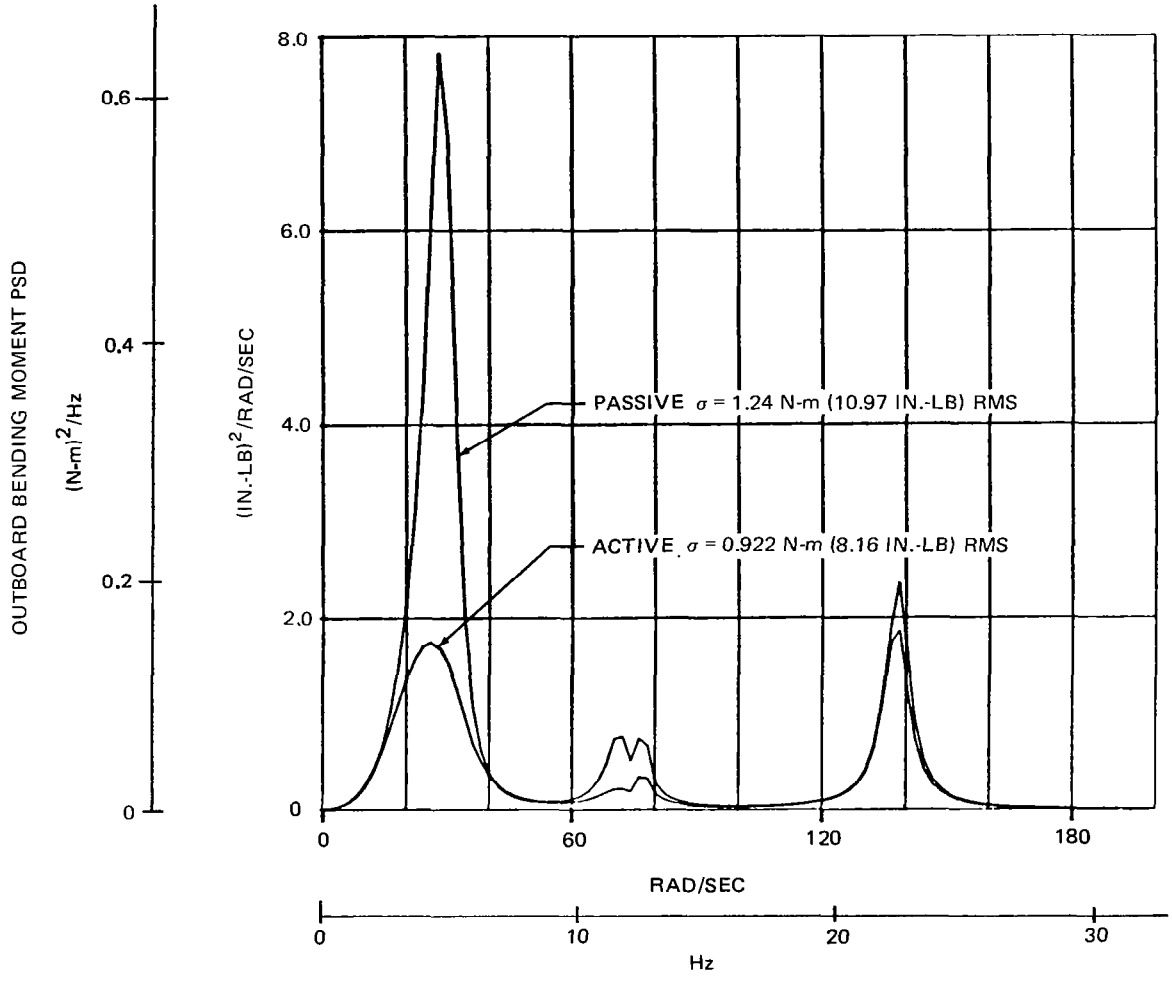

FIGURE 35. SEMISPAN OUTBOARD WING BENDING MOMENT PSD WITH THE TURBULENCE BANNER INSTALLED IN THE DOUGLAS WIND TUNNEL

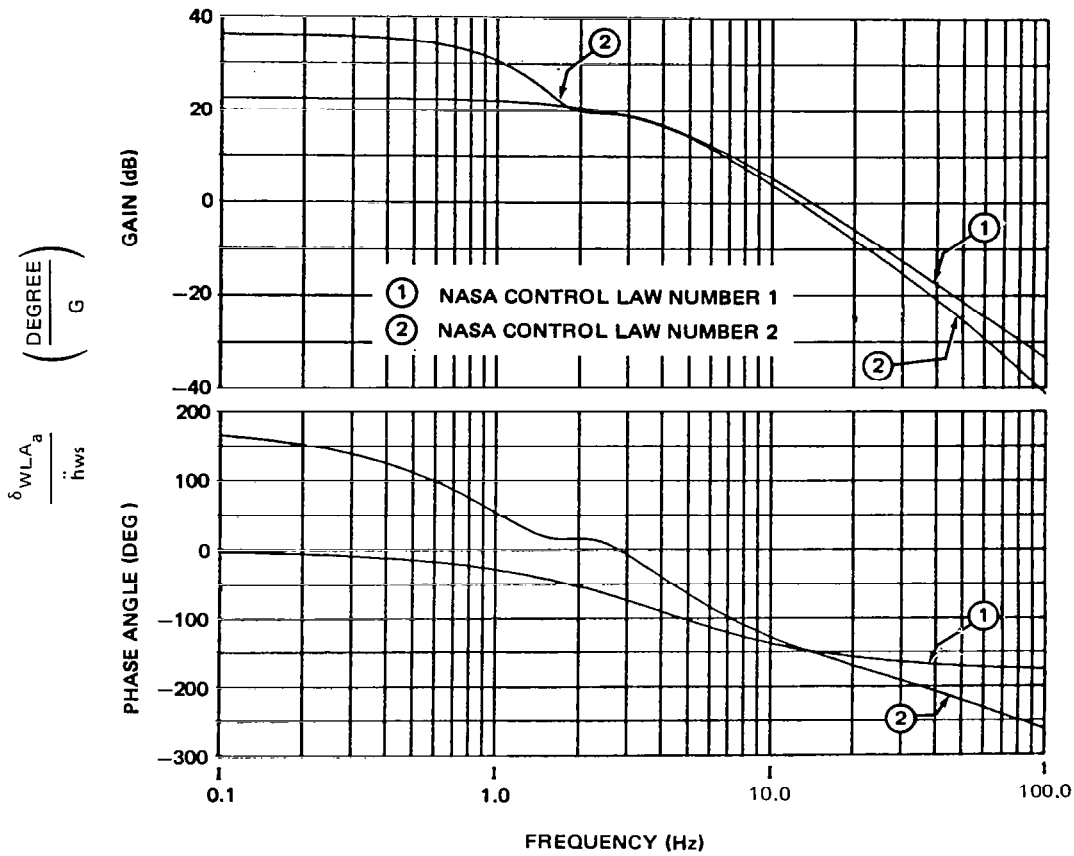

FIGURE 36. BODE DIAGRAMS OF ALTERNATE (NASA) CONTROL LAWS FOR THE SEMISPAN MODEL

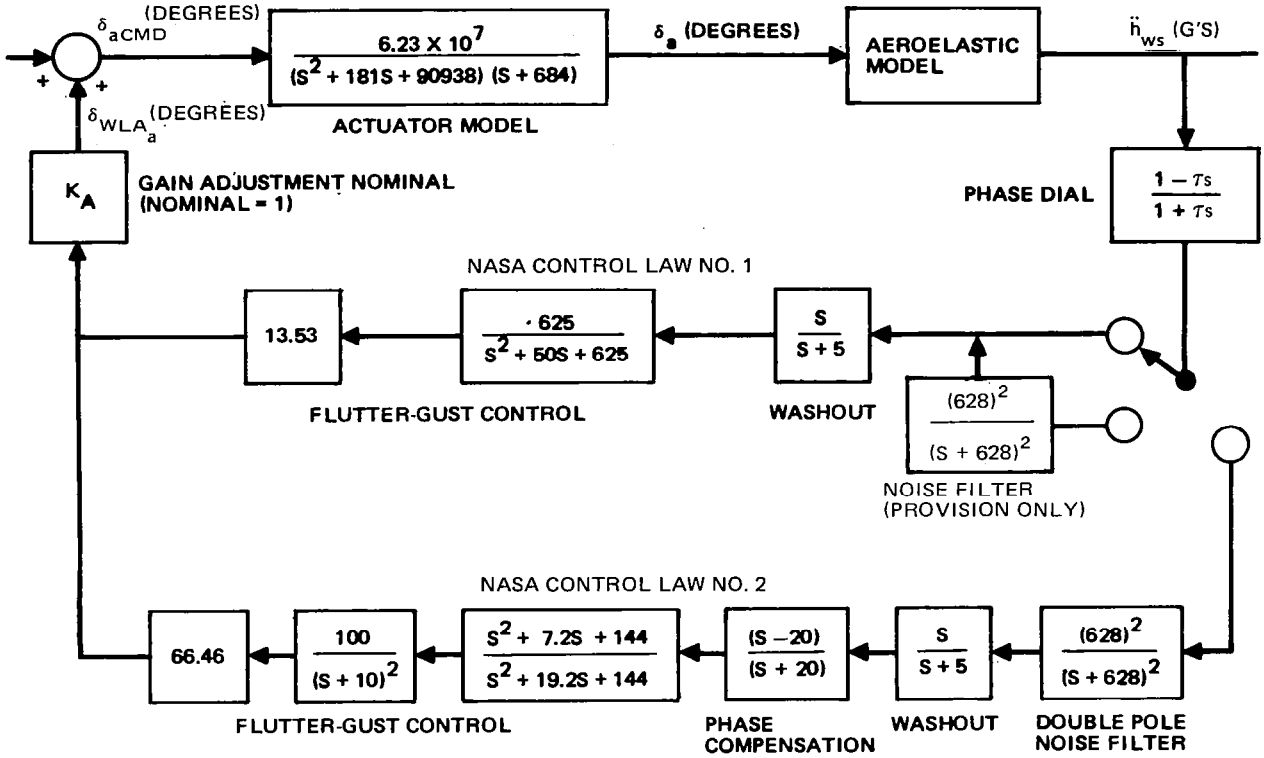

FIGURE 37. BLOCK DIAGRAMS OF ALTERNATE (NASA) CONTROL LAWS FOR THE SEMISPAN MODEL

For the full-span model, a notch filter was developed in an attempt to delay the occurrence of the 25 Hz mode instability. In addition, a lower gain was used than that which would provide the desired damping for the 12 Hz mode in order to improve the margins at the critical 25 Hz mode. This control law (A8) was not too different in other respects than that used for the semispan model. A flutter analysis using this control law together with elevator control law E5 verified the desired performance and predicted a 20 percent increase in flutter speed.

In synthesizing the aileron flutter suppression control law for the full-span model configuration with tip weights, several problems occurred that were not present for the semispan model. The 12 Hz flutter mode crossed the zero damping axis at a steep slope. At 20 percent above the flutter speed the damping ratio was −0.16, requiring a high gain for stabilization. The control law labeled A7 on Figure 31 shows this increased gain. As a consequence of this increased gain at high frequencies, an instability involving the actuator mode occurred above 40 Hz. Figure 38 illustrates this, showing a Nyquist plot of the aileron loop with the third order linear actuator model. It shows the passive flutter mode at 13.5 Hz and the actuator mode at 43.5 Hz both unstable. This plot was generated from the truncated, linearized equations of motion. Even though eight flexible modes are included in these equations, the highest frequency present is only 21 Hz so that the model characteristics at the actuator mode of 43.5 Hz are in doubt. Figure 39 is a replot of these characteristics using the structures tabular data, which include all of the model modes and unsteady aerodynamic effects, instead of the linear equations. The structures tabular data are available in the computer data bank together with the linearized equations.

AILERON CONTROL LAW (A7) WITHOUT ACTUATOR COMPENSATION
52 m/s (101 KNOTS), 10% FUEL

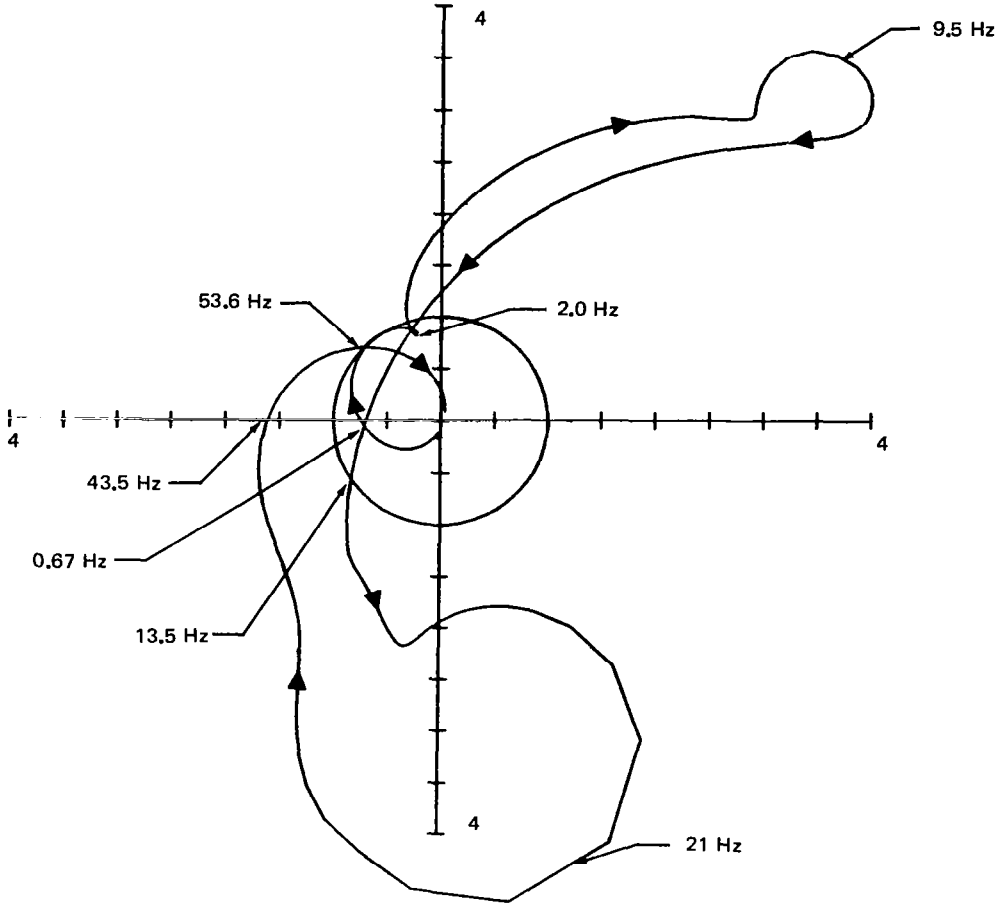

FIGURE 38. NYQUIST PLOT CALCULATED FROM ANALYTICAL DATA

AILERON CONTROL LAW (A7) WITHOUT ACTUATOR COMPENSATION
52 m/s (101 KNOTS), 10% FUEL

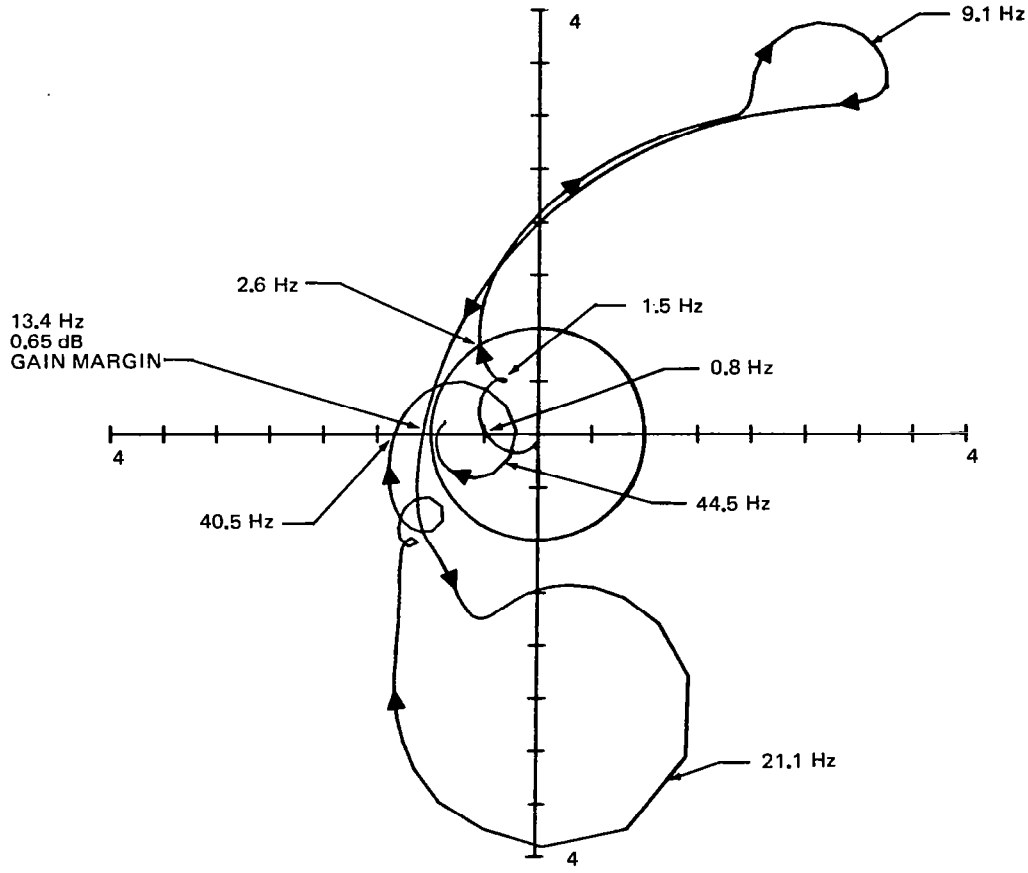

FIGURE 39. NYQUIST PLOT CALCULATED FROM TABULAR DATA

Note that the actuator instability still exists, but the flutter is now slightly stable. Because of such differences, which appear insignificant on a Bode plot with a log scale, final results were checked with plotted tabular data to confirm the linear system analysis. The check resulted in good agreement between control law synthesis calculations and analytical flutter analysis. Figure 39 verifies that a high-frequency instability was present and associated with the actuator mode. A second order lead-lag compensation filter was developed to stabilize this mode. This filter was included in the Bode plot of the aileron control law A7 in Figure 31. Figure 40 is a Nyquist plot of A7 with the compensation filter and with the elevator control law E4, using the plotted tabular model data. The plot is for a speed 20 percent above the passive flutter speed and predicts the flutter mode to be slightly stable (0.52 dB gain margin) and the actuator compensation filter to stabilize the high frequency modes.

AILERON CONTROL LAW (A7) AND ELEVATOR CONTROL LAW (E4)
52 m/s (101 KNOTS) 10% FUEL

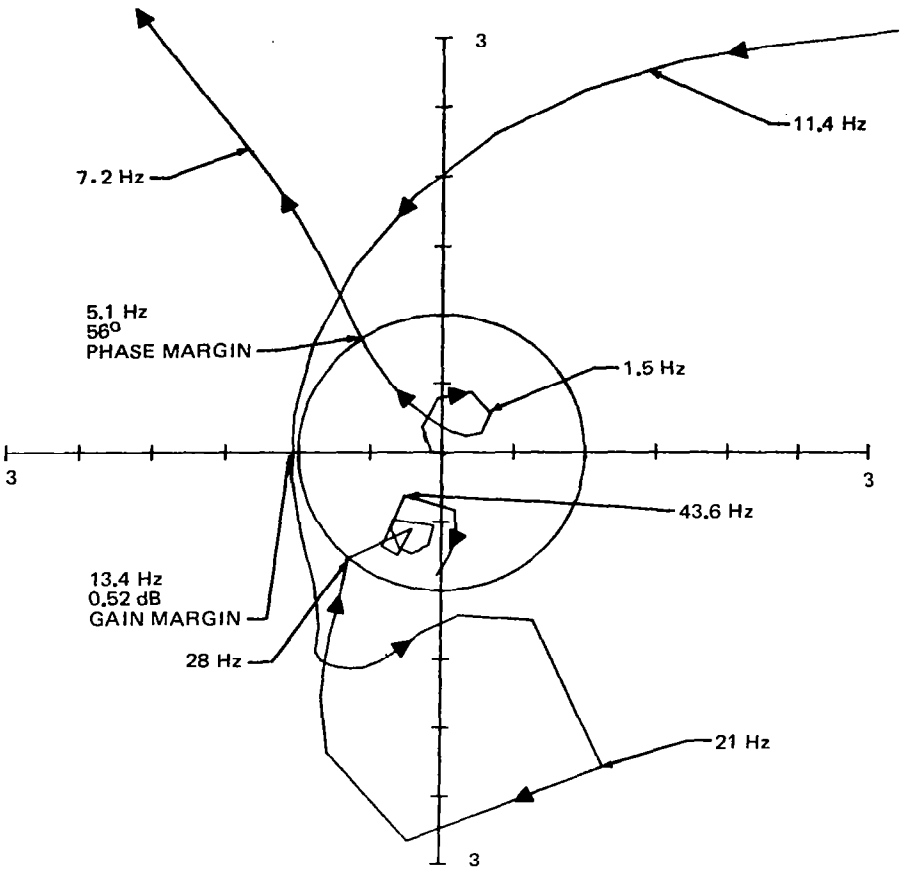

FIGURE 40. NYQUIST PLOT CALCULATED FROM TABULAR DATA

In order to create the Nyquist plot of Figure 40, it was necessary to compute the required coupling numerator from the plotted data. The system block diagram with a fuselage accelerometer, with output h_{FS}, feeding back to the elevator, added to the same aileron loop is:

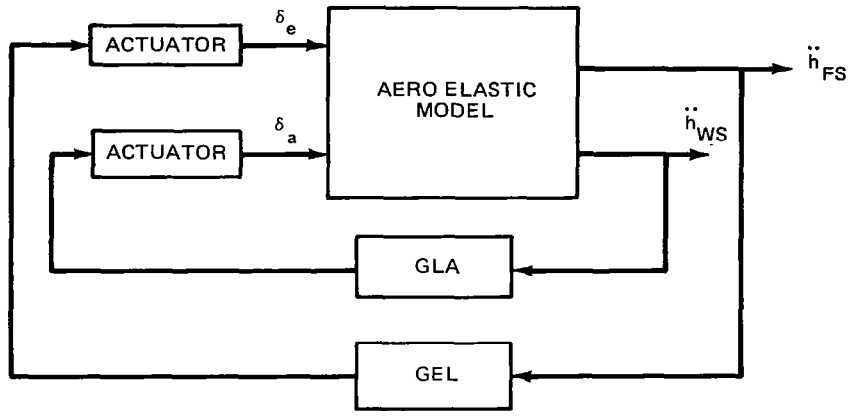

The corresponding open-loop transfer function is (neglecting actuator dynamics for simplicity)

$$\frac{(GLA)\, N_{\delta_a}^{\ddot{h}_{ws}}}{\Delta} + \frac{(GEL)\, N_{\delta_e}^{\ddot{h}_{fs}}}{\Delta} + \frac{(GLA)\,(GEL)\, N_{\delta_a}^{\ddot{h}_{ws}}\, {}_{\delta_e}^{\ddot{h}_{fs}}}{\Delta}$$

The data bank included plotted tabular data for all of the uncoupled transfer functions. With the program now able to cascade and add tabular data, the coupling transfer function can also be calculated, since

$$\frac{N_{\delta_a}^{\ddot{h}_{ws}}\, {}_{\delta_e}^{\ddot{h}_{fs}}}{\Delta} = \left(\frac{N_{\delta_a}^{\ddot{h}_{ws}}}{\Delta}\right)\left(\frac{N_{\delta_e}^{\ddot{h}_{fs}}}{\Delta}\right) - \left(\frac{N_{\delta_e}^{\ddot{h}_{ws}}}{\Delta}\right)\left(\frac{N_{\delta_a}^{\ddot{h}_{fs}}}{\Delta}\right)$$

An additional elevator control law, E3, was shown in Figure 32. This control law was developed before the methods of using the tabular data described above were utilized. Control law E3 resulted in a 5 Hz instability in the flutter analysis. Elevator control law E4 was developed using these tabular methods and, as shown in Figure 40 a phase margin of 56 degrees existed. This critical closed loop mode in the elevator loop was a combination of the short period (1.5 Hz) and fuselage first bending (11 Hz) open-loop modes.

Although the two configurations of the full-span model had different flutter characteristics, the gust response of the gust critical configuration (which involved the low-frequency modes and a heavy wing condition, 100 percent fuel) was not greatly changed. Figure 41 is the gust PSD for the full span model with and without the elevator loop active. A substantial reduction in the outboard bending moment PSD is shown with either control law.

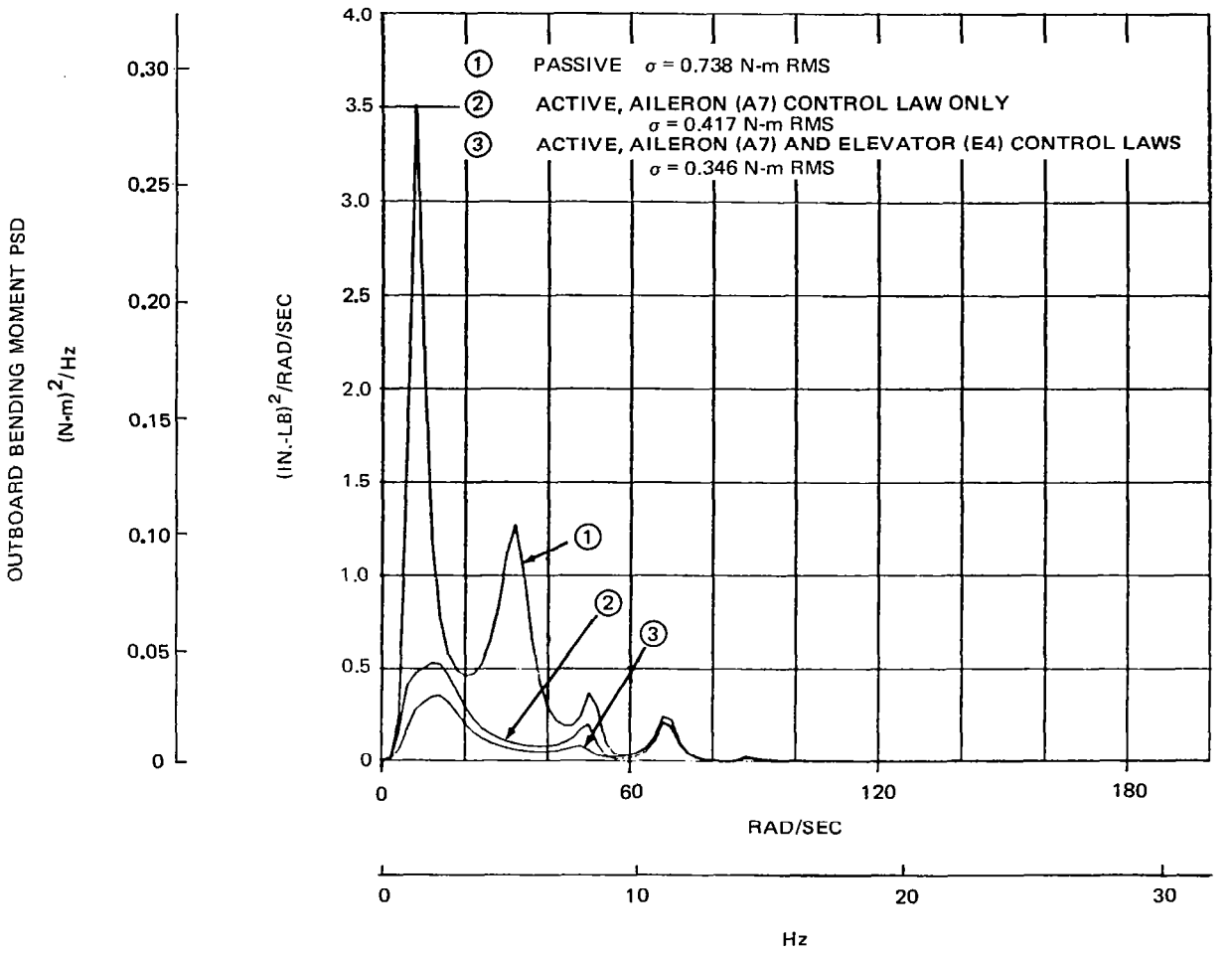

FIGURE 41. FULL SPAN MODEL OUTBOARD WING BENDING MOMENT PSD WITH THE TURBULENCE BANNER INSTALLED IN THE NORTHROP WIND TUNNEL

WIND TUNNEL TESTING AND ANALYSES

The results of the wind tunnel tests of the semispan and full span models are discussed in the order of testing. Three semispan tests and one full-span test were performed during the program. The first semispan test was performed using a Douglas control law, DAC CL 2.5. The second semispan test used alternate control laws, NASA CL 1 and NASA CL 2, developed by NASA Langley personnel. The third semispan test used both the Douglas and NASA control laws.

Semispan Flutter Tests

Prior to each tunnel test, zero-speed stability of the closed-loop system was checked by plucking the wing tip. For the DAC CL 2.5 at 140 percent of the design loop gain, this excitation initiated a zero-speed instability involving the 42.2 Hz wing torsion mode. This instability, illustrated in Figure 42, also occurred at some increased gain in the other tested flutter suppression control laws. Prevention using filter compensation is possible but may not be practical without degrading system performance. The zero-speed instability did not inhibit testing as the 42.2 Hz mode was stabilized by wind-on aerodynamic damping.

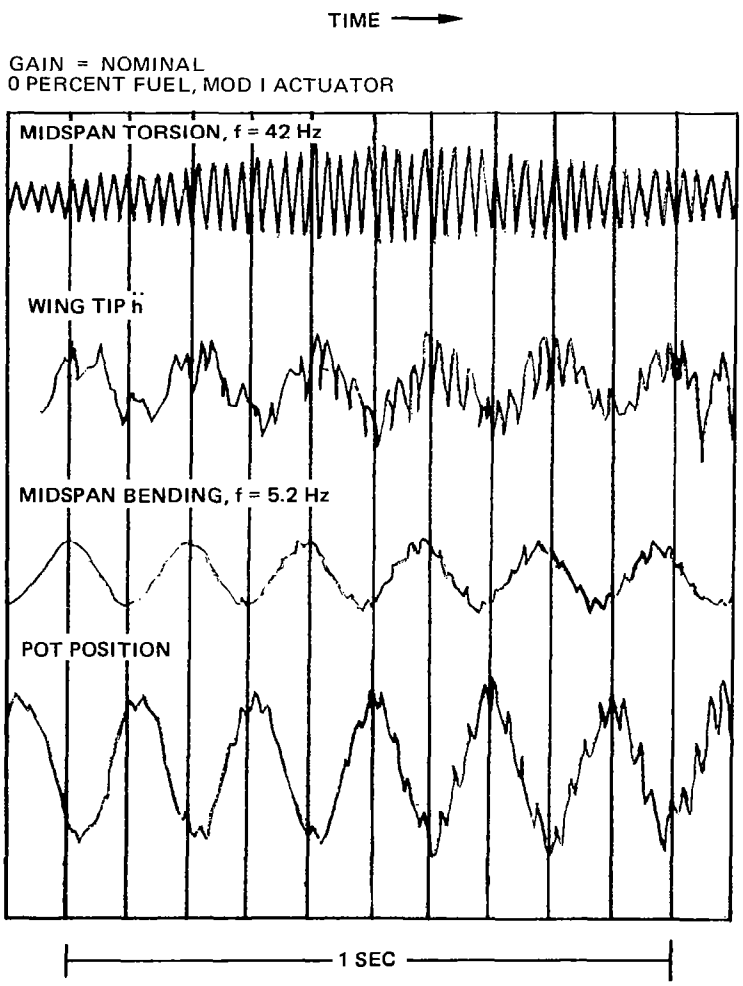

FIGURE 42. OSCILLOGRAPH TRACE OF ZERO-SPEED, 42 Hz AILERON INSTABILITY – SEMISPAN MODEL WITH NASA CL 1

Results of the semispan flutter tests, using DAC CL 2.5 at design gain, are shown in Figures 43 through 46 with analytical results plotted for comparison. Analytical results are in reasonable agreement with the test results. Any discrepancies may be accounted for by the aerodynamic and structural model representations, particularly the assumed value for structural damping. Sensitivity of the 12 Hz flutter mode to structural damping was shown by a test in which damping material was added to the pylon strut to increase the structural damping of the engine-pitch-wing mode from 0.01 to 0.014. The passive flutter speed increased from 47.8 m/s (93 KEAS) to 49.9 m/s (97 KEAS).

Flutter speed is a function of fuel quantity for both the open- and closed-loop cases, as shown in Figure 44. At the flutter-critical 10 percent fuel point, there is an improvement in the flutter speed due to the active control system. This increase is about 19 percent. For the intermediate off-design fuel levels the control law slightly degrades the flutter speed.

The flutter characteristics of the zero-fuel condition were measured for control law gain and phase variations. The results for gain changes are shown in Figure 45. At increased gain values the third wing-bending mode was driven unstable at speeds less than the passive flutter speed. The phase is referenced to 12 Hz (the frequency of the critical flutter mode).

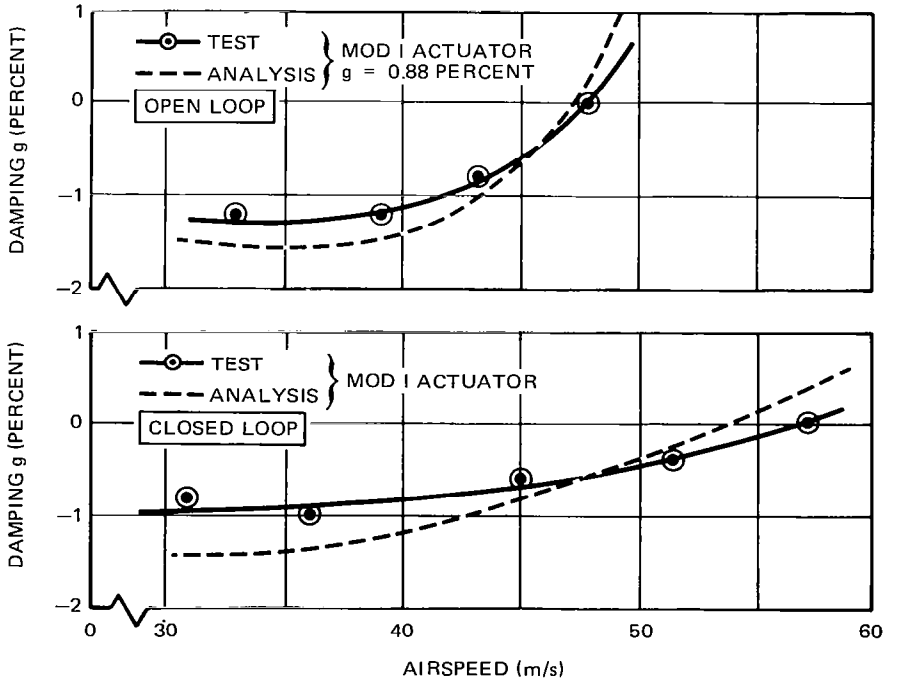

FIGURE 43. OPEN AND CLOSED LOOP SEMISPAN FLUTTER CHARACTERISTICS FOR THE ZERO FUEL CONFIGURATION, DAC CL 2.5

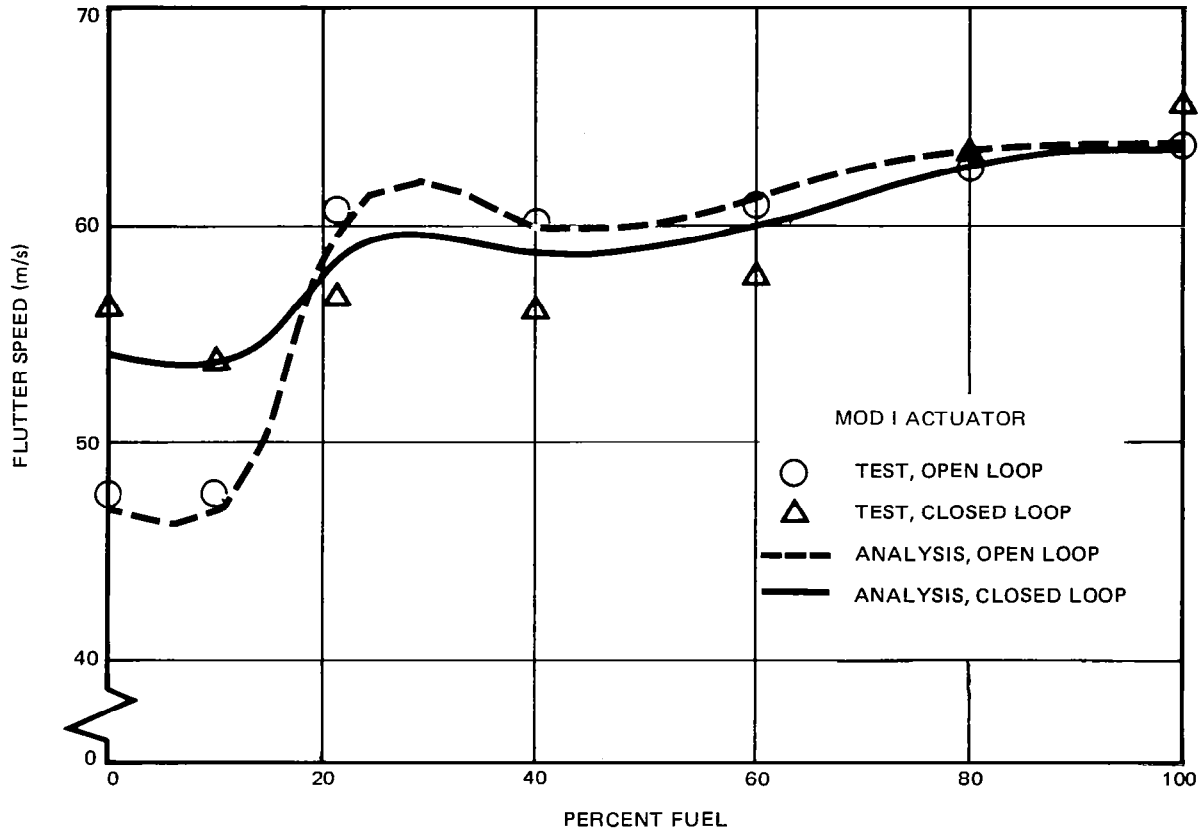

FIGURE 44. SEMISPAN MODEL FLUTTER SPEED VERSUS PERCENT FUEL, DAC CL 2.5

The results of tests conducted on the semispan model using control laws developed at NASA Langley are shown by plots of flutter speed versus gain (Figure 47) and structural damping versus flutter speed (Figures 48 through 53). Again, these results show the sensitivity of flutter speed to the zero-speed damping. For this reason, the zero-speed damping was measured prior to each tunnel run. For these tests, the maximum speed tested was 60.5 m/s (117 KEAS). Above that speed the higher frequency outer panel mode (on which the control laws had no significant effect) became unstable.

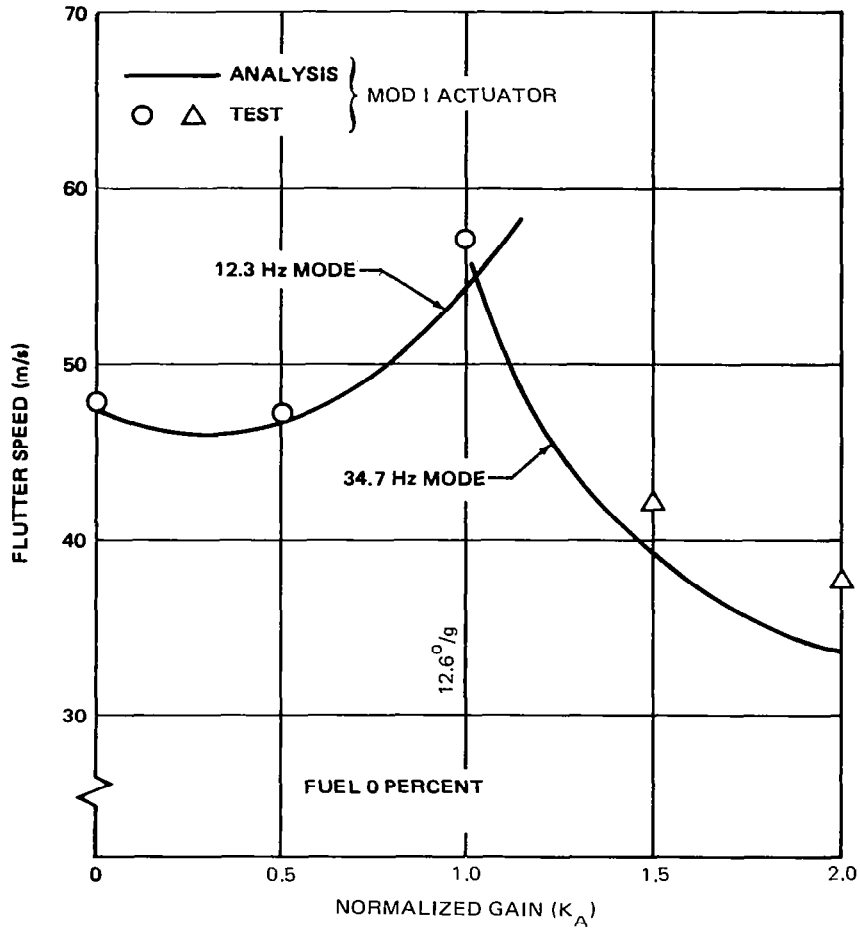

FIGURE 45. SEMISPAN MODEL FLUTTER SPEED VERSUS GAIN, DAC CL 2.5

During these tests it was discovered that results were not always repeatable. Also, a low frequency (4.26 Hz) filter instability occurred during the 30 degree phase lead check with NASA CL 2. Time histories of the open-loop actuator response at various frequencies indicated that the actuator was malfunctioning. Irregularities were most pronounced at small amplitudes. Time histories for the command signal and position potentiometer for the malfunctioning actuator are shown in Figures 54 and 55. As a result of the irregularities, the second test was terminated. The actuator improvement program, previously described, was then undertaken.

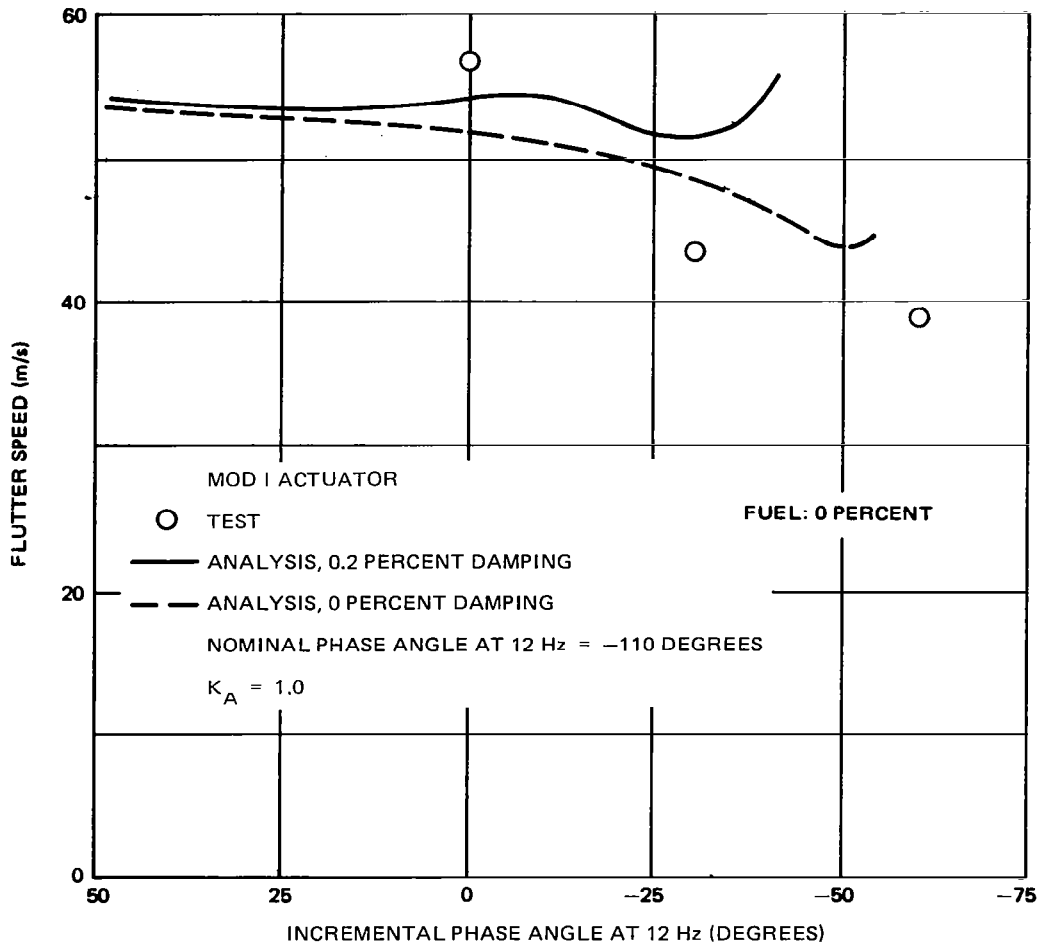

FIGURE 46. SEMISPAN MODEL FLUTTER SPEED VERSUS PHASE VARIATION, DAC CL 2.5

The third entry into the DLBWT completed the semispan model testing and verified the reliability of the actuator prior to full-span-model tests.

The results of the last semispan test are presented in Figures 56 through 58 along with comparisons with results of earlier tests. DAC 2.5 and NASA CL 1 were tested using the improved actuator, Mod II. Figure 56 is a plot of the flutter speed versus closed-loop gain using DAC CL 2.5. Flutter speed versus phase angle is also shown. The phase angle is referenced to the design phase of −110 degrees at 12 Hz; i.e., aileron position lags the control acceleration by 110 degrees. Note that the flutter speed with the closed-loop gain of $K_A = 1.25$ is 59.2 m/s (115 KEAS) or 24 percent greater than the passive flutter speed. The shift in the flutter speed from earlier tests was attributed to the Mod II actuator characteristics. Figure 57 presents the structural damping versus velocity of the passive and active cases and shows that test and analysis results are within 1 percent for the passive case and 2 percent for the active case.

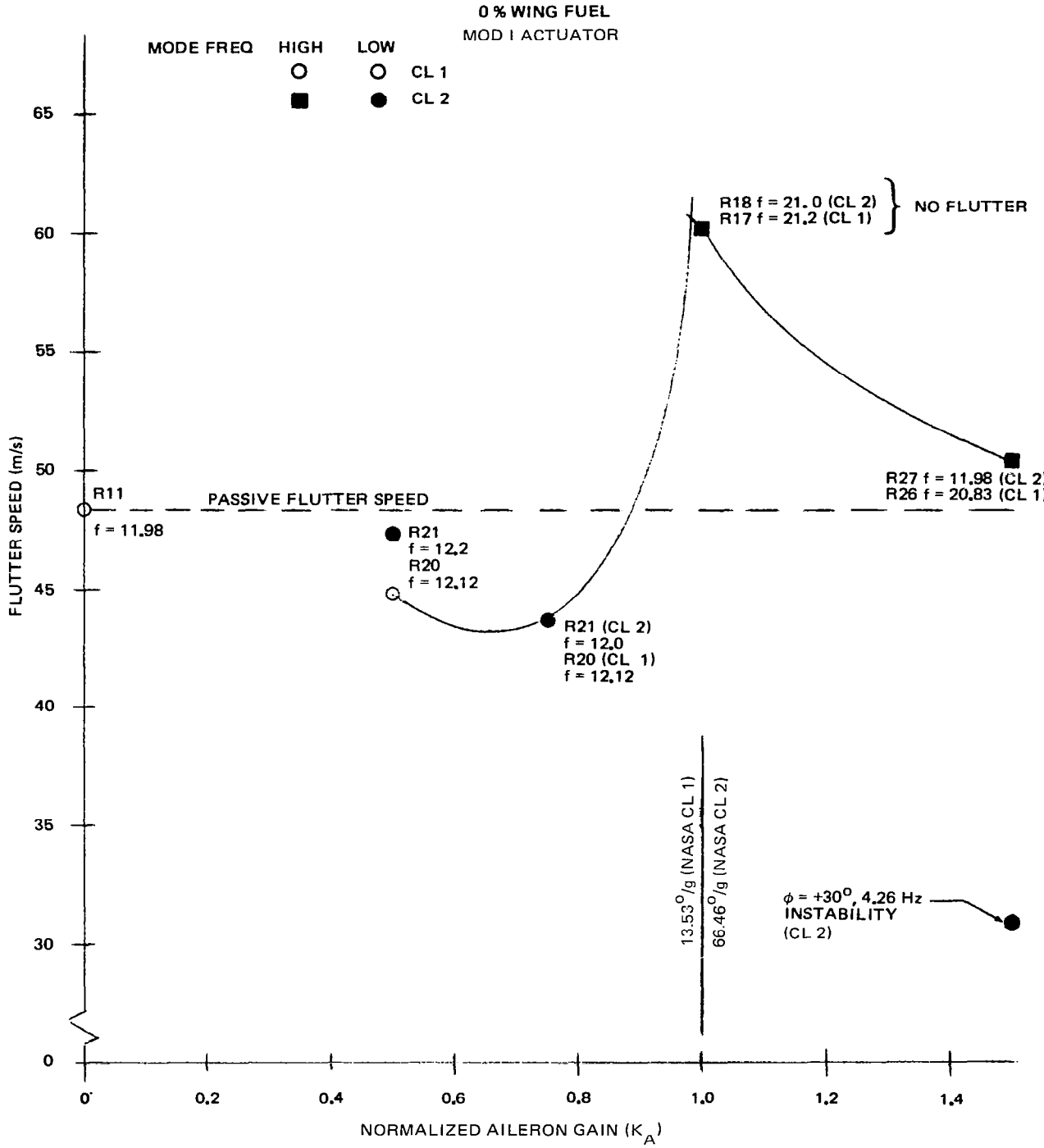

FIGURE 47. SEMISPAN MODEL FLUTTER SPEED VERSUS GAIN, COMPARISON OF NASA CL 1 AND CL 2

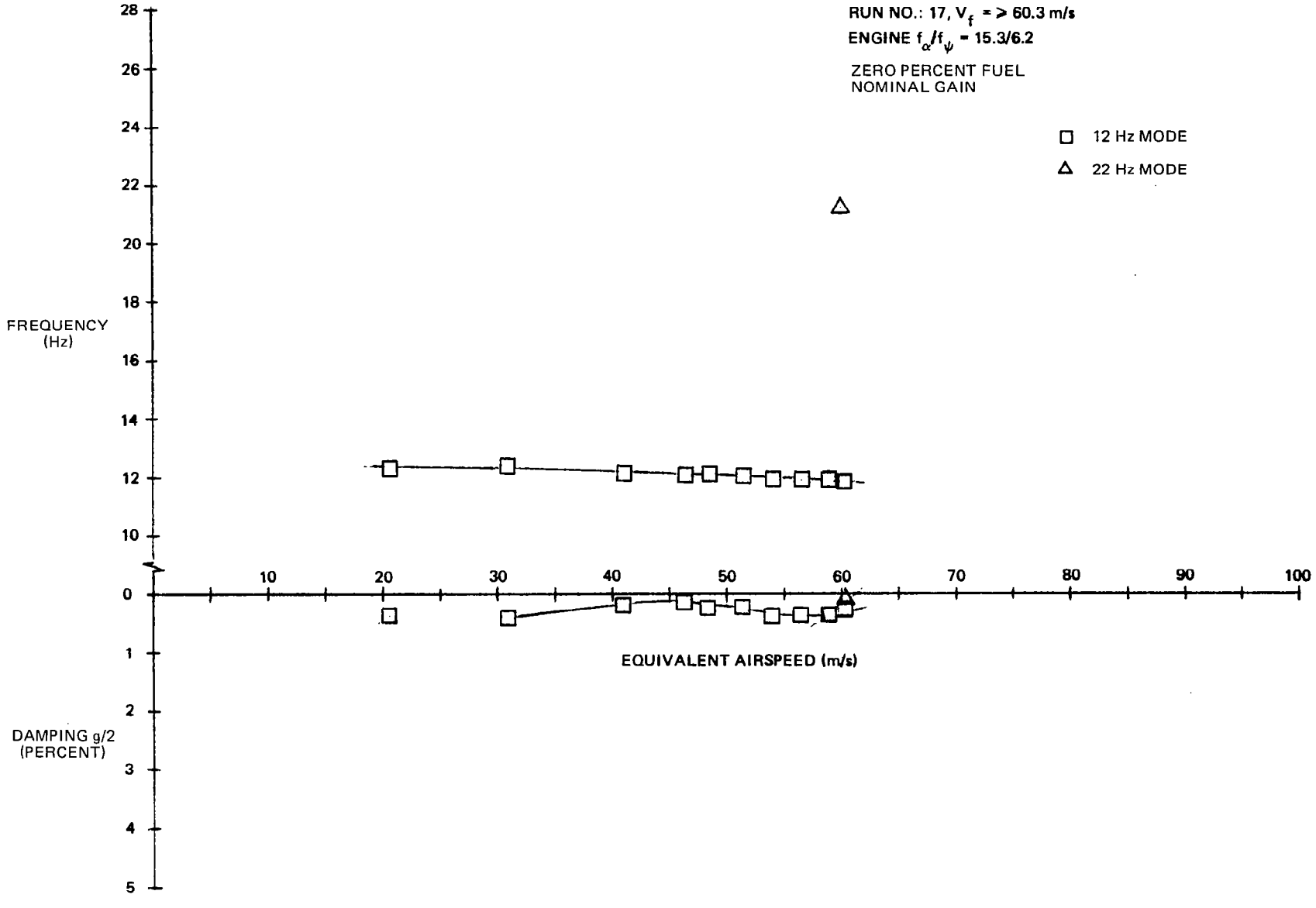

FIGURE 48. SEMISPAN FREQUENCY AND DAMPING FOR NASA CL 1

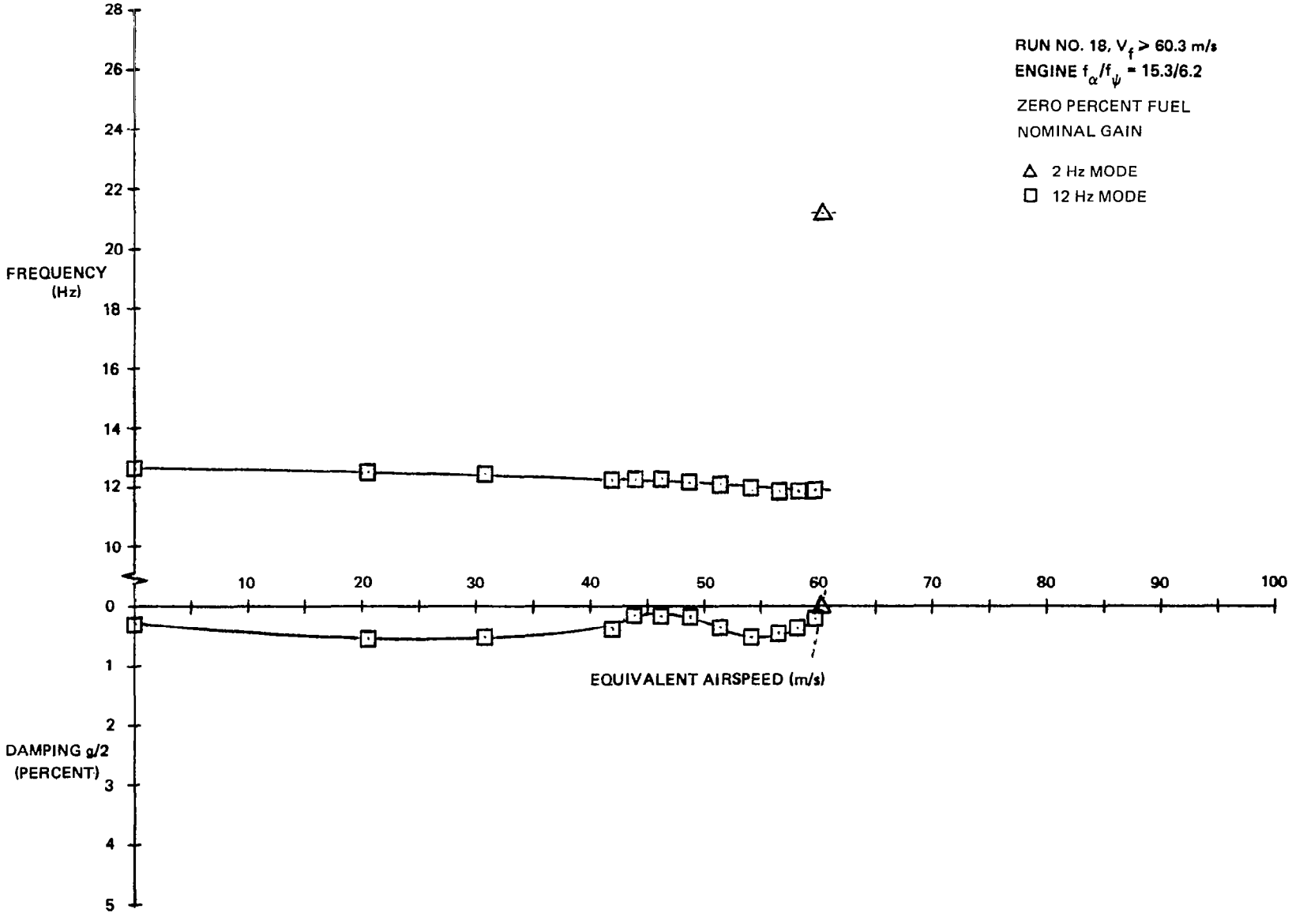

FIGURE 49. SEMISPAN FREQUENCY AND DAMPING FOR NASA CL 2

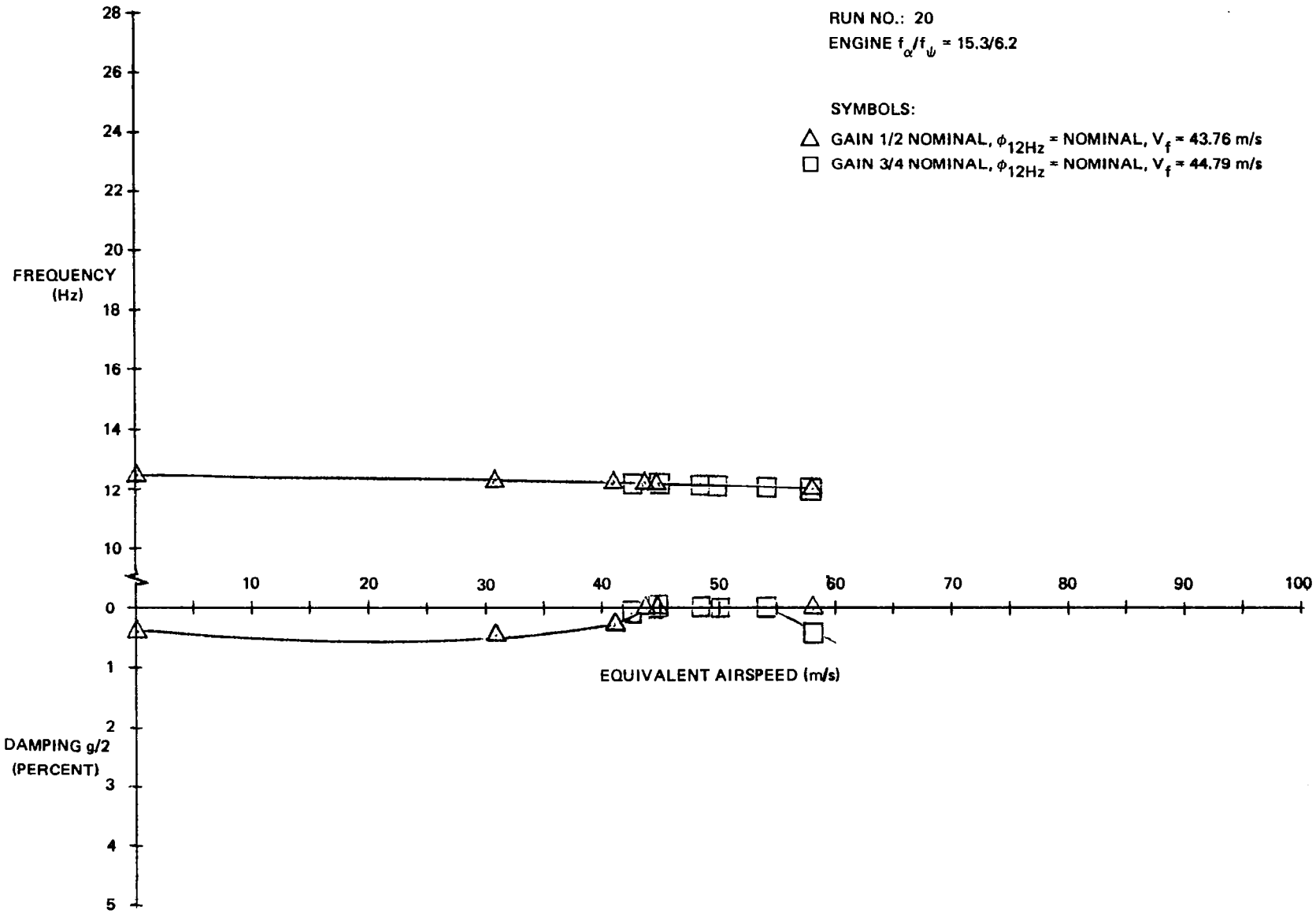

FIGURE 50. SEMISPAN FREQUENCY AND DAMPING FOR NASA CL 1 AT 1/2 AND 3/4 NOMINAL GAIN

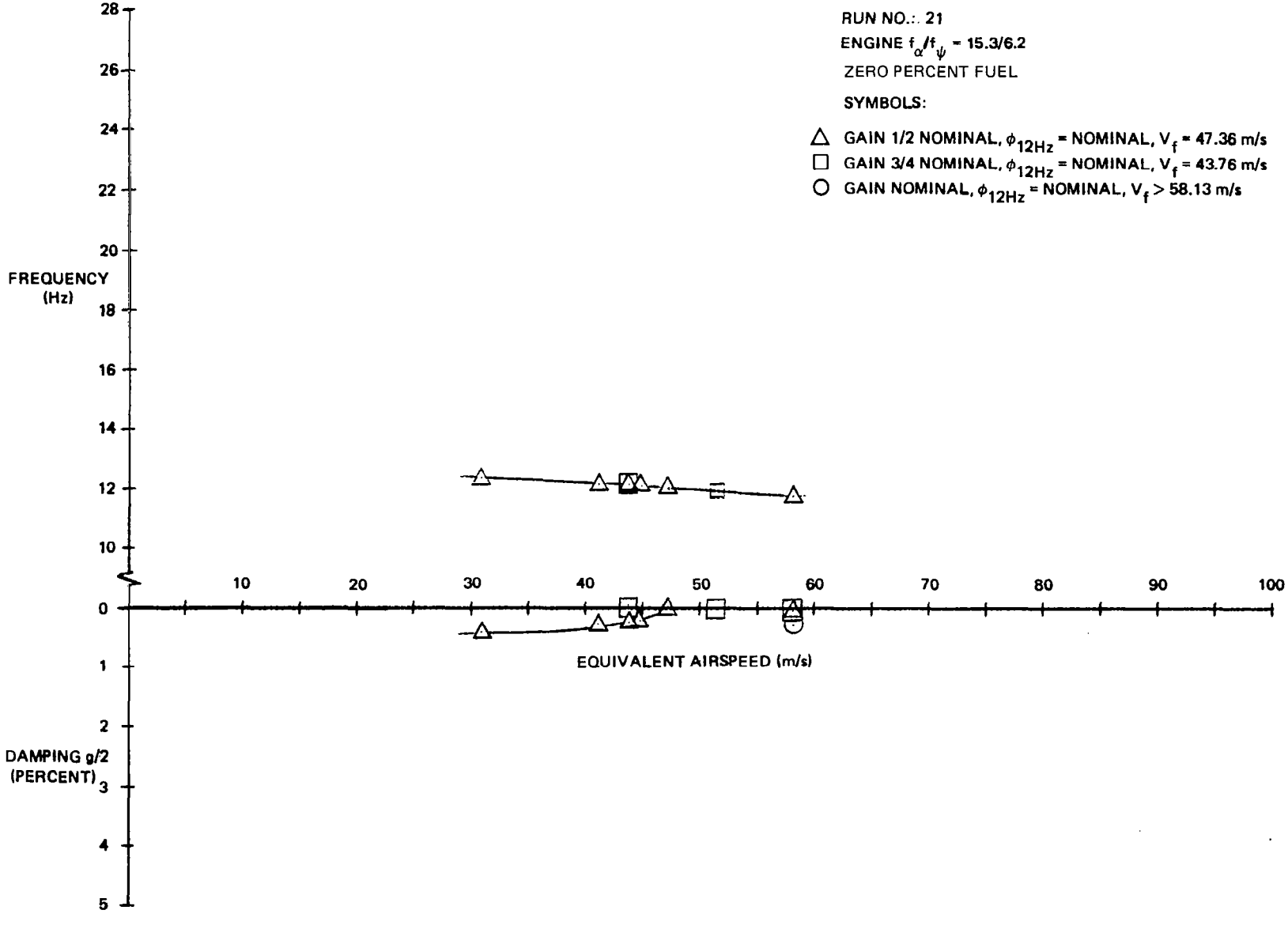

FIGURE 51. SEMISPAN FREQUENCY AND DAMPING FOR NASA CL 2 AT 1/2 AND 3/4 NOMINAL GAIN

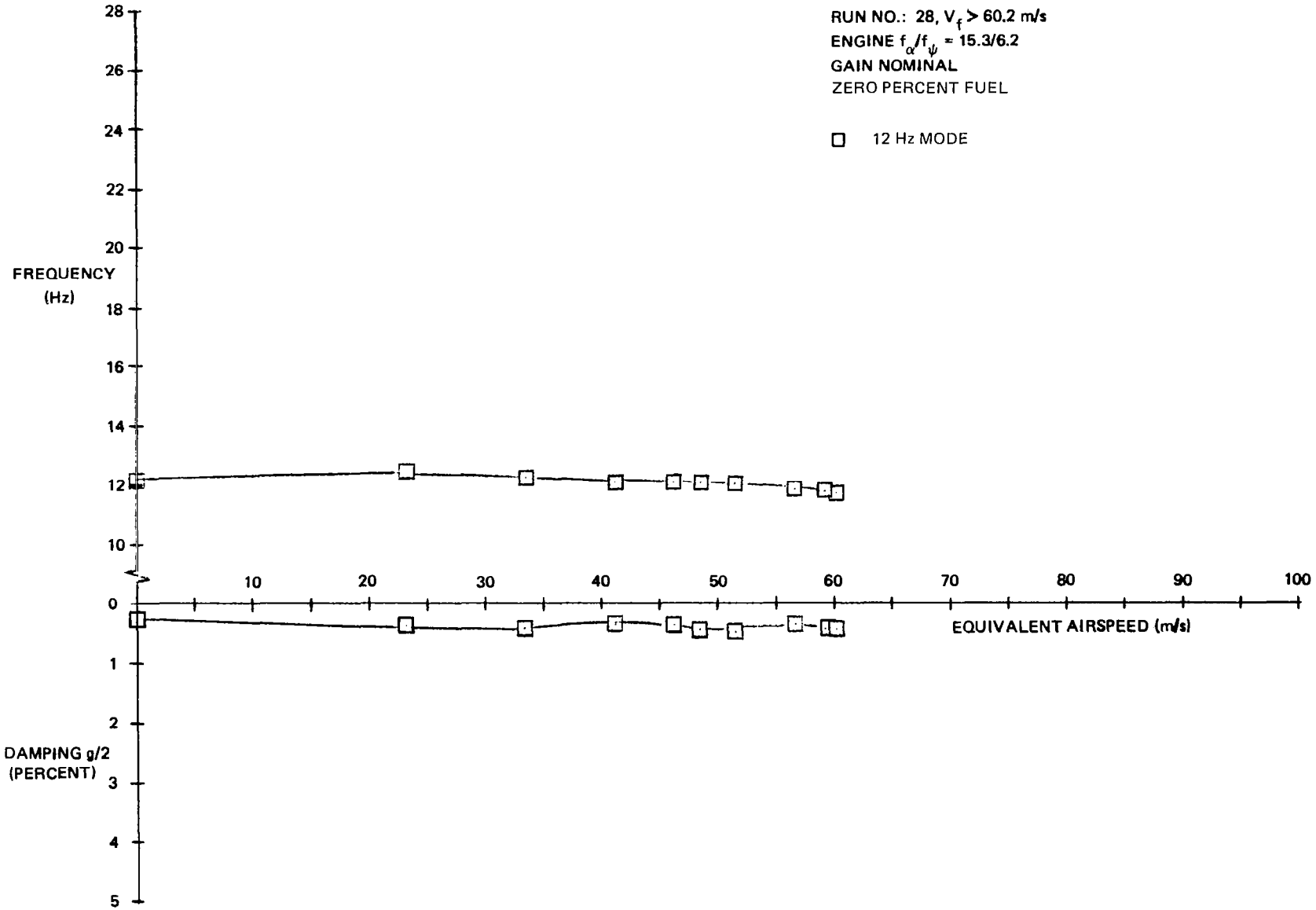

FIGURE 52. SEMISPAN FREQUENCY AND DAMPING FOR NASA CL 1 AT NOMINAL GAIN WITH A PHASE SHIFT AT 12 Hz OF +30 DEGREES

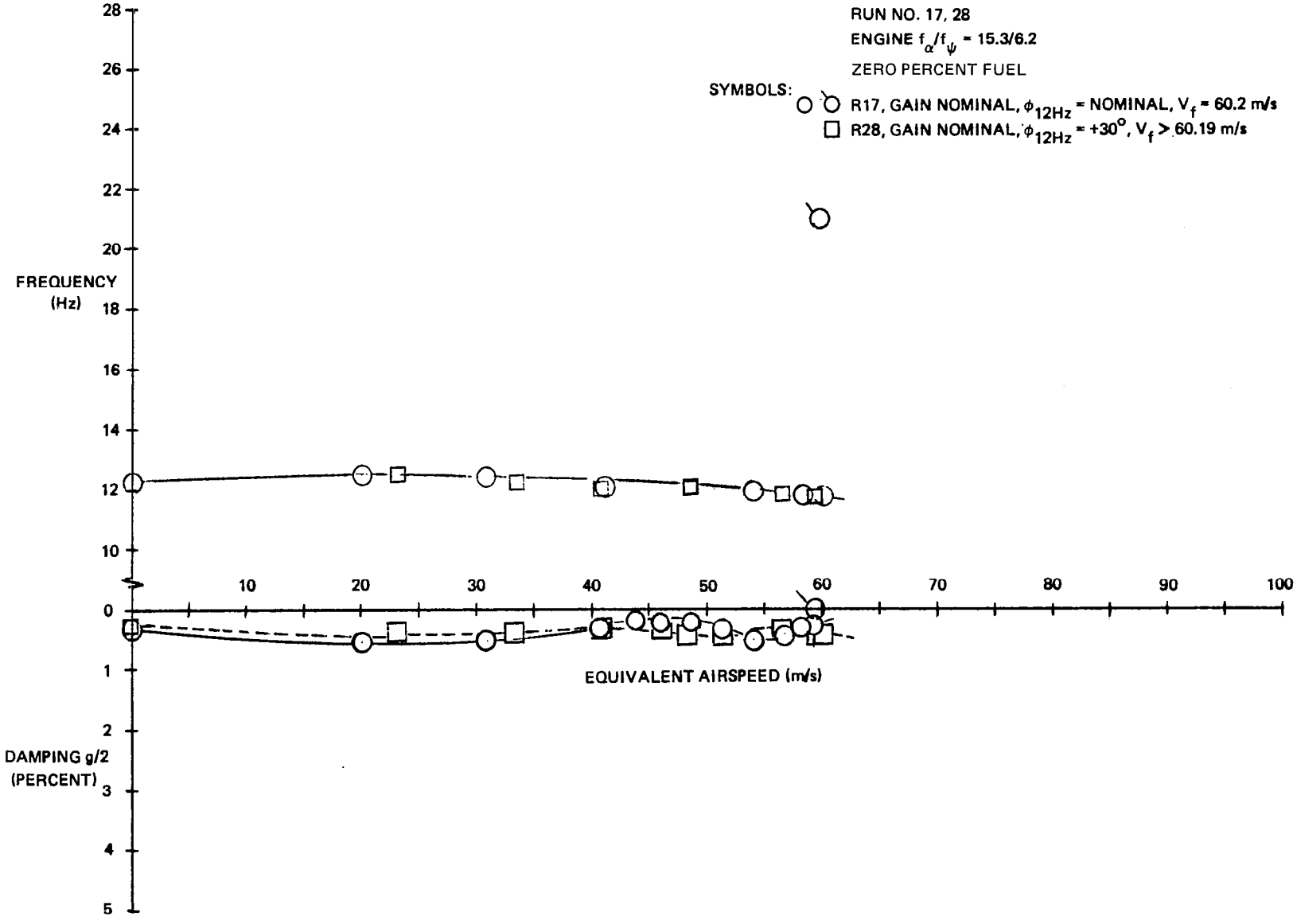

FIGURE 53. SEMISPAN FREQUENCY AND DAMPING FOR NASA CL 1 COMPARING NOMINAL PHASE AND A PHASE SHIFT OF +30 DEGREES AT 12 Hz

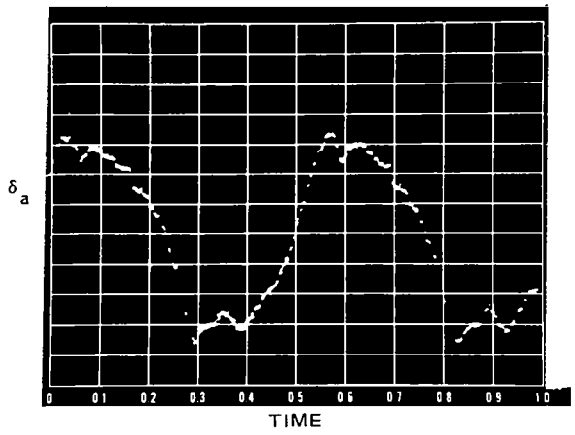

COMMAND SIGNAL δ_a = ± 1.5 DEG 4 Hz

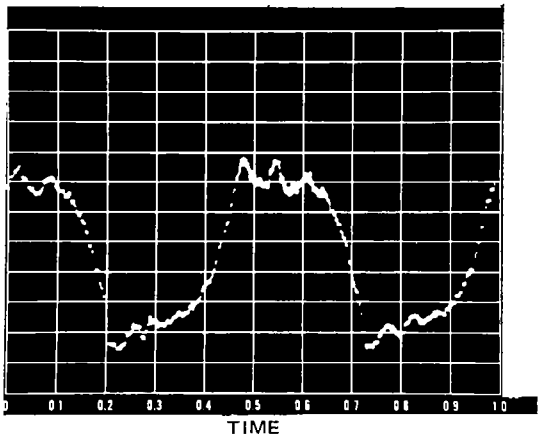

COMMAND SIGNAL δ_a = ± 5 DEG 4 Hz

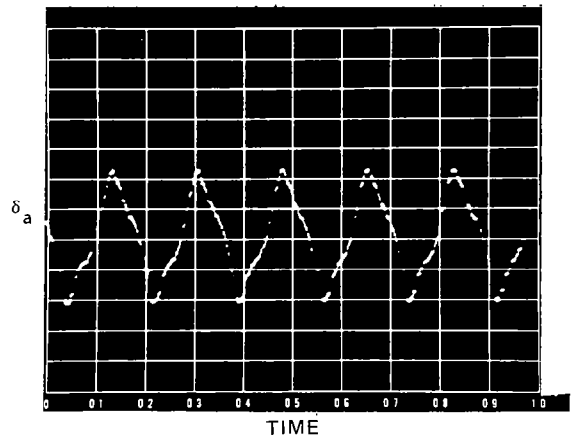

COMMAND SIGNAL δ_a = ± 1.5 DEG 12 Hz

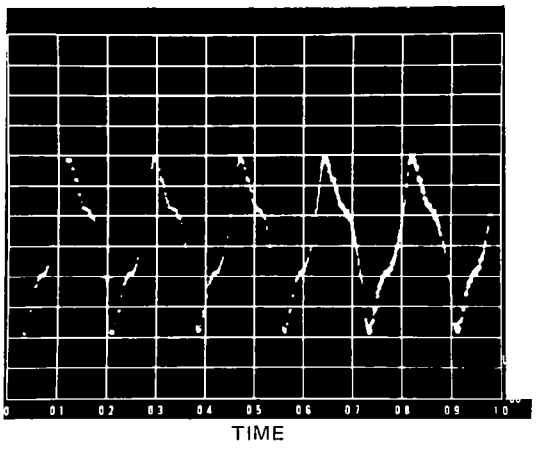

COMMAND SIGNAL δ_a = ± 5 DEG 12 Hz

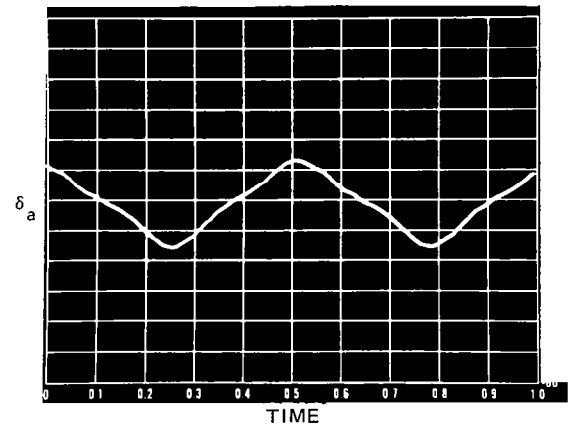

COMMAND SIGNAL δ_a = ± 5 DEG 20 Hz

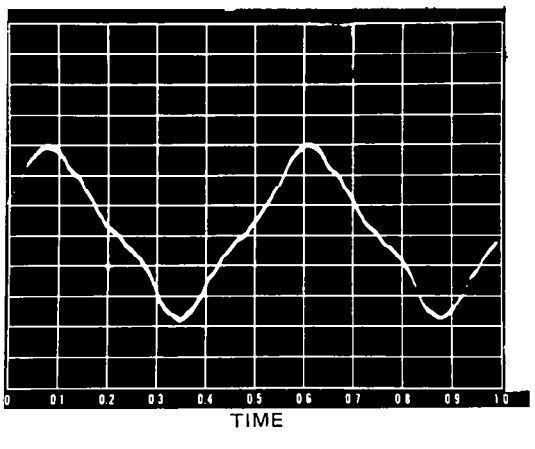

COMMAND SIGNAL δ_a = ± 1.5 DEG 20 Hz

FIGURE 54. ANALOG COMMAND SIGNAL VERSUS TIME

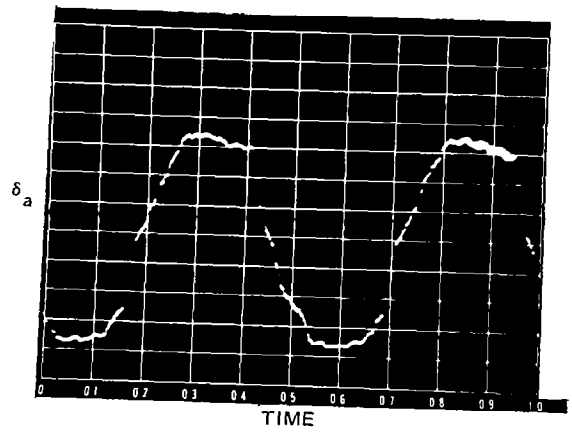

POT POSITION SIGNAL δ_a = ± 1.5 DEG 4 Hz

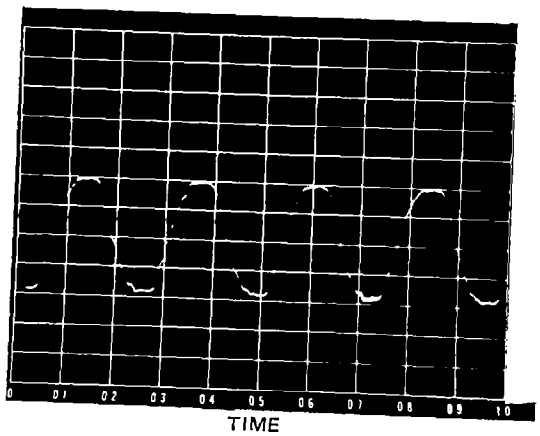

POT POSITION SIGNAL δ_a = ± 5 DEG 5 Hz

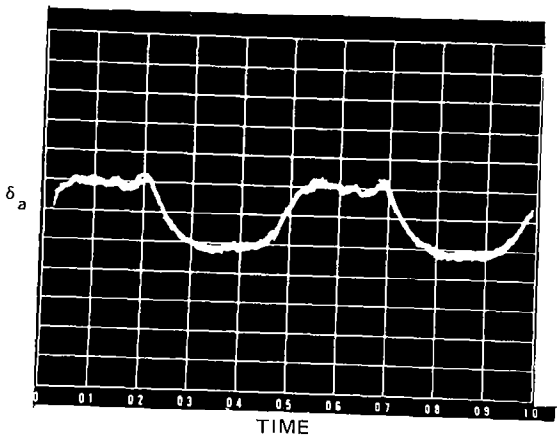

POT POSITION SIGNAL δ_a = ± 1.5 DEG 12 Hz

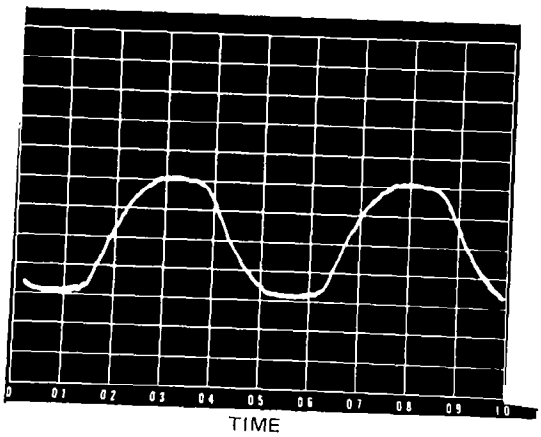

POT POSITION SIGNAL δ_a = ± 5 DEG 12 Hz

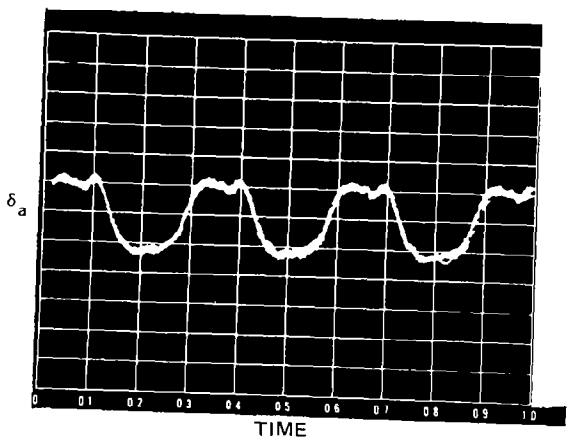

POT POSITION SIGNAL δ_a = ± 1.5 DEG 20 Hz

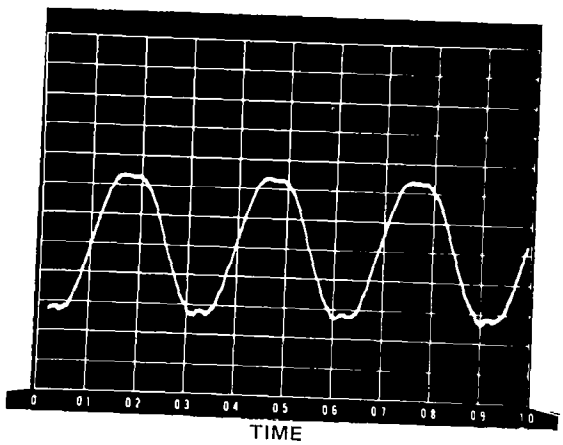

POT POSITION SIGNAL δ_a = ± 5 DEG 20 Hz

FIGURE 55. POT POSITION SIGNAL VERSUS TIME

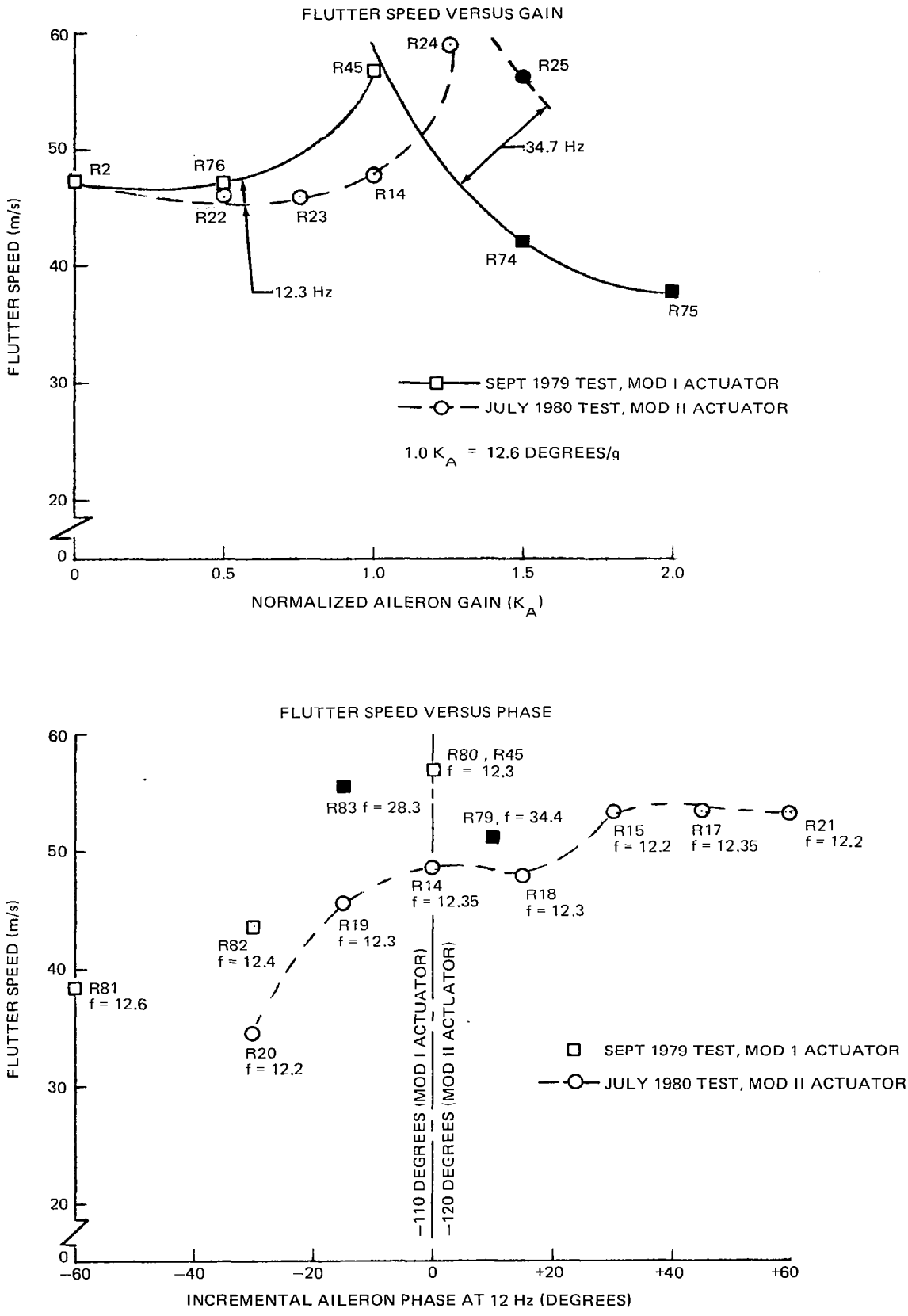

FIGURE 56. FLUTTER SPEED VERSUS GAIN AND PHASE FOR DAC C_L 2.5 – SEMISPAN MODEL

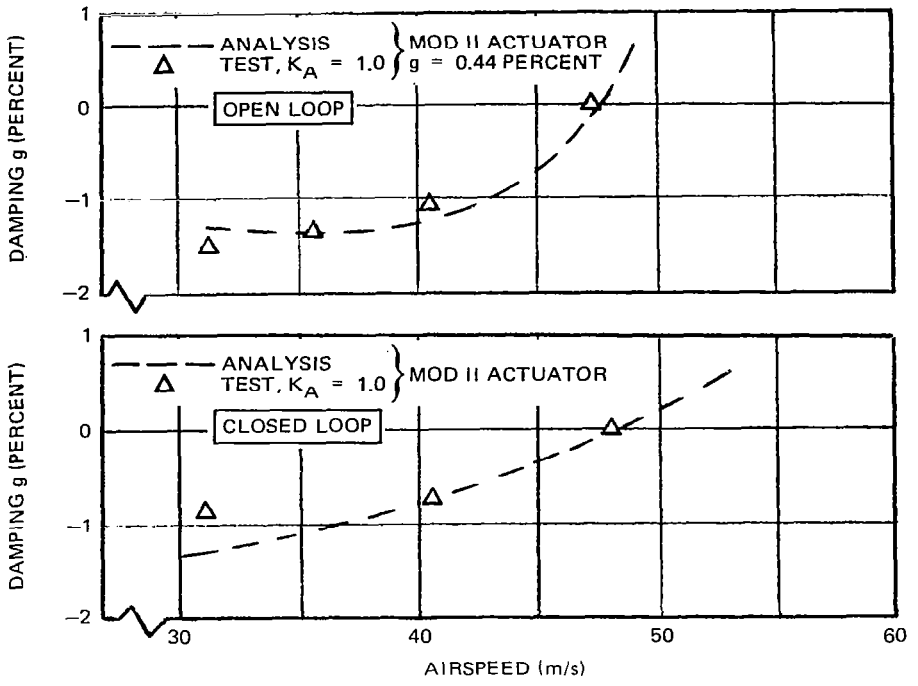

FIGURE 57. SEMISPAN MODEL DAMPING VERSUS VELOCITY – DAC CL 2.5

The results of gain and phase variations for the NASA CL 1 are shown in Figure 58. Here the test results show a flutter speed of 61.2 m/s (119 KEAS) or 28 percent over the passive speed. Tests were not carried out to higher speeds because of the presence of the high-frequency mode.

Semispan Transfer Functions

Static tests consisted of measuring the static response of the wing to aileron deflection as a function of airspeed. Wing spar bending and torsion moments were measured with strain gages located near the midspan and outboard stations. Results were compared to doublet lattice theoretical aerodynamics calculations using a 0.6 factor applied to the aileron forces as determined from available rigid wind tunnel model data. The test and calculated results are shown in Figures 59 and 60. These comparisons show reasonable agreement for the midspan bending moment and torque. However, the measured outboard torques were significantly less than the calculated values.

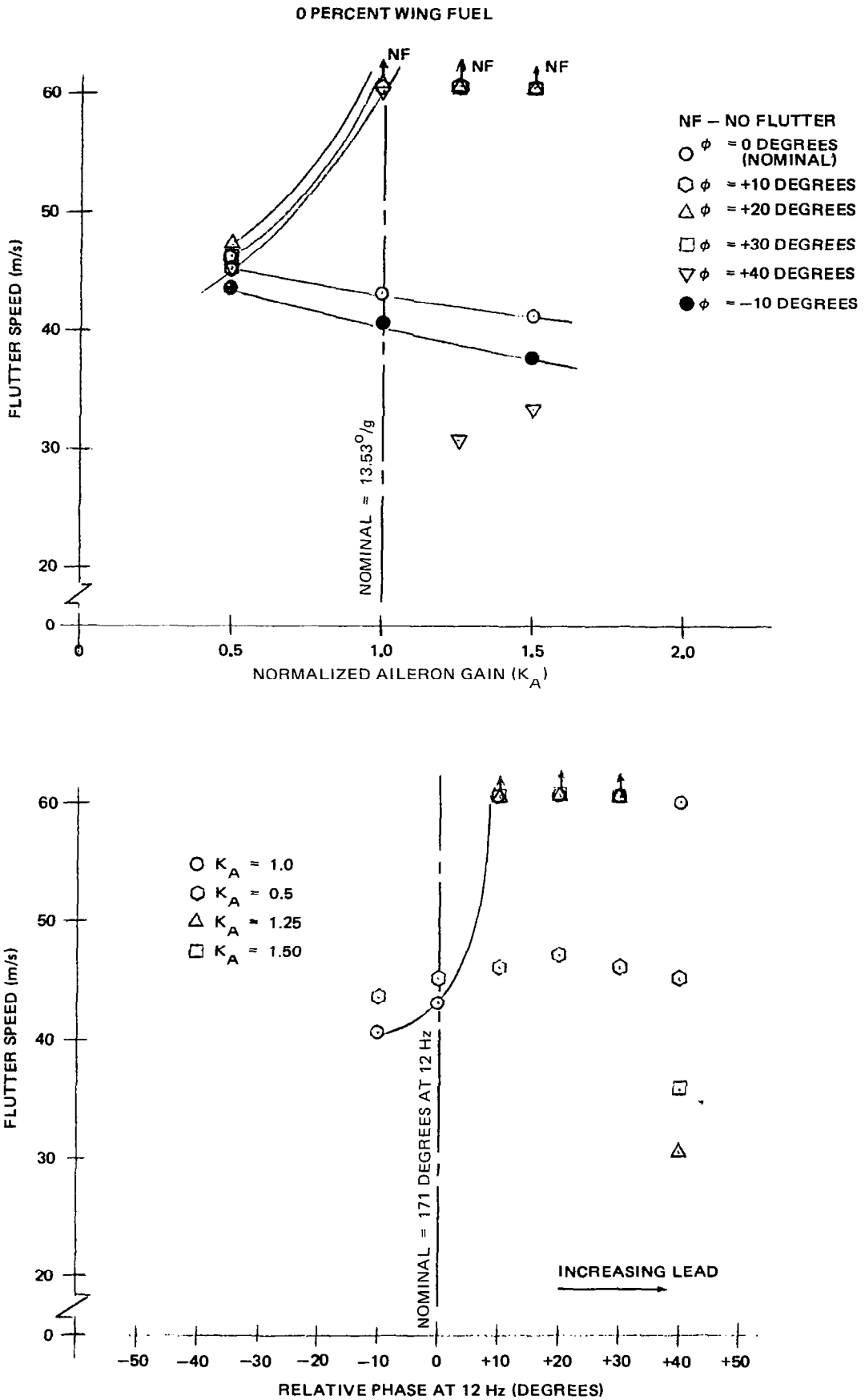

FIGURE 58. SEMISPAN FLUTTER SPEED VERSUS GAIN AND PHASE VARIATION USING NASA CL 1

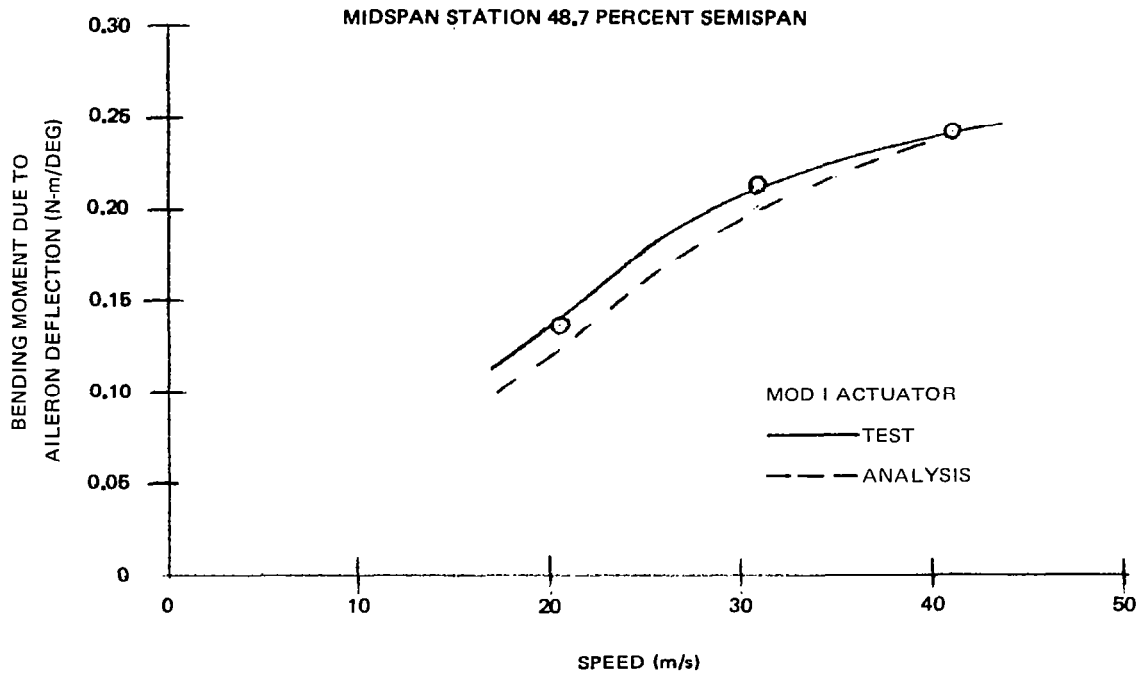

FIGURE 59. SEMISPAN WING STATIC BENDING MOMENT RESPONSE TO AILERON DEFLECTION

The discrepancy between test and calculation of the outboard section loads may be due to the assumption (used in the calculations) that the aileron hinge moments and shears were transmitted to the wing continuously along the spar. Actually, the hinge moment was transmitted to the wing through the aileron actuator only and the shear was transmitted through the three discrete hinge points (see Figure 3). Since the outboard torque gage was located outboard of the actuator, its reading did not reflect the effect of the aileron hinge moment.

The wing tip vertical and engine nacelle lateral acceleration responses to aileron harmonic oscillations were measured. The wing tip data were processed off-line from tape records and the nacelle data were processed on-line using a Spectral Dynamics 335A analyzer. These transfer functions, plotted in terms of dB response versus frequency, are presented in Figures 61 and 62. Predicted transfer functions are also shown for direct comparison. Figure 61, comparing wing tip accelerations, shows good agreement between test results and analysis. Agreement between test and analytical results is also shown for the first peak of the nacelle lateral acceleration response corresponding to the 6 Hz nacelle yaw mode (Figure 62). For the other modes, the nacelle lateral acceleration agreement is not good. Lack of agreement at the 12.3 Hz mode may be because this mode, as compared to the lateral motion, is characterized by a strong nacelle pitching motion and, because of accelerometer orientation, the lateral accelerometer measured a slight vertical component of pitching motion. Lack of agreement at other frequencies may be due to errors in predicting the unsteady aerodynamic forces on the nacelle.

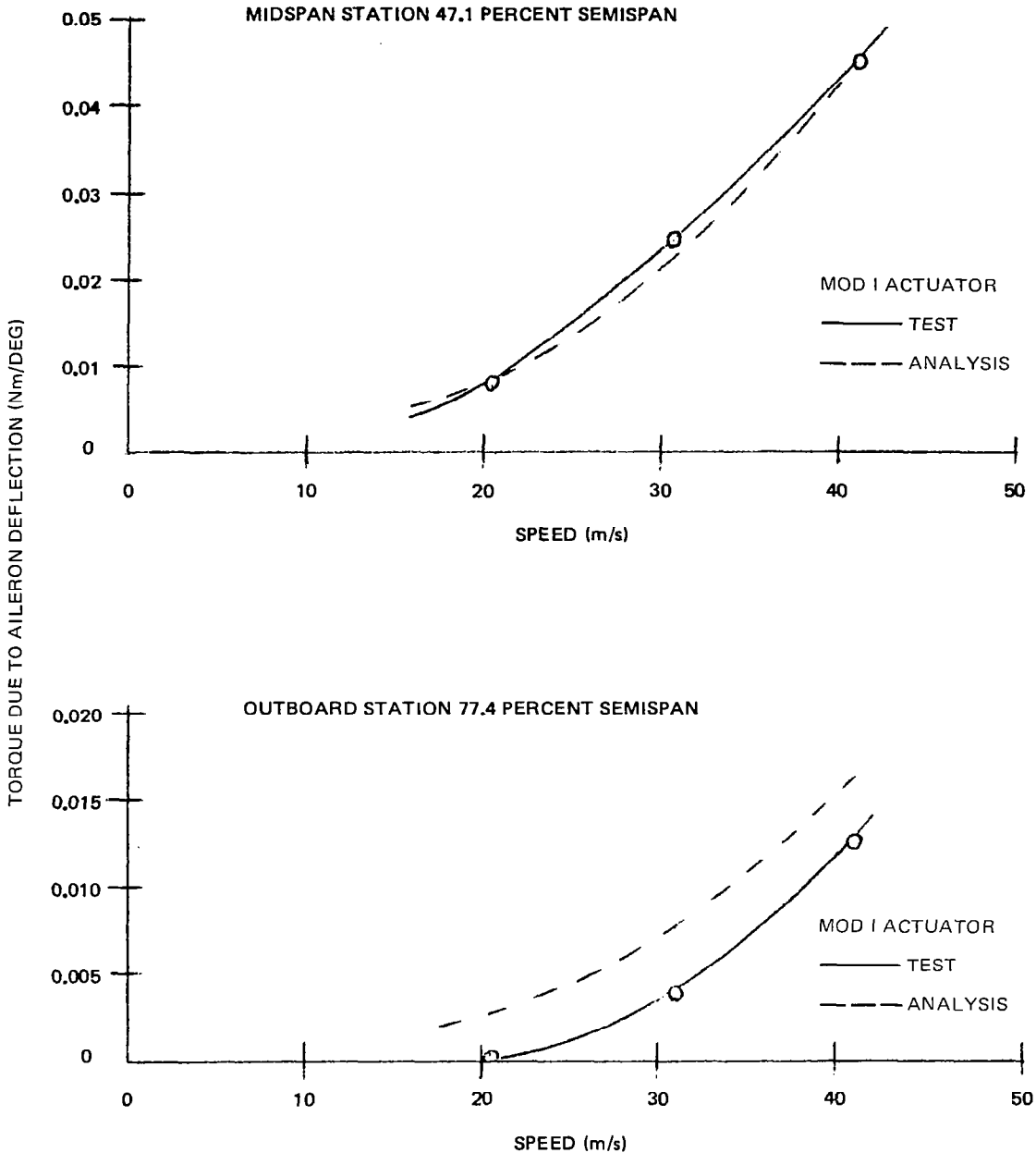

FIGURE 60. SEMISPAN WING STATIC TORQUE RESPONSE TO AILERON DEFLECTION

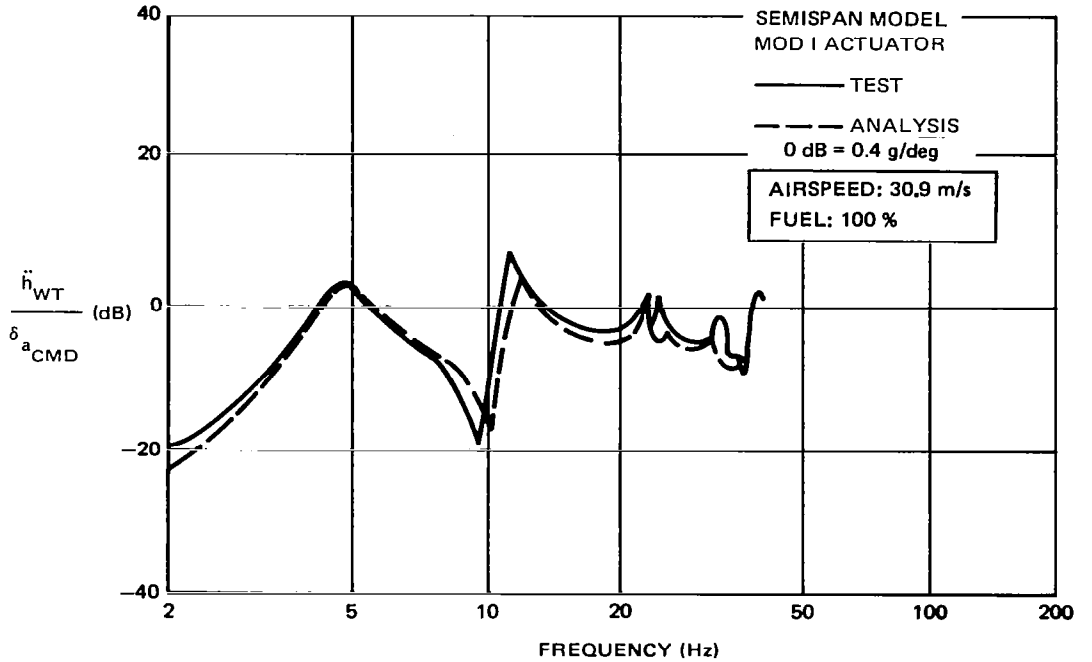

FIGURE 61. WING TIP ACCELERATION RESPONSE TO AILERON EXCITATION

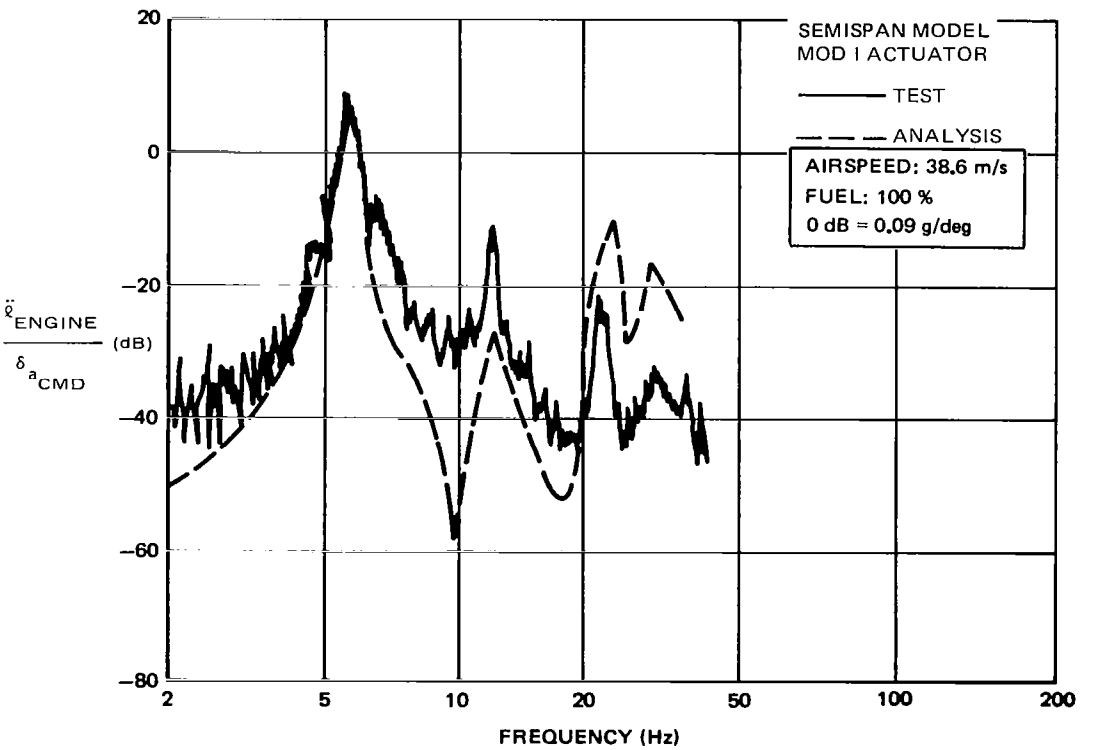

FIGURE 62. ENGINE LATERAL ACCELERATION RESPONSE TO AILERON EXCITATION

Semispan Gust Results

The response of the semispan wing to the turbulence field generated by the banner were obtained in terms of RMS and PSD data. Analytical correlations with the measured data were difficult because a complete description of the turbulence field exciting the model was not available. Limited data were available concerning turbulence RMS values and PSD at selected tunnel locations (see Tunnel Description and Model Installation), but no information was available concerning correlation of the turbulence at different tunnel locations. Consequently two types of analyses were performed:

1. One-dimensional — the turbulence field was assumed to be perfectly correlated across the tunnel test section.

2. Two-dimensional — the turbulence was assumed to be highly uncorrelated across the tunnel test section.

Considering the limited information available concerning the turbulence field, the two-dimensional analysis correlated reasonably well with the measured data. The one-dimensional analysis did not correlate well with the measured data. Consequently the PSD calculation of bending moment was based on the assumption of a two-dimensional gust field. Table 3 shows comparisons of midspan bending moments. The calculated PSDs, compared to test results, are shown in Figure 63 for the open-loop and closed-loop cases. The reasonable agreement between test and two-dimensional analytical results suggests that the nature of the turbulence was in fact two-dimensional.

TABLE 3
MIDSPAN BENDING MOMENT COMPARISONS
SEMISPAN MODEL, 100% FUEL, V = 30.9 m/s

DATA	RMS(NEWTON-METERS)
One-Dimensional Analysis	7.25
Two-Dimensional Analysis	1.48
Measured	1.68

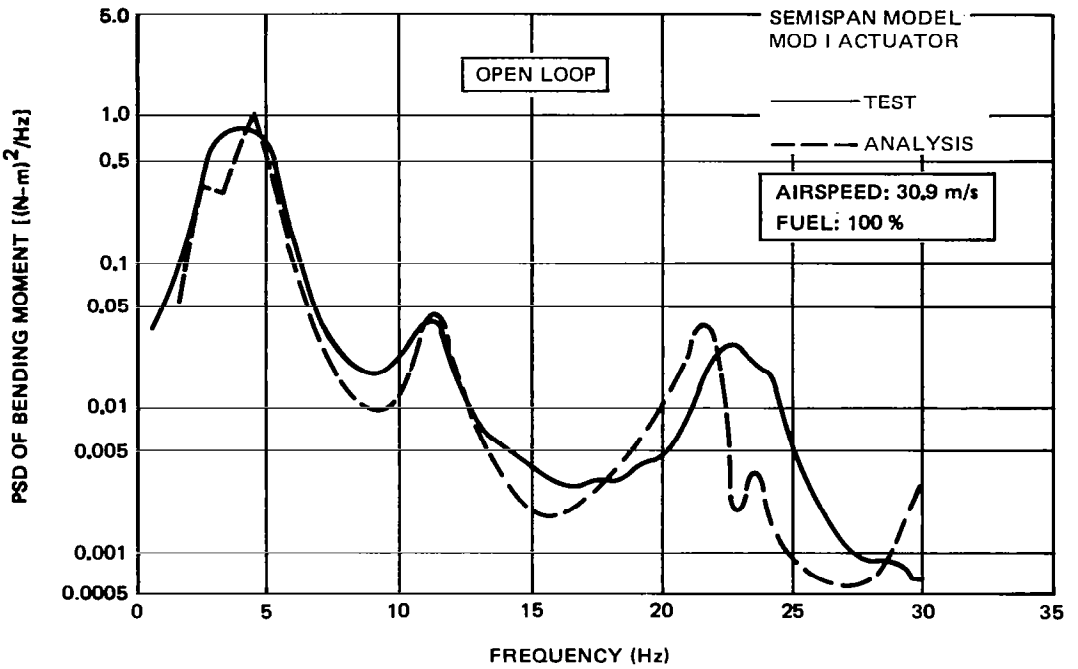

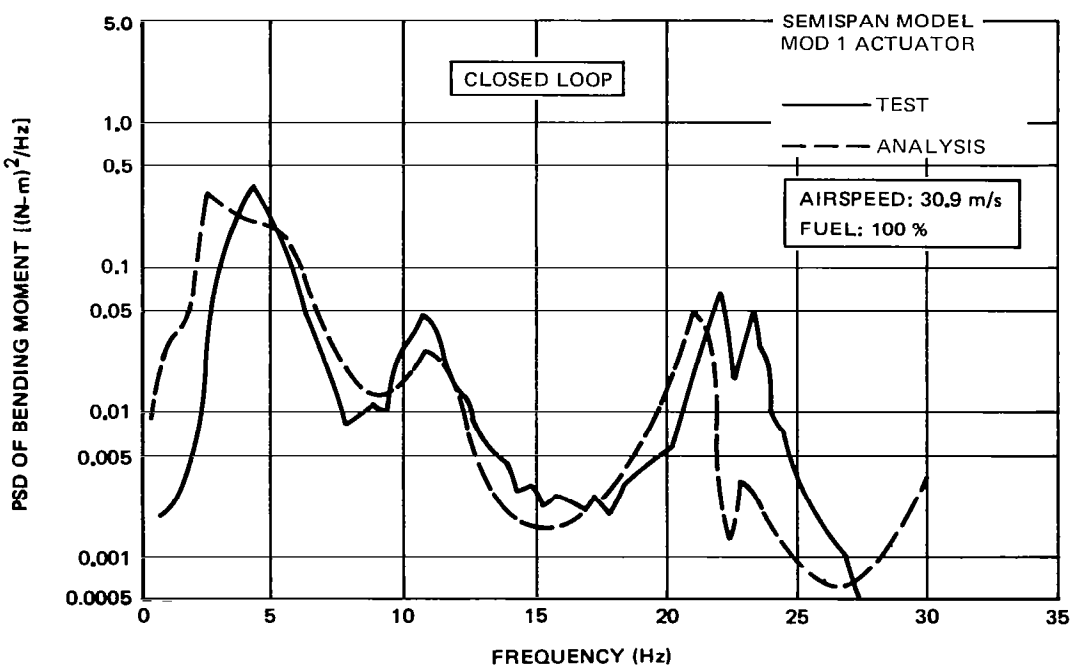

FIGURE 63. OPEN- AND CLOSED-LOOP POWER SPECTRUM DENSITY OF 49 PERCENT SPAN BENDING MOMENT DUE TO TURBULENCE

Comparison between the open- and closed-loop bending moments show the active control system (ACS) was effective in reducing the PSD load due to the first wing bending mode (the mode generating the highest loads). The system had little or no effect upon the 12.3 Hz torsion mode, and increased the PSD load due to the 23 Hz wing second-bending mode. The overall effect of the ACS was to reduce the midspan RMS bending moment by 22 to 40 percent depending upon speed, as shown by Figure 64. Measurements of the midspan torque at 30.9 m/s (60 KEAS) for 100 percent fuel showed that the ACS produced negligible changes in the midspan torque load.

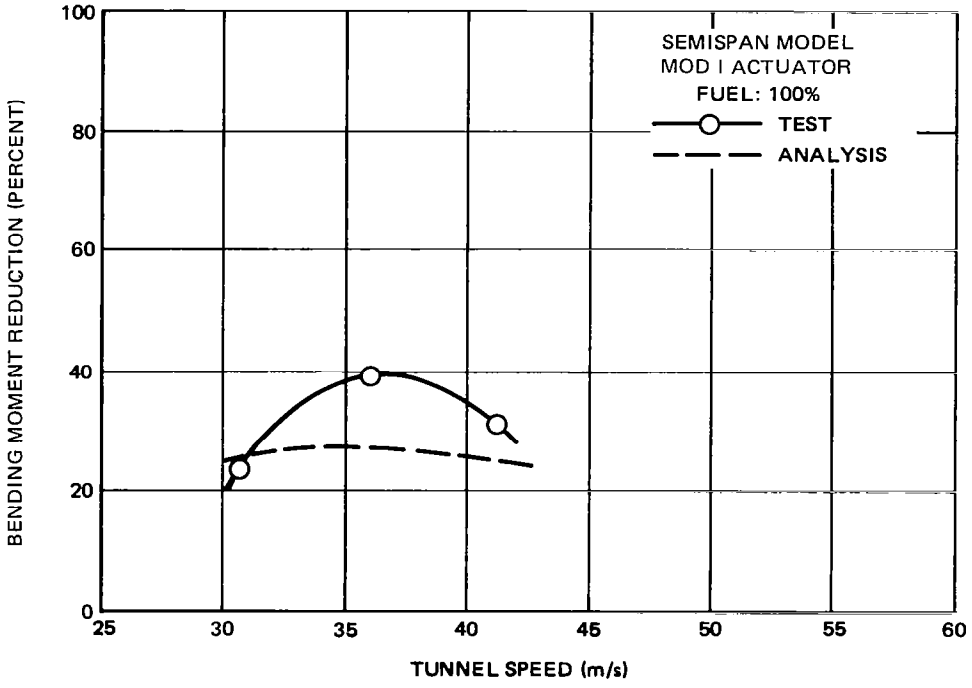

FIGURE 64. ACTIVE CONTROL SYSTEM REDUCTION OF RMS BENDING MOMENT AT 49 PERCENT SPAN

Full-Span Flutter Tests and Analyses

Following the semispan tests, the full-span model was tested. The test established passive and active flutter and gust response characteristics of the complete model. Two model configurations were tested. The first or baseline configuration was based directly upon a DC-10 derivative. For the second, or alternate, configuration, a weight was installed aft of the wing tip to produce a sharp flutter crossing (not typical of the DC-10). Test results were compared with analytical results to evaluate the active control laws and the methods involved.

The baseline configuration reflected a low wing fuel state (10 percent) and had a fuselage ballast of 4.5 kg (10 lb) at the model's center of gravity. This arrangement was used to reduce the passive flutter speed due to the 12 Hz mode without changing the flutter character and thereby achieve an adequate testing range for demonstrating margins. Reduction of the 12 Hz mode flut-

ter speed was important because of the existence of a higher frequency flutter mode (25 Hz) which was expected to set an upper limit on test speeds. Adequate separation of these modes allowed testing over a speed range which permitted demonstration of the effectiveness of control laws, developed mainly for the critical 12 Hz mode.

Several control laws were evaluated prior to tunnel entry. The evaluation resulted in the principal test control law, A7/E4. The control law identification, A7/E4, refers to the seventh and fourth modification of the aileron and elevator control laws, respectively. Midway through the test program another control law was tested and designated as A8/E5. Control law A8/E5 was based upon an updated aeroelastic representation of the model and resulted in aileron and elevator gains reduced to one-fourth and one-third, respectively, of A7/E4. Also, a 22 Hz notch filter was used in the A8 control law in an attempt to alleviate the detrimental effect of the 25 Hz wing mode. A notch filter was prepared to counter an anticipated 40 Hz servo instability at zero airspeed. The initial engagement of the control law A7 at the reference gain ($K_A = 1.0$) confirmed the 40 Hz instability. The notch filter, although adequate for the 40 Hz mode, introduced other instabilities with frequencies ranging from 50 to 180 Hz for the gain of $K_A = 1.0$. To avoid the 40 Hz instability this notch filter was eliminated and the gain was reduced to $K_A = 0.5$. Therefore, the closed-loop flutter tests were only performed with the A7 control law at reduced gain. The lower gain A8/E5 control laws avoided these instabilities.

The damping versus speed plot of Figure 65 shows the passive flutter speed of the baseline configuration was 54.0 m/s (105 KEAS) with a frequency of 12.7 Hz. The maximum subcritical structural damping, c/cc, was 1.5 percent. Unlike the semispan model, flutter onset of the full-span model was definite and moderately divergent. The analytically predicted passive flutter speed was 54.5 m/s (106 KEAS) with a frequency of 12.3 Hz. The calculated damping versus velocity of the 12 Hz mode (Figure 65) showed good comparison with test results.

After passive flutter speeds were established, closed-loop flutter tests were performed for several gain and phase settings. Plots of damping versus speed for control law 1/2 A7/E4 (the same as A7/E4 but with half the aileron gain) are shown in Figure 65 together with comparisons of analysis and passive results. Test results verified analytical predictions for the 1/2 A7/E4 control law. The critical 12 Hz mode was entirely suppressed with this control law (as predicted) and test damping data agreed well with analyses. At subcritical speeds there was no evidence of the 25 Hz flutter mode until flutter onset was imminent. The baseline configuration flutter speed with the 1/2 A7/E4 control law was 63 m/s (122.5 KEAS) with a frequency of 22.2 Hz. According to analyses, the 25 Hz mode passive flutter speed was reduced by the 1/2 A7/E4 control law from 67.5 m/s (131 KEAS) to 64.0 m/s (124.5 KEAS) with a flutter frequency of 26.3 Hz. Agreement between analyses and test was within 2 percent for the closed-loop flutter speed and within 16 percent for the frequency. The difference in flutter frequency was due to difficulty in predicting rapid frequency shifts of the high-frequency outer panel torsion mode near flutter onset. The 1/2 A7/E4 control law suppressed the critical 12 Hz mode entirely.

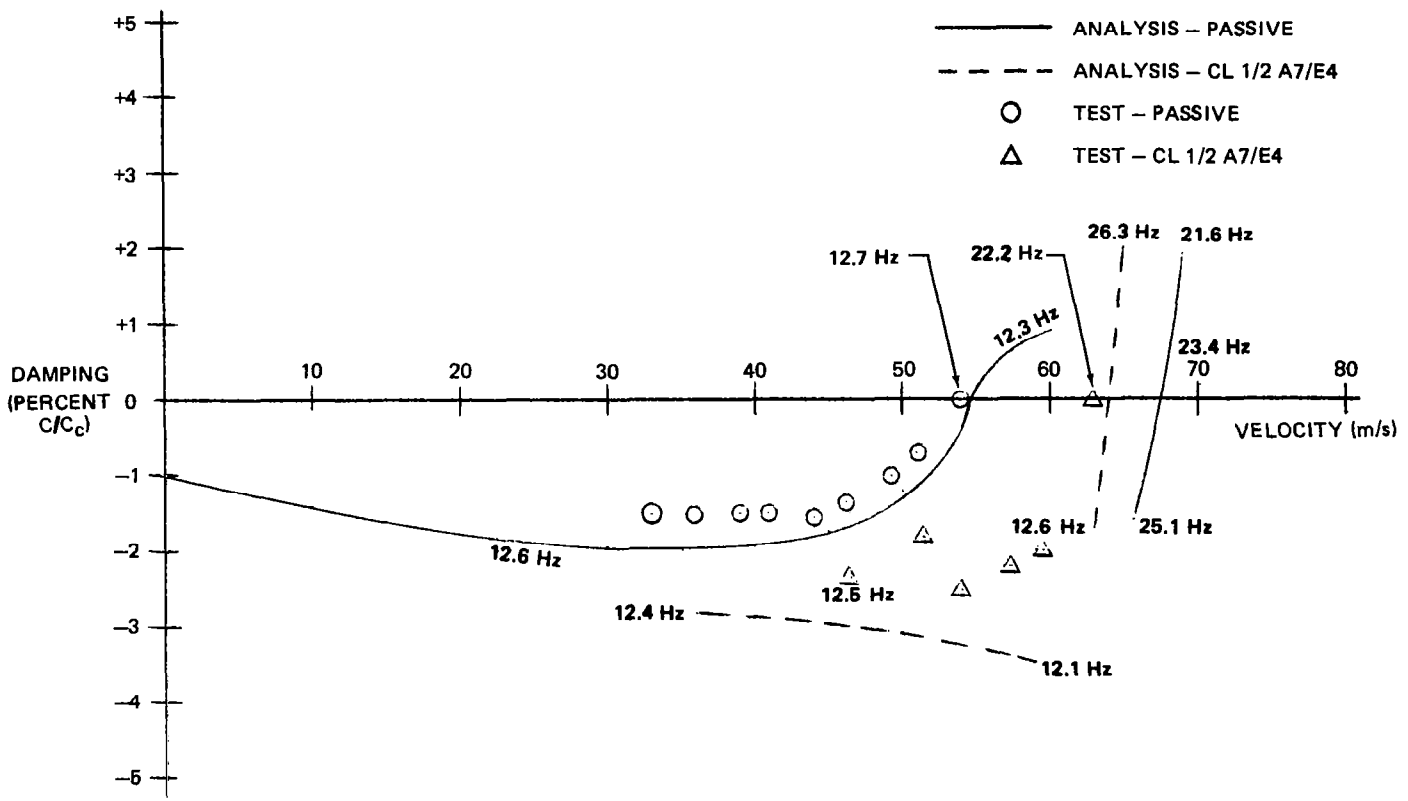

FIGURE 65. DAMPING VERSUS VELOCITY FOR THE FULL-SPAN MODEL – BASELINE CONFIGURATION

Gain variations were performed on the aileron part of the control law, A7. In the test, gain variations only up to $K_A = 0.5$ could be tested because of the high-frequency instabilities at higher gains. Figure 66 shows results of tests and analyses for gain variations. Except for zero gain (passive case), the higher frequency mode became unstable in the test or analyses results. Analysis predicts the flutter speed of the high frequency mode to decrease significantly with increasing gain. The test results do not confirm this result; rather, they seem to show a negligible effect of the aileron control law up to a gain of near 0.4, and then a small speed improvement at a gain of 0.5. However, the difference between test and analysis may be less than shown because the speeds plotted are the maximum speeds tested rather than actual flutter speeds. Because of the violence of this flutter mode, the runs were stopped when the test engineer judged that flutter was imminent.

Test results for gain variations of control law A8/E5 are also presented in Figure 66. As discussed, A8/E5 differed from A7/E4 in that the gains were reduced and the aileron loop was designed with a notch filter to suppress the outer wing 25 Hz mode. However, the improvement in using A8/E4 was less than expected.

Results of phase variations of control law A7 with $K_A = 0.5$ and 0.25 are included in Figure 67. The incremental phase of aileron rotation with respect to control acceleration has been noted lead (+) or lag (−) measured at 12 Hz. Analyses predicted only a moderate reduction in the flutter speed of the high-frequency flutter mode with increasing phase lag; however, the test results showed that increasing phase lag had a strong effect in flutter speed reduction, e.g., 30 degrees additional lag resulted in a flutter speed reduction of 20 percent as compared to a predicted reduction of 2 percent. Also, flutter at 30 degrees lag involved different modes than at zero phase. The ability to accurately predict the effects of phase variations requires further study.

The discussion of results so far has been centered upon the baseline configuration. An alternate configuration was tested and analyzed which featured a wing engine pylon of increased rigidity and the addition of a trailing wing tip boom with a 20 gram mass located 0.152 m (6 in.) aft of the elastic axis. The effect of these changes was to create a violent type of flutter at a frequency of 12 Hz characterized by pronounced wing tip torsion. Figure 68 shows the results of these tests and analysis, both passive and active. The analysis-test correlation is good for the passive case; $V_f =$ 43 m/s (83.6 KEAS) by analyses and $V_f = 42$ m/s (81.6 KEAS) from the test. Also, the sharp onset of the flutter is indicated by the test results, in that a 15 Hz mode was being tracked without evidence of another mode when the 12 Hz mode became unstable with a small increase in velocity. In fact, during one run, this unexpected rapid loss of damping resulted in wing tip damage. Figure 68 also shows that the analysis predicted an increase in flutter speed to 53 m/s (103 KEAS) with control law A7/E4. However, because of high-frequency instabilities with aileron gains above 0.5, the analytical result could not be verified by test. But, for a gain of 0.5, the analysis predicted a small change in flutter speed and the test confirmed this result.

An aileron gain variation was also tested on the alternate configuration with the wing sensors at the normal location and with the wing sensors moved outboard. Figure 69 shows the results of these tests. Control law A7.1/E4 refers to the case where each wing sensor was moved from the 48 percent span station to a station near the wing tip. Control law A7.1/E4 produced no improvement in flutter speed within the limited range of gains that could be tested. At $K_A = 0.375$ and 0.5 filter instabilities appeared and at $K_A = 1$ a high frequency structurally coupled instability developed.

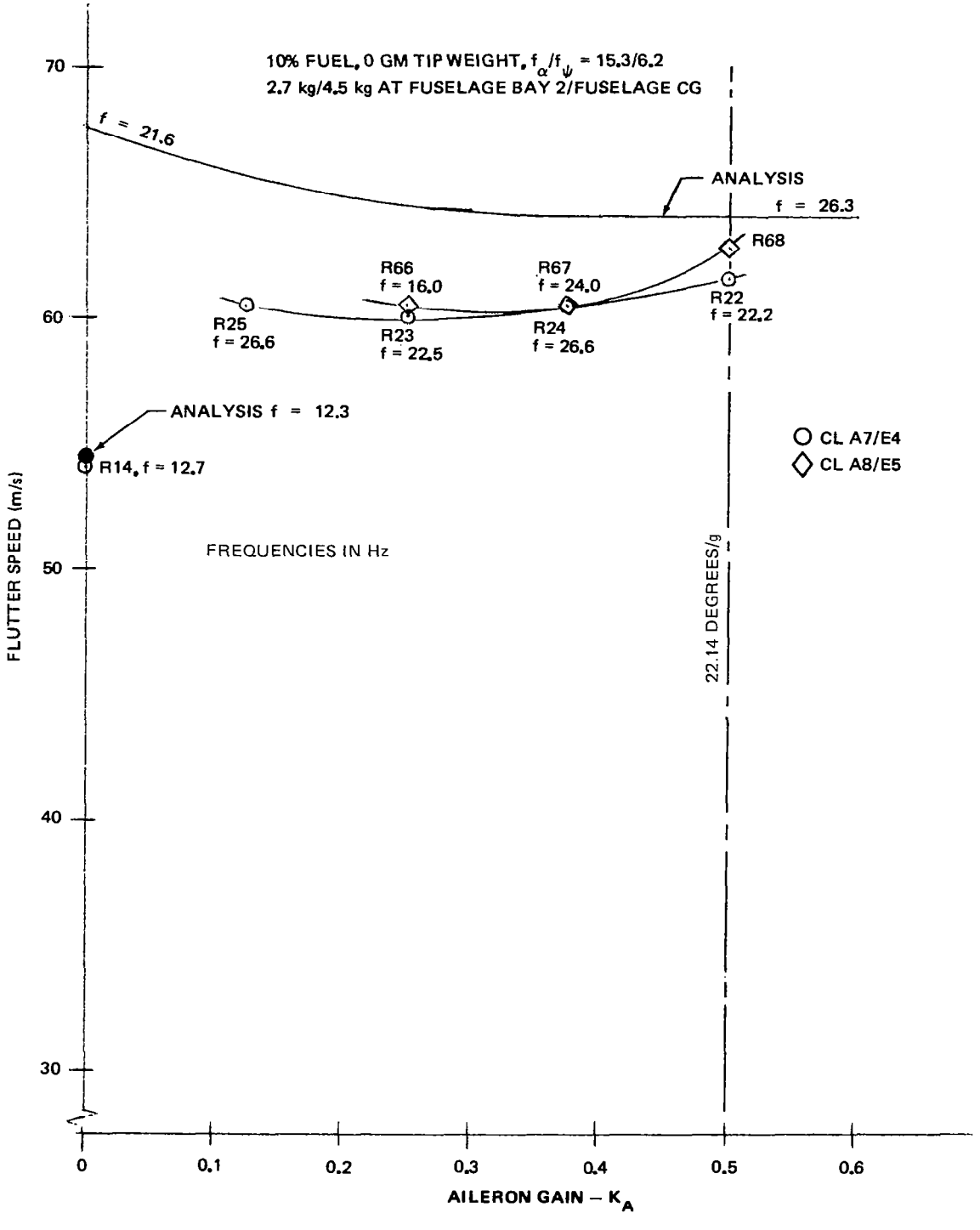

FIGURE 66. FLUTTER SPEED VERSUS GAIN FOR THE FULL-SPAN MODEL – BASELINE CONFIGURATION

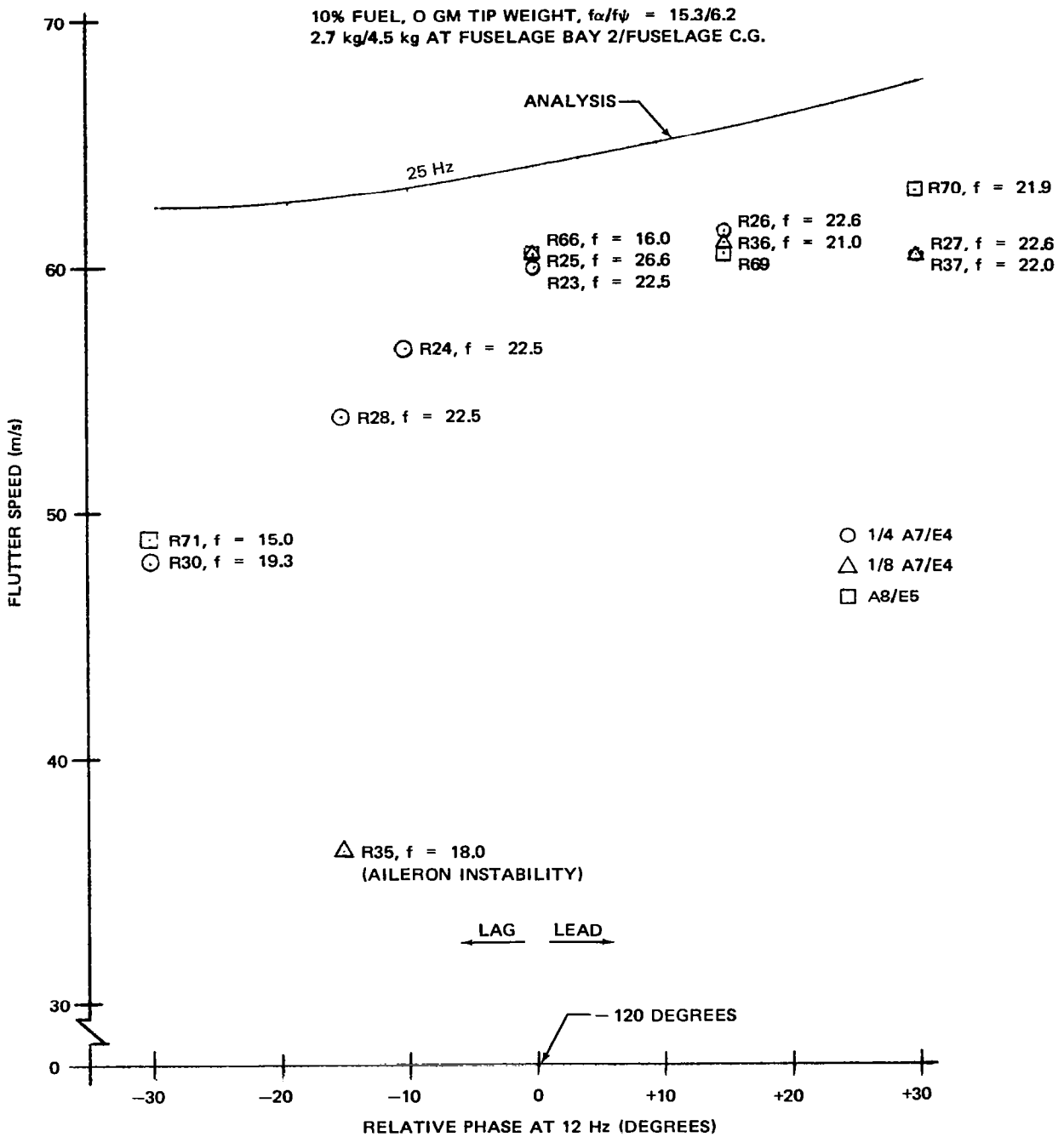

FIGURE 67. FLUTTER SPEED VERSUS PHASE VARIATION FOR THE FULL-SPAN MODEL – BASELINE CONFIGURATION

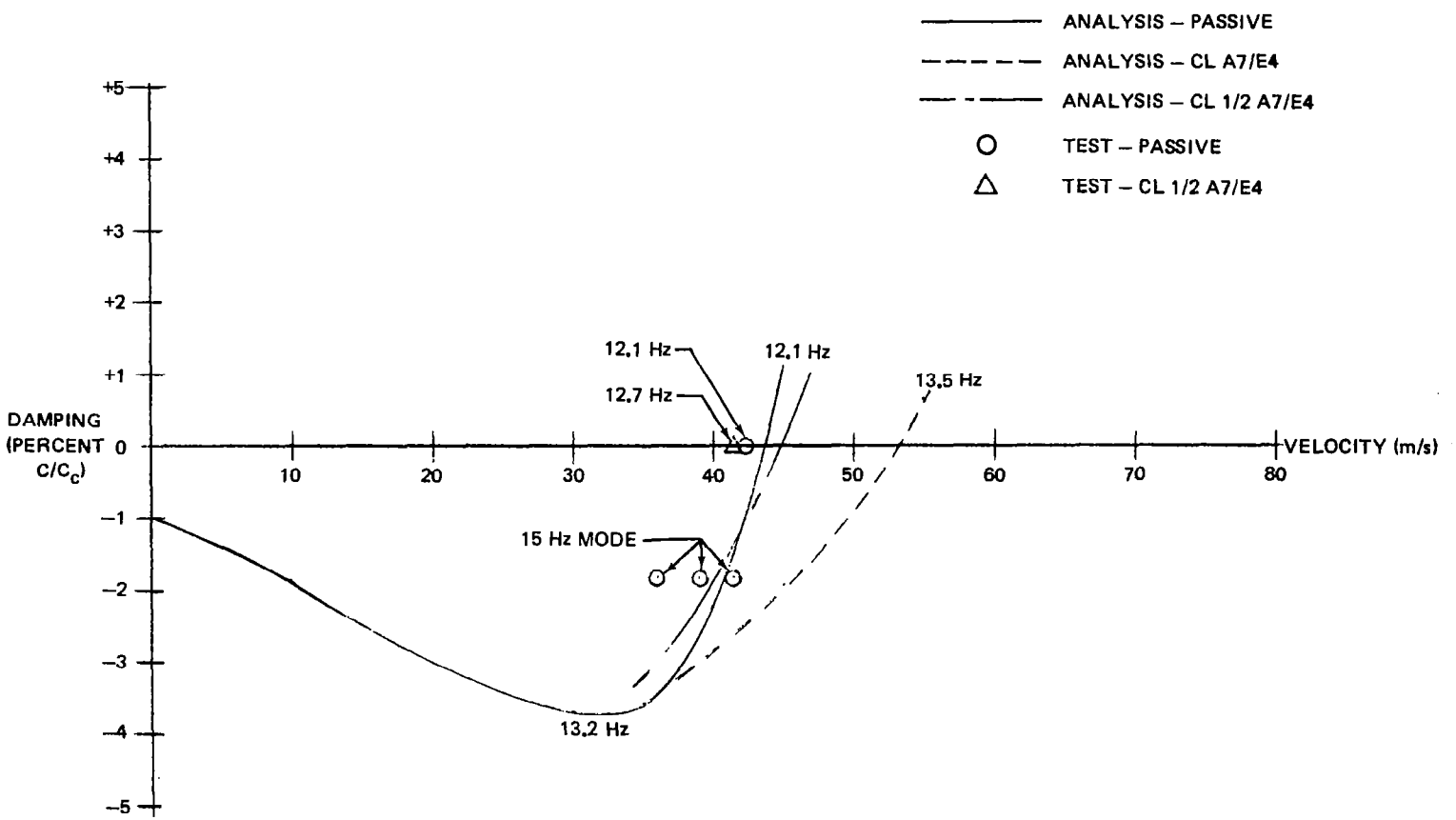

FIGURE 68. DAMPING VERSUS VELOCITY FOR THE FULL-SPAN MODEL – ALTERNATE CONFIGURATION

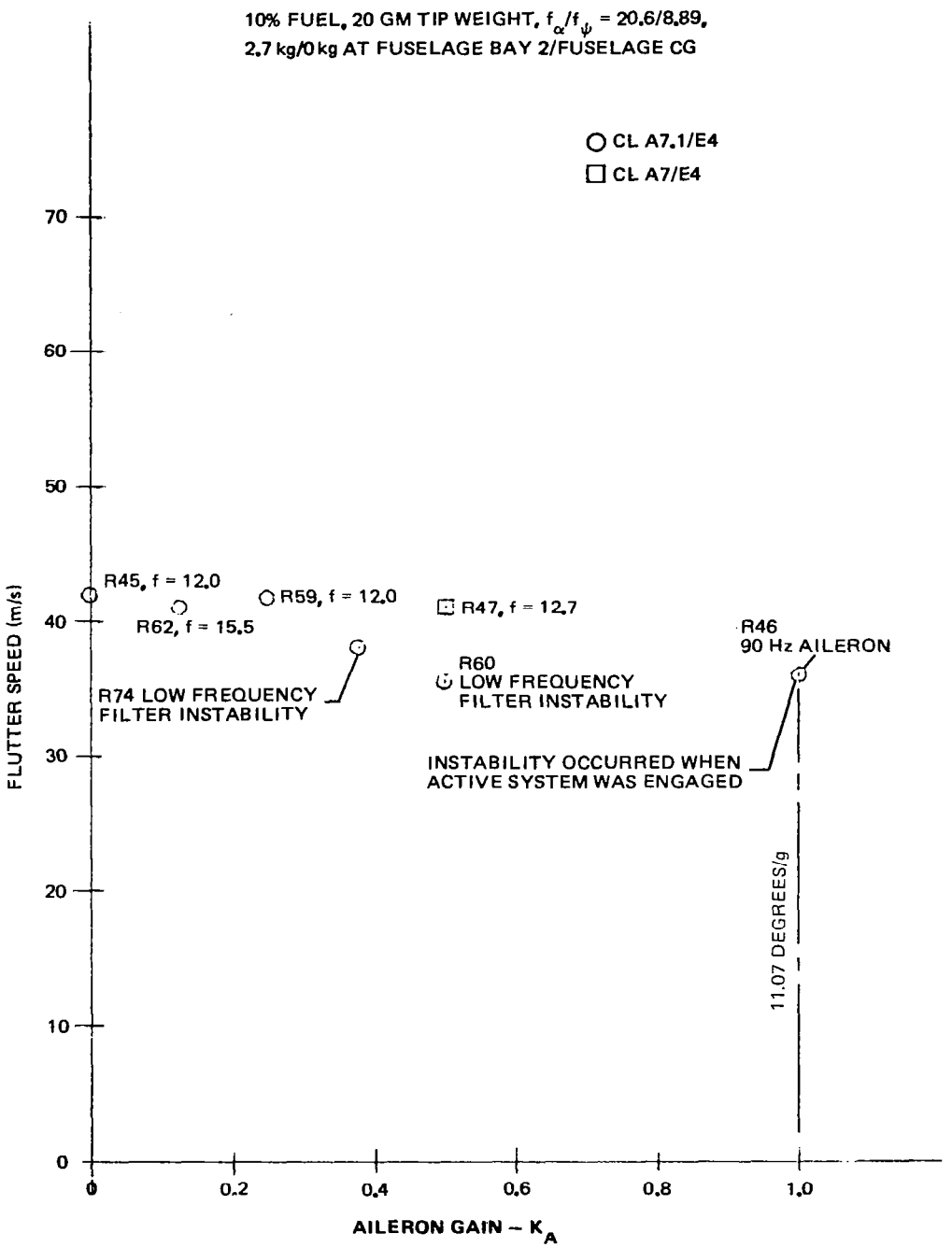

FIGURE 69. FLUTTER SPEED VERSUS GAIN FOR THE FULL-SPAN MODEL – ALTERNATE CONFIGURATION

Full-Span Transfer Functions

The transfer functions (TF) showing the relationships between model response and control surface inputs were investigated by analysis and tests at a speed of 38.6 m/s (75 KEAS). Symmetric and antisymmetric aileron inputs were used over a frequency range of 2 to 35 Hz for which wing loads, wing tip accelerations, and nacelle accelerations were measured and calculated. Similar data were taken for elevator harmonic inputs. The response to symmetric aileron oscillations are shown in Figures 70 through 72 and the response to elevator oscillations are shown in Figures 73 and 74. The antisymmetric aileron TF data are shown in Figure 75.

The calculated transfer functions show reasonably good agreement with measurements except as follows: agreement of predicted and measured lateral engine responses to symmetric aileron inputs is good for the dominant nacelle 6 Hz yaw and 23 Hz roll modes, but for the 9 Hz fuselage bending and 13 Hz wing nacelle pitch modes the calculated responses are in poor agreement with measured responses (Figure 71). As was the case for a similar difference noted for the semispan results, the disagreement may be due to a slight offset in the orientation of the nacelle lateral accelerometer relative to the theoretical axis causing the lateral accelerometer to respond erroneously to a small component of vertical motion. For example, a 5 degree offset would result in the lateral accelerometer responding to nearly 10 percent of the vertical motion. Since the nacelle vertical motion is 10 times the lateral motion in the 13 Hz mode, a 5 degree offset would account for the discrepancy.

Another discrepancy between analytical and test results is in the outboard wing bending moment response to aileron inputs (Figure 72). For this case, the predicted response is greater than the measured response over the entire frequency spectrum. As with the semispan model, this may be due to an assumption that aileron shear forces are transmitted to the wing continuously along the aileron leading edge and not through the actuator and the three discrete hinge points. Also, and perhaps more importantly, the analytical representation assumed the aileron stiffness did not significantly contribute to the wing bending stiffness. The aileron does, in fact, contribute a second load path, bypassing the outboard bending gage in the spar bending moment reaction. An illustration of the aileron, hinge arrangement, actuator, spar, and outboard bending moment strain gage assembly was shown earlier in Figure 3.

The response of the wing bending moment to elevator inputs (Figure 73) shows the predicted response to be higher than the test results at the 9 Hz fuselage bending mode. This may be due to aeroelastic effects being greater than predicted. The elevator shear loads in the analysis went directly into the horizontal stabilizer spar whereas, in fact, the loads are transferred to the spar through the trailing edges of the balsa sections. This resulted in the chordwise bending being greater than predicted thereby reducing elevator effectiveness.

Figure 73 shows that for the 9 Hz fuselage bending mode, the calculated cg response was higher than measured but the wing engine lateral response agreed well. In the 12 Hz mode, calculated and measured engine lateral response did not agree. The difficulties of predicting the wing engine response may be due to slight misalignment of the engine to the wing or an oversimplified aerodynamic model.

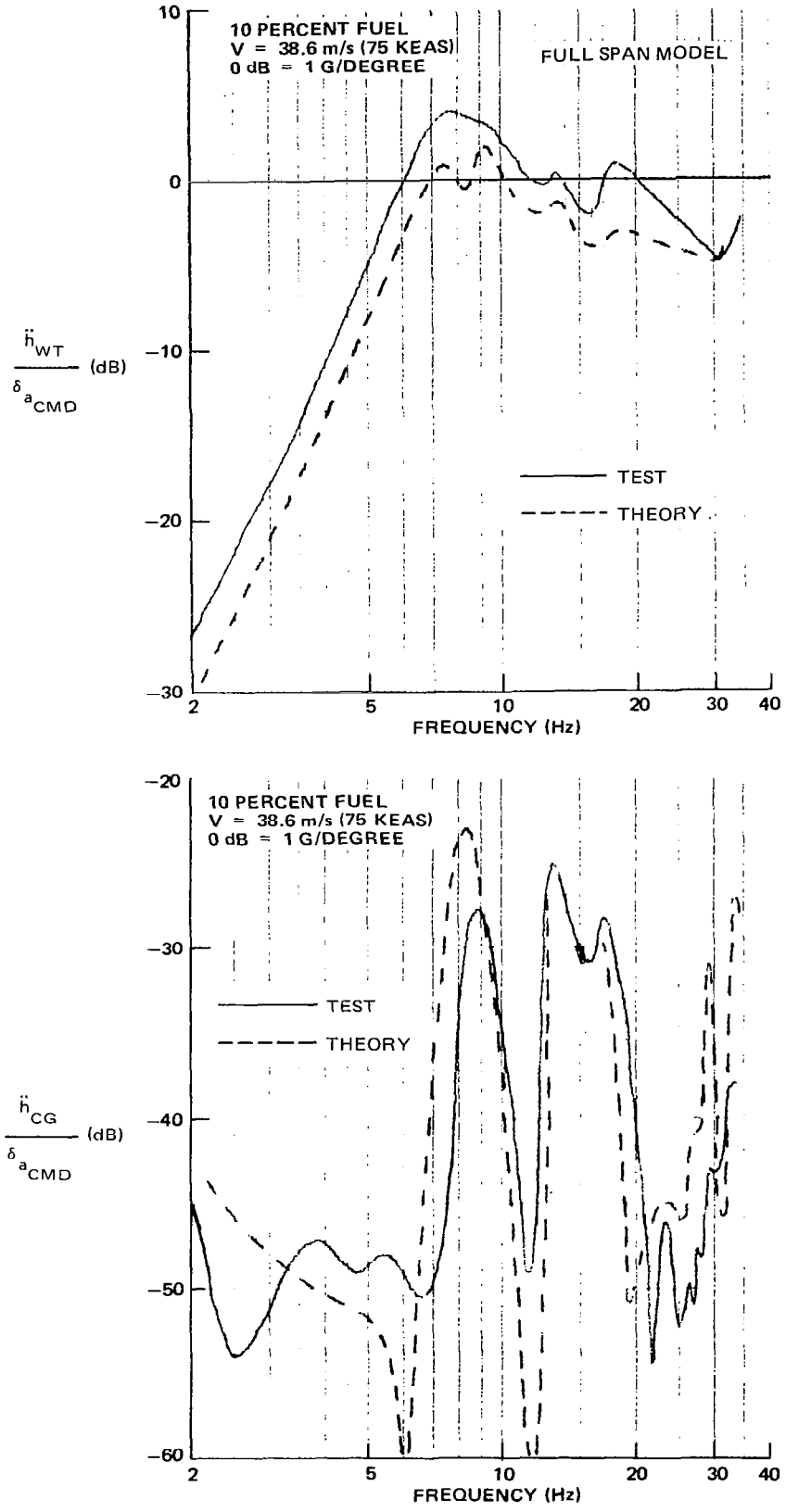

FIGURE 70. WING TIP AND FUSELAGE CG VERTICAL ACCELERATION RESPONSE TO COMMANDED AILERON EXCITATION

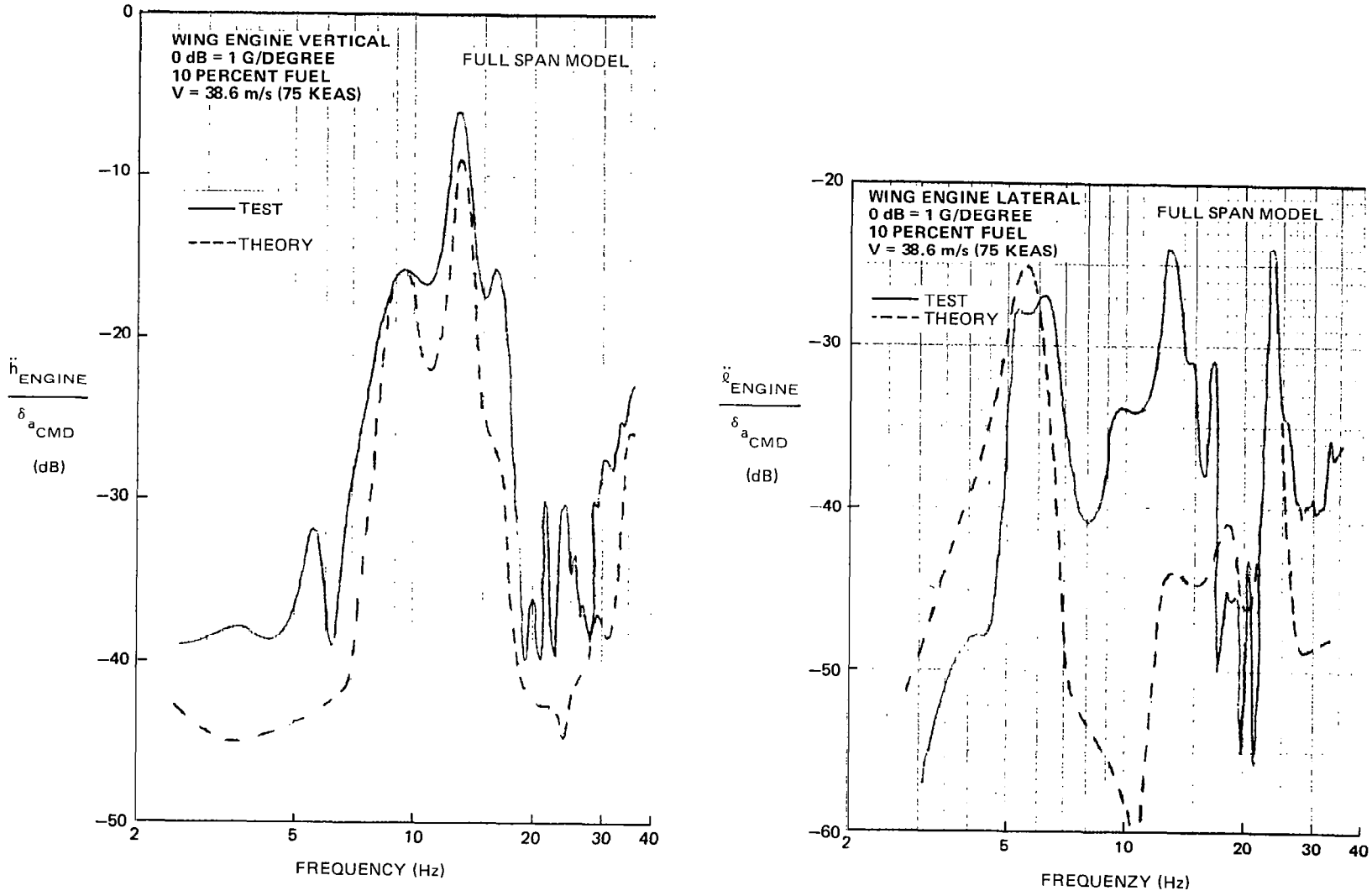

FIGURE 71. WING ENGINE VERTICAL AND LATERAL ACCELERATION RESPONSE TO COMMANDED AILERON EXCITATION

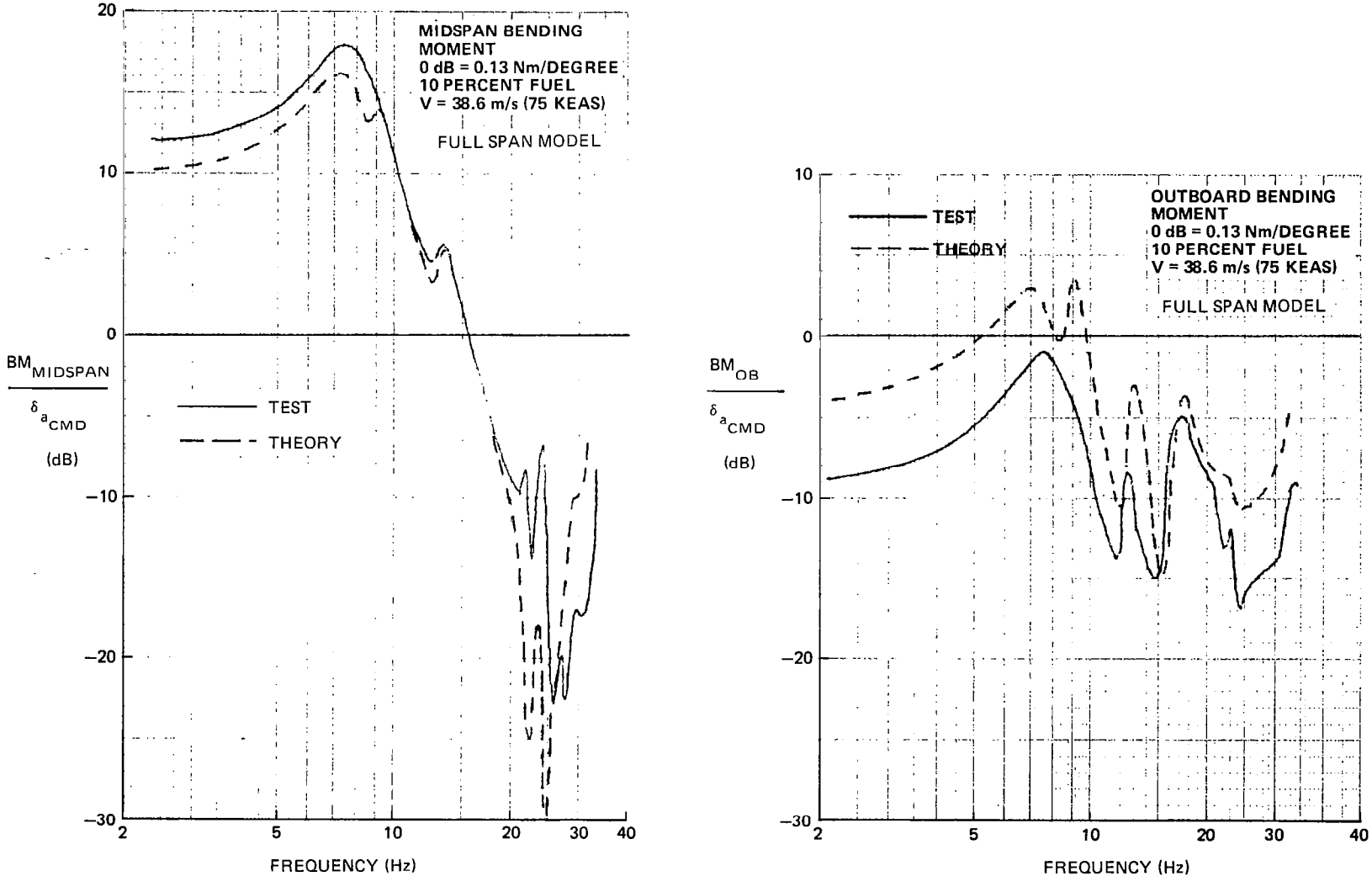

FIGURE 72. MIDSPAN AND OUTBOARD BENDING MOMENT RESPONSE TO COMMANDED AILERON EXCITATION

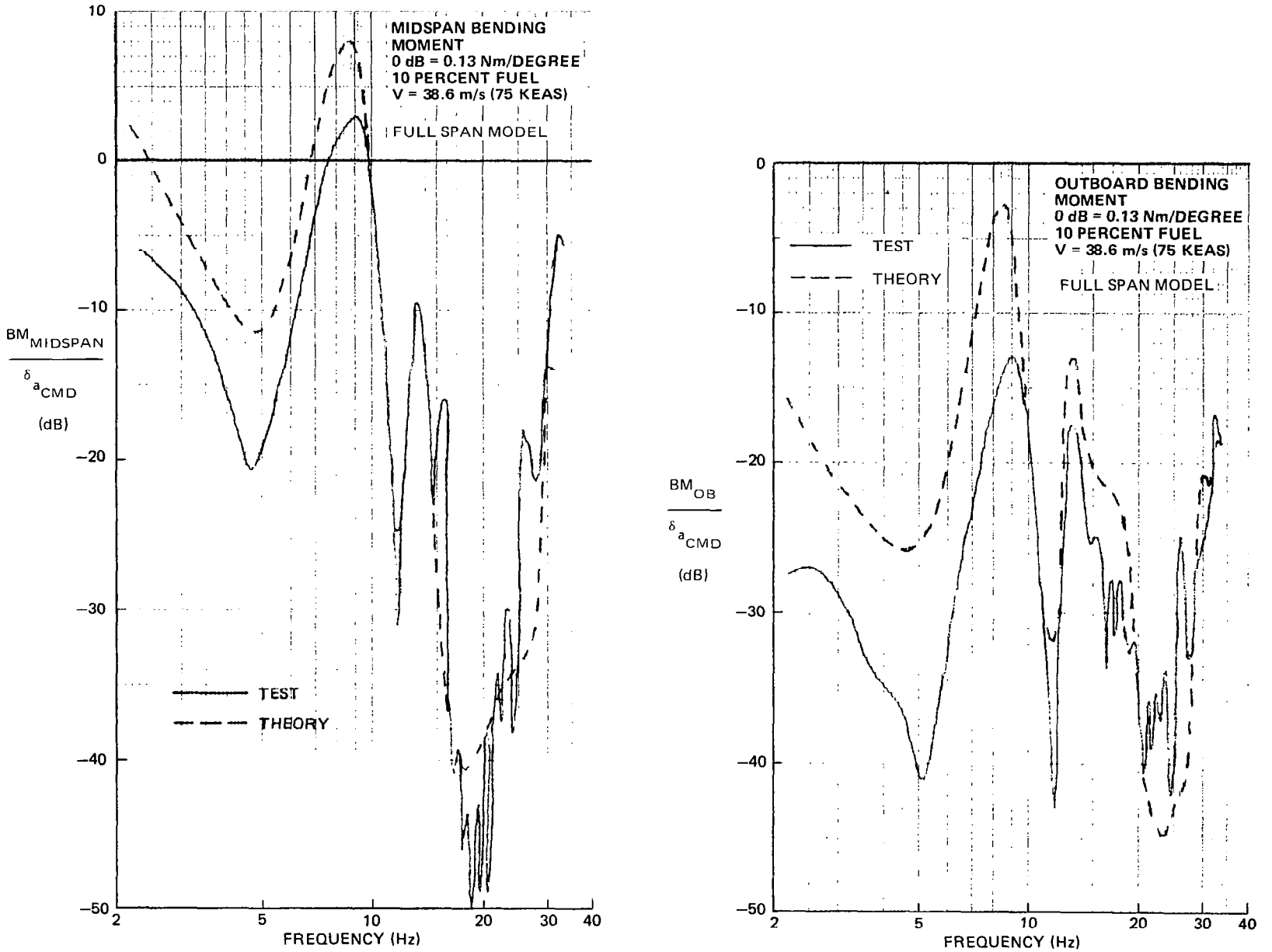

FIGURE 73. MIDSPAN AND OUTBOARD BENDING MOMENT RESPONSE TO COMMANDED ELEVATOR EXCITATION

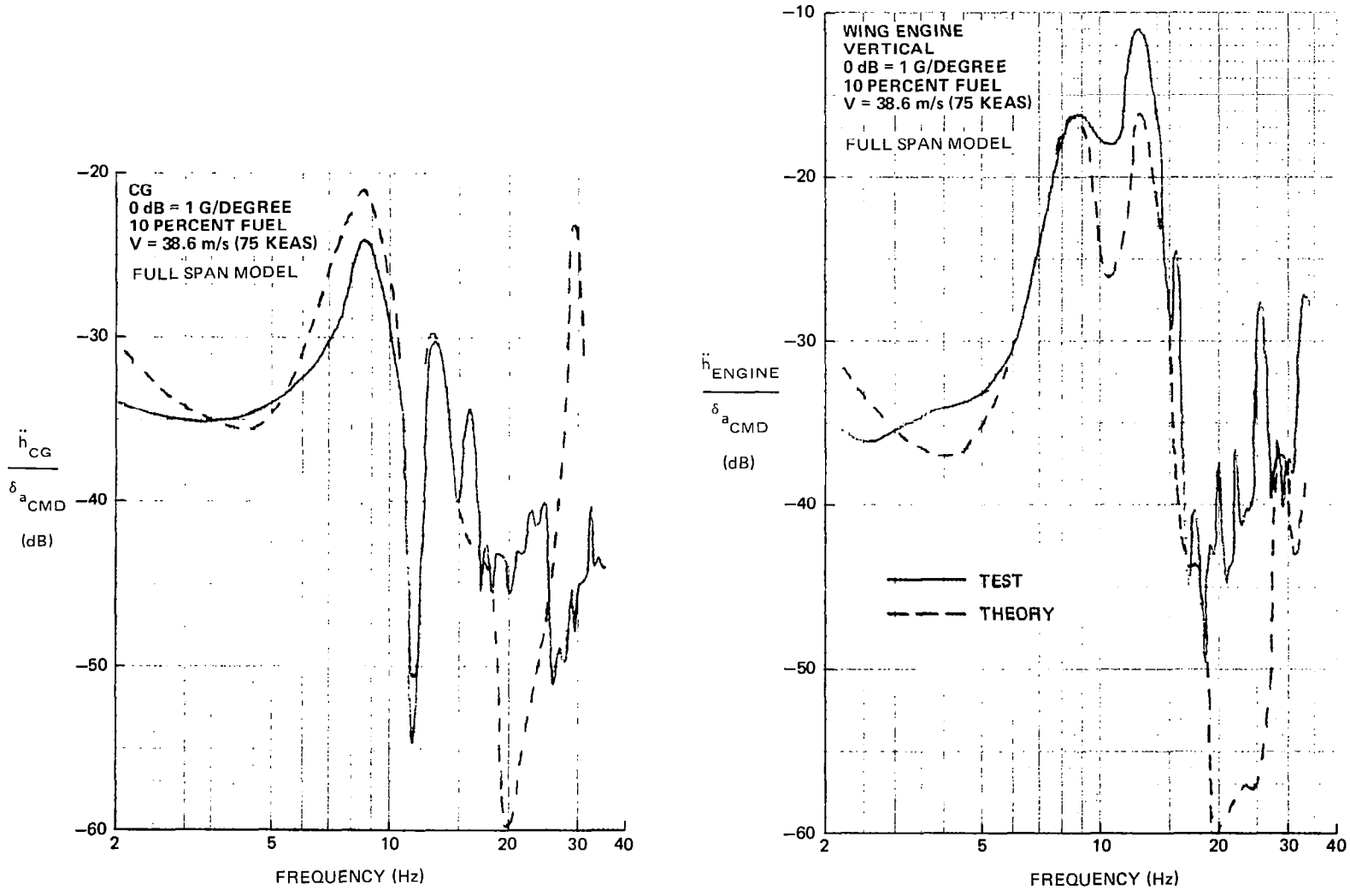

FIGURE 74. FUSELAGE CG AND WING ENGINE VERTICAL ACCELERATION RESPONSE TO COMMANDED ELEVATOR EXCITATION

Figure 75 shows that the measured responses of the left and right engines to pure antisymmetric open-loop aileron inputs disagree by 5 dB. A review of the left and right aileron inputs to the model showed that these inputs were of the same magnitude and 180 degrees out of phase. Therefore, it is concluded that the model itself was somewhat asymmetric. This is supported by observations made during resonant testing. Because it was not assumed in the theoretical analysis, the asymmetry indicated by Figure 75 represents a source of discrepancy between predicted and measured model response. Also, as was shown for the calculated aileron to engine TF, these antisymmetric test results indicate that the analytical engine motions in the 12 Hz mode were low with respect to the measured engine motion.

Full-Span Turbulence

Power spectra were computed and compared to test results for selected bending moments and accelerations. Analytical results, using a one-dimensional spectrum, as shown in Figure 76, indicate the active control system significantly reduced the short period mode and the symmetric structural mode responses. Figures 77 and 78 show that the active system reduces the loads for the structural modes but not for the rigid body short period mode. The short period gust loads were not accurately predicted because the analytical representation assumed a free-flying model and did not include the installation constraints consisting of a nose pitch damper, an instrumentation bundle, and the vertical slide rod.

Additional difficulty in correlating analytical and test results may have been due to model asymmetry and the nonhomogeneous gust field. This lack of homogenity is indicated by the response of the right wing being significantly larger than the response of the left wing as shown by comparing the PSD of the right wing tip accelerometer to the PSD of the average of the two wing tips (Figure 79). Further, since the control law constrained the ailerons to act symmetrically, the strong antisymmetric responses were not attenuated by the active system. Finally, a review of films of the model flying in the turbulence showed the model resting against the upper stops on the slide rod a significant amount of time, a flying characteristic not anticipated in analytical predictions.

The RMS bending moments give an indication of the overall level of response. Table 4 presents the midspan bending moments as measured and computed. As compared to test, analysis predicts higher loads when either a one-dimensional or a two-dimensional gust representation is used.

The predicted reduction in wing RMS bending moment due to the active system is shown in Table 5. Here, using the usual one-dimensional representation for gust loads predictions, the wing passive RMS bending moment of 3.4 N-m is higher by a factor of 10 than the comparable measured value given in Table 4. It is shown also that the active system reduces the midspan RMS bending moment by over 50 percent.

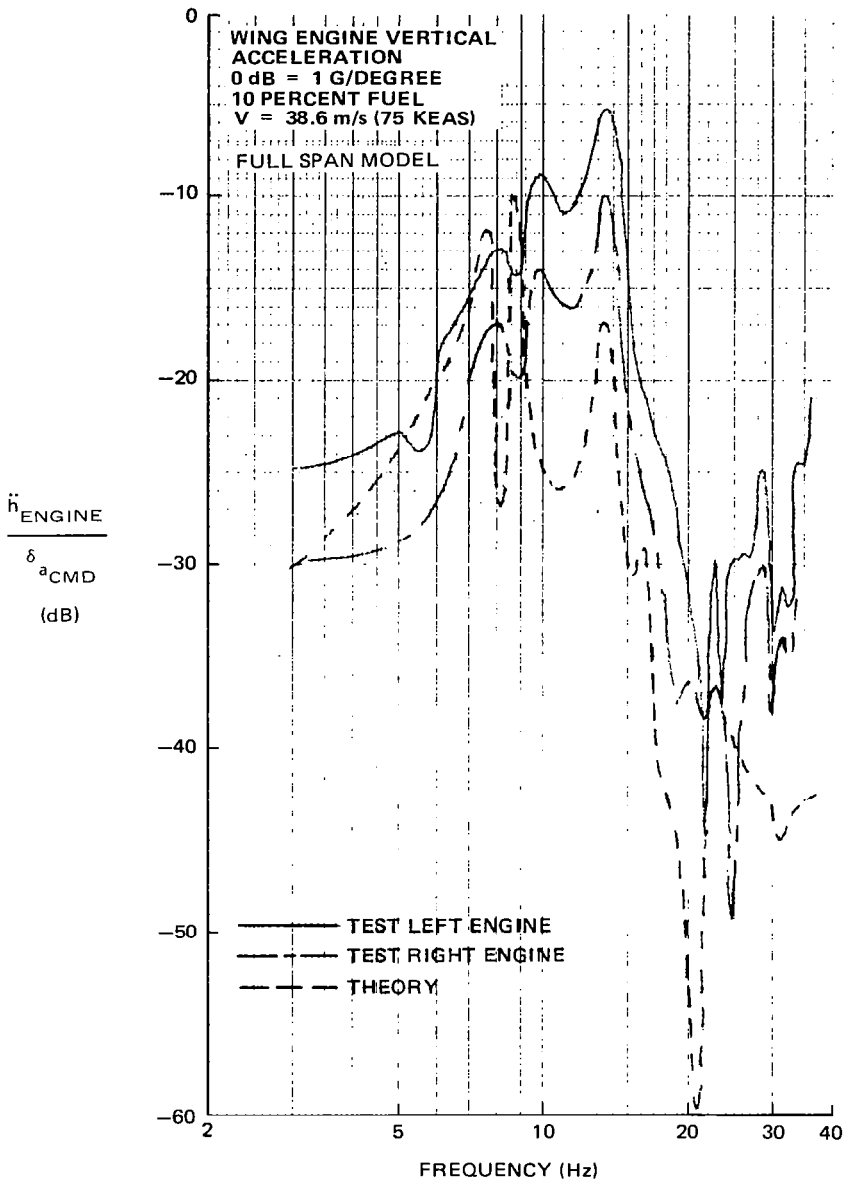

FIGURE 75. WING ENGINE VERTICAL ACCELERATION RESPONSE TO COMMANDED AILERON EXCITATION

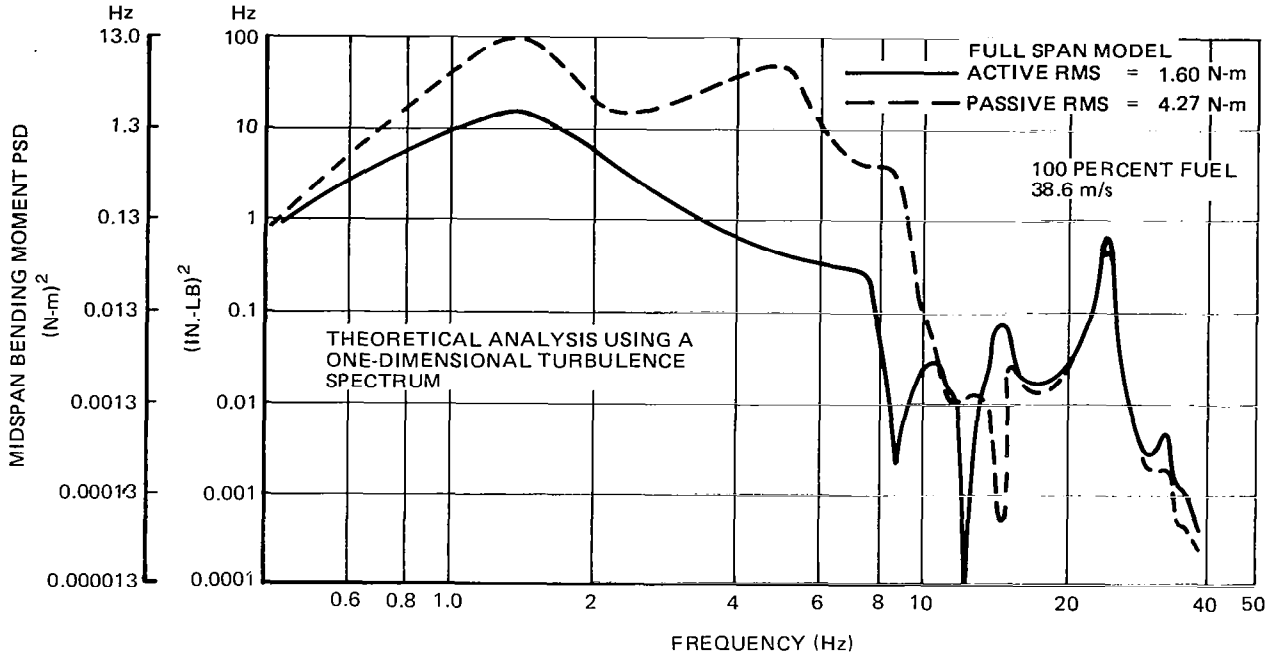

FIGURE 76. THEORETICAL MIDSPAN BENDING MOMENT POWER SPECTRAL DENSITY USING A ONE-DIMENSIONAL TURBULENCE SPECTRUM

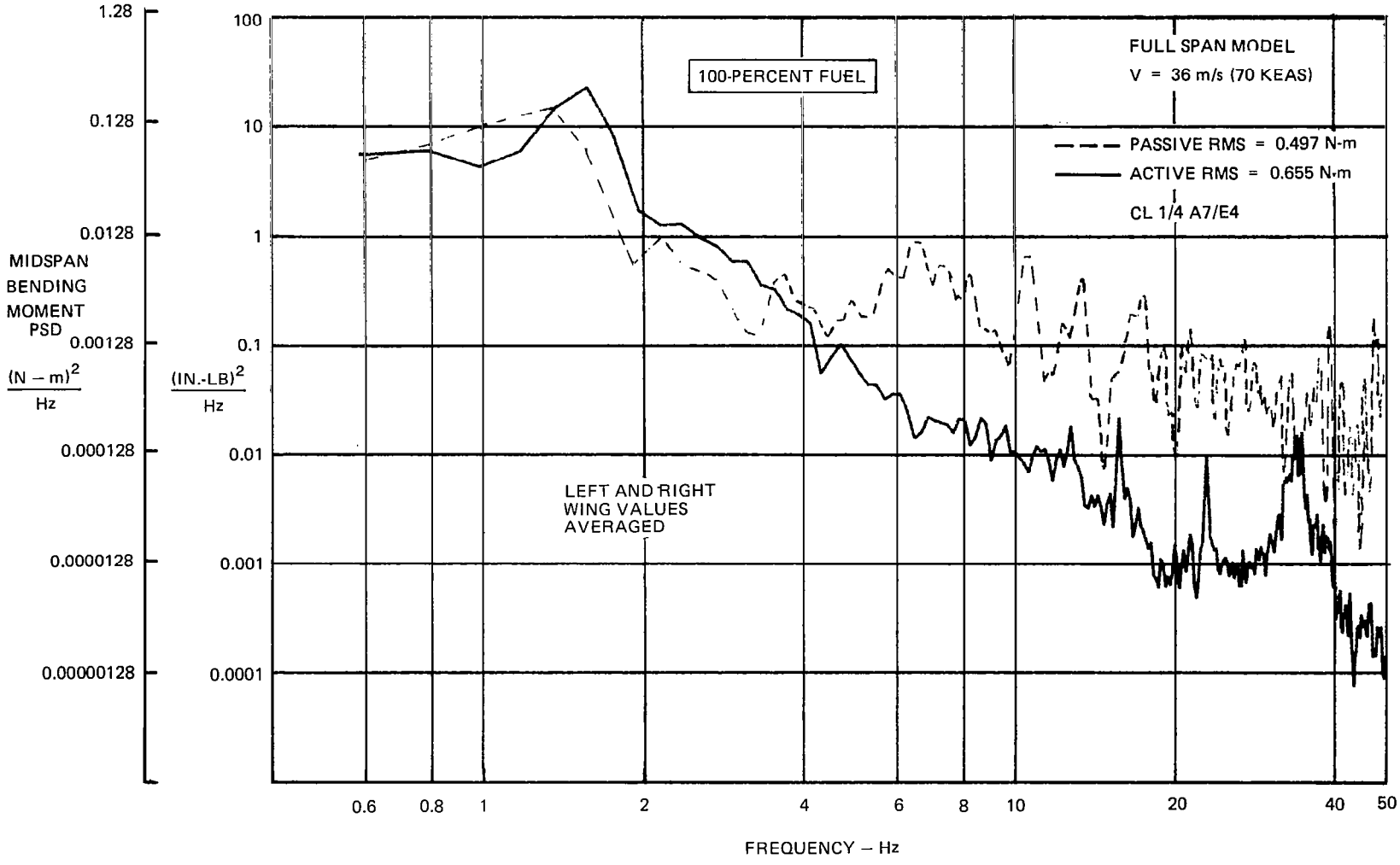

FIGURE 77. MIDSPAN BENDING MOMENT PSD DUE TO TURBULENCE – 100-PERCENT FUEL

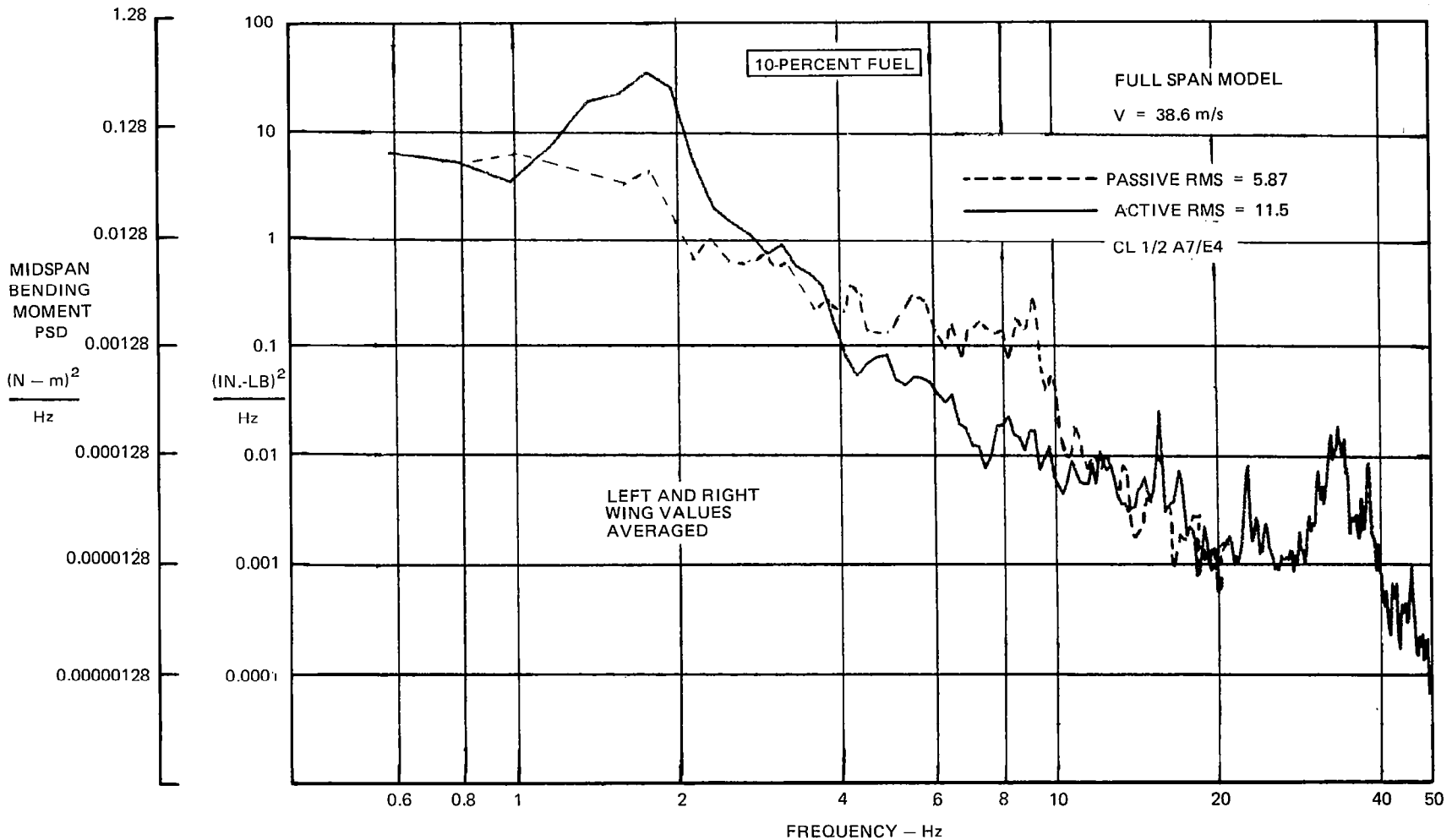

FIGURE 78. MIDSPAN BENDING MOMENT PSD DUE TO TURBULENCE – 10-PERCENT FUEL

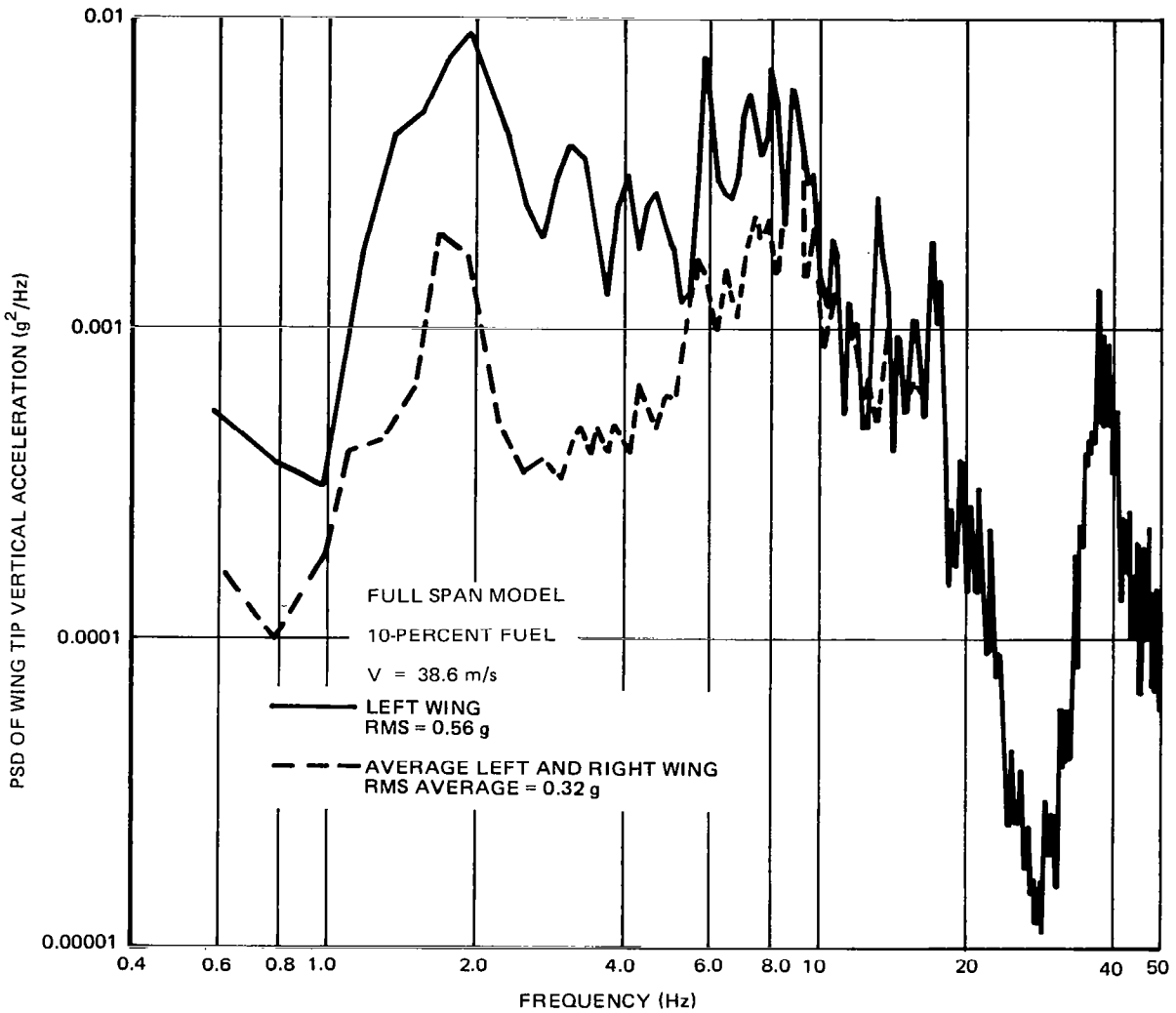

FIGURE 79. WING TIP VERTICAL ACCELERATION PSD DUE TO TURBULENCE

TABLE 4
MIDSPAN BENDING MOMENT COMPARISON
FULL SPAN MODEL, 10-PERCENT FUEL, V = 38.6 m/s

DATA	RMS(NEWTON-METERS)
One-Dimensional Analysis	3.398
Two-Dimensional Analysis	1.520
Measured (Right Side)	0.663
Measured (Averaged both sides)	0.331

TABLE 5
REDUCTIONS IN RMS BENDING MOMENT
FULL SPAN MODEL, V = 38.6 m/s
ONE-DIMENSIONAL ANALYSIS
10% FUEL

	LOCATION		PERCENT REDUCTION	
	MIDSPAN	OUTBOARD	MIDSPAN	OUTBOARD
Passive	3.398	0.573	-	-
Active	1.495	0.262	56	54

100% FUEL

Passive	4.27	0.62	-	-
Active	1.60	0.41	63	34

CONCLUSIONS

In general, the main objectives of the program were met:

1. The ability to increase flutter speed of the first critical flutter mode by using a relatively simple control system and control law was demonstrated on both models. For the semispan model, the flutter speed for the critical 10-percent fuel condition was increased by about 19 percent over the passive flutter speed; for the full-span model, the first critical flutter mode (12 Hz) was suppressed entirely. A second flutter mode (23 Hz) became unstable for the full-span model at speeds above the passive flutter speed for the basic 12-Hz mode, and an attempt to control this mode using a notch filter was unsuccessful. Also unsuccessful was an attempt to suppress a flutter mode that crossed sharply into the unstable region, as induced on the full-span model by adding weights behind the wing tips.

2. The active control system was also able, for the most part, to significantly reduce the gust loads caused by turbulence induced in the tunnel. There was one notable exception: contrary to analytical predictions, the active system actually increased the structural loads caused by short-period motion of the full-span model. This was believed to be the result of the effects of the model support system, which was not accounted for in the analyses.

3. For the flutter tests, the agreement between the analytical predictions and the mode shapes, frequencies, damping values, and transfer functions measured in the tests was generally good. For the gust load alleviation tests, the relative change in model resonse to turbulence was in agreement with analysis for the semispan model, but not for the full-span model. This was partly because of the simplistic model used to describe the turbulence field. The usual one-dimensional model of the turbulence gave predictions of higher gust loads than occurred. The predictions were better using a two-dimensional model, but were still not completely satisfactory.

4. Valuable engineering experience was obtained in the design, development, and testing of active control flexible models and related servo-system hardware and equipment.

APPENDIX A

BASIC DATA

Structural and aerodynamic data used to derive the analytical representation of the models are presented on the following pages. Figure A-1 presents the coordinate system and sign convention geometry used in analyses. Figures A-2 through A-6 and Tables A-1 through A-3 present geometrical data. Figures A-7 through A-12 present stiffness data. Tables A-4 through A-21 present mass data and Table A-22 presents aerodynamic correction factors.

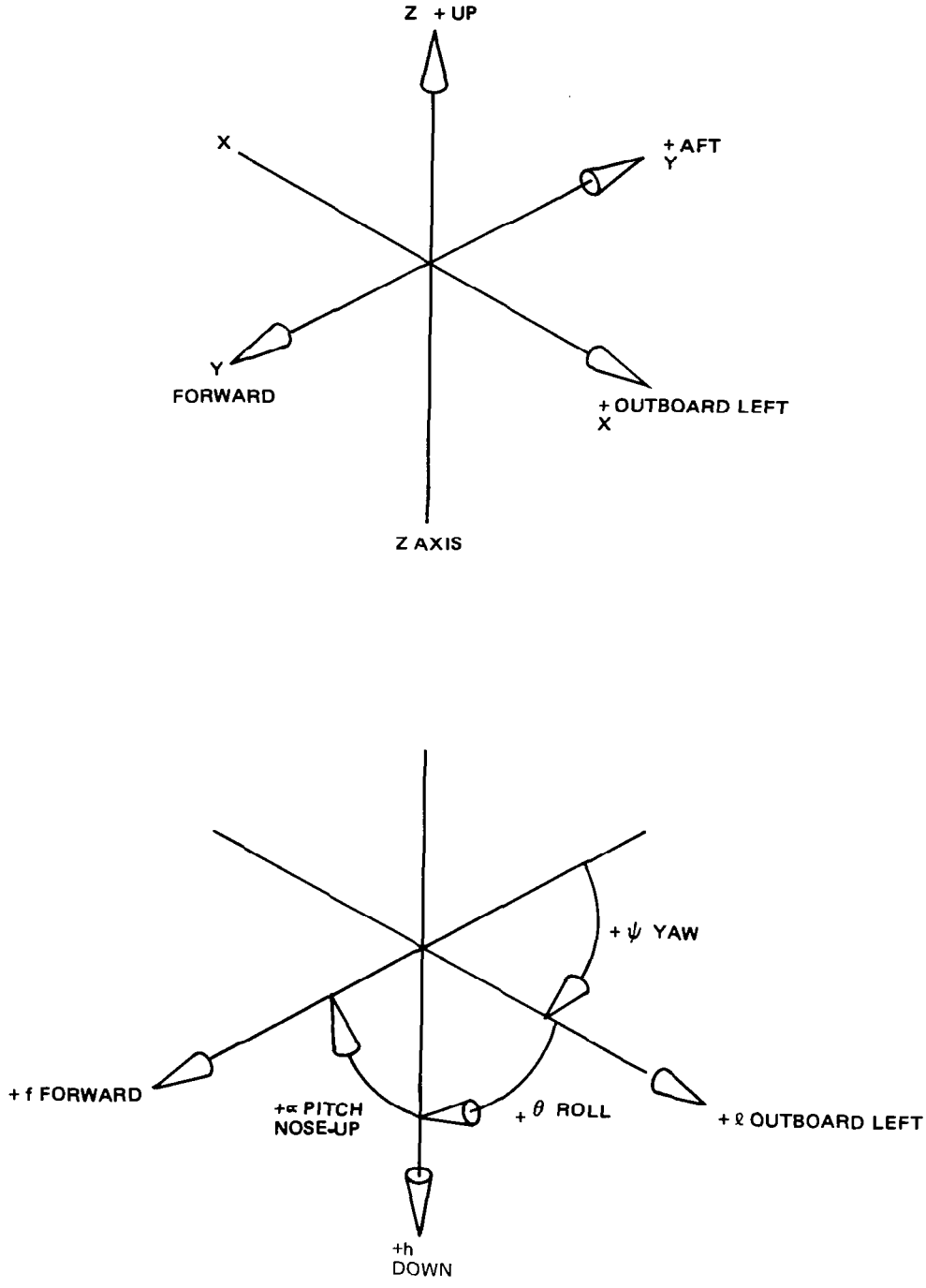

FIGURE A-1. ANALYTICAL SIGN CONVENTIONS AND COORDINATE SYSTEM

Λ_{EA} = 33.2264°
SPAR DIHEDRAL = 3.2333°
X_{EA} = 0.030 X_W

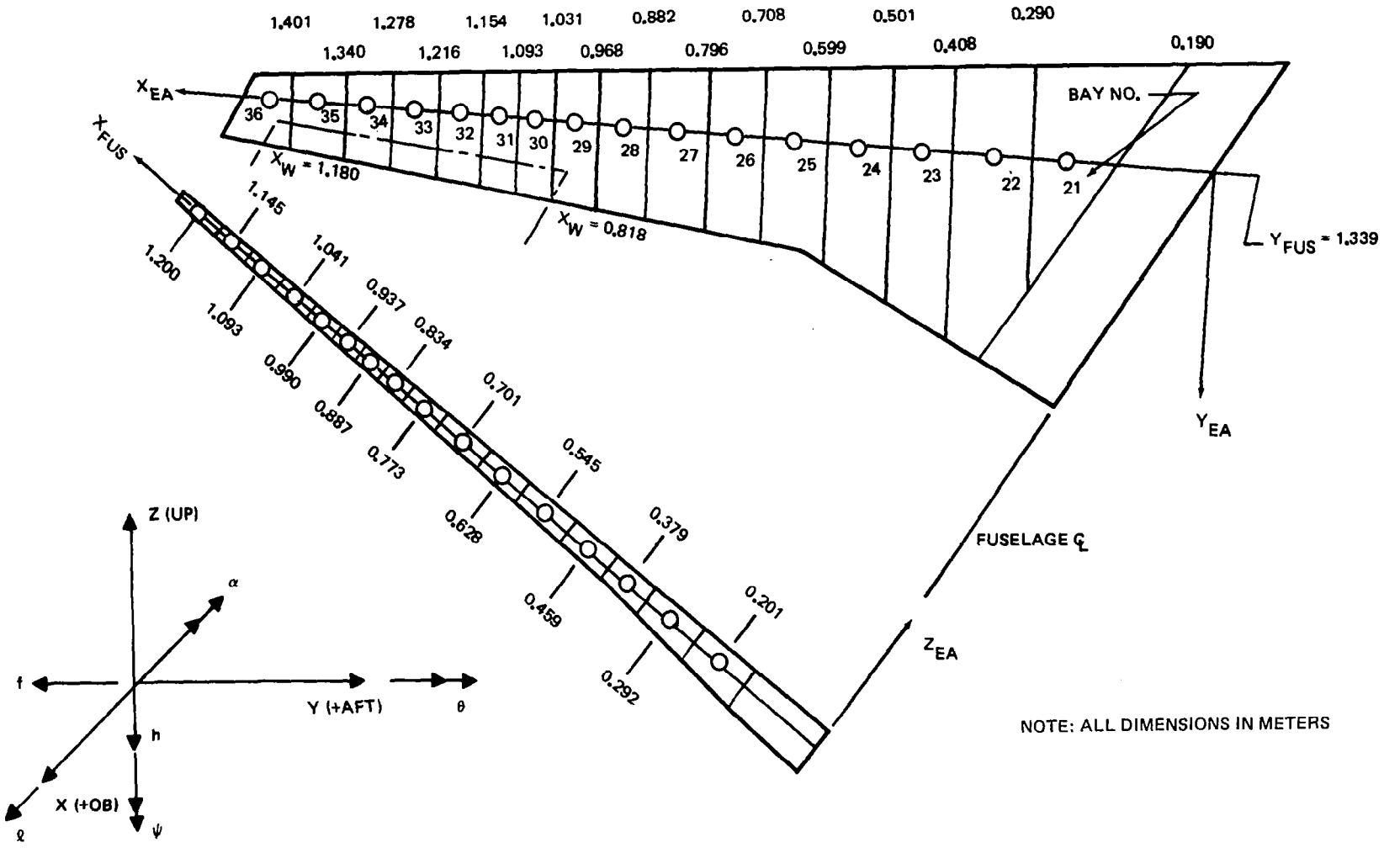

NOTE: ALL DIMENSIONS IN METERS

FIGURE A-2. WING BAY REFERENCE STATIONS

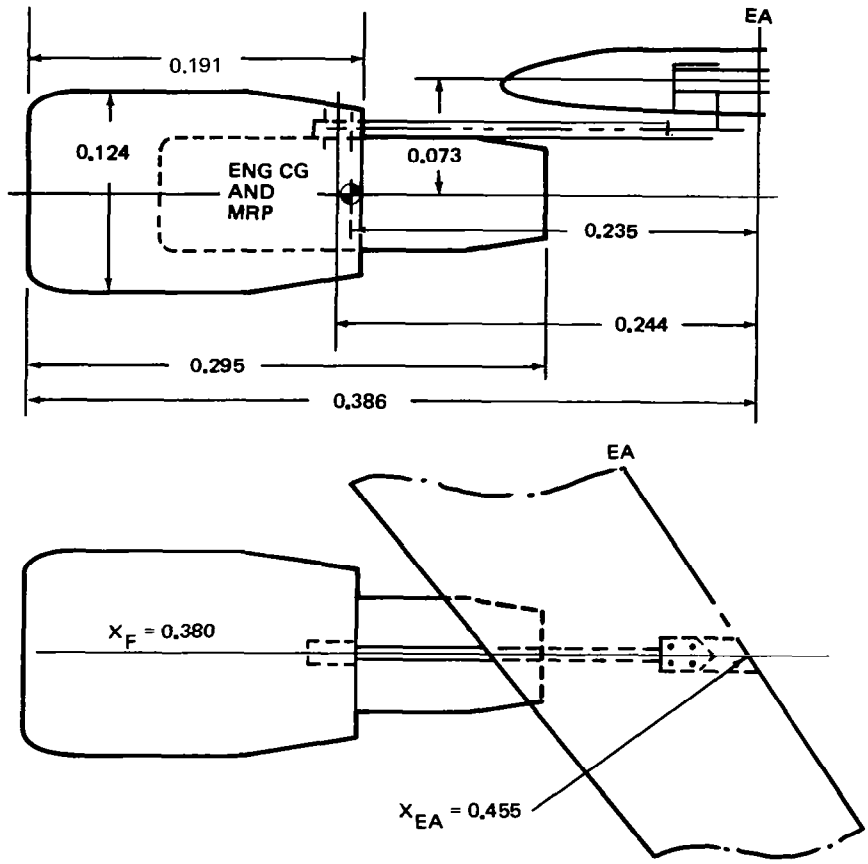

FIGURE A-3. WING ENGINE NACELLE GEOMETRY

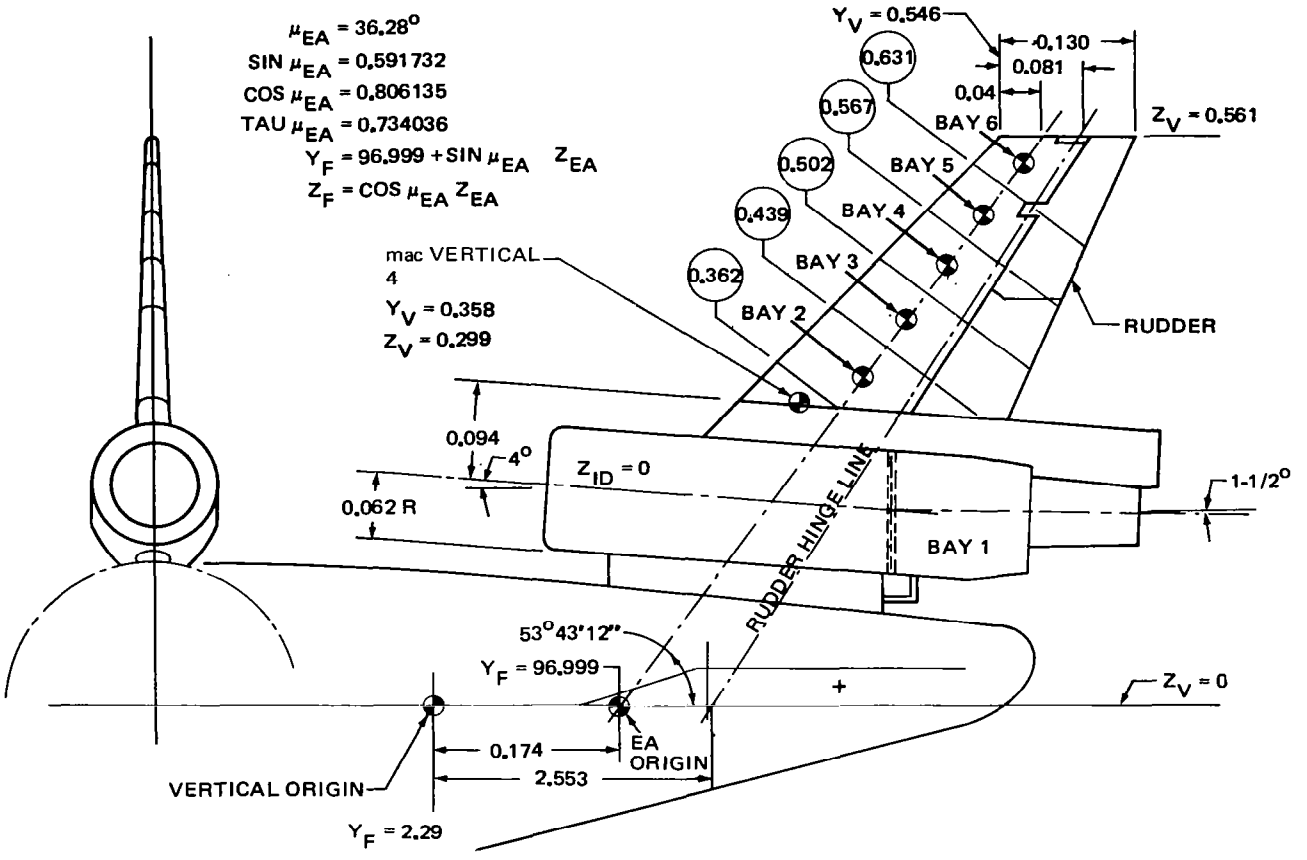

FIGURE A-4. VERTICAL STABILIZER GEOMETRY

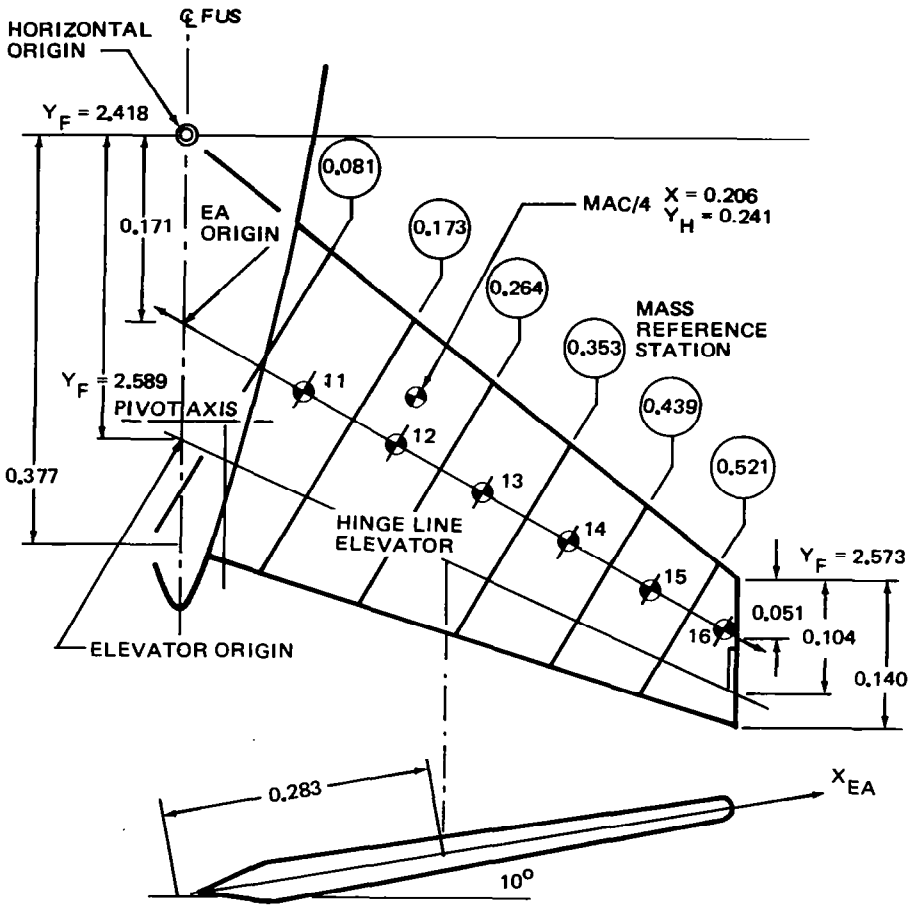

FIGURE A-5. HORIZONTAL STABILIZER GEOMETRY

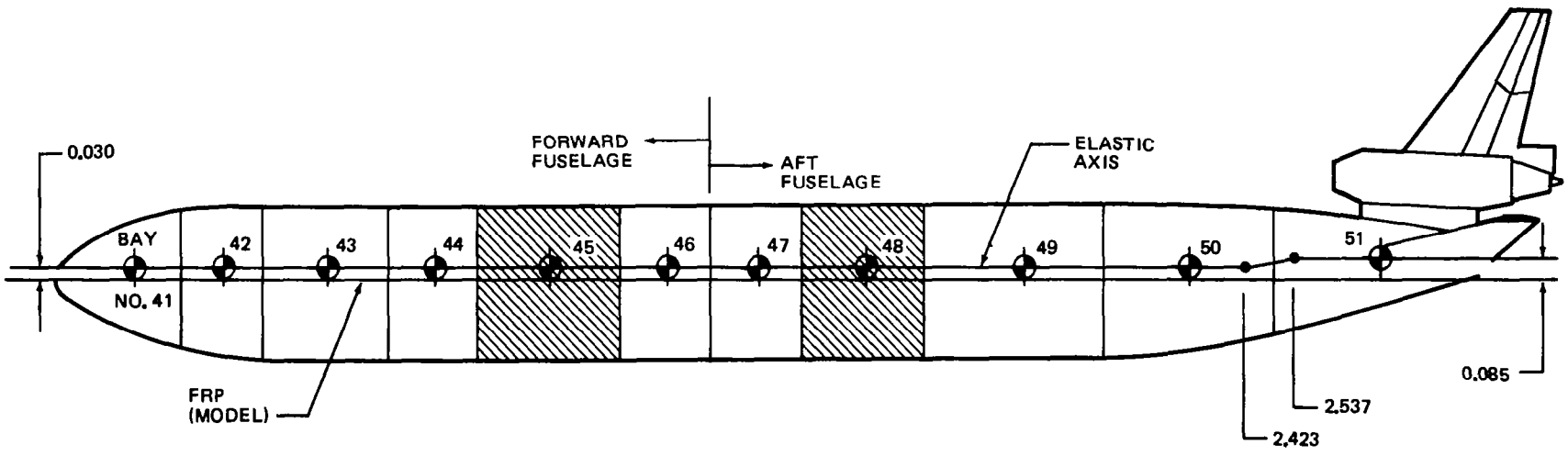

BAY NO.	REFERENCE AXIS		FUSELAGE COORDINATES		
	STATION (M)	LIMITS	X(+LT)	Y(+AFT)	Z(+UP)
41	0.151	−0.019 – 0.238	0	0.148	0
42	0.328	0.238 – 0.410	0	0.326	0
43	0.543	0.410 – 0.673	0	0.543	0
44	0.766	0.673 – 0.856	0	0.766	0
45	1.01	0.856 – 1.153	0	1.006	0
46	1.25	1.153 – 1.339	0	1.245	0
47	1.43	1.339 – 1.523	0	1.431	0
48	1.65	1.523 – 1.762	0	1.649	0
49	1.86	1.762 – 2.144	0	1.856	0
50	2.32	2.144 – 2.490	0	2.319	0
51	2.72	2.490 – 2.909	0	2.720	0.054

FIGURE A-6. FUSELAGE BAY LIMITS

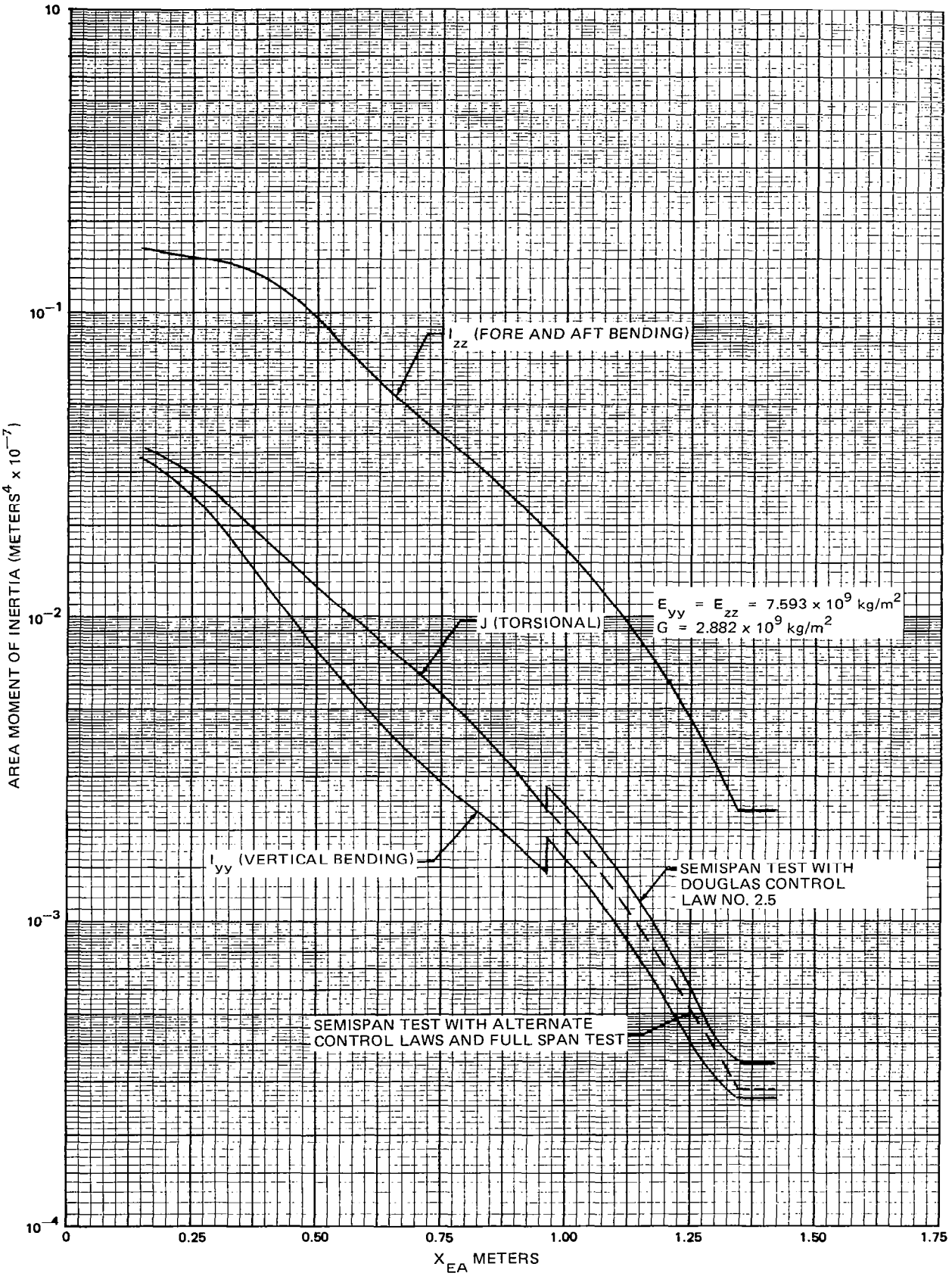

FIGURE A-7. WING SECTION PROPERTIES ALONG X_{EA}

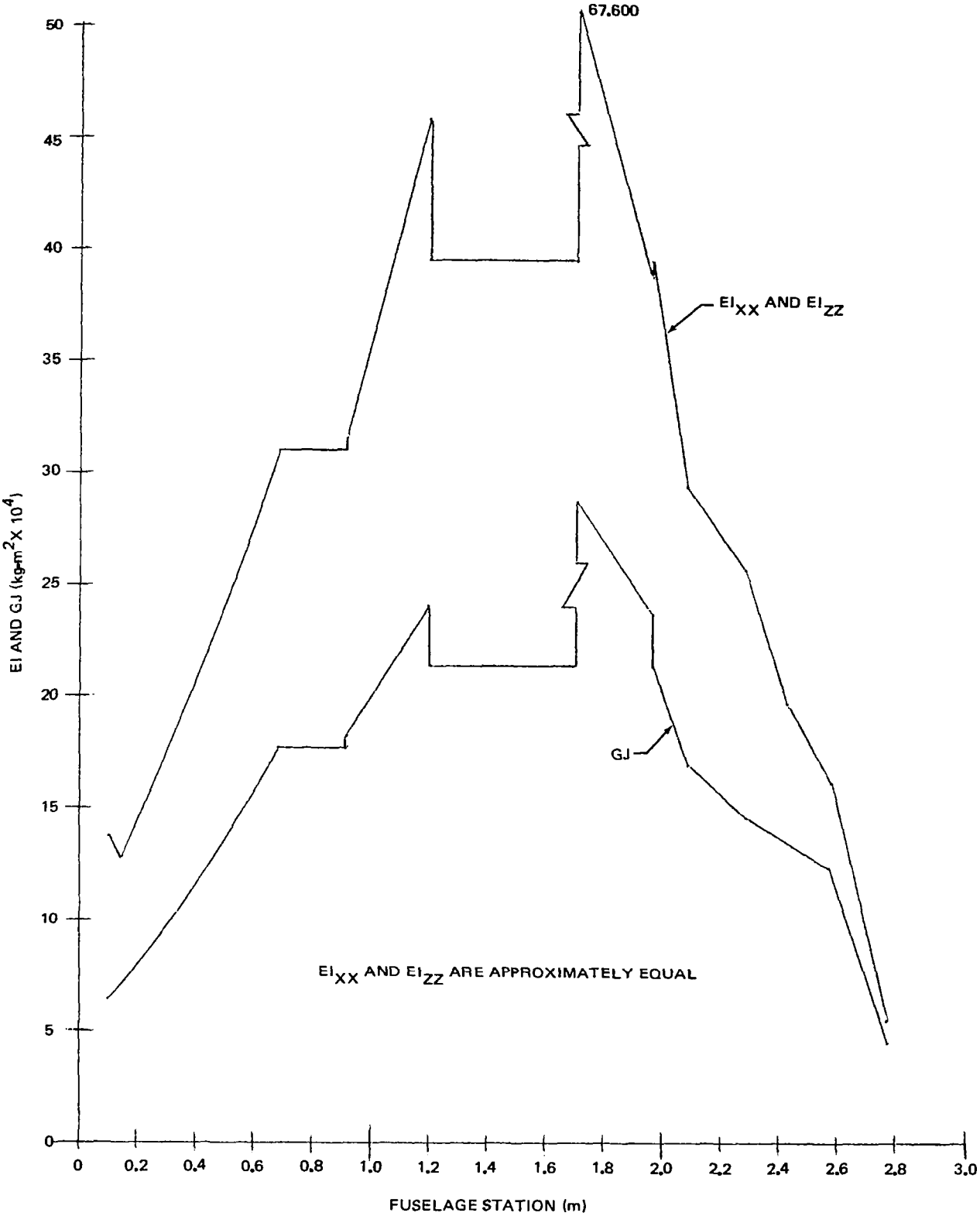

FIGURE A-8. FUSELAGE STIFFNESS PROPERTIES

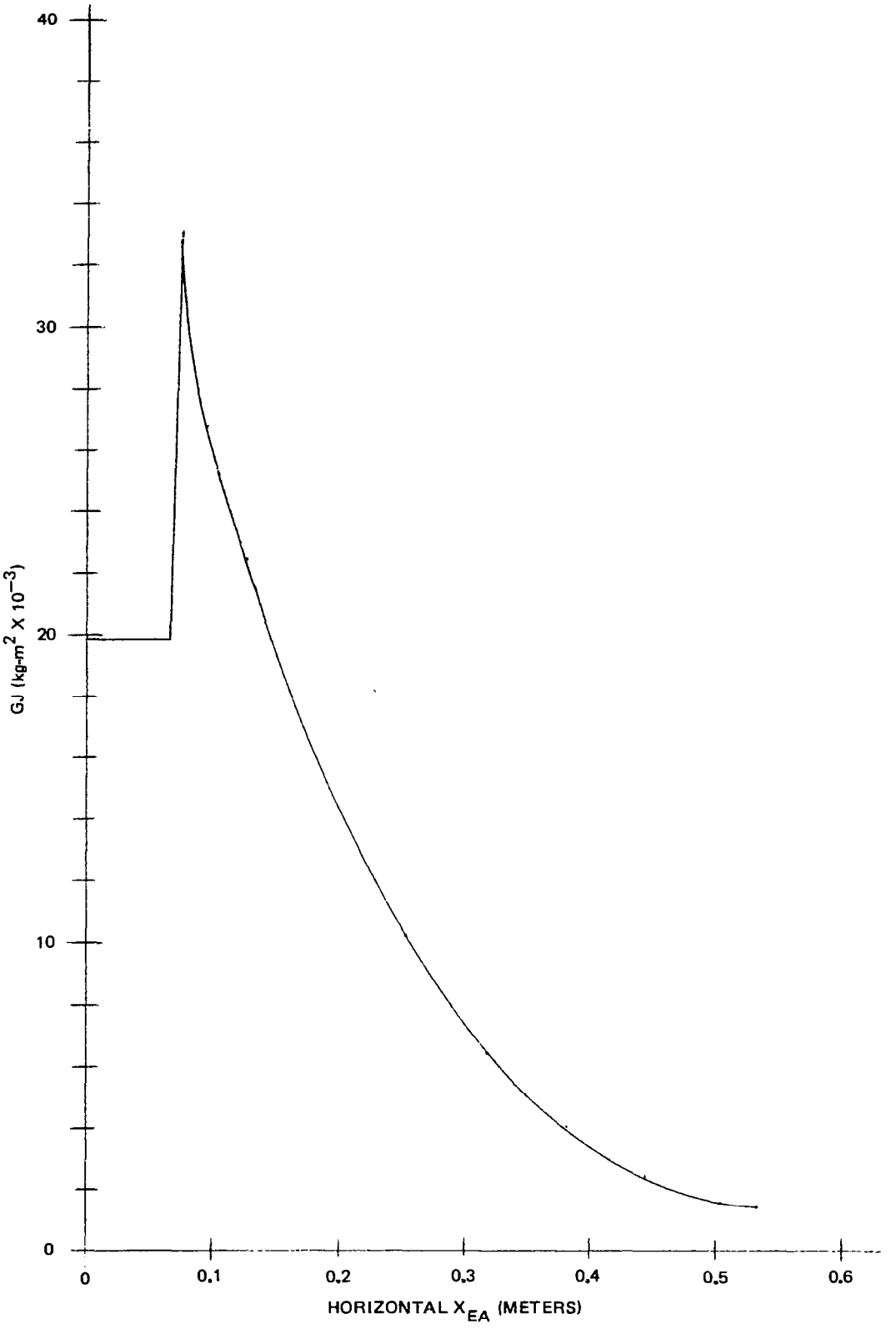

FIGURE A-9. HORIZONTAL STABILIZER STIFFNESS – GJ VERSUS X_{EA}

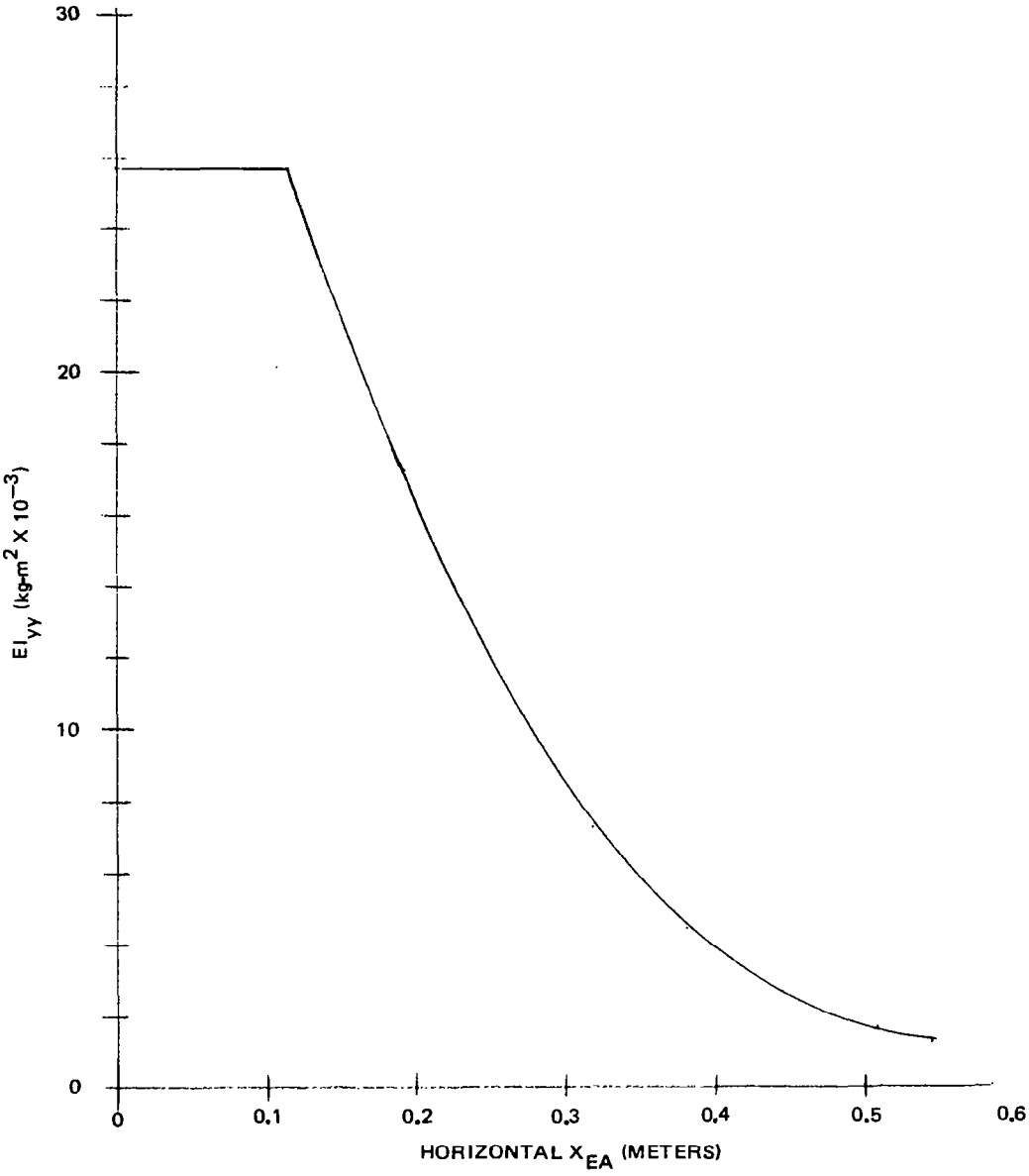

FIGURE A-10. HORIZONTAL STABILIZER STIFFNESS – EI_{yy} VERSUS X_{EA}

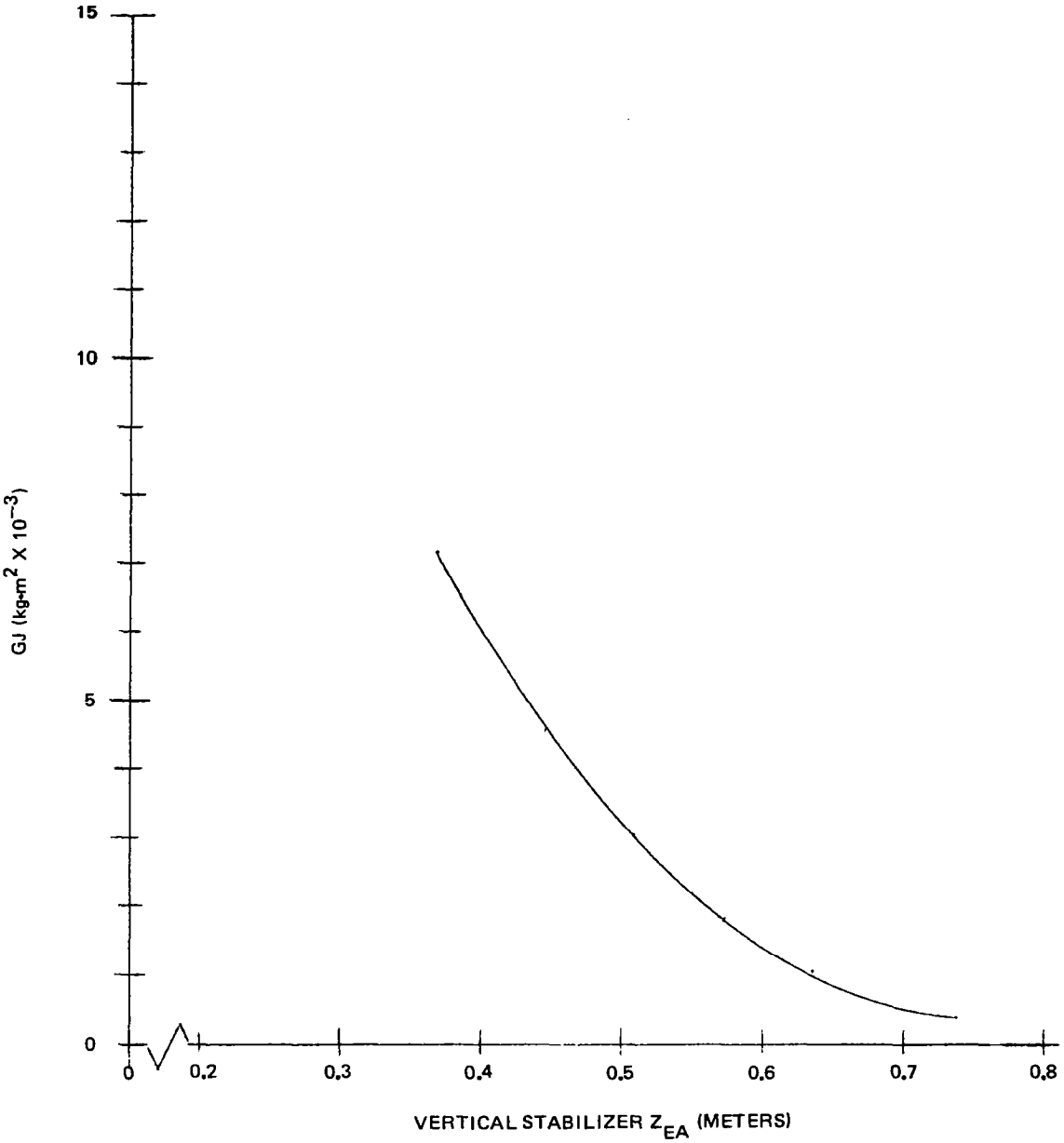

FIGURE A-11. VERTICAL STABILIZER STIFFNESS – GJ VERSUS Z_{EA}

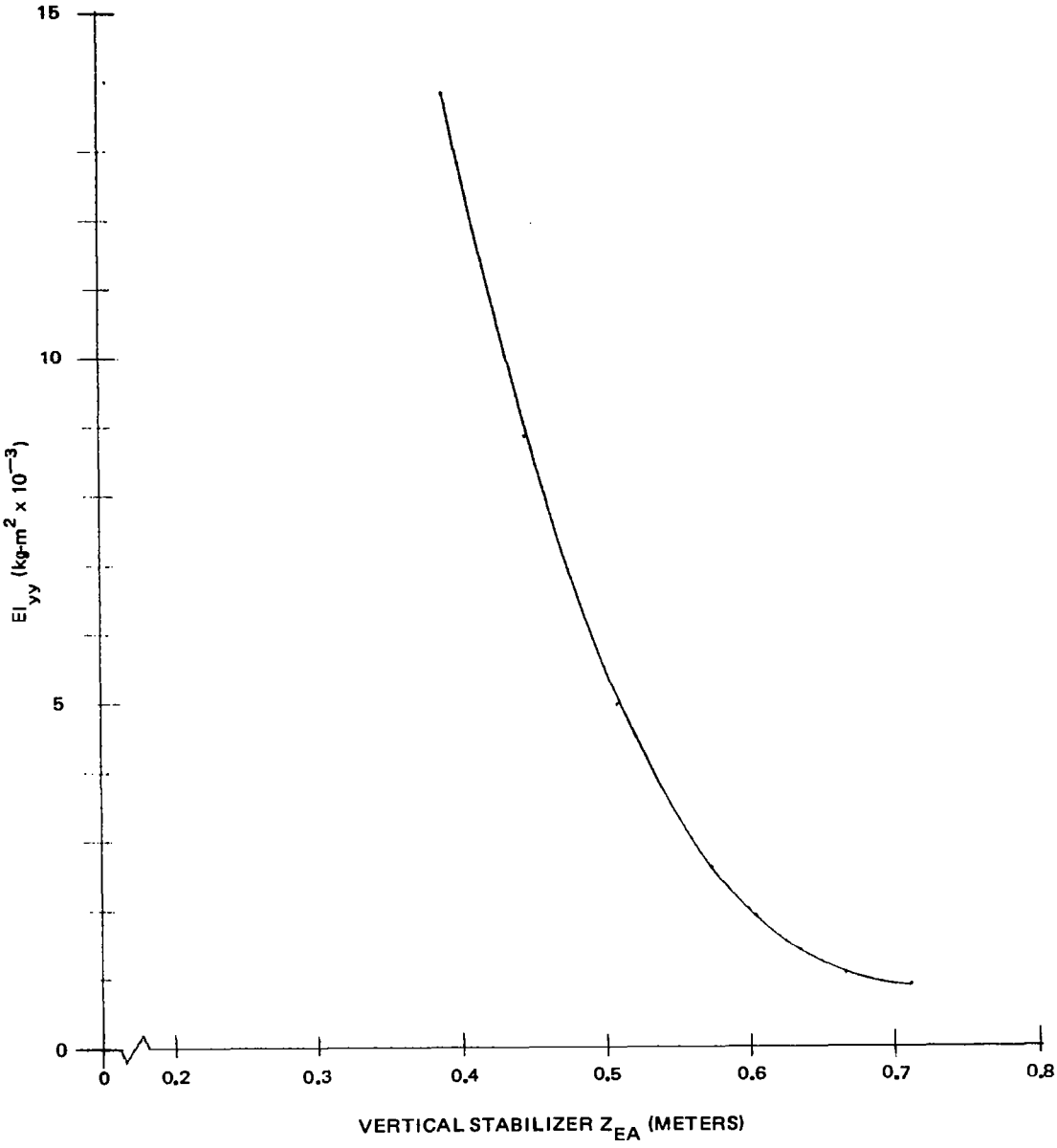

FIGURE A-12. VERTICAL STABILIZER STIFFNESS – EI_{yy} VERSUS Z_{EA}

Table A-1

Wing Bay Reference Stations

REFERENCE AXIS			FUSELAGE COORDINATES		
BAY	STATION	LIMITS	X	Y	Z
21	0.240	0.190 - 0.290	0.200	1.470	-0.064
22	0.350	0.290 - 0.408	0.292	1.531	-0.058
23	0.455	0.408 - 0.501	0.380	1.589	-0.053
24	0.550	0.501 - 0.599	0.459	1.640	-0.049
25	0.653	0.599 - 0.708	0.545	1.700	-0.044
26	0.751	0.708 - 0.796	0.627	1.751	-0.039
27	0.839	0.796 - 0.882	0.701	1.799	-0.035
28	0.926	0.882 - 0.968	0.773	1.846	-0.031
29	0.999	0.968 - 1.031	0.834	1.886	-0.028
30	1.062	1.031 - 1.093	0.887	1.921	-0.025
31	1.124	1.093 - 1.154	0.939	1.955	-0.022
32	1.185	1.154 - 1.216	0.990	1.989	-0.019
33	1.247	1.216 - 1.278	1.043	2.022	-0.016
34	1.309	1.278 - 1.340	1.093	2.056	-0.013
35	1.371	1.340 - 1.401	1.145	2.090	-0.010
36	1.437	1.401 - 1.473	1.200	2.126	-0.007

Coordinate Transformation

$$\begin{Bmatrix} X \\ Y \\ Z \end{Bmatrix}_{FUS} = \begin{bmatrix} 0.835180 & -0.547077 & -0.056402 \\ 0.547949 & 0.836512 & 0 \\ 0.047181 & -0.030905 & 0.998408 \end{bmatrix} \begin{Bmatrix} X \\ Y \\ Z \end{Bmatrix}_{EA} + \begin{Bmatrix} 0 \\ 1.339 \\ -0.075 \end{Bmatrix}$$

$$\begin{Bmatrix} X \\ Y \\ Z \end{Bmatrix}_{EA} = \begin{bmatrix} 0.835180 & 0.547949 & 0.047181 \\ -0.547077 & 0.836512 & -0.030905 \\ -0.056402 & 0 & 0.998408 \end{bmatrix} \begin{Bmatrix} X \\ Y \\ Z \end{Bmatrix}_{FUS} + \begin{Bmatrix} -0.730 \\ -1.122 \\ 0.079 \end{Bmatrix}$$

Engine Location

$X_{EA} = 0.323$ $\quad Y_{EA} = -0.194$ $\quad Z_{EA} = -0.073$

$X_{FUS} = 0.380$ $\quad Y_{FUS} = 1.353$ $\quad Z_{FUS} = -0.127$

Table A-2

Vertical Stabilizer Bay Reference Stations

Reference Axis			Fuselage Coordinates		
Bay	Station	Limits	X	Y	Z
2	0.4005	0.3624 - 0.4386	0	2.7008	0.3229
3	0.4704	0.4386 - 0.5021	0	2.742	0.3792
4	0.5349	0.5021 - 0.5674	0	2.780	0.4312
5	0.5992	0.5674 - 0.6309	0	2.818	0.4830
6	0.6637	0.6309 - 0.6962	0	2.856	0.5349

Coordinate Transformation

$$\begin{Bmatrix} X \\ Y \\ Z \end{Bmatrix}_{EA} = \begin{bmatrix} 1.0 & 0 & 0 \\ 0 & 0.806135 & -0.591732 \\ 0 & 0.591732 & 0.806135 \end{bmatrix} \begin{Bmatrix} X \\ Y \\ Z \end{Bmatrix}_{FUS} + \begin{bmatrix} 0 \\ -1.986 \\ -1.4578 \end{bmatrix}$$

Lower Vertical Stabilizer C.G.

$X_F = 0$ $\quad Y_F = 2.5809$ $\quad Z_F = 0.15966$

Table A-3

Horizontal Stabilizer Bay Reference Stations

Reference Station			Fuselage Coordinates		
Bay	Station	Limits	X	Y	Z
1	0.1280	0.0810 - 0.175	0.1091	2.6530	0.0370
2	0.21971	0.1750 - 0.2644	0.1873	2.6989	0.05077
3	0.3089	0.2644 - 0.353	0.2633	2.7435	0.06418
4	0.3961	0.353 - 0.4389	0.3377	2.7872	0.0773176
5	0.4798	0.4389 - 0.5207	0.4091	2.829	0.0899
6	0.5569	0.5207 - 0.5722	0.4749	2.8677	0.1015

Coordinate Transformation

$$\begin{Bmatrix} X \\ Y \\ Z \end{Bmatrix}_{EA} = \begin{bmatrix} 0.852616 & 0.500444 & 0.150339 \\ -0.492841 & 0.865769 & -0.086901 \\ -0.173648 & 0 & 0.984808 \end{bmatrix} \begin{Bmatrix} X \\ Y \\ Z \end{Bmatrix}_{F} + \begin{bmatrix} -1.1724 \\ -2.0222 \\ -0.0175 \end{bmatrix}$$

Table A-4

Engine Mass Properties and
Cantilevered Pylon Frequencies

Engine Mass Properties

WEIGHT - kg		0.927
C.G.	X_{FUS}-m	0.3804 Outboard from fuselage and to engine
	Y_{FUS}-m	0.2428 Forward from wing elastic axis to engine C.G.
	Z - m	-0.073 Down from wing elastic axis to engine c.g.
I_{PITCH} - kg-m^2 ABOUT C.G.		4.6472×10^{-3}
I_{ROLL} - kg-m^2 ABOUT C.G.		8.077×10^{-4}
I_{YAW} - kg-m^2 ABOUT C.G		4.9862×10^{-3}

Cantilevered Pylon Frequencies (Hz)

	-85 PYLON	-13 PYLON
PITCH	15.3	20.6
YAW	6.2	8.89
ROLL	23.31	31.0

TABLE A-5

MODEL MASS DATA – WING ZERO FUEL

MODE NO. 664

BAY	MASS	MX	MY	MZ	IXX	IYY
21	0.42	0.0	-0.01	0.0	0.14471E-02	0.47936E-03
22	0.42	0.0	0.02	0.0	0.34110E-02	0.28713E-03
23	0.25	0.0	0.01	0.0	0.16000E-02	0.10918E-03
24	0.19	0.0	0.00	0.0	0.80418E-03	0.10693E-03
25	0.21	0.0	0.01	0.0	0.85401E-03	0.11685E-03
26	0.13	0.0	0.00	0.0	0.56691E-03	0.88989E-04
27	0.12	0.0	0.00	0.0	0.38774E-03	0.79274E-04
28	0.11	0.0	0.00	0.0	0.33445E-03	0.56917E-04
29	0.05	0.0	0.00	0.0	0.86092E-04	0.16417E-04
30	0.05	0.0	0.00	0.0	0.74123E-04	0.12729E-04
31	0.08	0.0	0.00	0.0	0.17300E-03	0.15773E-04
32	0.03	0.0	0.00	0.0	0.41437E-04	0.10418E-04
33	0.03	0.0	0.00	0.0	0.27595E-04	0.83985E-05
34	0.03	0.0	0.00	0.0	0.30141E-04	0.82815E-05
35	0.03	0.0	0.00	0.0	0.21625E-04	0.63794E-05
36	0.02	0.0	0.00	0.0	0.17880E-04	0.12642E-04

BAY	IZZ	IXY	IYZ	IXZ
21	0.19871E-02	0.0	0.0	0.0
22	0.35516E-02	0.0	0.0	0.0
23	0.16481E-02	0.0	0.0	0.0
24	0.88436E-03	0.0	0.0	0.0
25	0.95690E-03	0.0	0.0	0.0
26	0.60633E-03	0.0	0.0	0.0
27	0.42610E-03	0.0	0.0	0.0
28	0.38048E-03	0.0	0.0	0.0
29	0.10520E-03	0.0	0.0	0.0
30	0.85360E-04	0.0	0.0	0.0
31	0.18781E-03	0.0	0.0	0.0
32	0.50567E-04	0.0	0.0	0.0
33	0.35116E-04	0.0	0.0	0.0
34	0.37691E-04	0.0	0.0	0.0
35	0.27068E-04	0.0	0.0	0.0
36	0.29556E-04	0.0	0.0	0.0

NOTE:

Units of Mass: $kg/m/sec^2$

Units of Inertia: $kg\text{-}m^2/m/sec^2$

Units of Unbalance: $kg\text{-}m/m/sec^2$

TABLE A-6
MODEL MASS DATA — 10-PERCENT WING FUEL

MODE NO. 1450

BAY	MASS	MX	MY	MZ	IXX	IYY
21	0.59	0.0	0.00	0.0	0.33512E-02	0.66910E-03
22	0.61	0.0	0.02	0.0	0.40040E-02	0.41606E-03
23	0.40	0.0	0.01	0.0	0.18687E-02	0.17350E-03
24	0.20	0.0	0.00	0.0	0.88588E-03	0.11661E-03
25	0.21	0.0	0.01	0.0	0.88890E-03	0.11913E-03
26	0.13	0.0	0.00	0.0	0.56691E-03	0.88989E-04
27	0.12	0.0	0.00	0.0	0.38774E-03	0.79274E-04
28	0.13	0.0	0.00	0.0	0.33445E-03	0.56917E-04
29	0.07	0.0	0.00	0.0	0.86092E-04	0.16417E-04
30	0.05	0.0	0.00	0.0	0.74123E-04	0.12729E-04
31	0.08	0.0	0.00	0.0	0.17300E-03	0.15773E-04
32	0.03	0.0	0.00	0.0	0.41437E-04	0.10418E-04
33	0.03	0.0	0.00	0.0	0.27595E-04	0.83985E-05
34	0.04	0.0	0.00	0.0	0.32189E-04	0.82815E-05
35	0.03	0.0	0.00	0.0	0.21625E-04	0.63794E-05
36	0.02	0.0	0.00	0.0	0.17880E-04	0.12642E-04

BAY	IZZ	IXY	IYZ	IXZ
21	0.27733E-02	0.0	0.0	0.0
22	0.51453E-02	0.0	0.0	0.0
23	0.26199E-02	0.0	0.0	0.0
24	0.96454E-03	0.0	0.0	0.0
25	0.97549E-03	0.0	0.0	0.0
26	0.45191E-03	0.0	0.0	0.0
27	0.35640E-03	0.0	0.0	0.0
28	0.27197E-03	0.0	0.0	0.0
29	0.88989E-04	0.0	0.0	0.0
30	0.76757E-04	0.0	0.0	0.0
31	0.12844E-03	0.0	0.0	0.0
32	0.49923E-04	0.0	0.0	0.0
33	0.35086E-04	0.0	0.0	0.0
34	0.35525E-04	0.0	0.0	0.0
35	0.26981E-04	0.0	0.0	0.0
36	0.28532E-04	0.0	0.0	0.0

NOTE:

Units of Mass: $kg/m/sec^2$
Units of Inertia: $kg\text{-}m^2/m/sec^2$
Units of Unbalance: $kg\text{-}m/m/sec^2$

TABLE A-7

MODEL MASS DATA – 10-PERCENT WING FUEL PLUS 20-GRAM TIP WEIGHT

MODE NO.	1574					
BAY	MASS	MX	MY	MZ	IXX	IYY
21	0.59	0.0	0.00	0.0	0.33521E-02	0.66928E-03
22	0.61	0.0	0.02	0.0	0.40050E-02	0.41618E-03
23	0.40	0.0	0.01	0.0	0.18692E-02	0.17356E-03
24	0.20	0.0	0.00	0.0	0.88612E-03	0.11664E-03
25	0.21	0.0	0.01	0.0	0.88913E-03	0.11916E-03
26	0.13	0.0	0.00	0.0	0.56691E-03	0.88989E-04
27	0.12	0.0	0.00	0.0	0.38774E-03	0.79274E-04
28	0.11	0.0	0.00	0.0	0.33445E-03	0.56917E-04
29	0.05	0.0	0.00	0.0	0.86092E-04	0.16417E-04
30	0.05	0.0	0.00	0.0	0.74123E-04	0.12729E-04
31	0.08	0.0	0.00	0.0	0.17300E-03	0.15773E-04
32	0.03	0.0	0.00	0.0	0.41437E-04	0.10418E-04
33	0.03	0.0	0.00	0.0	0.27595E-04	0.83985E-05
34	0.03	0.0	0.00	0.0	0.30141E-04	0.82815E-05
35	0.03	0.0	0.00	0.0	0.21625E-04	0.63794E-05
36	0.04	0.00	0.00	0.0	0.34262E-03	0.15201E-03

BAY	IZZ	IXY	IYZ	IXZ
21	0.27740E-02	0.0	0.0	0.0
22	0.51467E-02	0.0	0.0	0.0
23	0.26205E-02	0.0	0.0	0.0
24	0.96480E-03	0.0	0.0	0.0
25	0.97575E-03	0.0	0.0	0.0
26	0.60633E-03	0.0	0.0	0.0
27	0.42610E-03	0.0	0.0	0.0
28	0.38048E-03	0.0	0.0	0.0
29	0.10520E-03	0.0	0.0	0.0
30	0.85360E-04	0.0	0.0	0.0
31	0.18781E-03	0.0	0.0	0.0
32	0.50567E-04	0.0	0.0	0.0
33	0.35116E-04	0.0	0.0	0.0
34	0.37691E-04	0.0	0.0	0.0
35	0.27068E-04	0.0	0.0	0.0
36	0.49367E-03	0.21274E-03	0.0	0.0

NOTE:

Units of Mass: $kg/m/sec^2$

Units of Inertia: $kg\text{-}m^2/m/sec^2$

Units of Unbalance: $kg\text{-}m/m/sec^2$

TABLE A-8
MODEL MASS DATA – 21.5 PERCENT WING FUEL

MODE NO. 1015 BAY	MASS	MX	MY	MZ	IXX	IYY
21	0.74	0.0	0.01	0.0	0.41656E-02	0.83830E-03
22	0.64	0.0	0.03	0.0	0.41899E-02	0.43915E-03
23	0.41	0.0	0.01	0.0	0.19341E-02	0.17520E-03
24	0.21	0.0	0.00	0.0	0.86592E-03	0.11881E-03
25	0.21	0.0	0.01	0.0	0.88796E-03	0.11913E-03
26	0.13	0.0	0.00	0.0	0.56691E-03	0.88989E-04
27	0.12	0.0	0.00	0.0	0.38774E-03	0.79274E-04
28	0.11	0.0	0.00	0.0	0.33445E-03	0.56917E-04
29	0.17	0.0	0.00	0.0	0.16504E-03	0.59141E-04
30	0.15	0.0	0.00	0.0	0.12908E-03	0.48665E-04
31	0.16	0.0	0.00	0.0	0.27417E-03	0.40588E-04
32	0.10	0.0	0.00	0.0	0.73070E-04	0.34706E-04
33	0.08	0.0	0.00	0.0	0.43192E-04	0.29819E-04
34	0.07	0.0	0.00	0.0	0.39856E-04	0.21830E-04
35	0.06	0.0	0.00	0.0	0.28649E-04	0.16914E-04
36	0.02	0.0	0.00	0.0	0.17880E-04	0.12642E-04

BAY	IZZ	IXY	IYZ	IXZ
21	0.34751E-02	0.0	0.0	0.0
22	0.54319E-02	0.0	0.0	0.0
23	0.26448E-02	0.0	0.0	0.0
24	0.98263E-03	0.0	0.0	0.0
25	0.97569E-03	0.0	0.0	0.0
26	0.60633E-03	0.0	0.0	0.0
27	0.42610E-03	0.0	0.0	0.0
28	0.38048E-03	0.0	0.0	0.0
29	0.24657E-03	0.0	0.0	0.0
30	0.17063E-03	0.0	0.0	0.0
31	0.29851E-03	0.0	0.0	0.0
32	0.10421E-03	0.0	0.0	0.0
33	0.68154E-04	0.0	0.0	0.0
34	0.59902E-04	0.0	0.0	0.0
35	0.43836E-04	0.0	0.0	0.0
36	0.29556E-04	0.0	0.0	0.0

NOTE:

Units of Mass: $kg/m/sec^2$
Units of Inertia: $kg\text{-}m^2/m/sec^2$
Units of Unbalance: $kg\text{-}m/m/sec^2$

TABLE A-9

MODEL MASS DATA – 40 PERCENT WING FUEL

MODE NO.	1008					
BAY	MASS	MX	MY	MZ	IXX	IYY
21	1.02	0.0	0.01	0.0	0.65691E-02	0.11598E-02
22	0.83	0.0	0.03	0.0	0.46891E-02	0.56800E-03
23	0.60	0.0	0.01	0.0	0.21740E-02	0.25974E-03
24	0.40	0.0	0.01	0.0	0.10812E-02	0.22805E-03
25	0.34	0.0	0.01	0.0	0.98737E-03	0.19047E-03
26	0.15	0.0	0.00	0.0	0.60929E-03	0.10251E-03
27	0.12	0.0	0.00	0.0	0.38774E-03	0.79274E-04
28	0.11	0.0	0.00	0.0	0.33445E-03	0.56917E-04
29	0.17	0.0	0.00	0.0	0.16504E-03	0.59141E-04
30	0.15	0.0	0.00	0.0	0.12908E-03	0.48665E-04
31	0.16	0.0	0.00	0.0	0.27417E-03	0.40588E-04
32	0.10	0.0	0.00	0.0	0.73070E-04	0.34706E-04
33	0.08	0.0	0.00	0.0	0.43192E-04	0.29819E-04
34	0.07	0.0	0.00	0.0	0.39856E-04	0.21830E-04
35	0.06	0.0	0.00	0.0	0.28649E-04	0.16914E-04
36	0.02	0.0	0.00	0.0	0.17880E-04	0.12642E-04

BAY	IZZ	IXY	IYZ	IXZ
21	0.48076E-02	0.0	0.0	0.0
22	0.70256E-02	0.0	0.0	0.0
23	0.39207E-02	0.0	0.0	0.0
24	0.18863E-02	0.0	0.0	0.0
25	0.15599E-02	0.0	0.0	0.0
26	0.61555E-03	0.0	0.0	0.0
27	0.42610E-03	0.0	0.0	0.0
28	0.38048E-03	0.0	0.0	0.0
29	0.24657E-03	0.0	0.0	0.0
30	0.17063E-03	0.0	0.0	0.0
31	0.29851E-03	0.0	0.0	0.0
32	0.10421E-03	0.0	0.0	0.0
33	0.68154E-04	0.0	0.0	0.0
34	0.59902E-04	0.0	0.0	0.0
35	0.43836E-04	0.0	0.0	0.0
36	0.29556E-04	0.0	0.0	0.0

NOTE:

Units of Mass: $kg/m/sec^2$

Units of Inertia: $kg\text{-}m^2/m/sec^2$

Units of Unbalance: $kg\text{-}m/m/sec^2$

TABLE A-10
MODEL MASS DATA – 60 PERCENT WING FUEL

MODE NO. 1007

BAY	MASS	MX	MY	MZ	IXX	IYY
21	1.27	0.0	0.01	0.0	0.76723E-02	0.14356E-02
22	1.00	0.0	0.03	0.0	0.50456E-02	0.68291E-03
23	0.75	0.0	0.01	0.0	0.23243E-02	0.32263E-03
24	0.55	0.0	0.01	0.0	0.11637E-02	0.31484E-03
25	0.49	0.0	0.01	0.0	0.11046E-02	0.27712E-03
26	0.25	0.0	0.00	0.0	0.66814E-03	0.17262E-03
27	0.18	0.0	0.00	0.0	0.42671E-03	0.12489E-03
28	0.13	0.0	0.00	0.0	0.34329E-03	0.66778E-04
29	0.17	0.0	0.00	0.0	0.16504E-03	0.59141E-04
30	0.15	0.0	0.00	0.0	0.12908E-03	0.48665E-04
31	0.16	0.0	0.00	0.0	0.27417E-03	0.40588E-04
32	0.10	0.0	0.00	0.0	0.73070E-04	0.34706E-04
33	0.08	0.0	0.00	0.0	0.43192E-04	0.29819E-04
34	0.07	0.0	0.00	0.0	0.39856E-04	0.21830E-04
35	0.06	0.0	0.00	0.0	0.28649E-04	0.16914E-04
36	0.02	0.0	0.00	0.0	0.17880E-04	0.12642E-04

BAY	IZZ	IXY	IYZ	IXZ
21	0.59677E-02	0.0	0.0	0.0
22	0.84473E-02	0.0	0.0	0.0
23	0.48703E-02	0.0	0.0	0.0
24	0.26039E-02	0.0	0.0	0.0
25	0.22694E-02	0.0	0.0	0.0
26	0.11762E-02	0.0	0.0	0.0
27	0.67132E-03	0.0	0.0	0.0
28	0.44644E-03	0.0	0.0	0.0
29	0.24657E-03	0.0	0.0	0.0
30	0.17063E-03	0.0	0.0	0.0
31	0.29851E-03	0.0	0.0	0.0
32	0.10421E-03	0.0	0.0	0.0
33	0.68154E-04	0.0	0.0	0.0
34	0.59902E-04	0.0	0.0	0.0
35	0.43836E-04	0.0	0.0	0.0
36	0.29556E-04	0.0	0.0	0.0

NOTE:

Units of Mass: $kg/m/sec^2$
Units of Inertia: $kg\text{-}m^2/m/sec^2$
Units of Unbalance: $kg\text{-}m/m/sec^2$

TABLE A-11
MODEL MASS DATA – 80 PERCENT WING FUEL

MODE NO. 996

BAY	MASS	MX	MY	MZ	IXX	IYY
21	1.50	0.0	0.01	0.0	0.76597E-02	0.17031E-02
22	1.15	0.0	0.03	0.0	0.53601E-02	0.78334E-03
23	0.84	0.0	0.01	0.0	0.24560E-02	0.35964E-03
24	0.67	0.0	0.01	0.0	0.12691E-02	0.38121E-03
25	0.65	0.0	0.01	0.0	0.12020E-02	0.36553E-03
26	0.38	0.0	0.00	0.0	0.73775E-03	0.25842E-03
27	0.32	0.0	0.00	0.0	0.49970E-03	0.21862E-03
28	0.20	0.0	0.00	0.0	0.39022E-03	0.10672E-03
29	0.17	0.0	0.00	0.0	0.16504E-03	0.59141E-04
30	0.15	0.0	0.00	0.0	0.12908E-03	0.48665E-04
31	0.16	0.0	0.00	0.0	0.27417E-03	0.40588E-04
32	0.10	0.0	0.00	0.0	0.73070E-04	0.34706E-04
33	0.08	0.0	0.00	0.0	0.43192E-04	0.29819E-04
34	0.07	0.0	0.00	0.0	0.39856E-04	0.21830E-04
35	0.06	0.0	0.00	0.0	0.28649E-04	0.16914E-04
36	0.02	0.0	0.00	0.0	0.17880E-04	0.12642E-04

BAY	IZZ	IXY	IYZ	IXZ
21	0.70597E-02	0.0	0.0	0.0
22	0.96894E-02	0.0	0.0	0.0
23	0.54289E-02	0.0	0.0	0.0
24	0.31529E-02	0.0	0.0	0.0
25	0.29934E-02	0.0	0.0	0.0
26	0.17608E-02	0.0	0.0	0.0
27	0.11752E-02	0.0	0.0	0.0
28	0.71349E-03	0.0	0.0	0.0
29	0.24657E-03	0.0	0.0	0.0
30	0.17063E-03	0.0	0.0	0.0
31	0.29851E-03	0.0	0.0	0.0
32	0.10421E-03	0.0	0.0	0.0
33	0.68154E-04	0.0	0.0	0.0
34	0.59902E-04	0.0	0.0	0.0
35	0.43836E-04	0.0	0.0	0.0
36	0.29556E-04	0.0	0.0	0.0

NOTE:

Units of Mass: $kg/m/sec^2$
Units of Inertia: $kg\text{-}m^2/m/sec^2$
Units of Unbalance: $kg\text{-}m/m/sec^2$

TABLE A-12
MODEL MASS DATA — 100-PERCENT WING FUEL

MODE NO. 736

BAY	MASS	MX	MY	MZ	IXX	IYY
21	2.09	0.0	-0.01	0.0	0.75537E-02	0.29647E-02
22	1.48	0.0	0.04	0.0	0.61690E-02	0.17073E-02
23	0.84	0.0	0.02	0.0	0.40786E-02	0.58895E-03
24	0.68	0.0	0.01	0.0	0.14382E-02	0.63785E-03
25	0.68	0.0	0.01	0.0	0.15555E-02	0.74966E-03
26	0.41	0.0	0.01	0.0	0.96919E-03	0.24098E-03
27	0.34	0.0	0.00	0.0	0.52232E-03	0.20955E-03
28	0.22	0.0	0.00	0.0	0.42118E-03	0.94022E-04
29	0.17	0.0	0.00	0.0	0.16504E-03	0.59141E-04
30	0.15	0.0	0.00	0.0	0.12908E-03	0.48665E-04
31	0.16	0.0	0.00	0.0	0.27417E-03	0.40588E-04
32	0.10	0.0	0.00	0.0	0.73070E-04	0.34706E-04
33	0.08	0.0	0.00	0.0	0.43192E-04	0.29819E-04
34	0.07	0.0	0.00	0.0	0.39856E-04	0.21830E-04
35	0.06	0.0	0.00	0.0	0.28649E-04	0.16914E-04
36	0.02	0.0	0.00	0.0	0.17880E-04	0.12642E-04

BAY	IZZ	IXY	IYZ	IXZ
21	0.94067E-02	0.0	0.0	0.0
22	0.74974E-02	0.0	0.0	0.0
23	0.37327E-02	0.0	0.0	0.0
24	0.19022E-02	0.0	0.0	0.0
25	0.21023E-02	0.0	0.0	0.0
26	0.11162E-02	0.0	0.0	0.0
27	0.70866E-03	0.0	0.0	0.0
28	0.49528E-03	0.0	0.0	0.0
29	0.24657E-03	0.0	0.0	0.0
30	0.17063E-03	0.0	0.0	0.0
31	0.29851E-03	0.0	0.0	0.0
32	0.10421E-03	0.0	0.0	0.0
33	0.68154E-04	0.0	0.0	0.0
34	0.59902E-04	0.0	0.0	0.0
35	0.43836E-04	0.0	0.0	0.0
36	0.29556E-04	0.0	0.0	0.0

NOTE:

UNITS OF MASS: $kg/m/sec^2$

UNITS OF INERTIA: $kg\text{-}m^2/m/sec^2$

UNITS OF UNBALANCE: $kg\text{-}m/m/sec^2$

TABLE A-13

MODEL MASS DATA – FORWARD FUSELAGE WITH 13.2 kg NOSE BALLAST

MODE NO. 2151

BAY	MASS	MX	MY	MZ	IXX	IYY
41	0.32	0.0	0.0	0.0	0.32877E-02	0.17821E-02
42	1.56	0.0	0.0	0.0	0.90130E-03	0.25181E-02
43	0.35	0.0	0.0	0.0	0.37296E-02	0.92076E-02
44	0.24	0.0	0.0	0.0	0.12115E-02	0.28444E-02
45	0.42	0.0	0.0	0.0	0.57502E-02	0.39886E-02
46	0.78	0.0	0.0	0.0	0.41393E-02	0.86853E-02

BAY	IZZ	IXY	IYZ	IXZ
41	0.32877E-02	0.0	0.0	0.0
42	0.90130E-03	0.0	0.0	0.0
43	0.37296E-02	0.0	0.0	0.0
44	0.12115E-02	0.0	0.0	0.0
45	0.57502E-02	0.0	0.0	0.0
46	0.41393E-02	0.0	0.0	0.0

TABLE A-14

MODEL MASS DATA – AFT FUSELAGE

MODE NO. 1266

BAY	MASS	MX	MY	MZ	IXX	IYY
47	0.77	0.0	0.0	0.0	0.39915E-02	0.85814E-02
48	0.59	0.0	0.0	0.0	0.23645E-02	0.46411E-02
49	0.79	0.0	0.0	0.0	0.41744E-02	0.64379E-02
50	0.37	0.0	0.0	0.0	0.67817E-02	0.32862E-02
51	0.70	0.0	0.0	0.0	0.18747E-01	0.53069E-02

BAY	IZZ	IXY	IYZ	IXZ
47	0.39915E-02	0.0	0.0	0.0
48	0.23645E-02	0.0	0.0	0.0
49	0.41744E-02	0.0	0.0	0.0
50	0.67817E-02	0.0	0.0	0.0
51	0.18747E-01	0.0	0.0	0.0

NOTE:

UNITS OF MASS: kg/m/sec^2

UNITS OF INERTIA: kg-m^2/m/sec^2

UNITS OF UNBALANCE: kg-m/m/sec^2

TABLE A-15
MODEL MASS DATA – UPPER VERTICAL STABILIZER

MODE NO. 1220

BAY	MASS	MX	MY	MZ	IXX	IYY
2	0.01	0.0	0.0	0.0	0.18875E-04	0.0
3	0.02	0.0	0.0	0.0	0.39783E-04	0.0
4	0.02	0.0	0.0	0.0	0.33389E-04	0.0
5	0.01	0.0	0.0	0.0	0.19255E-04	0.0
6	0.02	0.0	0.0	0.0	0.27858E-04	0.0

BAY	IZZ	IXY	IYZ	IXZ
2	0.0	0.0	0.0	0.0
3	0.0	0.0	0.0	0.0
4	0.0	0.0	0.0	0.0
5	0.0	0.0	0.0	0.0
6	0.0	0.0	0.0	0.0

TABLE A-16
MODEL MASS DATA – LOWER VERTICAL STABILIZER
(INCLUDES AFT ENGINE DUCT)

MODE NO. 1265

BAY	MASS	MX	MY	MZ	IXX	IYY
1	0.24	0.0	0.0	0.0	0.22064E-02	0.14181E-02

BAY	IZZ	IXY	IYZ	IXZ
1	0.30229E-02	0.0	0.0	0.0

NOTE:

UNITS OF MASS: kg/m/sec^2

UNITS OF INERTIA: kg-m^2/m/sec^2

UNITS OF UNBALANCE: kg-m/m/sec^2

TABLE A-17

MODEL MASS DATA – HORIZONTAL STABILIZER

MODE NO.	1231					
BAY	MASS	MX	MY	MZ	IXX	IYY
11	0.09	0.0	0.0	0.0	0.38133E-03	0.0
12	0.06	0.0	0.0	0.0	0.25558E-03	0.0
13	0.05	0.0	0.0	0.0	0.16724E-03	0.0
14	0.04	0.0	0.0	0.0	0.10371E-03	0.0
15	0.03	0.0	0.0	0.0	0.58087E-04	0.0
16	0.02	0.0	0.0	0.0	0.32102E-04	0.0

BAY	IZZ	IXY	IYZ	IXZ
11	0.0	0.0	0.0	0.0
12	0.0	0.0	0.0	0.0
13	0.0	0.0	0.0	0.0
14	0.0	0.0	0.0	0.0
15	0.0	0.0	0.0	0.0
16	0.0	0.0	0.0	0.0

NOTE:

UNITS OF MASS: kg/m/sec^2

UNITS OF INERTIA: kg-m^2/m/sec^2

UNITS OF UNBALANCE: kg-m/m/sec^2

TABLE A-18
MODEL MASS DATA – TAIL ENGINE

MODE NO.	1176					
BAY	MASS	MX	MY	MZ	IXX	IYY
56	0.45	0.0	0.0	0.0	0.19226E-02	0.43017E-03

BAY	IZZ	IXY	IYZ	IXZ
56	0.17530E-02	0.0	0.0	0.0

TABLE A-19
MODEL MASS DATA – WING ENGINE

MODE NO.	799					
BAY	MASS	MX	MY	MZ	IXX	IYY
30	0.93	0.0	-0.01	0.0	0.46971E-02	0.80819E-03

BAY	IZZ	IXY	IYZ	IXZ
39	0.45359E-02	0.0	0.0	0.0

NOTE:

UNITS OF MASS: kg/m/sec^2

UNITS OF INERTIA: kg-m^2/m/sec^2

UNITS OF UNBALANCE: kg-m/m/sec^2

Table A-20

Aileron Mass Properties

Weight, grams	40.1
X_{CG}, meters (measured from inboard end of aileron)	0.164
Y_{CG}, meters (measured aft of hinge line)	0.10
Z_{CG}, meters	0
$I_{ROLL\ CG}$, g-m^2	0.504
$I_{YAW\ CG}$, g-m^2	0.388
$I_{PITCH\ CG}$, g-m^2	0.005

Table A-21

Elevator Mass Properties

Weight, grams	39.4
X_{CG}, meters (measured from inboard end of elevator)	0.095
Y_{CG}, meters (measured aft of hinge line)	0.022
Z_{CG}, meters	0
$I_{ROLL\ CG}$, g-m^2	0.158
I_{HL}, deg	0.043

Table A-22

Aerodynamics Correction Factors

BAY	LIFT DUE TO h	LIFT DUE TO α	MOMENT DUE TO h	MOMENT DUE TO α
24	.94	.94	.94	.94
25	.946	.946	.946	.946
26	.952	.952	.952	.952
27	.952	.952	.952	.952
28	.945	.945	.945	.945
29	.937	.937	.937	.937
30	.933	.933	.933	.933
31	.925	.925	.925	.925
32	.931	.931	.931	.931
33	.954	.954	.954	.954
34	.948	.948	.948	.948
35	.917	.917	.917	.917
36	.833	.833	.675	.675

APPENDIX B

ANALOG COMPUTER DIAGRAMS

This section contains schematic diagrams of the COMCOR 175 analog computer. Figure B-1 presents a schematic diagram of the servo-amplifier. Figures B-2 through B-4 present schematic diagrams of the aileron and elevator control laws for the full-span model. Figure B-5 presents a schematic of the hydraulic dump circuit.

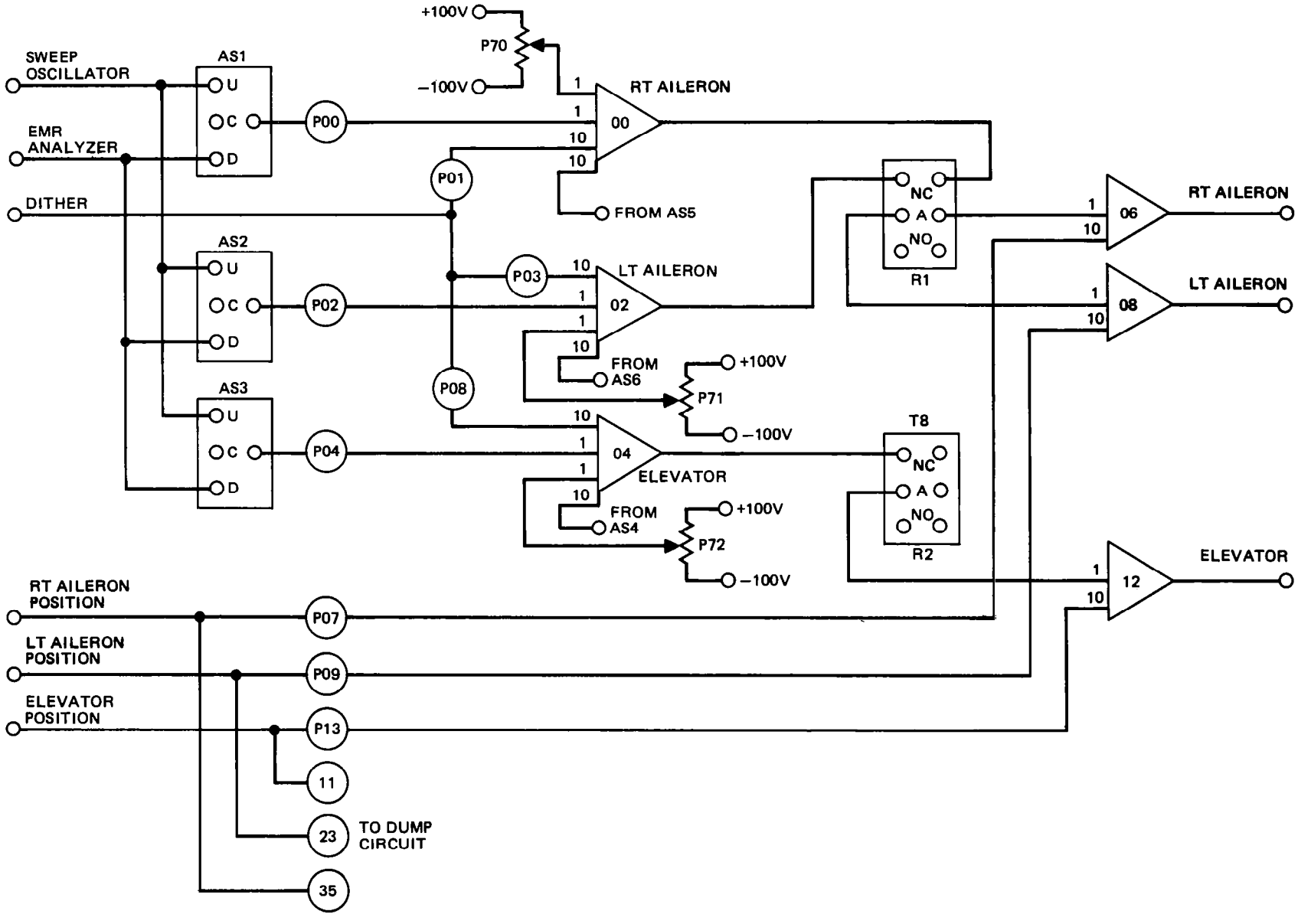

FIGURE B-1. SERVO-AMPLIFIER SCHEMATIC – ANALOG COMPUTER

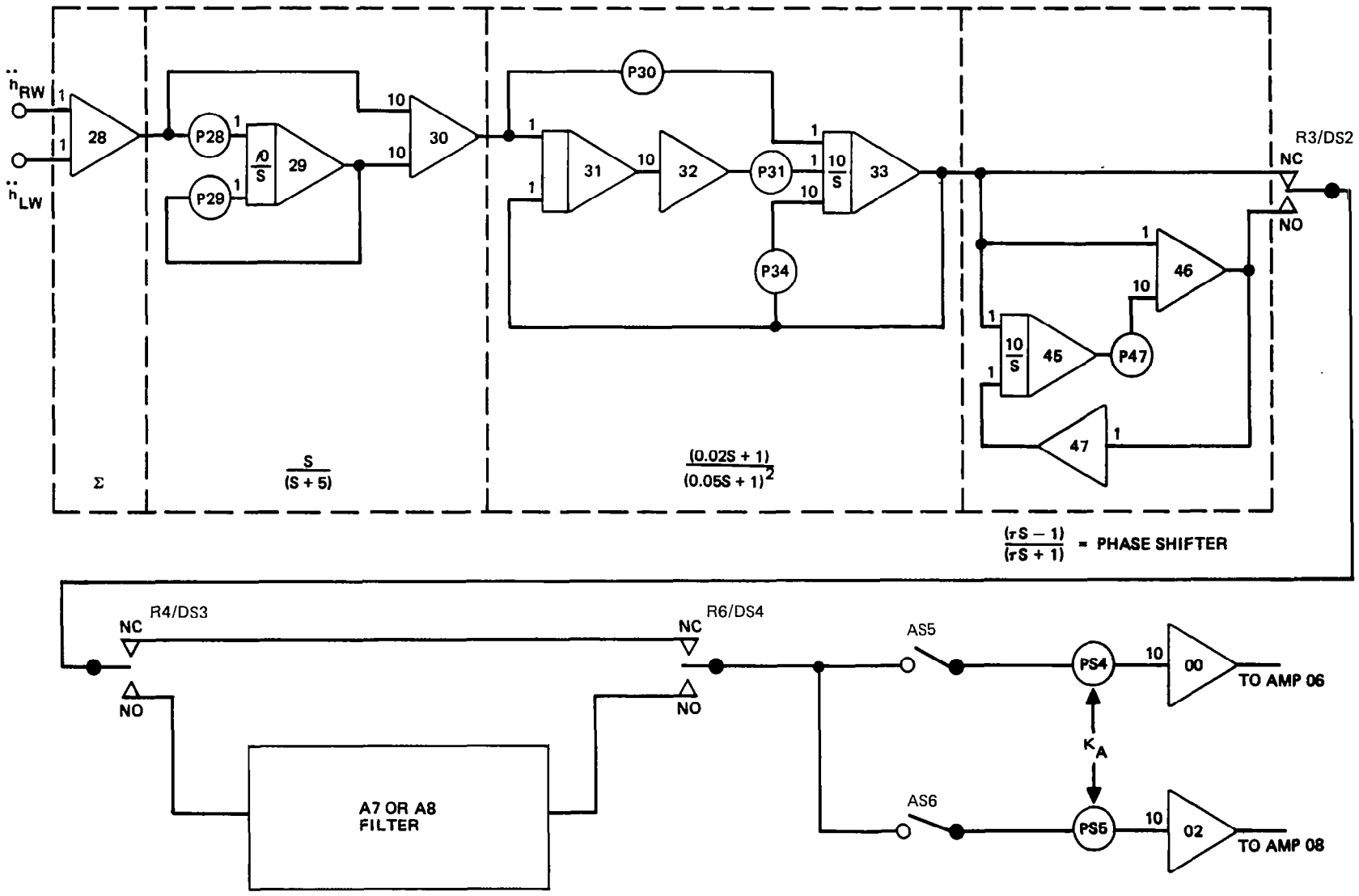

FIGURE B-2. FULL SPAN MODEL AILERON CONTROL LAW – ANALOG COMPUTER

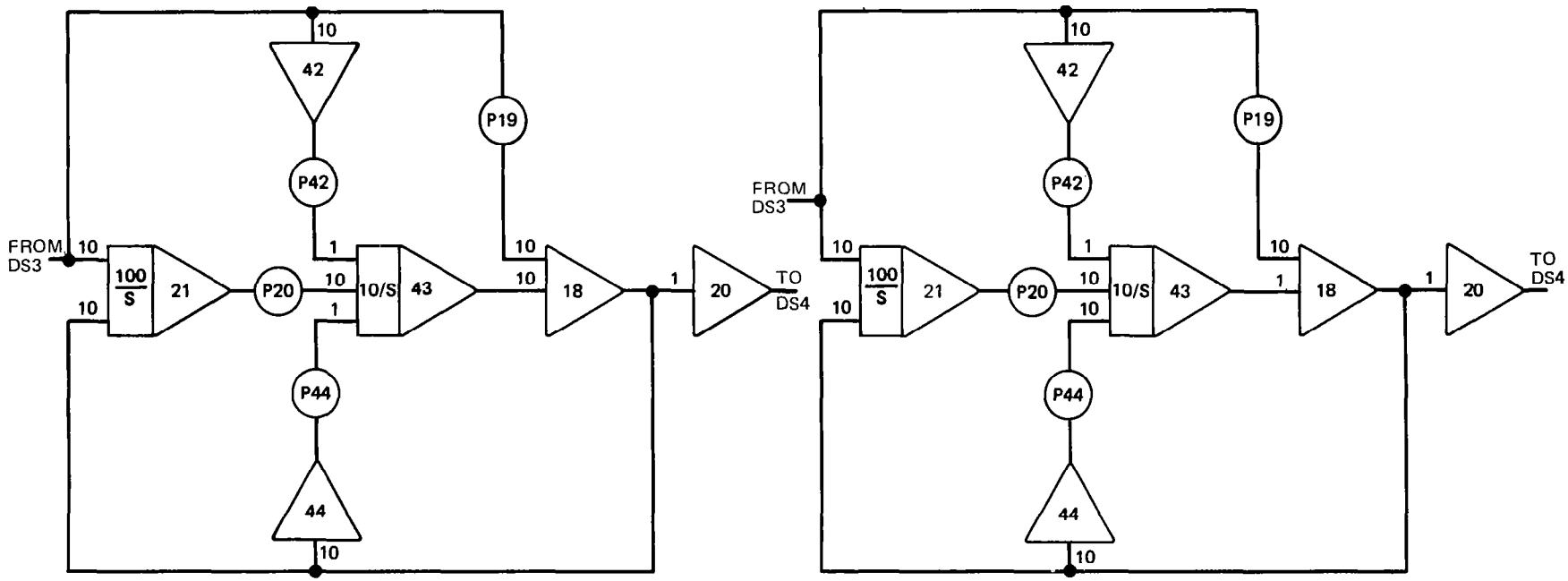

$$A7 = \frac{(140^2)(S^2 + 100S + 250^2)}{(250^2)(S^2 + 500S + 140^2)}$$

$$A8 = \frac{S^2 + 56S + 140^2}{S^2 + 196S + 140^2}$$

POT NUMBER	POT SETTING A7	A8
P28	0.5000	0.5000
P29	0.5000	0.5000
P30	0.8000	0.8000
P31	0.4000	0.4000
P34	0.4000	0.4000
P19	0.4000	0.1000
P20	0.2500	0.1960
P42	0.4000	0.5600
P44	0.5000	0.1960
P54	$K_{A7}/[0.78(2)]$	$K_{A8}/[0.78(2)]$
P55	$K_{A7}/[0.78(2)]$	$K_{A8}/[0.78(2)]$

FIGURE B-3. NOTCH FILTERS – FULL SPAN MODEL AILERON CONTROL LAW

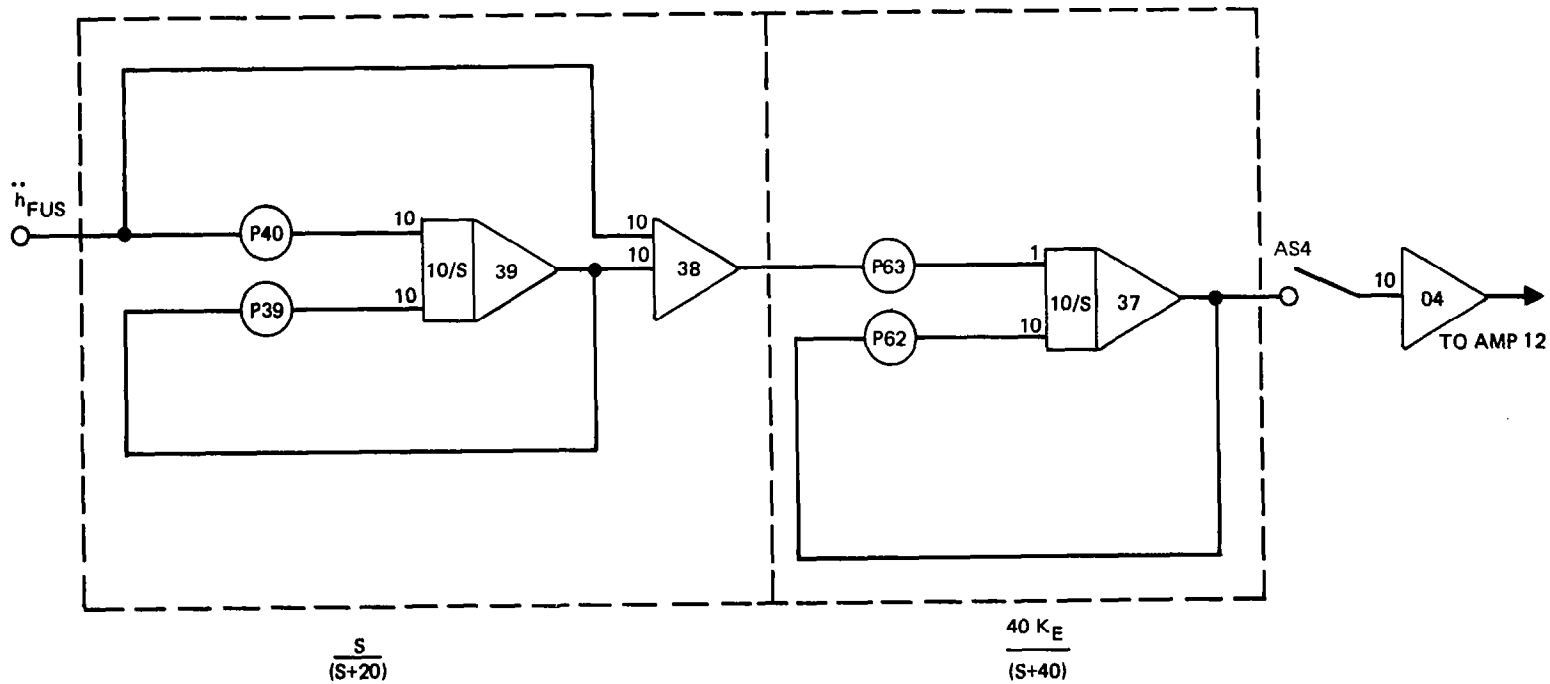

POT NUMBER	POT SETTING FOR E4	E5
39	0.2000	0.2000
40	0.2000	0.2000
62	0.4000	0.4000
63	$40K_E16$	$40K_E/18$

FIGURE B-4. FULL SPAN MODEL ELEVATOR CONTROL LAW – ANALOG COMPUTER

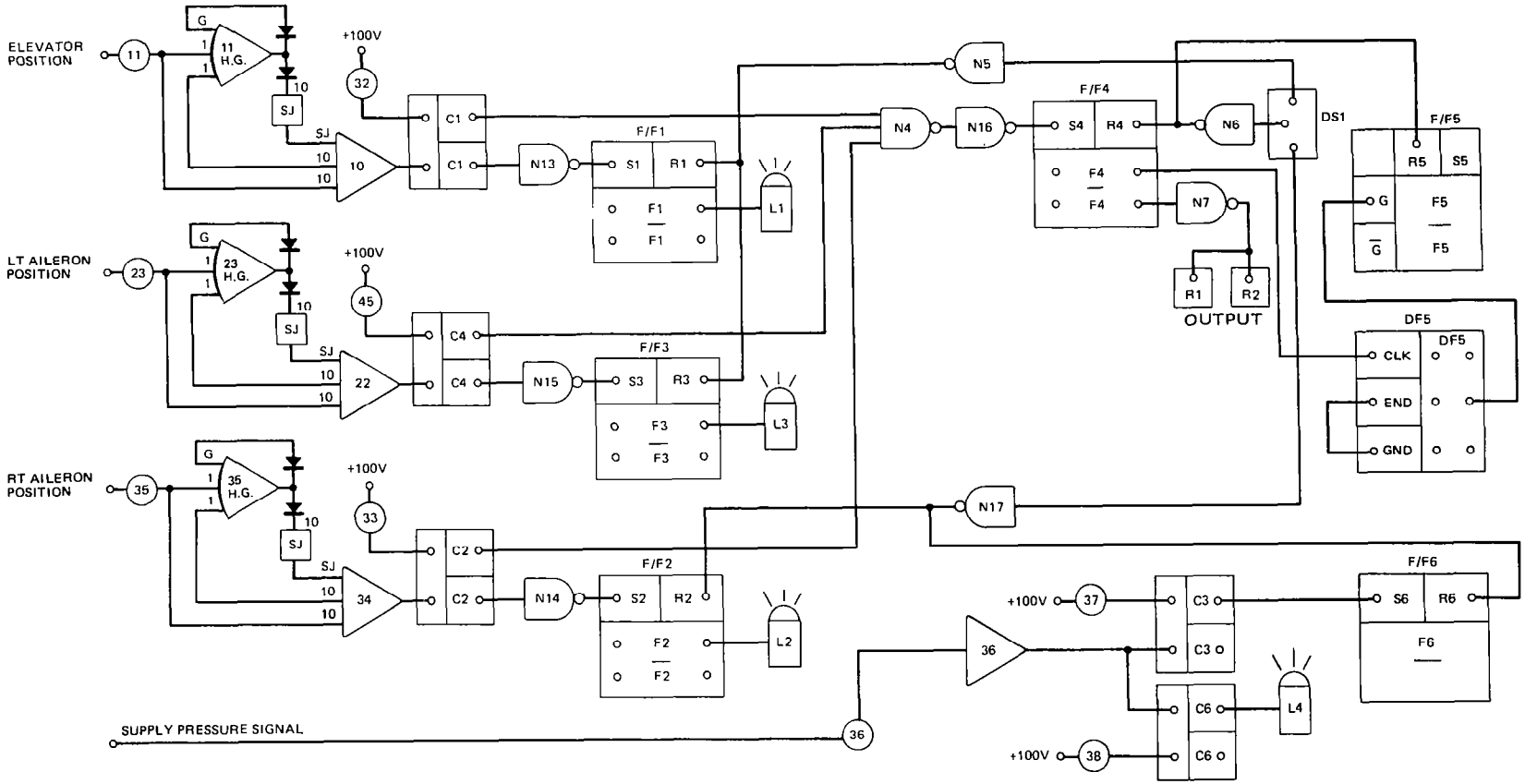

FIGURE B-5. HYDRAULIC DUMP CIRCUIT – ANALOG COMPUTER

APPENDIX C

GROUND VIBRATION TEST DATA

Mode shapes and frequencies of the semispan model measured in the ground vibration test are presented in Figures C-1 through C-8 and Table C-1. Analytical predictions are included for comparison. Measured and analytical symmetric mode shapes of the full-span model in the alternate configuration are presented in Figures C-9 through C-13. Analytical mode shapes and frequencies of the full-span model in the baseline configuration are presented in Figures C-14 through C-25. Measured frequencies of the full-span model are presented in Table C-2. Calculated orthogonal modes of the full-span model are presented in Tables C-3 through C-38.

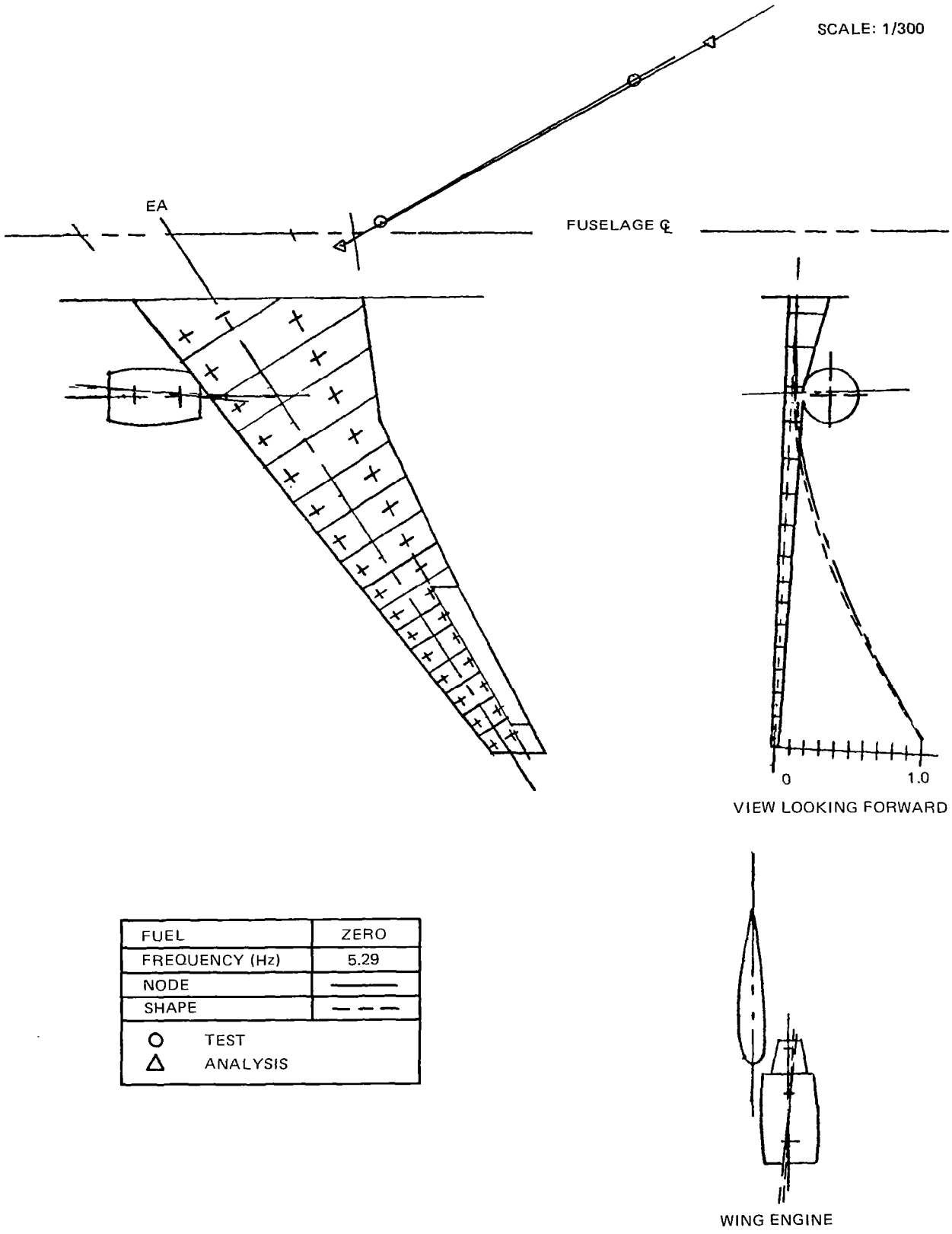

FIGURE C-1. SEMISPAN VIBRATION MODES – FIRST WING BENDING

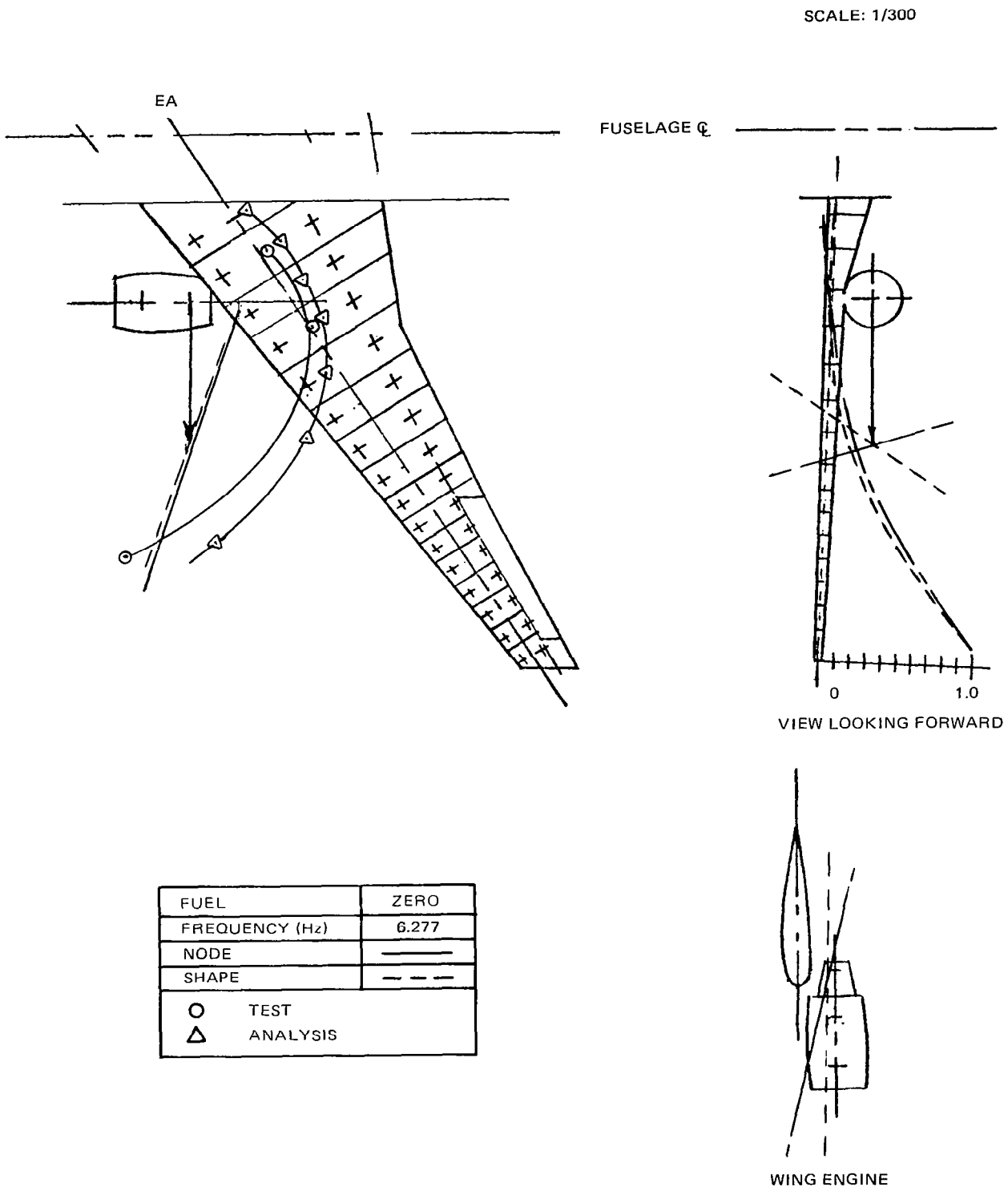

FIGURE C-2. SEMISPAN VIBRATION MODES – ENGINE YAW

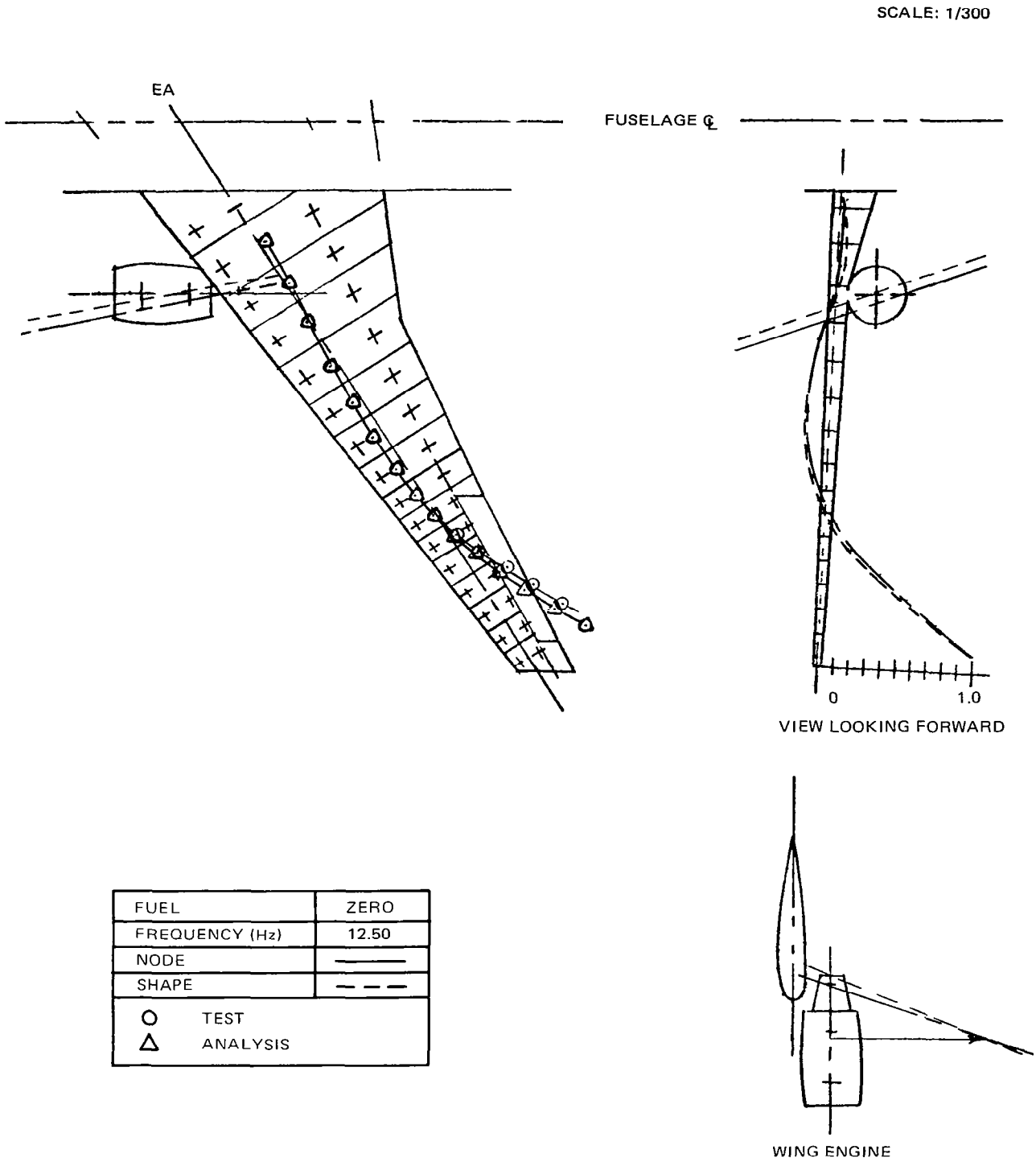

FIGURE C-3. SEMISPAN VIBRATION MODES – FIRST WING TORSION AND ENGINE PITCH

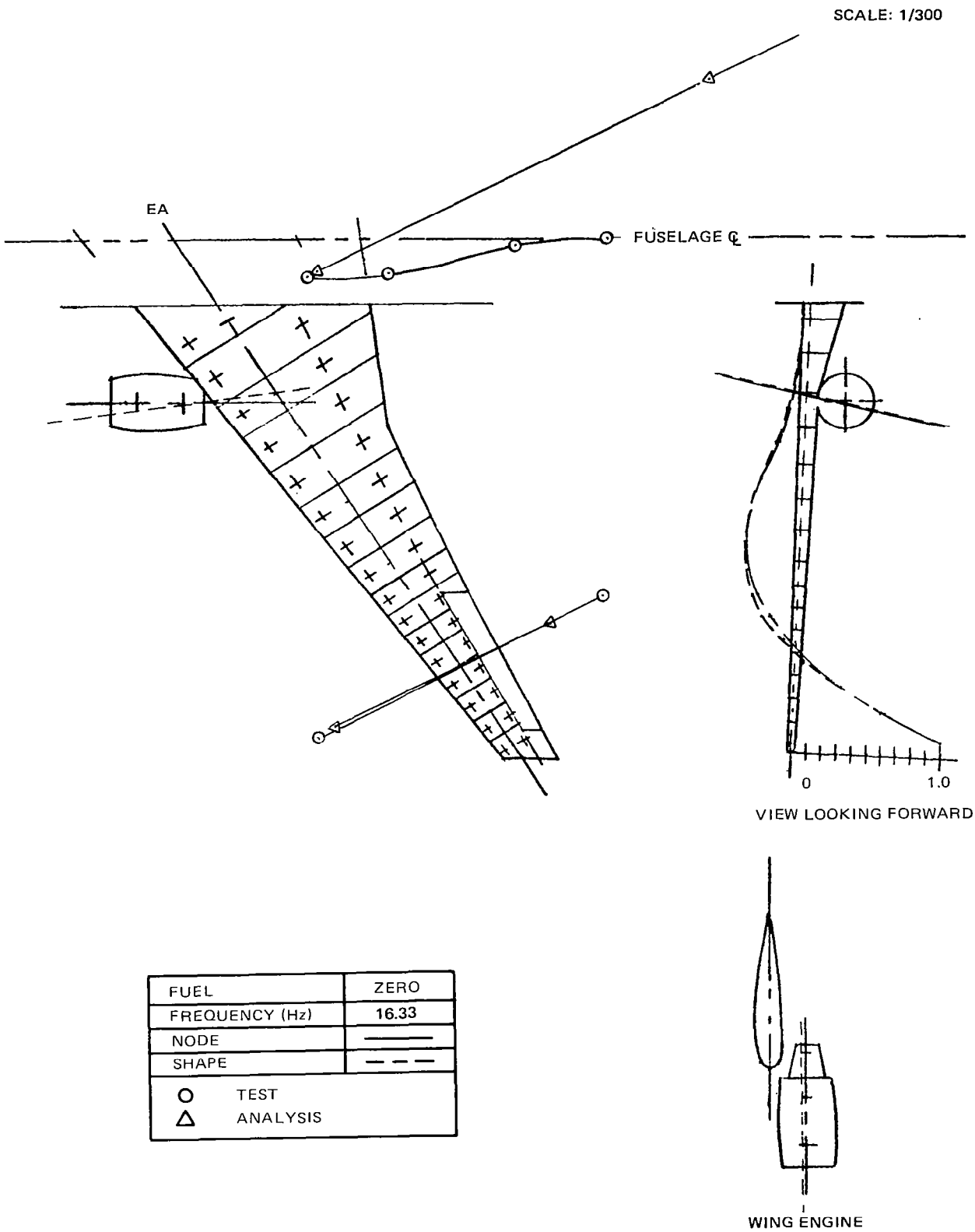

FIGURE C-4. SEMISPAN VIBRATION MODES – SECOND WING BENDING

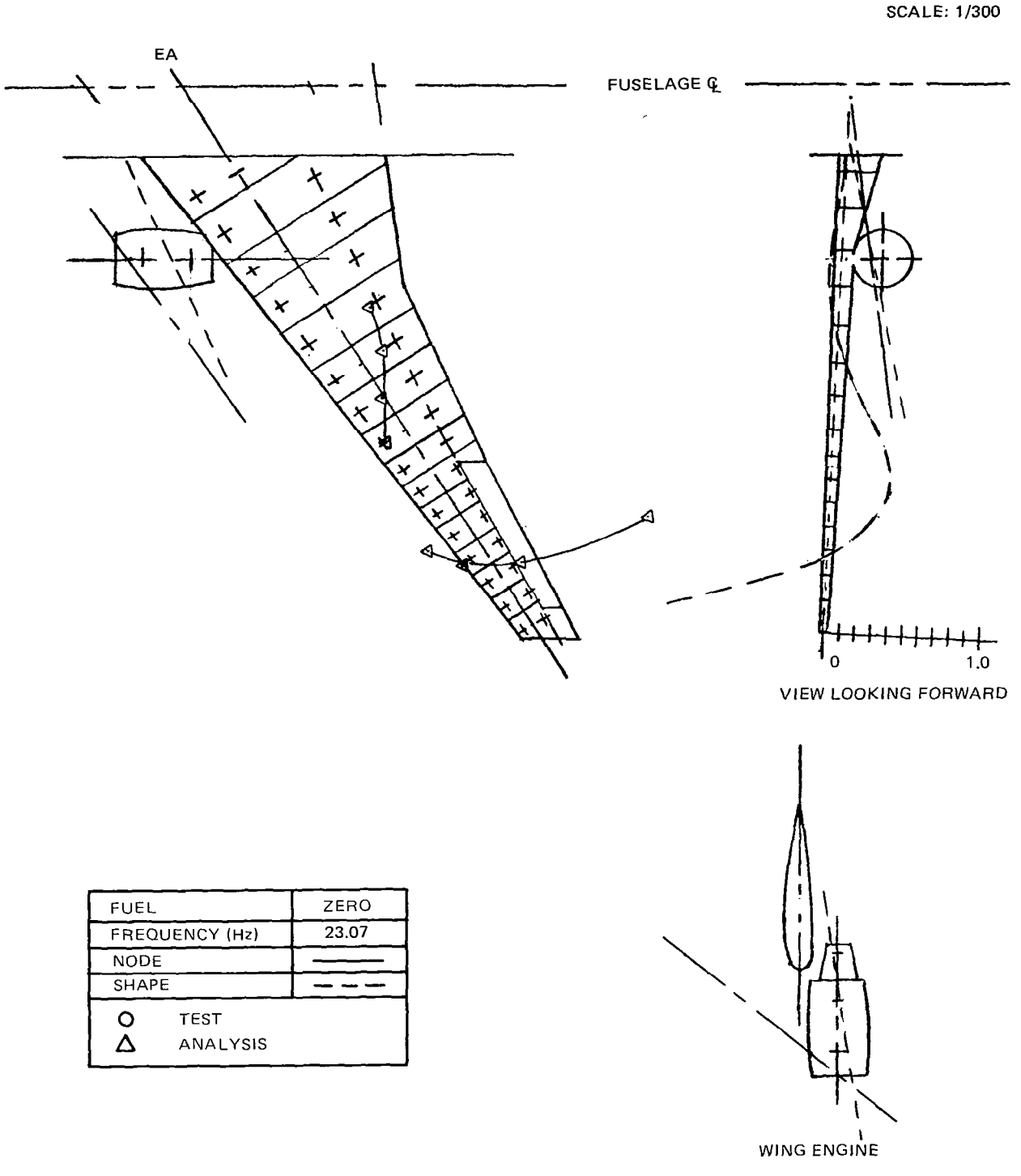

FIGURE C-5. SEMISPAN VIBRATION MODES – ENGINE ROLL

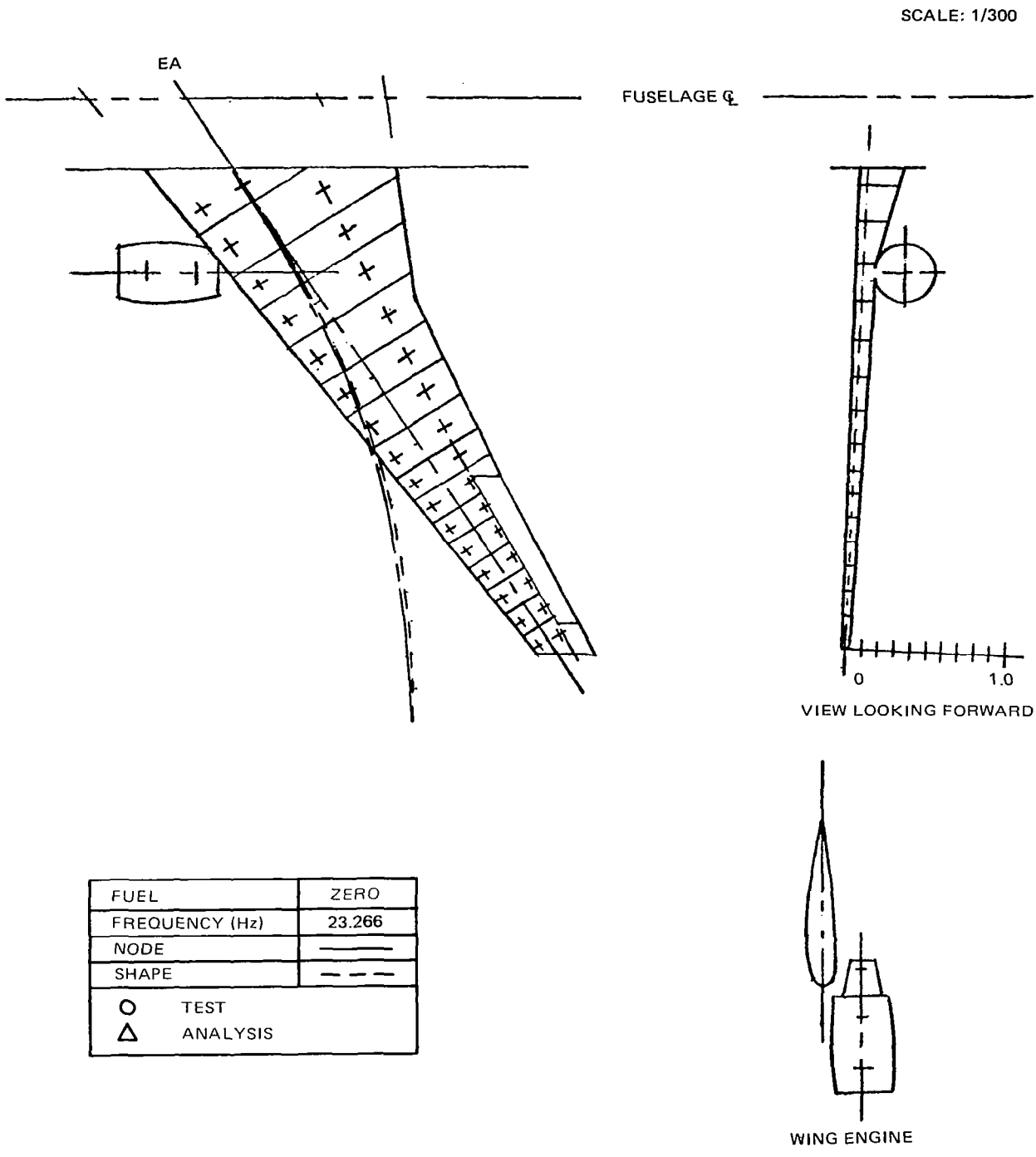

FIGURE C-6. SEMISPAN VIBRATION MODES – WING FORE AND AFT BENDING

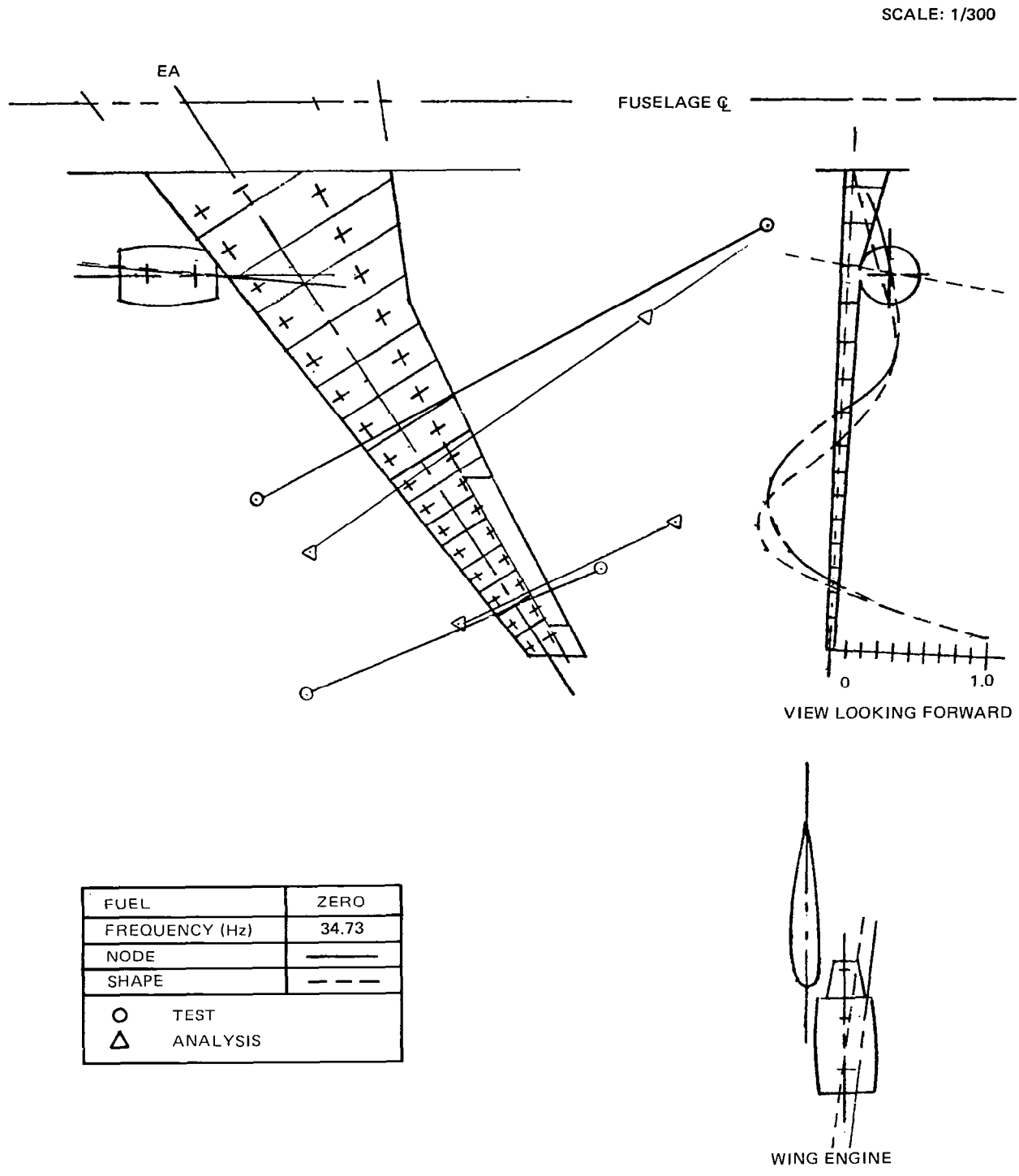

FIGURE C-7. SEMISPAN VIBRATION MODES – THIRD WING BENDING

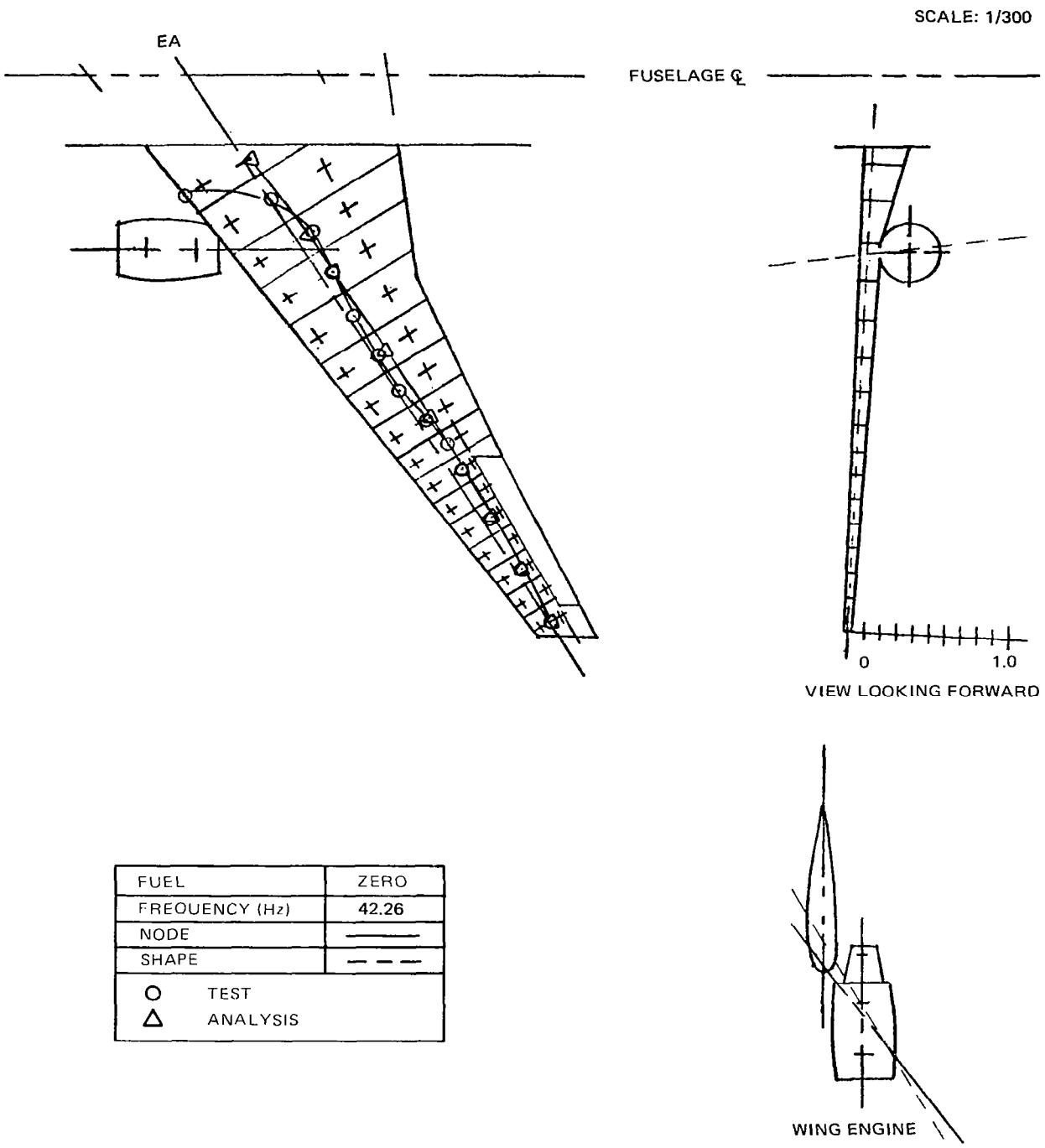

FIGURE C-8. SEMISPAN VIBRATION MODES – SECOND WING TORSION

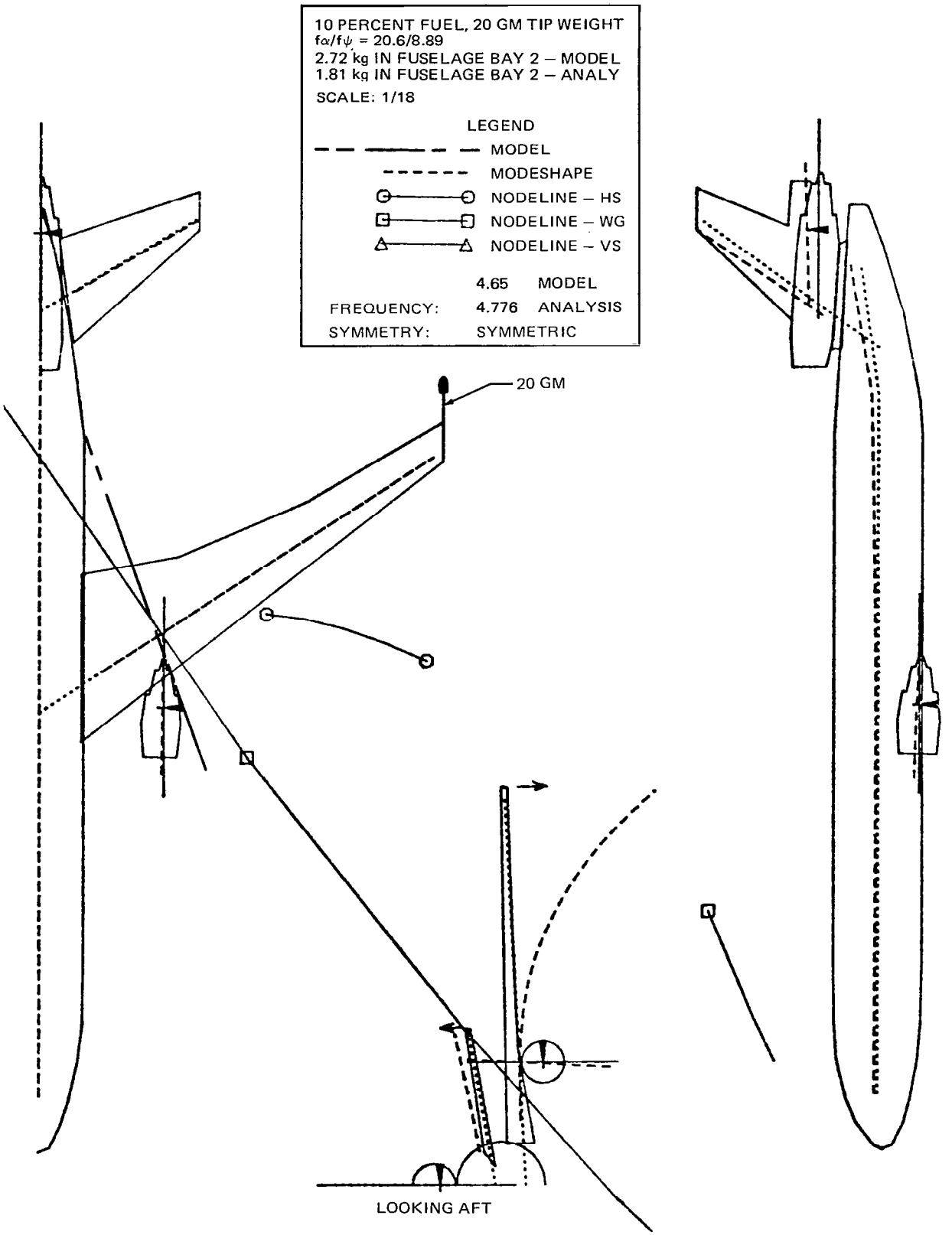

FIGURE C-9. FULL-SPAN MODE SHAPE – FIRST WING BENDING

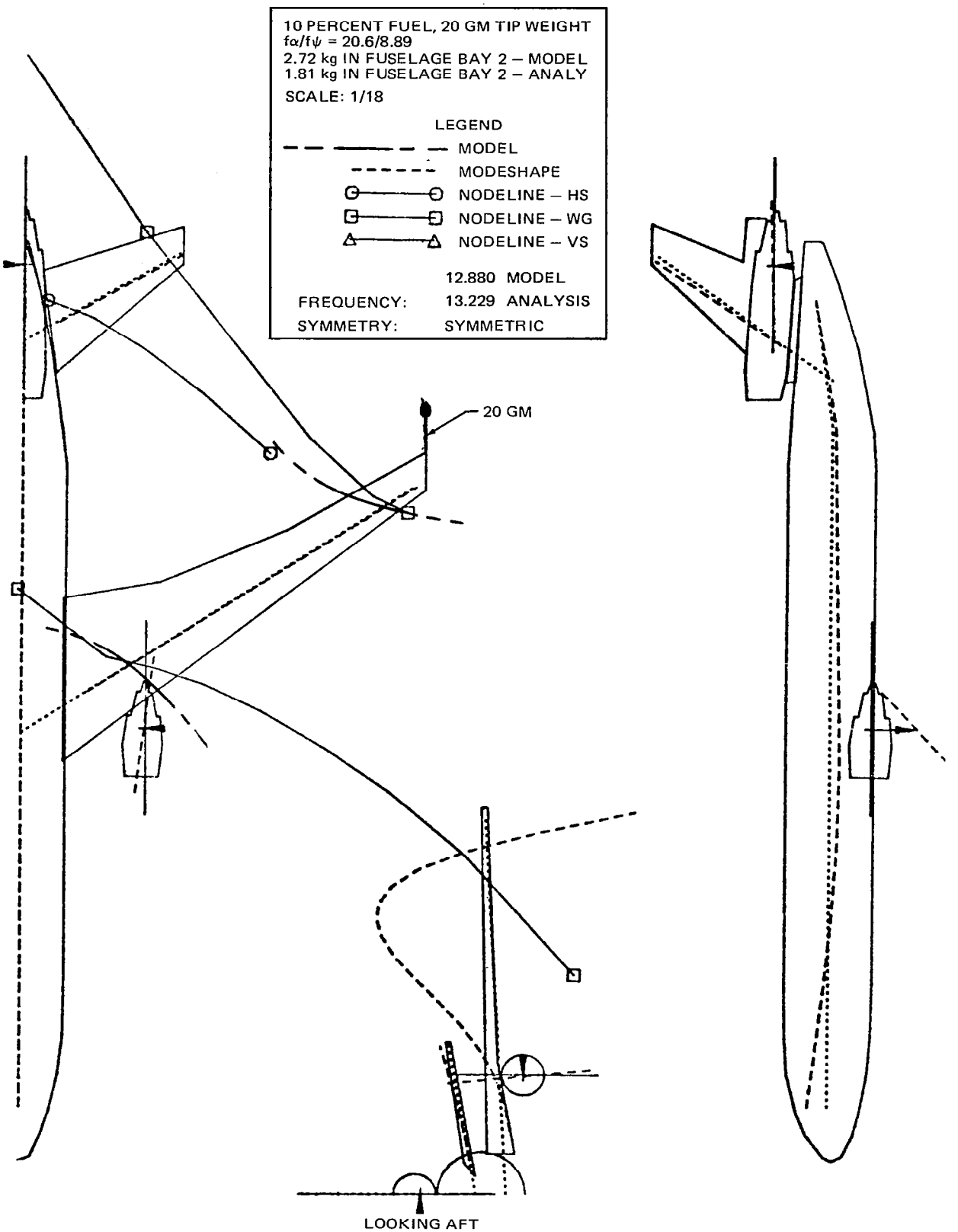

FIGURE C-10. FULL-SPAN MODE SHAPE – INNER WING TORSION

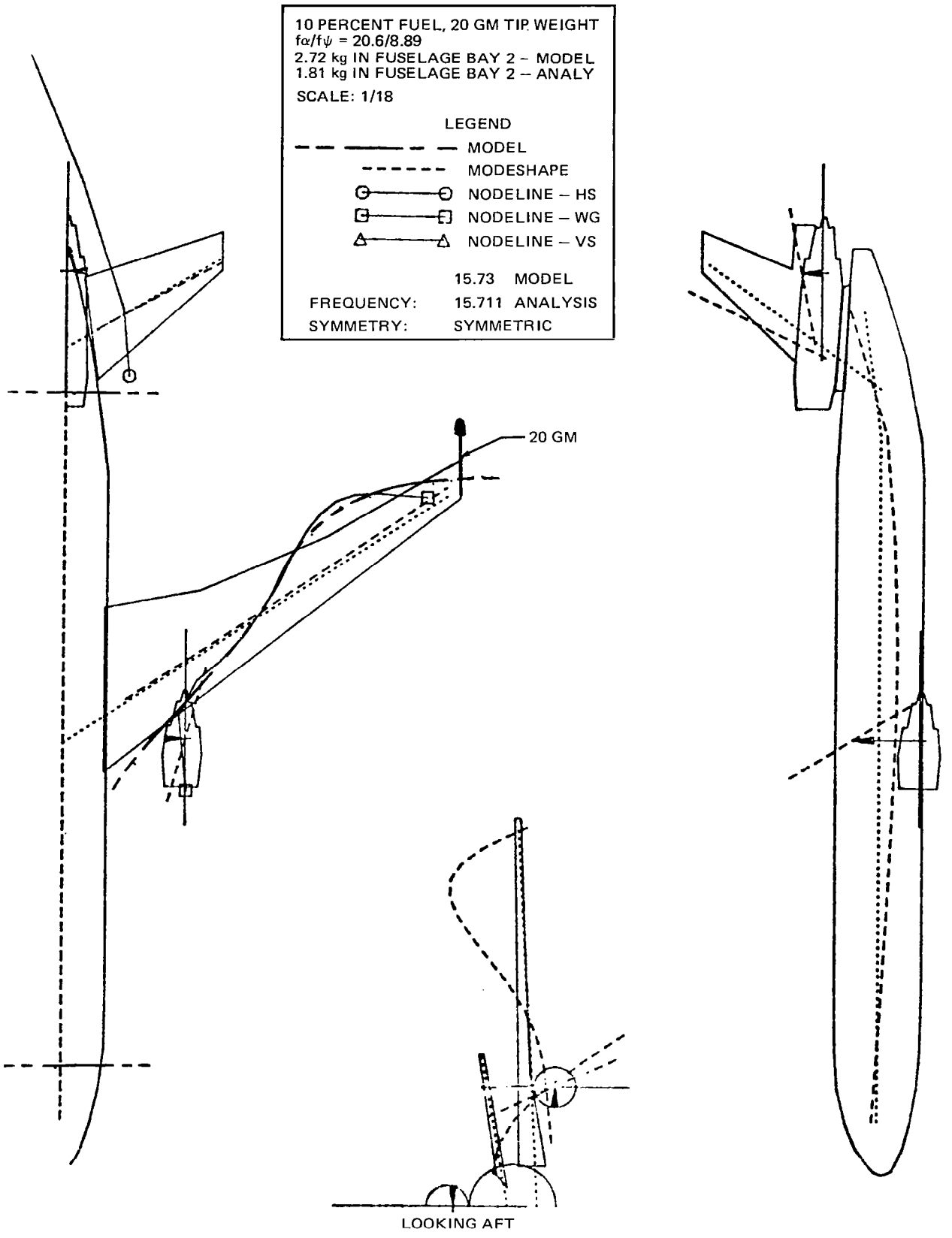

FIGURE C-11. FULL-SPAN MODE SHAPE – ENGINE AND WING PITCH

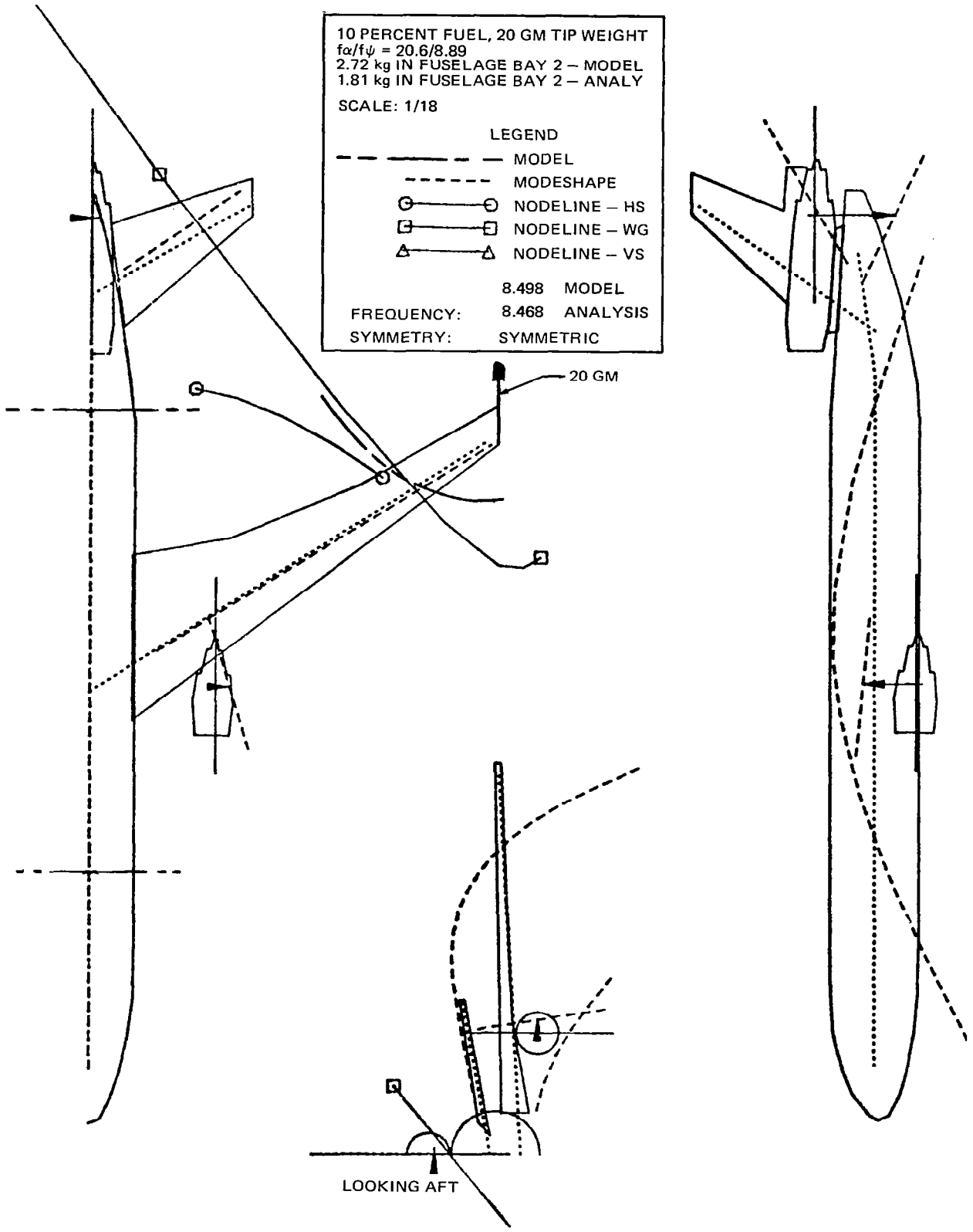

FIGURE C-12. FULL-SPAN MODE SHAPE – FIRST FUSELAGE VERTICAL BENDING

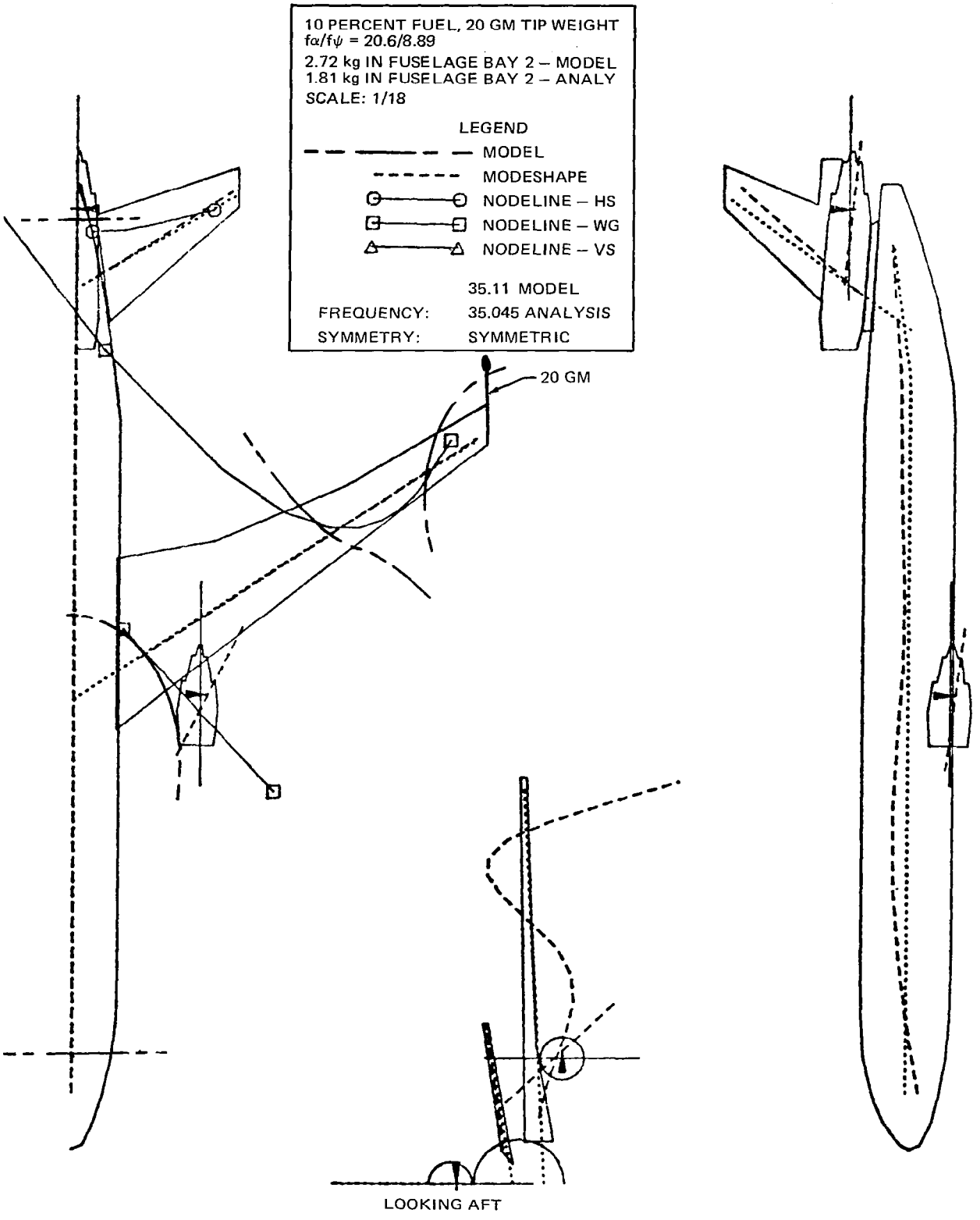

FIGURE C-13. FULL-SPAN MODE SHAPE – HIGHER WING MODE

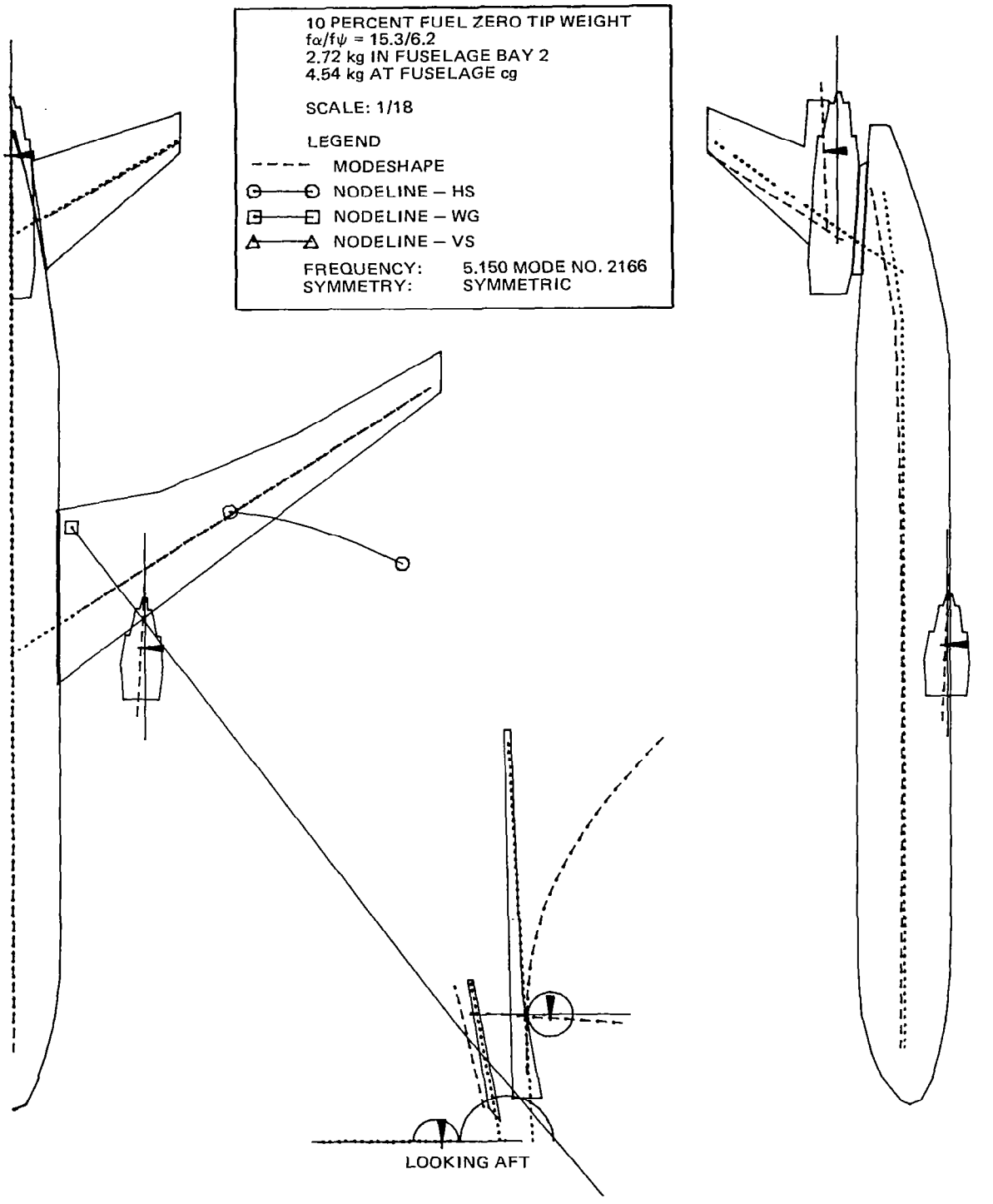

FIGURE C-14. FULL-SPAN MODE SHAPE – FIRST WING BENDING

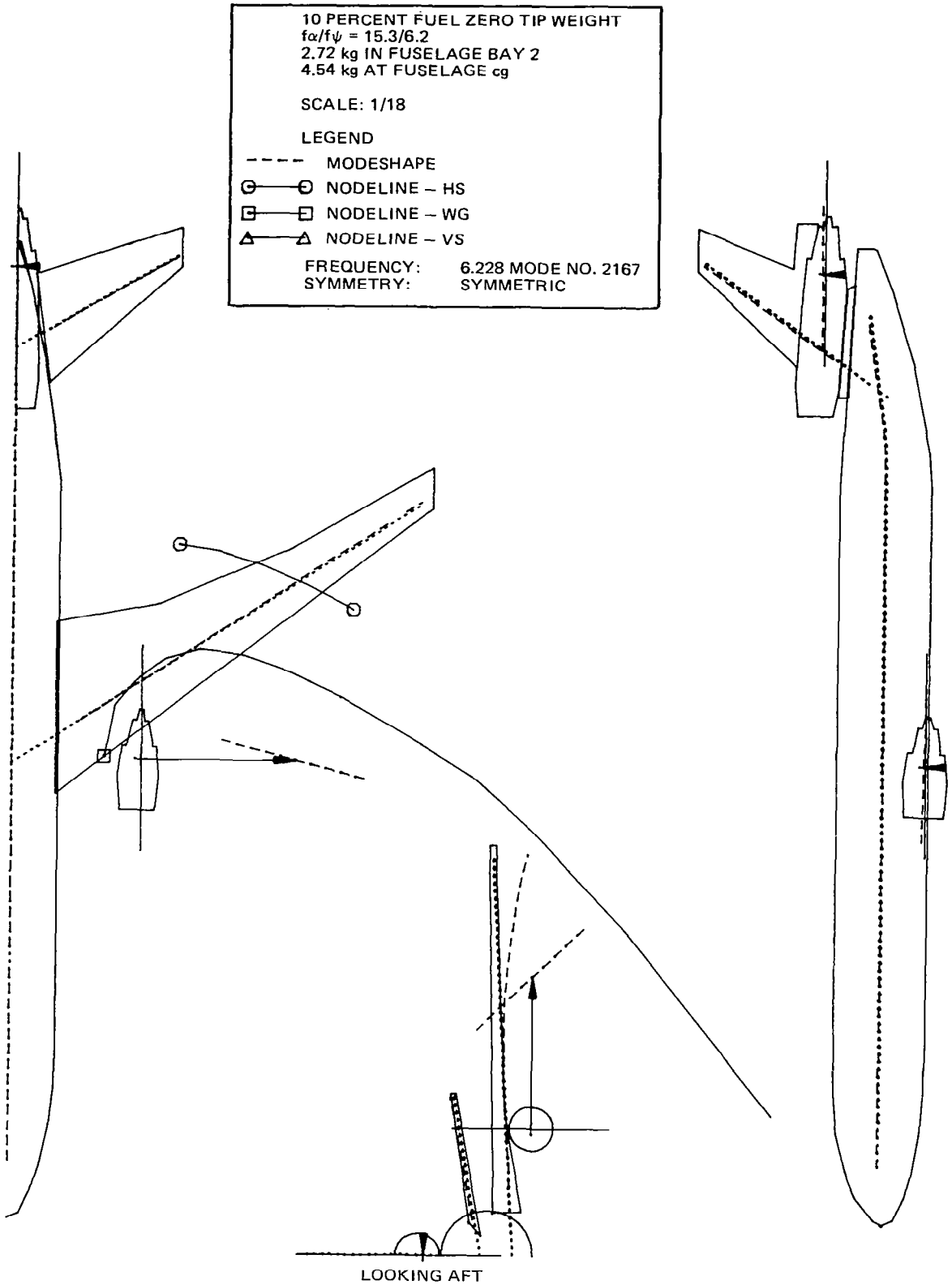

FIGURE C-15. FULL-SPAN MODE SHAPE – WING ENGINE YAW

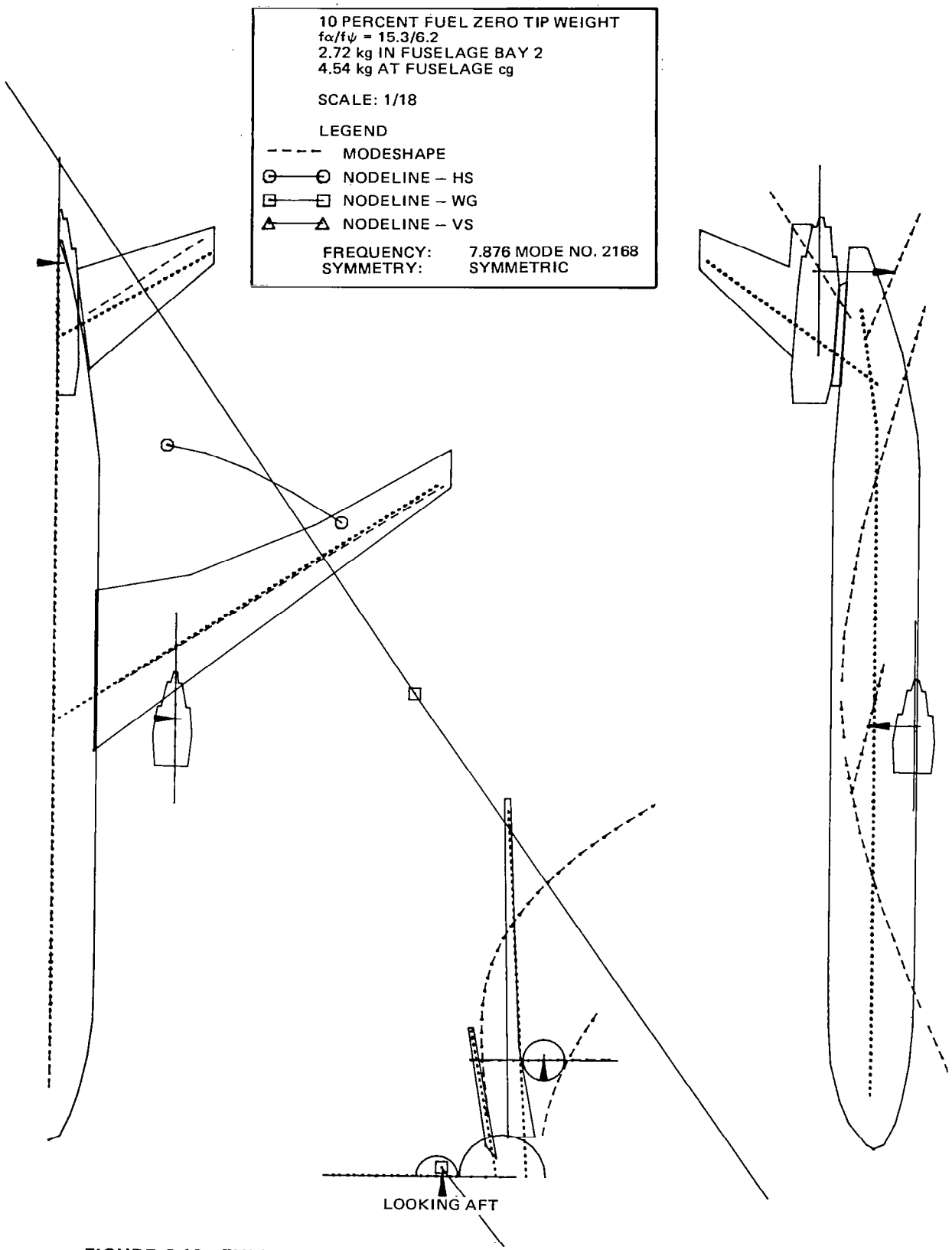

FIGURE C-16. FULL-SPAN MODE SHAPE – FIRST FUSELAGE VERTICAL BENDING

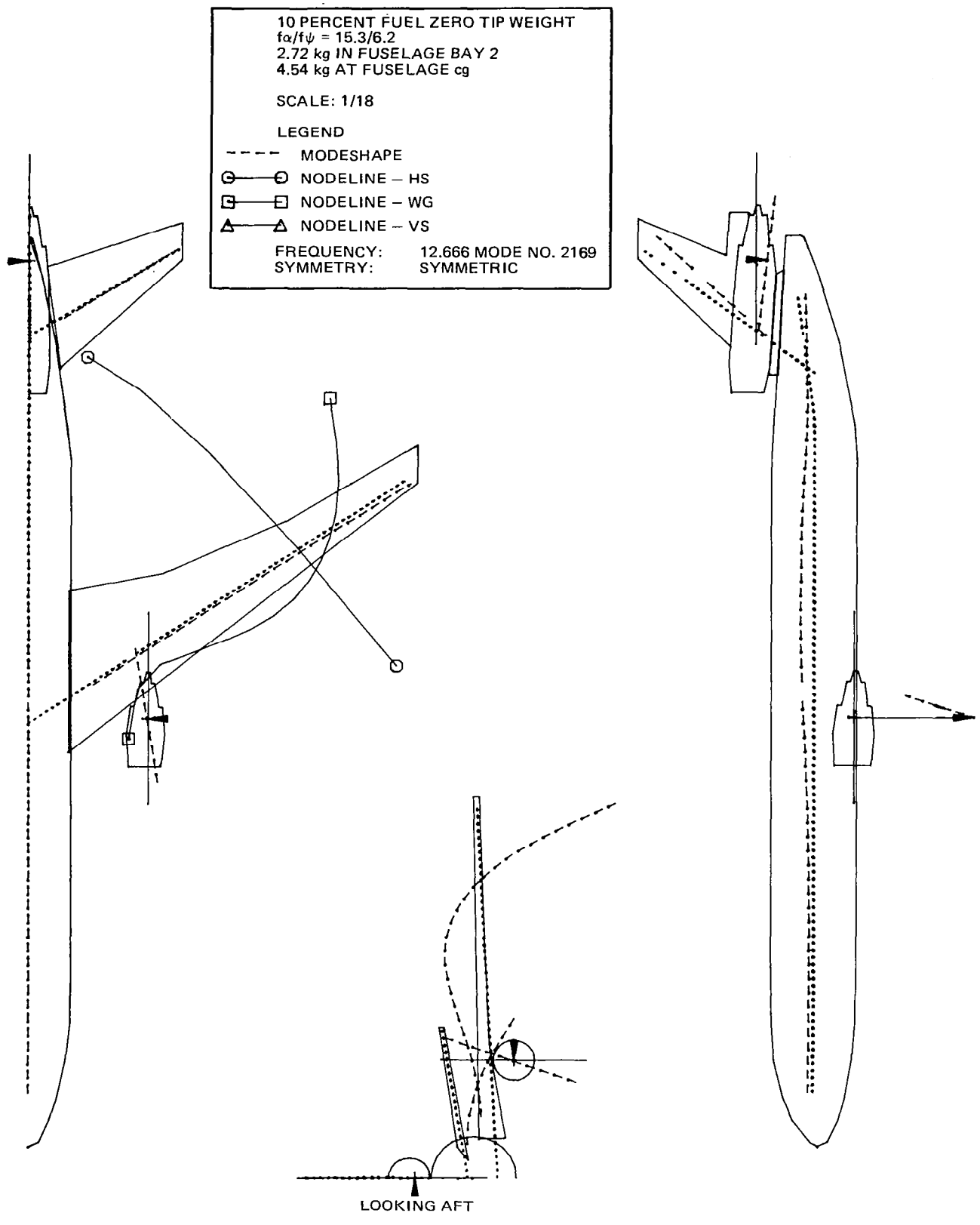

FIGURE C-17. FULL-SPAN MODE SHAPE – WING INNER PANEL TORSION

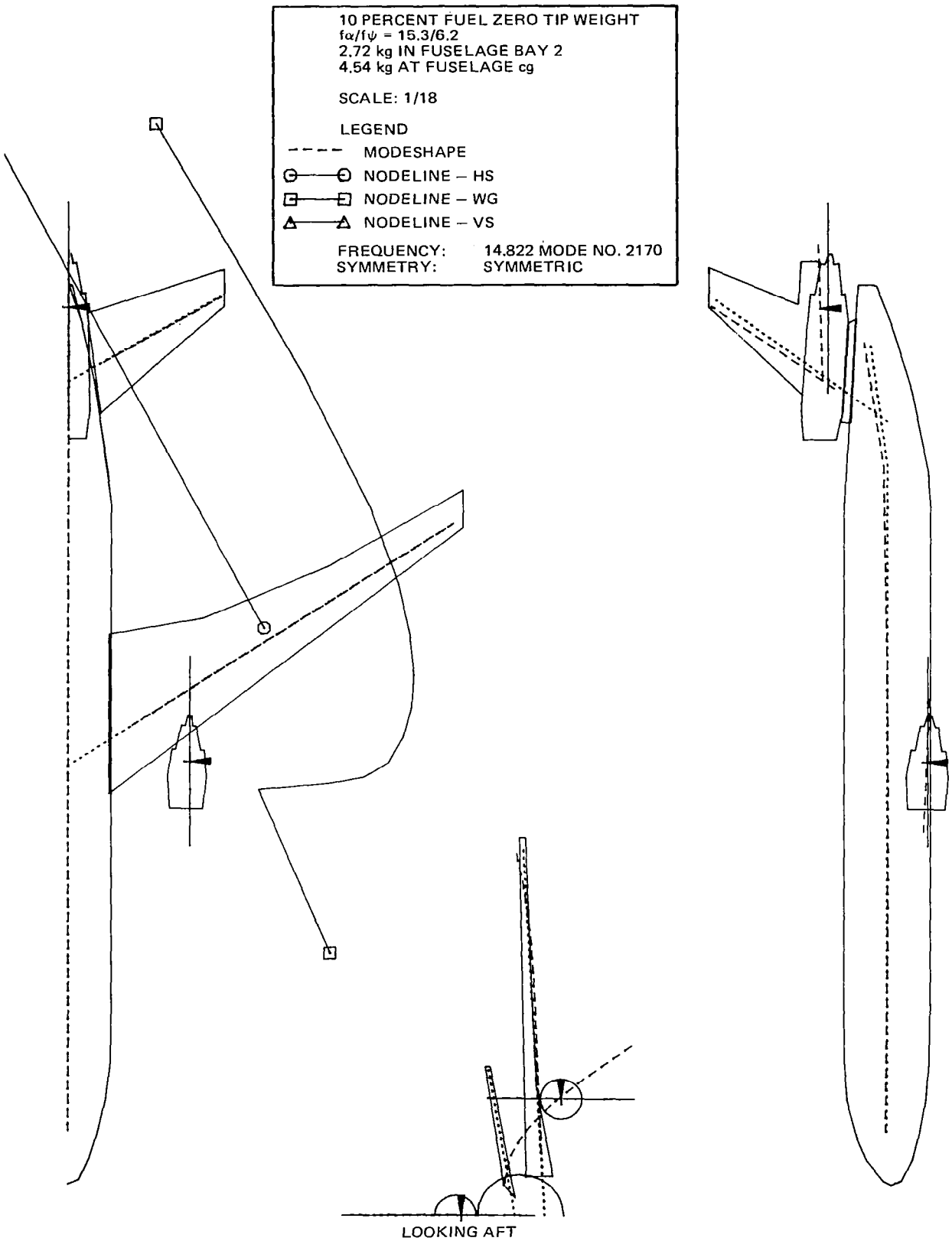

FIGURE C-18. FULL-SPAN MODE SHAPE – HORIZONTAL STABILIZER VERTICAL BENDING

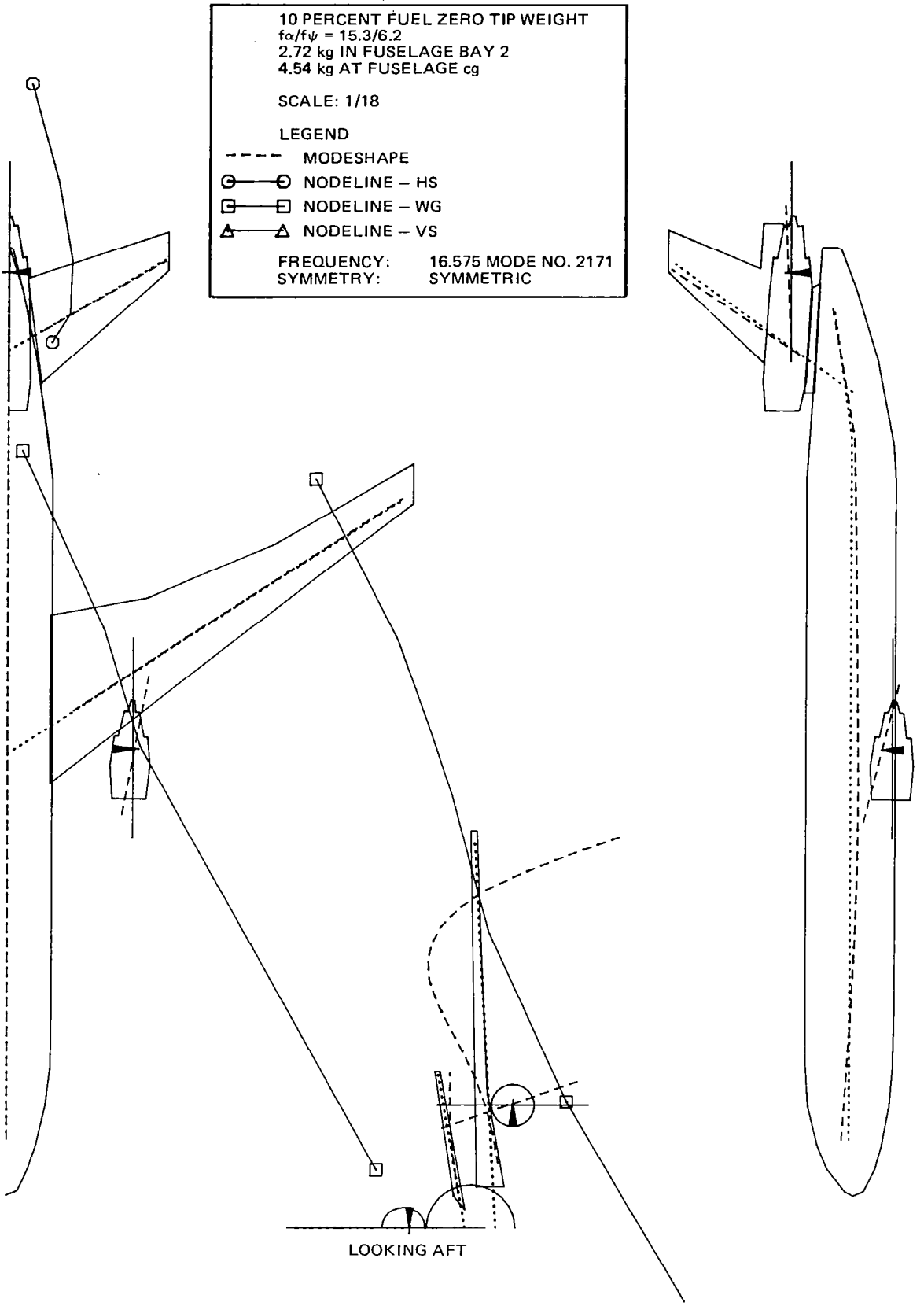

FIGURE C-19. FULL-SPAN MODE SHAPE – ENGINE AND WING PITCH

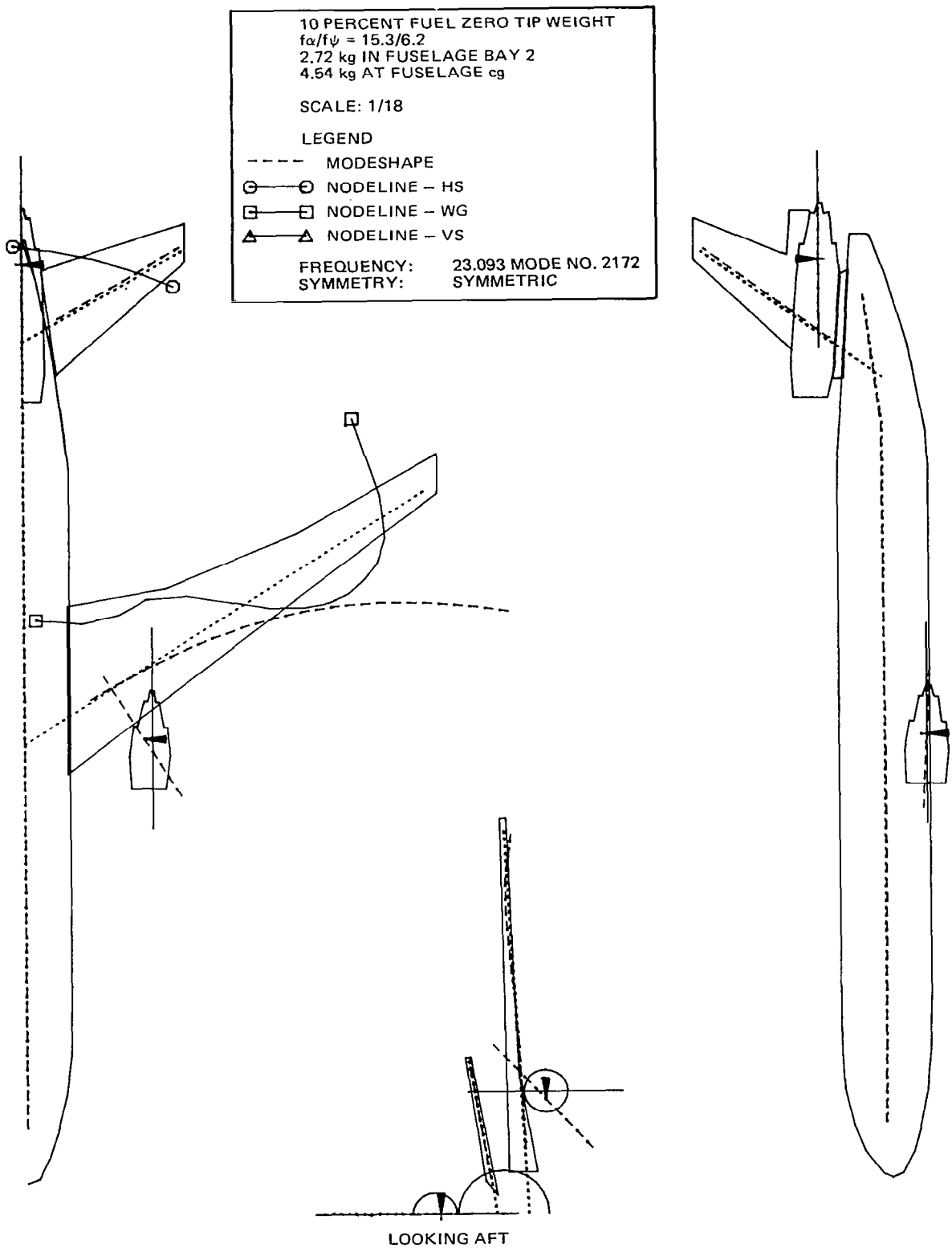

FIGURE C-20. FULL-SPAN MODE SHAPE – WING FORE AND AFT BENDING

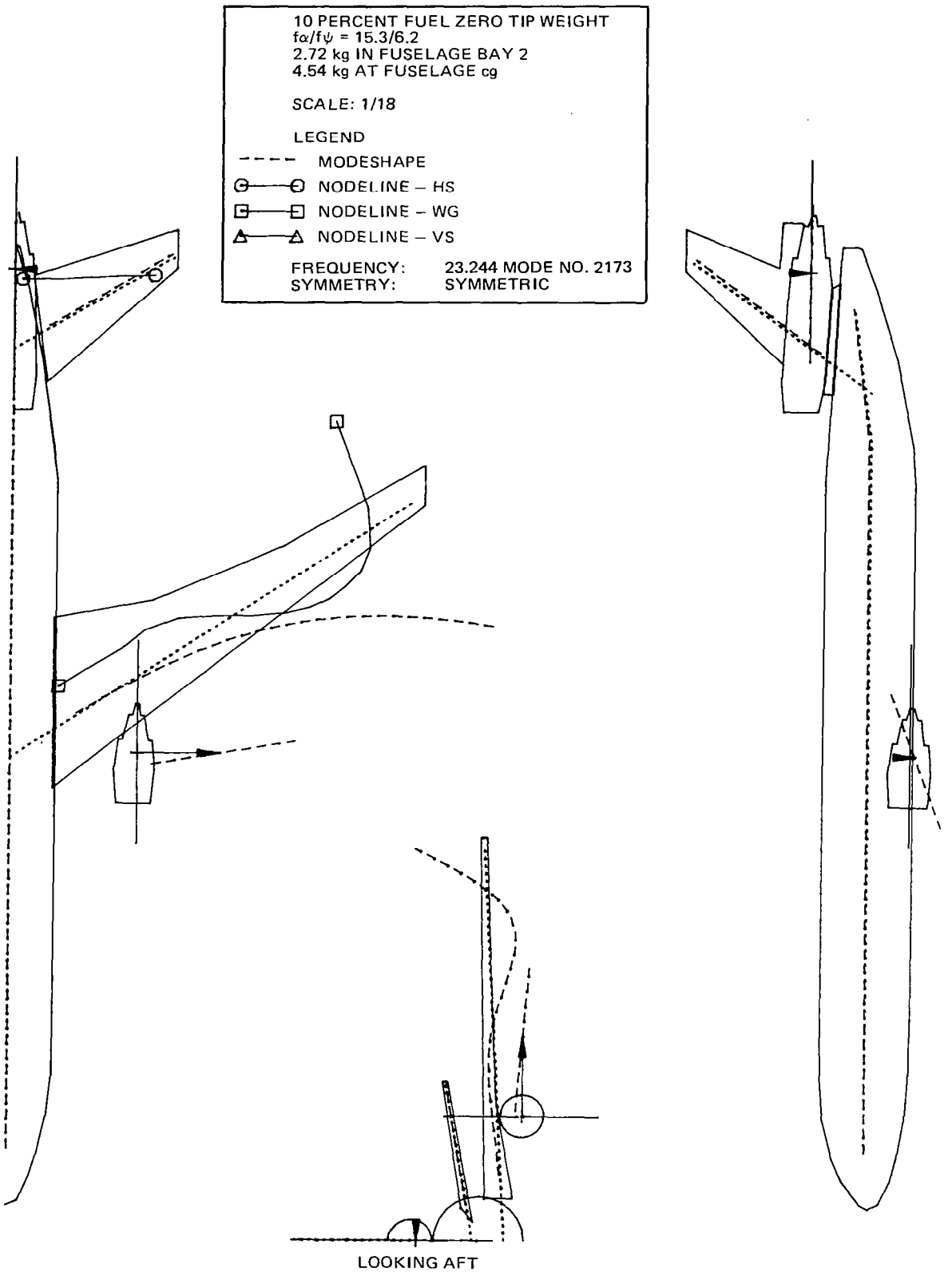

FIGURE C-21. FULL-SPAN MODE SHAPE – WING ENGINE ROLL

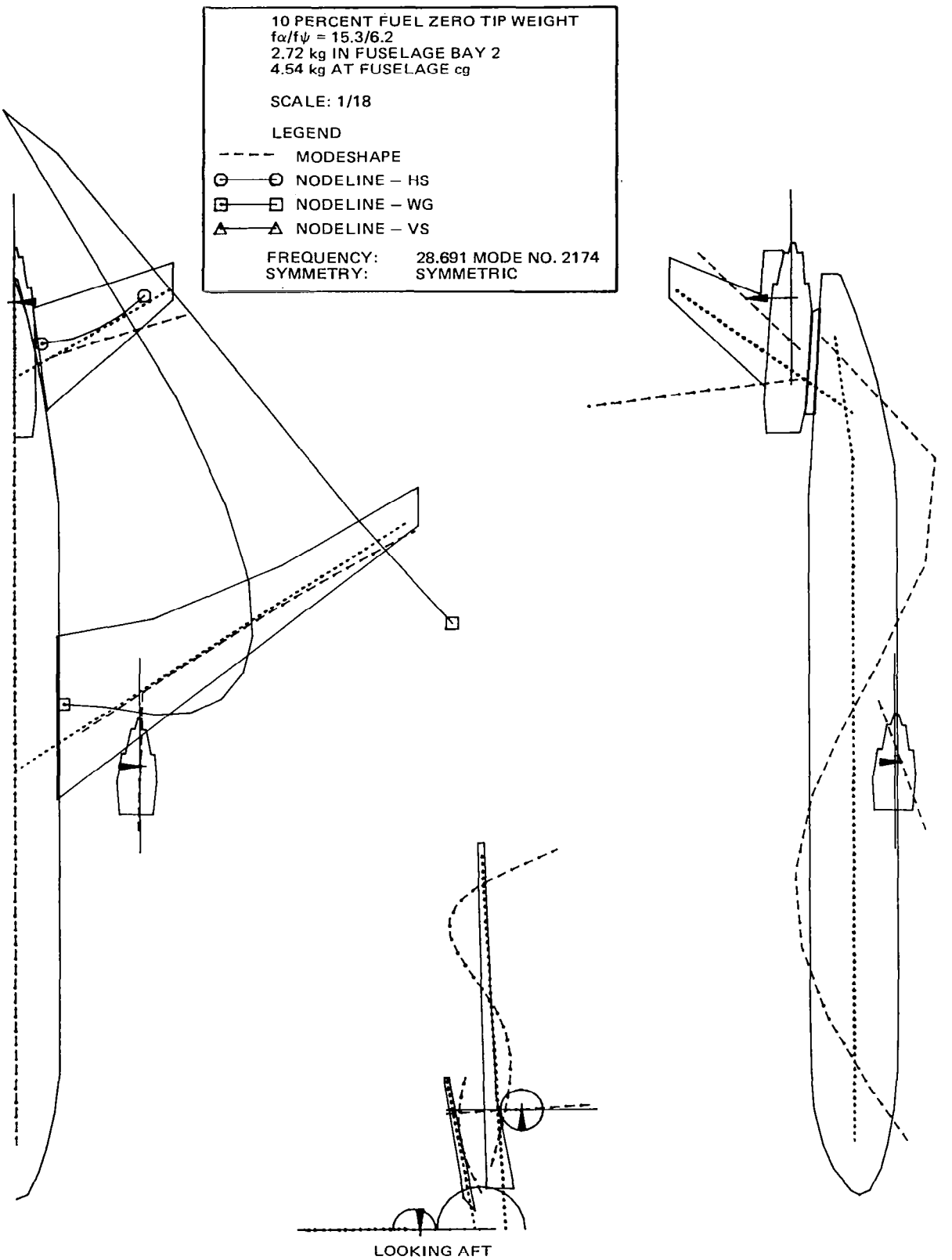

FIGURE C-22. FULL-SPAN MODE SHAPE – FUSELAGE SECOND VERTICAL BENDING

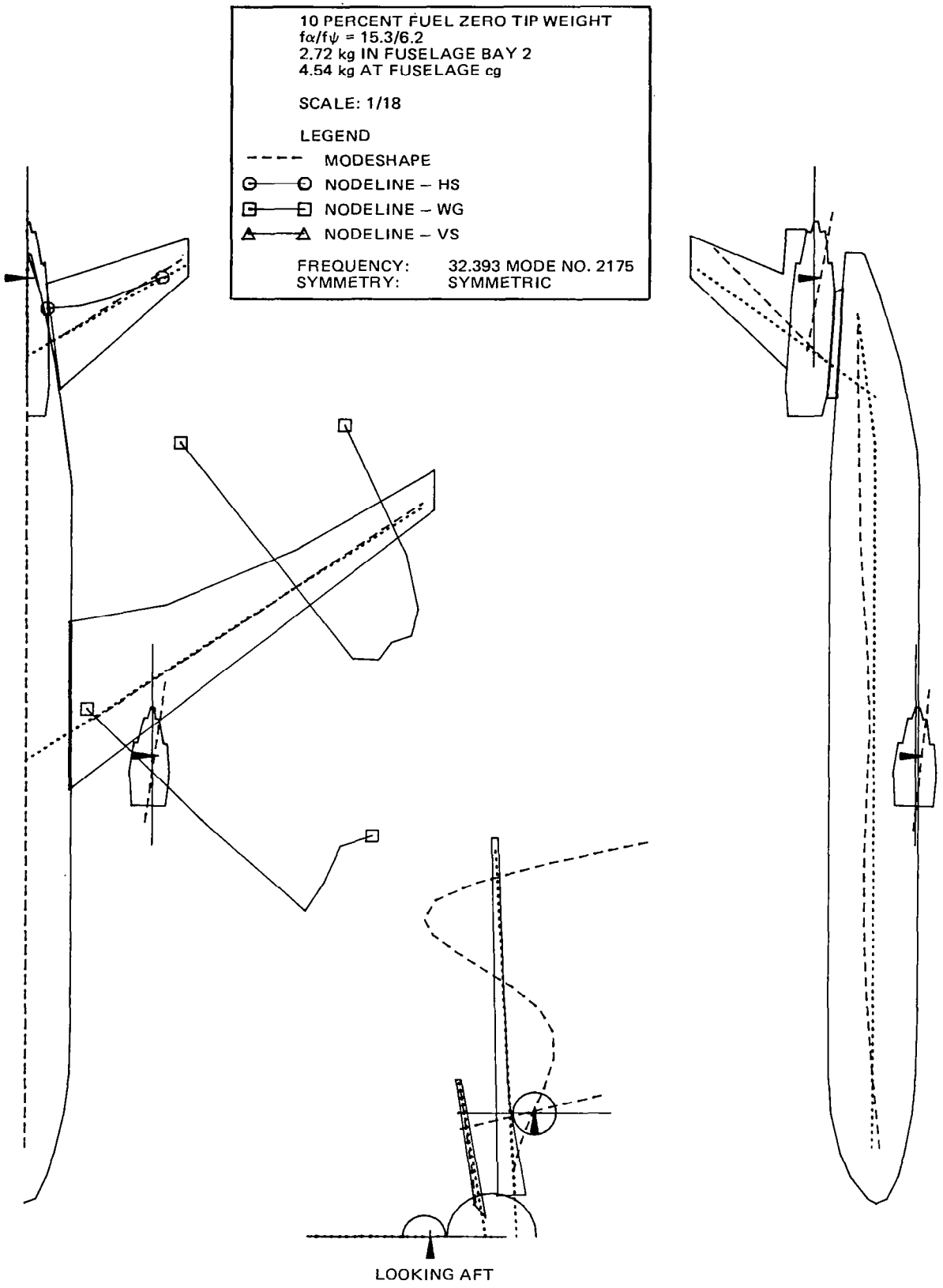

FIGURE C-23. FULL-SPAN MODE SHAPE – HIGHER WING MODE (32.393 Hz)

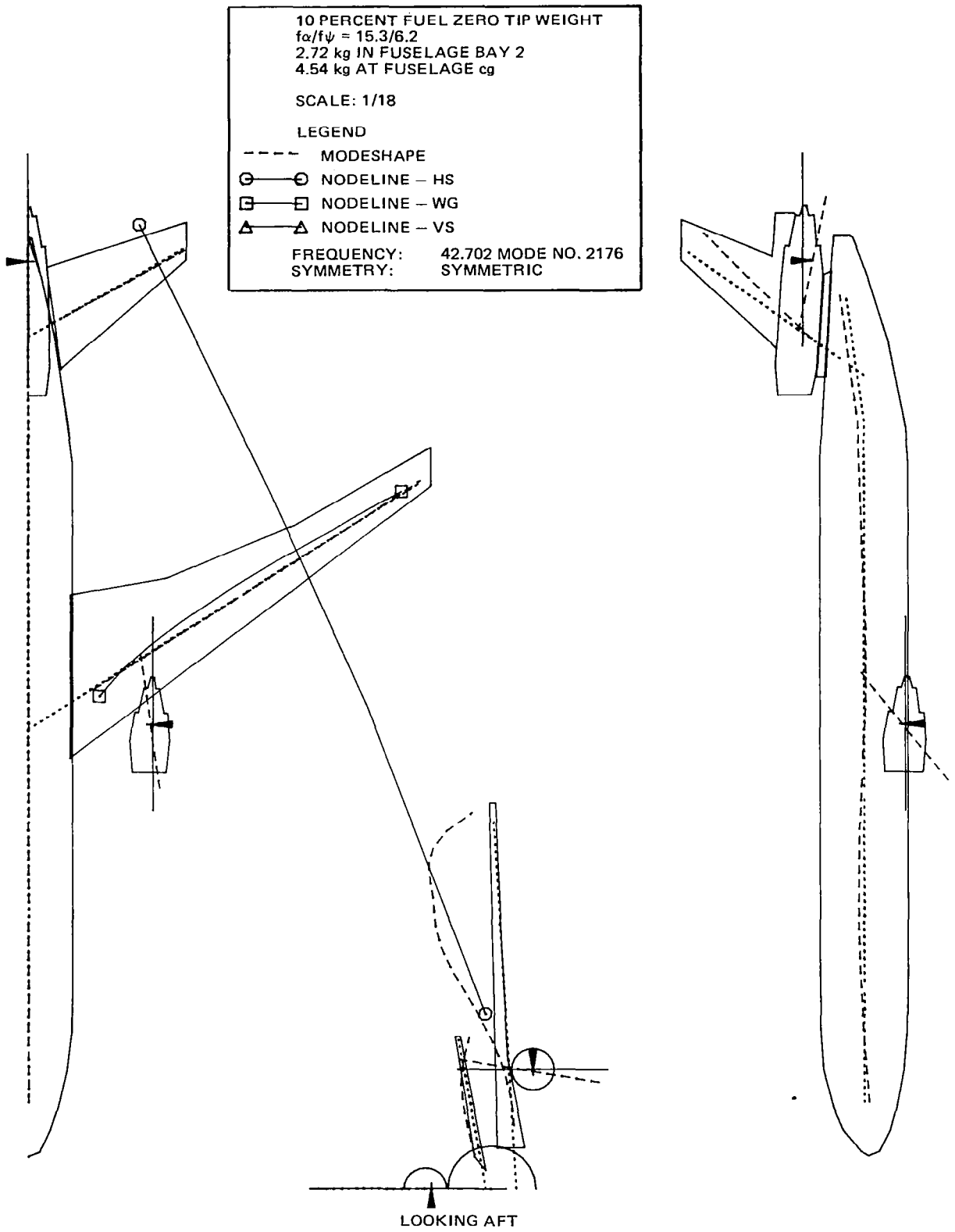

FIGURE C-24. FULL-SPAN MODE SHAPE – HIGHER WING MODE (42.702 Hz)

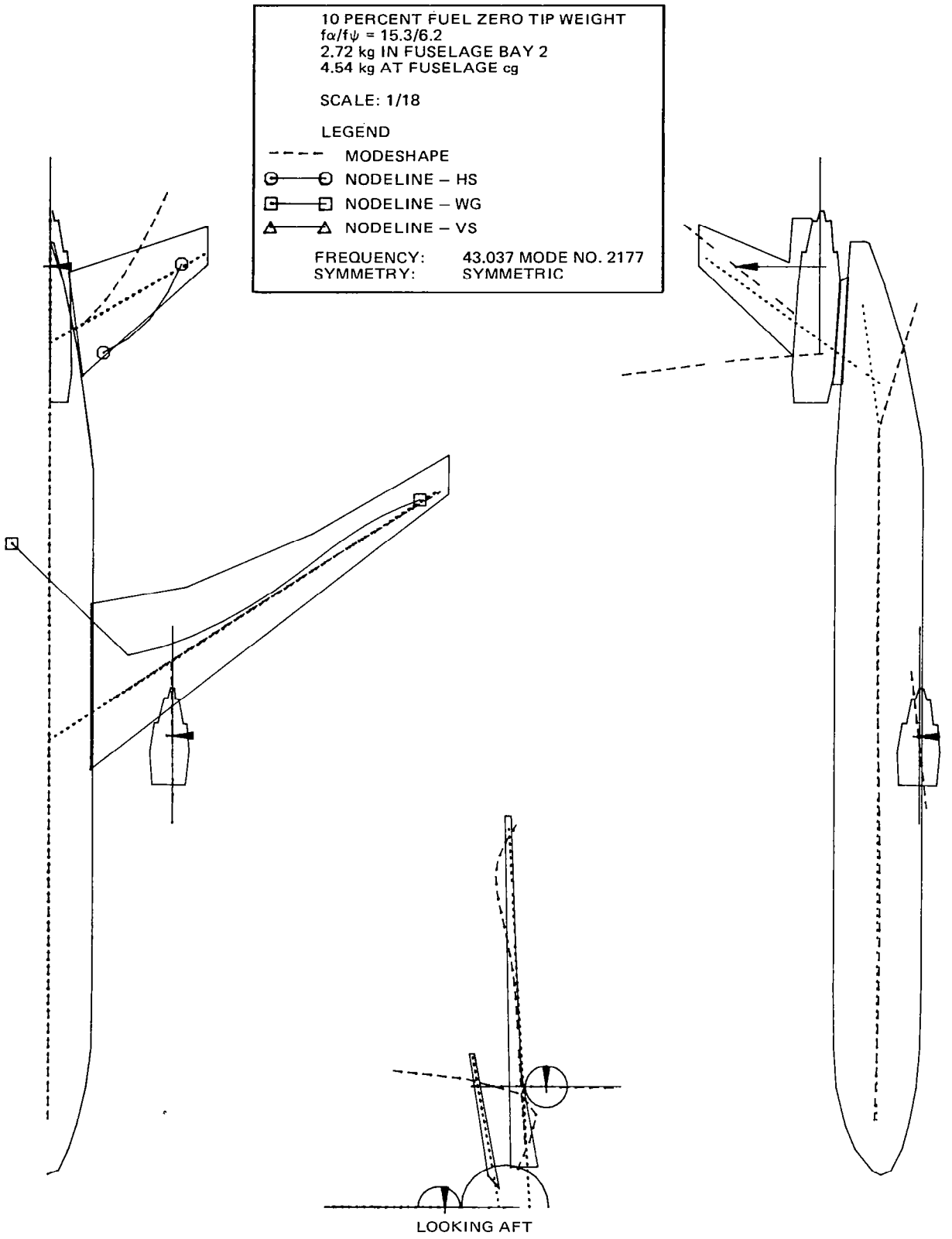

FIGURE C-25. FULL-SPAN MODE SHAPE – HORIZONTAL STABILIZER MODE

Table C-1

Measured and Analytical Frequencies - Semispan Model

ZERO PERCENT WING FUEL

MEASURED FREQUENCY (Hz)		ANALYTICAL FREQ. (Hz)
1st Entry	2nd Entry	
5.3	5.2	5.2
6.3	6.5	6.2
12.5	12.6	12.4
16.3	16.2	16.3
23.1	23.1	23.3
34.7	34.0	33.2
42.3	42.0	42.2

Table C-2

Symmetric Measured Frequencies - Full Span Model

MODE DESCRIPTION	10% Wing Fuel			100% Wing Fuel		
Wing Tip Weight	0 GM	10 GM	20 GM	0 GM	10 GM	20 GM
1st Wing Bending	5.0 Hz	4.7 Hz	4.7 Hz	3.9 Hz	3.8 Hz	3.6 Hz
Engine Yaw/ Fus. Vert. Bend.	8.9	8.8	8.8	8.3	8.3	8.1
Fus. Vert. Bending	9.0	8.8	9.0	-	-	-
Engine Pitch/ Wing Torsion	14.7	13.9	12.8	11.7	11.2	10.7
Engine Pitch	-	16.3	15.6	15.7	15.3	14.8
2nd Wing Bending	17.8	-	-	-	-	-
Wing Fore and Aft Bend.	-	21.0	20.7	-	20.0	-
Higher Wing Mode	-	23.2	25.3	24.6	26.0	-
Engine Roll	31.0	31.4	31.4	-	-	32.0
Outer Wing Torsion	41.6	-	35.2	33.8	-	35.9

TABLE C-3
SYMMETRIC MODE SHAPE –
10-PERCENT WING FUEL, NO TIP WEIGHT, 4.54 kg IN BAY 47

MODE NO. 2163 FREQ = 0.0 GENERALIZED MASS= 0.08

BAY	H	ALPH	THET	F	L	PSI
1	0.0	0.0	0.0	-0.592E+00	-0.806E+00	0.0
2	0.0	0.0	0.0	-0.592E+00	-0.806E+00	0.0
3	0.0	0.0	0.0	-0.592E+00	-0.806E+00	0.0
4	0.0	0.0	0.0	-0.592E+00	-0.806E+00	0.0
5	0.0	0.0	0.0	-0.592E+00	-0.806E+00	0.0
6	0.0	0.0	0.0	-0.592E+00	-0.806E+00	0.0
7	0.0	0.0	0.0	0.0	0.0	0.0
8	0.0	0.0	0.0	0.0	0.0	0.0
9	0.0	0.0	0.0	0.0	0.0	0.0
10	0.0	0.0	0.0	0.0	0.0	0.0
11	0.985E+00	0.0	0.0	-0.869E-01	-0.15CE+CC	0.0
12	0.985E+00	0.0	0.0	-0.869E-01	-0.150E+00	0.0
13	0.985E+00	0.0	0.0	-0.869E-01	-0.15CE+00	0.0
14	0.985E+00	0.0	0.0	-0.869E-01	-0.15CE+CC	0.0
15	0.985E+00	0.0	0.0	-0.869E-01	-0.150E+00	0.0
16	0.985E+00	0.0	0.0	-0.869E-01	-0.15CE+00	0.0
17	0.0	0.0	0.0	0.0	0.C	0.0
18	0.0	0.0	0.0	0.0	0.0	0.0
19	0.0	0.0	0.0	0.0	0.0	0.0
20	0.0	0.0	0.0	0.0	0.C	0.0
21	0.998E+00	0.0	0.0	-0.309E-01	-0.472E-01	0.0
22	0.998E+00	0.0	0.0	-0.309E-01	-0.472E-01	0.0
23	0.998E+00	0.0	0.0	-0.309E-01	-0.472E-01	0.0
24	0.998E+00	0.0	0.0	-0.309E-01	-0.472E-01	0.0
25	0.998E+00	0.0	0.0	-0.309E-01	-0.472E-01	0.0
26	0.998E+00	0.0	0.0	-0.309E-01	-0.472E-01	0.0
27	0.998E+00	0.0	0.0	-0.309E-01	-0.472E-01	0.0
28	0.998E+00	0.0	0.0	-0.309E-01	-0.472E-01	0.0
29	0.998E+00	0.0	0.0	-0.309E-01	-0.472E-01	0.0
30	0.998E+00	0.0	0.0	-0.309E-01	-0.472E-01	0.0
31	0.998E+00	0.0	0.0	-0.309E-01	-0.472E-01	0.0
32	0.998E+00	0.0	0.0	-0.309E-01	-0.472E-01	0.0
33	0.998E+00	0.0	0.0	-0.309E-01	-0.472E-01	0.0
34	0.998E+00	0.0	0.0	-0.309E-01	-0.472E-01	0.0
35	0.998E+00	0.0	0.0	-0.309E-01	-0.472E-01	0.0
36	0.998E+00	0.0	0.0	-0.309E-01	-0.472E-01	0.0
37	0.0	0.0	0.0	0.0	0.0	0.0
38	0.0	0.0	0.0	0.0	0.0	0.0
39	0.100E+01	0.0	0.0	0.0	0.0	0.0
40	0.0	0.0	0.0	0.0	0.0	0.0
41	0.100E+01	0.0	0.0	0.0	0.0	0.0
42	0.100E+01	0.0	0.0	0.0	0.0	0.0
43	0.100E+01	0.0	0.0	0.0	0.0	0.0
44	0.100E+01	0.0	0.0	0.0	0.0	0.0
45	0.100E+01	0.0	0.0	0.0	0.0	0.0
46	0.100E+01	0.0	0.0	0.0	0.0	0.0
47	0.100E+01	0.0	0.0	0.0	0.0	0.0
48	0.100E+01	0.0	0.0	0.0	0.0	0.0
49	0.100E+01	0.0	0.0	0.0	0.0	0.0
50	0.100E+01	0.0	0.0	0.0	0.0	0.0
51	0.100E+01	0.0	0.0	0.0	0.0	0.0
52	0.0	0.0	0.0	0.0	0.0	0.0
53	0.0	0.0	0.0	0.0	0.0	0.0
54	0.0	0.0	0.0	0.0	0.0	0.0
55	0.0	0.0	0.0	0.0	0.0	0.0
56	0.100E+01	0.0	0.0	-0.262E-01	0.0	0.0

TABLE C-4
SYMMETRIC MODE SHAPE –
10-PERCENT WING FUEL, NO TIP WEIGHT, 4.54 kg IN BAY 47

MODE NO. 2164 FREQ = 0.0 GENERALIZED MASS= 62.78

BAY	H	ALPH	THET	F	L	PSI
1	0.154E-04	0.0	0.0	-0.340E+02	-0.357E+02	-0.100E+01
2	0.168E-04	0.0	0.0	-0.420E+02	-0.357E+02	-0.100E+01
3	0.173E-04	0.0	0.0	-0.447E+02	-0.357E+02	-0.100E+01
4	0.178E-04	0.0	0.0	-0.473E+02	-0.357E+02	-0.100E+01
5	0.183E-04	0.0	0.0	-0.498E+02	-0.357E+02	-0.100E+01
6	0.188E-04	0.0	0.0	-0.523E+02	-0.357E+02	-0.100E+01
7	0.0	0.0	0.0	0.0	0.0	0.0
8	0.0	0.0	0.0	0.0	0.0	0.0
9	0.0	0.0	0.0	0.0	0.0	0.0
10	0.0	0.0	0.0	0.0	0.0	0.0
11	0.509E+02	0.853E+00	0.493E+00	-0.576E+01	-0.705E+01	-0.174E+00
12	0.527E+02	0.853E+00	0.493E+00	-0.638E+01	-0.705E+01	-0.174E+00
13	0.545E+02	0.853E+00	0.493E+00	-0.699E+01	-0.705E+01	-0.174E+00
14	0.562E+02	0.853E+00	0.493E+00	-0.759E+01	-0.705E+01	-0.174E+00
15	0.578E+02	0.853E+00	0.493E+00	-0.816E+01	-0.705E+01	-0.174E+00
16	0.593E+02	0.853E+00	0.493E+00	-0.869E+01	-0.705E+01	-0.174E+00
17	0.0	0.0	0.0	0.0	0.0	0.0
18	0.0	0.0	0.0	0.0	0.0	0.0
19	0.0	0.0	0.0	0.0	0.0	0.0
20	0.0	0.0	0.0	0.0	0.0	0.0
21	0.517E+01	0.835E+00	0.547E+00	0.193E+01	-0.161E+01	-0.564E-01
22	0.753E+01	0.835E+00	0.547E+00	0.169E+01	-0.162E+01	-0.564E-01
23	0.980E+01	0.835E+00	0.547E+00	0.145E+01	-0.161E+01	-0.564E-01
24	0.118E+02	0.835E+00	0.547E+00	0.125E+01	-0.162E+01	-0.564E-01
25	0.141E+02	0.835E+00	0.547E+00	0.102E+01	-0.162E+01	-0.564E-01
26	0.162E+02	0.835E+00	0.547E+00	0.796E+00	-0.161E+01	-0.564E-01
27	0.181E+02	0.835E+00	0.547E+00	0.604E+00	-0.162E+01	-0.564E-01
28	0.199E+02	0.835E+00	0.547E+00	0.412E+00	-0.162E+01	-0.564E-01
29	0.215E+02	0.835E+00	0.547E+00	0.246E+00	-0.161E+01	-0.564E-01
30	0.229E+02	0.835E+00	0.547E+00	0.112E+00	-0.162E+01	-0.564E-01
31	0.242E+02	0.835E+00	0.547E+00	-0.299E-01	-0.162E+01	-0.564E-01
32	0.255E+02	0.835E+00	0.547E+00	-0.163E+00	-0.162E+01	-0.564E-01
33	0.269E+02	0.835E+00	0.547E+00	-0.304E+00	-0.161E+01	-0.564E-01
34	0.282E+02	0.835E+00	0.547E+00	-0.438E+00	-0.162E+01	-0.564E-01
35	0.295E+02	0.835E+00	0.547E+00	-0.579E+00	-0.161E+01	-0.564E-01
36	0.309E+02	0.835E+00	0.547E+00	-0.724E+00	-0.162E+01	-0.564E-01
37	0.0	0.0	0.0	0.0	0.0	0.0
38	0.0	0.0	0.0	0.0	0.0	0.0
39	0.567E+00	0.100E+01	0.0	0.498E+01	0.0	0.0
40	0.0	0.0	0.0	0.0	0.0	0.0
41	-0.469E+02	0.100E+01	0.0	0.0	0.0	0.0
42	-0.399E+02	0.100E+01	0.0	0.0	0.0	0.0
43	-0.313E+02	0.100E+01	0.0	0.0	0.0	0.0
44	-0.226E+02	0.100E+01	0.0	0.0	0.0	0.0
45	-0.131E+02	0.100E+01	0.0	0.0	0.0	0.0
46	-0.366E+01	0.100E+01	0.0	0.0	0.0	0.0
47	0.362E+01	0.100E+01	0.0	0.0	0.0	0.0
48	0.122E+02	0.100E+01	0.0	0.0	0.0	0.0
49	0.254E+02	0.100E+01	0.0	0.0	0.0	0.0
50	0.386E+02	0.100E+01	0.0	0.0	0.0	0.0
51	0.544E+02	0.100E+01	0.0	-0.214E+01	0.0	0.0
52	0.0	0.0	0.0	0.0	0.0	0.0
53	0.0	0.0	0.0	0.0	0.0	0.0
54	0.0	0.0	0.0	0.0	0.0	0.0
55	0.0	0.0	0.0	0.0	0.0	0.0
56	0.585E+02	0.100E+01	0.0	-0.885E+01	0.0	0.0

TABLE C-5
SYMMETRIC MODE SHAPE –
10-PERCENT WING FUEL, NO TIP WEIGHT, 4.54 kg IN BAY 47

MODE NO. 2165 FREQ = 0.0 GENERALIZED MASS= 0.08

BAY	H	ALPH	THET	F	L	PSI
1	0.0	0.0	0.0	0.806E+00	-0.592E+00	0.0
2	0.0	0.0	0.0	0.806E+00	-0.592E+00	0.0
3	0.0	0.0	0.0	0.806E+00	-0.592E+00	0.0
4	0.0	0.0	0.0	0.806E+00	-0.592E+00	0.0
5	0.0	0.0	0.0	0.806E+00	-0.592E+00	0.0
6	0.0	0.0	0.0	0.806E+00	-0.592E+00	0.0
7	0.0	0.0	0.0	0.0	0.0	0.0
8	0.0	0.0	0.0	0.0	0.0	0.0
9	0.0	0.0	0.0	0.0	0.0	0.0
10	0.0	0.0	0.0	0.0	0.0	0.0
11	0.0	0.0	0.0	0.866E+00	-0.500E+00	0.0
12	0.0	0.0	0.0	0.866E+00	-0.500E+00	0.0
13	0.0	0.0	0.0	0.866E+00	-0.500E+00	0.0
14	0.0	0.0	0.0	0.866E+00	-0.500E+00	0.0
15	0.0	0.0	0.0	0.866E+00	-0.500E+00	0.0
16	0.0	0.0	0.0	0.866E+00	-0.500E+00	0.0
17	0.0	0.0	0.0	0.0	0.0	0.0
18	0.0	0.0	0.0	0.0	0.0	0.0
19	0.0	0.0	0.0	0.0	0.0	0.0
20	0.0	0.0	0.0	0.0	0.0	0.0
21	0.0	0.0	0.0	0.837E+00	-0.548E+00	0.0
22	0.0	0.0	0.0	0.837E+00	-0.548E+00	0.0
23	0.0	0.0	0.0	0.837E+00	-0.548E+00	0.0
24	0.0	0.0	0.0	0.837E+00	-0.548E+00	0.0
25	0.0	0.0	0.0	0.837E+00	-0.548E+00	0.0
26	0.0	0.0	0.0	0.837E+00	-0.548E+00	0.0
27	0.0	0.0	0.0	0.837E+00	-0.548E+00	0.0
28	0.0	0.0	0.0	0.837E+00	-0.548E+00	0.0
29	0.0	0.0	0.0	0.837E+00	-0.548E+00	0.0
30	0.0	0.0	0.0	0.837E+00	-0.548E+00	0.0
31	0.0	0.0	0.0	0.837E+00	-0.548E+00	0.0
32	0.0	0.0	0.0	0.837E+00	-0.548E+00	0.0
33	0.0	0.0	0.0	0.837E+00	-0.548E+00	0.0
34	0.0	0.0	0.0	0.837E+00	-0.548E+00	0.0
35	0.0	0.0	0.0	0.837E+00	-0.548E+00	0.0
36	0.0	0.0	0.0	0.837E+00	-0.548E+00	0.0
37	0.0	0.0	0.0	0.0	0.0	0.0
38	0.0	0.0	0.0	0.0	0.0	0.0
39	0.0	0.0	0.0	0.100E+01	0.0	0.0
40	0.0	0.0	0.0	0.0	0.0	0.0
41	0.0	0.0	0.0	0.100E+01	0.0	0.0
42	0.0	0.0	0.0	0.100E+01	0.0	0.0
43	0.0	0.0	0.0	0.100E+01	0.0	0.0
44	0.0	0.0	0.0	0.100E+01	0.0	0.0
45	0.0	0.0	0.0	0.100E+01	0.0	0.0
46	0.0	0.0	0.0	0.100E+01	0.0	0.0
47	0.0	0.0	0.0	0.100E+01	0.0	0.0
48	0.0	0.0	0.0	0.100E+01	0.0	0.0
49	0.0	0.0	0.0	0.100E+01	0.0	0.0
50	0.0	0.0	0.0	0.100E+01	0.0	0.0
51	0.0	0.0	0.0	0.100E+01	0.0	0.0
52	0.0	0.0	0.0	0.0	0.0	0.0
53	0.0	0.0	0.0	0.0	0.0	0.0
54	0.0	0.0	0.0	0.0	0.0	0.0
55	0.0	0.0	0.0	0.0	0.0	0.0
56	0.262E-01	0.0	0.0	0.100E+01	0.0	0.0

TABLE C-6
SYMMETRIC MODE SHAPE –
10-PERCENT WING FUEL, NO TIP WEIGHT, 4.54 kg IN BAY 47

MODE NO. 2166 FREQ = 5.15 GENERALIZED MASS= 0.00

BAY	H	ALPH	THET	F	L	PSI
1	0.121E-08	0.0	0.0	0.457E-01	0.452E-01	0.191E-02
2	0.133E-08	0.0	0.0	0.612E-01	0.452E-01	0.195E-02
3	0.137E-08	0.0	0.0	0.666E-01	0.452E-01	0.195E-02
4	0.141E-08	0.0	0.0	0.715E-01	0.452E-01	0.195E-02
5	0.145E-08	0.0	0.0	0.765E-01	0.452E-01	0.195E-02
6	0.148E-08	0.0	0.0	0.814E-01	0.452E-01	0.195E-02
7	0.0	0.0	0.0	0.0	0.0	0.0
8	0.0	0.0	0.0	0.0	0.0	0.0
9	0.0	0.0	0.0	0.0	0.0	0.0
10	0.0	0.0	0.0	0.0	0.0	0.0
11	-0.683E-01	-0.166E-02	-0.118E-02	0.691E-02	0.988E-02	0.34CE-03
12	-0.733E-01	-0.166E-02	-0.159E-02	0.815E-02	0.988E-02	0.345E-03
13	-0.796E-01	-0.167E-02	-0.198E-02	0.936E-02	0.988E-02	0.348E-03
14	-0.870E-01	-0.168E-02	-0.234E-02	0.106E-01	0.988E-02	0.351E-03
15	-0.952E-01	-0.168E-02	-0.261E-02	0.117E-01	0.988E-02	0.353E-03
16	-0.103E+00	-0.168E-02	-0.273E-02	0.128E-01	0.988E-02	0.353E-03
17	0.0	0.0	0.0	0.0	0.0	0.0
18	0.0	0.0	0.0	0.0	0.0	0.0
19	0.0	0.0	0.0	0.0	0.0	0.0
20	0.0	0.0	0.0	0.0	0.0	0.0
21	-0.687E-02	-0.304E-04	0.778E-03	-0.884E-03	0.115E-02	-0.336E-05
22	-0.494E-03	0.562E-04	0.199E-02	-0.893E-03	0.115E-02	-0.157E-05
23	0.112E-01	0.174E-03	0.382E-02	-0.897E-03	0.115E-02	-0.285E-07
24	0.299E-01	0.299E-03	0.630E-02	-0.896E-03	0.115E-02	0.414E-06
25	0.626E-01	0.491E-03	0.993E-02	-0.893E-03	0.115E-02	0.841E-06
26	0.109E+00	0.740E-03	0.144E-01	-0.890E-03	0.115E-02	0.106E-05
27	0.167E+00	0.106E-02	0.192E-01	-0.886E-03	0.115E-02	0.993E-06
28	0.241E+00	0.148E-02	0.243E-01	-0.883E-03	0.115E-02	0.589E-06
29	0.318E+00	0.187E-02	0.283E-01	-0.882E-03	0.115E-02	-0.103E-06
30	0.391E+00	0.225E-02	0.313E-01	-0.883E-03	0.115E-02	-0.936E-06
31	0.471E+00	0.272E-02	0.345E-01	-0.887E-03	0.115E-02	-0.2CCE-05
32	0.559E+00	0.300E-02	0.379E-01	-0.893E-03	0.115E-02	-0.324E-05
33	0.656E+00	0.340E-02	0.413E-01	-0.903E-03	0.115E-02	-0.469E-05
34	0.761E+00	0.397E-02	0.446E-01	-0.916E-03	0.115E-02	-0.633E-05
35	0.872E+00	0.447E-02	0.466E-01	-0.934E-03	0.115E-02	-0.774E-05
36	0.100E+01	0.485E-02	0.473E-01	-0.955E-03	0.115E-02	-0.827E-05
37	0.0	0.0	0.0	0.0	0.0	0.0
38	0.0	0.0	0.0	0.0	0.0	0.0
39	-0.108E-01	0.252E-02	0.402E-02	0.551E-02	-0.239E-01	0.311E-02
40	-0.384E-03	0.0	0.248E-03	0.0	-0.840E-04	0.0
41	-0.251E-01	0.484E-03	0.0	-0.157E-02	0.0	0.0
42	-0.218E-01	0.479E-03	0.0	-0.157E-02	0.0	0.0
43	-0.178E-01	0.447E-03	0.0	-0.157E-02	0.0	0.0
44	-0.141E-01	0.382E-03	0.0	-0.157E-02	0.0	0.0
45	-0.110E-01	0.273E-03	0.0	-0.157E-02	0.0	0.0
46	-0.903E-02	0.143E-03	0.0	-0.157E-02	0.0	0.0
47	-0.884E-02	-0.197E-03	0.0	-0.157E-02	0.0	0.0
48	-0.130E-01	-0.767E-03	0.0	-0.157E-02	0.0	0.0
49	-0.263E-01	-0.112E-02	0.0	-0.157E-02	0.0	0.0
50	-0.448E-01	-0.167E-02	0.0	-0.157E-02	0.0	0.0
51	-0.758E-01	-0.198E-02	0.0	0.236E-02	0.0	0.0
52	0.0	0.0	0.0	0.0	0.0	0.0
53	0.0	0.0	0.0	0.0	0.0	0.0
54	0.0	0.0	0.0	0.0	0.0	0.0
55	0.0	0.0	0.0	0.0	0.0	0.0
56	-0.827E-01	-0.197E-02	0.0	0.121E-01	-0.158E-14	-0.429E-15

TABLE C-7
SYMMETRIC MODE SHAPE –
10-PERCENT WING FUEL, NO TIP WEIGHT, 4.54 kg IN BAY 47

MODE NO. 2167 FREQ = 6.23 GENERALIZED MASS= 0.01

BAY	H	ALPH	THET	F	L	PSI
1	0.117E-08	0.0	0.0	0.973E-02	0.771E-02	0.510E-03
2	0.128E-08	0.0	0.0	0.139E-01	0.771E-02	0.522E-03
3	0.132E-08	0.0	0.0	0.153E-01	0.771E-02	0.522E-03
4	0.136E-08	0.0	0.0	0.166E-01	0.771E-02	0.522E-03
5	0.139E-08	0.0	0.0	0.180E-01	0.771E-02	0.522E-03
6	0.143E-08	0.0	0.0	0.193E-01	0.771E-02	0.522E-03
7	0.0	0.0	0.0	0.0	0.0	0.0
8	0.0	0.0	0.0	0.0	0.0	0.0
9	0.0	0.0	0.0	0.0	0.0	0.0
10	0.0	0.0	0.0	0.0	0.0	0.0
11	-0.134E-01	-0.443E-03	-0.326E-03	0.192E-02	0.16CE-02	0.913E-04
12	-0.148E-01	-0.445E-03	-0.457E-03	0.225E-02	0.16CE-02	0.932E-04
13	-0.166E-01	-0.448E-03	-0.584E-03	0.258E-02	0.16CE-02	0.946E-04
14	-0.188E-01	-0.451E-03	-0.705E-03	0.291E-02	0.16CE-02	0.957E-04
15	-0.213E-01	-0.452E-03	-0.796E-03	0.322E-02	0.16CE-02	0.964E-04
16	-0.238E-01	-0.453E-03	-0.834E-03	0.352E-02	0.16CE-02	0.967E-04
17	0.0	0.0	0.0	0.0	0.0	0.0
18	0.0	0.0	0.0	0.0	0.0	0.0
19	0.0	0.0	0.0	0.0	0.0	0.0
20	0.0	0.0	0.0	0.0	0.0	0.0
21	0.143E-02	0.277E-03	-0.109E-03	0.141E-03	-0.279E-03	-0.788E-04
22	0.481E-03	0.688E-03	-0.264E-03	-0.523E-03	-0.279E-03	-0.198E-03
23	-0.665E-03	0.123E-02	-0.241E-03	-0.155E-02	-0.279E-03	-0.296E-03
24	-0.104E-02	0.131E-02	0.856E-04	-0.277E-02	-0.279E-03	-0.361E-03
25	0.684E-03	0.142E-02	0.848E-03	-0.439E-02	-0.279E-03	-0.433E-03
26	0.614E-02	0.162E-02	0.208E-02	-0.617E-02	-0.279E-03	-0.487E-03
27	0.159E-01	0.188E-02	0.361E-02	-0.792E-02	-0.279E-03	-0.515E-03
28	0.311E-01	0.217E-02	0.525E-02	-0.968E-02	-0.279E-03	-0.512E-03
29	0.483E-01	0.239E-02	0.651E-02	-0.111E-01	-0.279E-03	-0.478E-03
30	0.652E-01	0.257E-02	0.737E-02	-0.122E-01	-0.279E-03	-0.426E-03
31	0.842E-01	0.273E-02	0.821E-02	-0.132E-01	-0.279E-03	-0.352E-03
32	0.105E+00	0.259E-02	0.908E-02	-0.139E-01	-0.279E-03	-0.260E-03
33	0.129E+00	0.232E-02	0.101E-01	-0.144E-01	-0.279E-03	-0.148E-03
34	0.155E+00	0.186E-02	0.114E-01	-0.146E-01	-0.279E-03	-0.173E-04
35	0.184E+00	0.148E-02	0.124E-01	-0.145E-01	-0.279E-03	0.980E-04
36	0.218E+00	0.137E-02	0.128E-01	-0.142E-01	-0.279E-03	0.142E-03
37	0.0	0.0	0.0	0.0	0.0	0.0
38	0.0	0.0	0.0	0.0	0.0	0.0
39	-0.104E-01	0.124E-02	-0.546E-01	0.200E-02	0.10CE+01	-0.206E+00
40	0.587E-04	0.0	-0.380E-04	0.0	0.128E-04	0.0
41	-0.669E-02	0.217E-03	0.0	0.170E-03	0.0	0.0
42	-0.518E-02	0.215E-03	0.0	0.170E-03	0.0	0.0
43	-0.338E-02	0.203E-03	0.0	0.170E-03	0.0	0.0
44	-0.169E-02	0.180E-03	0.0	0.170E-03	0.0	0.0
45	-0.162E-03	0.142E-03	0.0	0.170E-03	0.0	0.0
46	0.977E-03	0.976E-04	0.0	0.170E-03	0.0	0.0
47	0.143E-02	-0.151E-05	0.0	0.170E-03	0.0	0.0
48	0.698E-03	-0.164E-03	0.0	0.170E-03	0.0	0.0
49	-0.238E-02	-0.269E-03	0.0	0.170E-03	0.0	0.0
50	-0.704E-02	-0.434E-03	0.0	0.170E-03	0.0	0.0
51	-0.153E-01	-0.530E-03	0.0	0.121E-02	0.0	0.0
52	0.0	0.0	0.0	0.0	0.0	0.0
53	0.0	0.0	0.0	0.0	0.0	0.0
54	0.0	0.0	0.0	0.0	0.0	0.0
55	0.0	0.0	0.0	0.0	0.0	0.0
56	-0.171E-01	-0.528E-03	0.0	0.362E-02	-0.444E-15	-0.12CE-15

TABLE C-8
SYMMETRIC MODE SHAPE –
10-PERCENT WING FUEL, NO TIP WEIGHT, 4.54 kg IN BAY 47

MODE NO. 2168 FREQ = 7.88 GENERALIZED MASS= 0.01

BAY	H	ALPH	THET	F	L	PSI
1	-0.731E-07	0.0	0.0	-0.270E+00	-0.168E+00	-0.217E-01
2	-0.801E-07	0.0	0.0	-0.447E+00	-0.168E+00	-0.223E-01
3	-0.825E-07	0.0	0.0	-0.508E+00	-0.168E+00	-0.223E-01
4	-0.848E-07	0.0	0.0	-0.565E+00	-0.168E+00	-0.223E-01
5	-0.870E-07	0.0	0.0	-0.621E+00	-0.168E+00	-0.223E-01
6	-0.893E-07	0.0	0.0	-0.678E+00	-0.168E+00	-0.223E-01
7	0.0	0.0	0.0	0.0	0.0	0.0
8	0.0	0.0	0.0	0.0	0.0	0.0
9	0.0	0.0	0.0	0.0	0.0	0.0
10	0.0	0.0	0.0	0.0	0.0	0.0
11	0.359E+00	0.189E-01	0.147E-01	-0.452E-01	-0.463E-01	-0.390E-02
12	0.425E+00	0.191E-01	0.218E-01	-0.595E-01	-0.463E-01	-0.400E-02
13	0.514E+00	0.193E-01	0.290E-01	-0.736E-01	-0.463E-01	-0.406E-02
14	0.626E+00	0.195E-01	0.360E-01	-0.877E-01	-0.463E-01	-0.412E-02
15	0.754E+00	0.196E-01	0.413E-01	-0.101E+00	-0.463E-01	-0.415E-02
16	0.883E+00	0.196E-01	0.435E-01	-0.114E+00	-0.463E-01	-0.416E-02
17	0.0	0.0	0.0	0.0	0.0	0.0
18	0.0	0.0	0.0	0.0	0.0	0.0
19	0.0	0.0	0.0	0.0	0.0	0.0
20	0.0	0.0	0.0	0.0	0.0	0.0
21	-0.239E+00	-0.324E-02	-0.294E-02	0.820E-02	0.107E-01	0.292E-03
22	-0.252E+00	-0.192E-02	-0.265E-02	0.945E-02	0.108E-01	0.297E-03
23	-0.260E+00	-0.106E-04	-0.973E-03	0.107E-01	0.107E-01	0.299E-03
24	-0.260E+00	-0.158E-03	0.136E-02	0.118E-01	0.108E-01	0.319E-03
25	-0.246E+00	-0.311E-03	0.559E-02	0.132E-01	0.108E-01	0.344E-03
26	-0.214E+00	-0.299E-03	0.116E-01	0.146E-01	0.107E-01	0.367E-03
27	-0.161E+00	-0.167E-03	0.189E-01	0.159E-01	0.108E-01	0.385E-03
28	-0.825E-01	0.726E-04	0.273E-01	0.172E-01	0.108E-01	0.399E-03
29	0.803E-02	0.384E-03	0.345E-01	0.184E-01	0.107E-01	0.406E-03
30	0.985E-01	0.728E-03	0.401E-01	0.194E-01	0.108E-01	0.407E-03
31	0.204E+00	0.123E-02	0.466E-01	0.204E-01	0.107E-01	0.404E-03
32	0.327E+00	0.187E-02	0.539E-01	0.213E-01	0.108E-01	0.397E-03
33	0.467E+00	0.293E-02	0.615E-01	0.223E-01	0.107E-01	0.386E-03
34	0.626E+00	0.458E-02	0.686E-01	0.232E-01	0.108E-01	0.370E-03
35	0.800E+00	0.610E-02	0.730E-01	0.241E-01	0.107E-01	0.355E-03
36	0.100E+01	0.713E-02	0.742E-01	0.250E-01	0.108E-01	0.349E-03
37	0.0	0.0	0.0	0.0	0.0	0.0
38	0.0	0.0	0.0	0.0	0.0	0.0
39	-0.313E+00	0.127E-01	-0.921E-03	0.225E-01	0.876E-03	0.136E-03
40	0.347E-03	0.0	-0.225E-03	0.0	0.759E-04	0.0
41	0.611E+00	-0.241E-01	0.0	0.128E-01	0.0	0.0
42	0.443E+00	-0.238E-01	0.0	0.128E-01	0.0	0.0
43	0.245E+00	-0.221E-01	0.0	0.128E-01	0.0	0.0
44	0.644E-01	-0.189E-01	0.0	0.128E-01	0.0	0.0
45	-0.902E-01	-0.136E-01	0.0	0.128E-01	0.0	0.0
46	-0.192E+00	-0.763E-02	0.0	0.128E-01	0.0	0.0
47	-0.226E+00	-0.155E-02	0.0	0.128E-01	0.0	0.0
48	-0.209E+00	0.537E-02	0.0	0.128E-01	0.0	0.0
49	-0.975E-01	0.100E-01	0.0	0.128E-01	0.0	0.0
50	0.879E-01	0.179E-01	0.0	0.128E-01	0.0	0.0
51	0.439E+00	0.227E-01	0.0	-0.310E-01	0.0	0.0
52	0.0	0.0	0.0	0.0	0.0	0.0
53	0.0	0.0	0.0	0.0	0.0	0.0
54	0.0	0.0	0.0	0.0	0.0	0.0
55	0.0	0.0	0.0	0.0	0.0	0.0
56	0.516E+00	0.226E-01	0.0	-0.127E-00	0.212E-13	0.575E-14

TABLE C-9
SYMMETRIC MODE SHAPE –
10-PERCENT WING FUEL, NO TIP WEIGHT, 4.54 kg IN BAY 47

MODE NO. 2169 FREQ = 12.67 GENERALIZED MASS= 0.01

BAY	H	ALPH	THET	F	L	PSI
1	-0.514E-07	0.0	0.0	-0.149E-01	-0.269E-02	-0.625E-02
2	-0.564E-07	0.0	0.0	-0.665E-01	-0.280E-02	-0.652E-02
3	-0.581E-07	0.0	0.0	-0.844E-01	-0.280E-02	-0.652E-02
4	-0.597E-07	0.0	0.0	-0.101E+00	-0.280E-02	-0.652E-02
5	-0.613E-07	0.0	0.0	-0.117E+00	-0.280E-02	-0.652E-02
6	-0.629E-07	0.0	0.0	-0.134E+00	-0.281E-02	-0.652E-02
7	0.0	0.0	0.0	0.0	0.0	0.0
8	0.0	0.0	0.0	0.0	0.0	0.0
9	0.0	0.0	0.0	0.0	0.0	0.0
10	0.0	0.0	0.0	0.0	0.0	0.0
11	0.349E-01	0.569E-02	0.743E-02	0.138E-01	-0.143E-01	-0.115E-02
12	0.764E-01	0.581E-02	0.157E-01	0.962E-02	-0.143E-01	-0.115E-02
13	0.147E+00	0.597E-02	0.248E-01	0.560E-02	-0.143E-01	-0.114E-02
14	0.249E+00	0.612E-02	0.343E-01	0.166E-02	-0.143E-01	-0.114E-02
15	0.375E+00	0.622E-02	0.420E-01	-0.210E-02	-0.143E-01	-0.114E-02
16	0.509E+00	0.625E-02	0.451E-01	-0.558E-02	-0.143E-01	-0.114E-02
17	0.0	0.0	0.0	0.0	0.0	0.0
18	0.0	0.0	0.0	0.0	0.0	0.0
19	0.0	0.0	0.0	0.0	0.0	0.0
20	0.0	0.0	0.0	0.0	0.0	0.0
21	-0.867E-01	-0.102E-01	-0.157E-02	0.181E-01	-0.595E-02	0.127E-03
22	-0.979E-01	-0.253E-01	-0.404E-02	0.185E-01	-0.594E-02	0.898E-04
23	-0.127E+00	-0.453E-01	-0.114E-01	0.190E-01	-0.595E-02	0.146E-03
24	-0.173E+00	-0.472E-01	-0.128E-01	0.196E-01	-0.594E-02	0.177E-03
25	-0.225E+00	-0.492E-01	-0.122E-01	0.204E-01	-0.593E-02	0.224E-03
26	-0.266E+00	-0.509E-01	-0.827E-02	0.214E-01	-0.595E-02	0.279E-03
27	-0.282E+00	-0.522E-01	-0.720E-03	0.224E-01	-0.594E-02	0.338E-03
28	-0.266E+00	-0.535E-01	0.107E-01	0.237E-01	-0.594E-02	0.403E-03
29	-0.218E+00	-0.542E-01	0.224E-01	0.249E-01	-0.595E-02	0.465E-03
30	-0.151E+00	-0.545E-01	0.327E-01	0.261E-01	-0.593E-02	0.520E-03
31	-0.560E-01	-0.548E-01	0.456E-01	0.275E-01	-0.594E-02	0.576E-03
32	0.736E-01	-0.544E-01	0.610E-01	0.289E-01	-0.594E-02	0.630E-03
33	0.243E+00	-0.535E-01	0.781E-01	0.306E-01	-0.595E-02	0.685E-03
34	0.455E+00	-0.521E-01	0.955E-01	0.323E-01	-0.594E-02	0.741E-03
35	0.704E+00	-0.506E-01	0.107E+00	0.342E-01	-0.595E-02	0.782E-03
36	0.100E+01	-0.491E-01	0.111E+00	0.363E-01	-0.594E-02	0.796E-03
37	0.0	0.0	0.0	0.0	0.0	0.0
38	0.0	0.0	0.0	0.0	0.0	0.0
39	0.829E+00	-0.170E+00	0.192E-01	-0.307E+00	-0.798E-02	-0.514E-02
40	-0.122E-02	0.0	0.792E-03	0.0	-0.268E-03	0.0
41	-0.375E-01	0.519E-03	0.0	0.269E-01	0.0	0.0
42	-0.340E-01	0.483E-03	0.0	0.269E-01	0.0	0.0
43	-0.309E-01	0.179E-03	0.0	0.269E-01	0.0	0.0
44	-0.318E-01	-0.431E-03	0.0	0.269E-01	0.0	0.0
45	-0.405E-01	-0.145E-02	0.0	0.269E-01	0.0	0.0
46	-0.598E-01	-0.271E-02	0.0	0.269E-01	0.0	0.0
47	-0.815E-01	-0.249E-02	0.0	0.269E-01	0.0	0.0
48	-0.939E-01	-0.403E-03	0.0	0.269E-01	0.0	0.0
49	-0.852E-01	0.125E-02	0.0	0.269E-01	0.0	0.0
50	-0.465E-01	0.462E-02	0.0	0.269E-01	0.0	0.0
51	0.568E-01	0.695E-02	0.0	0.146E-01	0.0	0.0
52	0.0	0.0	0.0	0.0	0.0	0.0
53	0.0	0.0	0.0	0.0	0.0	0.0
54	0.0	0.0	0.0	0.0	0.0	0.0
55	0.0	0.0	0.0	0.0	0.0	0.0
56	0.768E-01	0.667E-02	0.0	-0.924E-02	0.112E-13	0.304E-14

TABLE C-10
SYMMETRIC MODE SHAPE –
10-PERCENT WING FUEL, NO TIP WEIGHT, 4.54 kg IN BAY 47

MODE NO. 2170 FREQ = 14.82 GENERALIZED MASS= 0.00

BAY	H	ALPH	THET	F	L	PSI
1	-0.345E-08	0.0	0.0	0.273E-01	0.261E-01	0.137E-02
2	-0.378E-08	0.0	0.0	0.396E-01	0.262E-01	0.159E-02
3	-0.390E-08	0.0	0.0	0.440E-01	0.262E-01	0.159E-02
4	-0.400E-08	0.0	0.0	0.480E-01	0.262E-01	0.159E-02
5	-0.411E-08	0.0	0.0	0.521E-01	0.262E-01	0.159E-02
6	-0.422E-08	0.0	0.0	0.561E-01	0.262E-01	0.159E-02
7	0.0	0.0	0.0	0.0	0.0	0.0
8	0.0	0.0	0.0	0.0	0.0	0.0
9	0.0	0.0	0.0	0.0	0.0	0.0
10	0.0	0.0	0.0	0.0	0.0	0.0
11	-0.293E-01	-0.733E-03	0.933E-02	0.414E-02	0.544E-02	0.163E-03
12	0.393E-01	-0.755E-03	0.292E-01	0.477E-02	0.544E-02	0.186E-03
13	0.181E+00	-0.784E-03	0.518E-01	0.546E-02	0.544E-02	0.203E-03
14	0.401E+00	-0.811E-03	0.767E-01	0.618E-02	0.544E-02	0.216E-03
15	0.689E+00	-0.829E-03	0.969E-01	0.691E-02	0.544E-02	0.225E-03
16	0.100E+01	-0.835E-03	0.105E+00	0.759E-02	0.544E-02	0.228E-03
17	0.0	0.0	0.0	0.0	0.0	0.0
18	0.0	0.0	0.0	0.0	0.0	0.0
19	0.0	0.0	0.0	0.0	0.0	0.0
20	0.0	0.0	0.0	0.0	0.0	0.0
21	0.476E-02	-0.978E-04	0.154E-04	-0.132E-02	0.560E-03	0.116E-04
22	0.540E-02	0.143E-03	0.241E-03	-0.128E-02	0.560E-03	0.921E-05
23	0.699E-02	0.454E-03	0.552E-03	-0.124E-02	0.560E-03	0.634E-05
24	0.947E-02	0.542E-03	0.765E-03	-0.123E-02	0.560E-03	0.256E-05
25	0.129E-01	0.658E-03	0.900E-03	-0.123E-02	0.561E-03	-0.239E-05
26	0.163E-01	0.769E-03	0.828E-03	-0.124E-02	0.560E-03	-0.739E-05
27	0.187E-01	0.879E-03	0.498E-03	-0.128E-02	0.560E-03	-0.118E-04
28	0.194E-01	0.996E-03	-0.136E-03	-0.133E-02	0.560E-03	-0.159E-04
29	0.179E-01	0.106E-02	-0.866E-03	-0.138E-02	0.560E-03	-0.189E-04
30	0.150E-01	0.110E-02	-0.155E-02	-0.142E-02	0.561E-03	-0.210E-04
31	0.102E-01	0.113E-02	-0.244E-02	-0.148E-02	0.560E-03	-0.226E-04
32	0.295E-02	0.107E-02	-0.355E-02	-0.153E-02	0.560E-03	-0.235E-04
33	-0.722E-02	0.966E-03	-0.480E-02	-0.159E-02	0.560E-03	-0.241E-04
34	-0.205E-01	0.782E-03	-0.611E-02	-0.165E-02	0.560E-03	-0.242E-04
35	-0.366E-01	0.582E-03	-0.698E-02	-0.171E-02	0.560E-03	-0.238E-04
36	-0.561E-01	0.416E-03	-0.727E-02	-0.178E-02	0.560E-03	-0.235E-04
37	0.0	0.0	0.0	0.0	0.0	0.0
38	0.0	0.0	0.0	0.0	0.0	0.0
39	-0.697E-02	0.244E-02	0.291E-03	0.340E-02	-0.115E-03	-0.192E-03
40	-0.615E-04	0.0	0.398E-04	0.0	-0.134E-04	0.0
41	-0.990E-02	0.642E-03	0.0	-0.847E-03	0.0	0.0
42	-0.547E-02	0.622E-03	0.0	-0.847E-03	0.0	0.0
43	-0.459E-03	0.536E-03	0.0	-0.847E-03	0.0	0.0
44	0.361E-02	0.381E-03	0.0	-0.847E-03	0.0	0.0
45	0.612E-02	0.143E-03	0.0	-0.847E-03	0.0	0.0
46	0.630E-02	-0.110E-03	0.0	-0.847E-03	0.0	0.0
47	0.446E-02	-0.448E-03	0.0	-0.847E-03	0.0	0.0
48	-0.108E-02	-0.810E-03	0.0	-0.847E-03	0.0	0.0
49	-0.131E-01	-0.946E-03	0.0	-0.847E-03	0.0	0.0
50	-0.261E-01	-0.103E-02	0.0	-0.847E-03	0.0	0.0
51	-0.412E-01	-0.694E-03	0.0	0.143E-02	0.0	0.0
52	0.0	0.0	0.0	0.0	0.0	0.0
53	0.0	0.0	0.0	0.0	0.0	0.0
54	0.0	0.0	0.0	0.0	0.0	0.0
55	0.0	0.0	0.0	0.0	0.0	0.0
56	-0.530E-01	-0.171E-02	0.0	0.766E-02	-0.868E-14	-0.235E-14

TABLE C-11
SYMMETRIC MODE SHAPE –
10-PERCENT WING FUEL, NO TIP WEIGHT, 4.54 kg IN BAY 47

MODE NO. 2171 FREQ = 16.57 GENERALIZED MASS= 0.00

BAY	H	ALPH	THET	F	L	PSI
1	-0.115E-07	0.0	0.0	0.681E-02	-0.745E-02	0.200E-02
2	-0.126E-07	0.0	0.0	0.236E-01	-0.740E-02	0.214E-02
3	-0.130E-07	0.0	0.0	0.295E-01	-0.740E-02	0.214E-02
4	-0.133E-07	0.0	0.0	0.349E-01	-0.740E-02	0.214E-02
5	-0.137E-07	0.0	0.0	0.403E-01	-0.740E-02	0.214E-02
6	-0.140E-07	0.0	0.0	0.457E-01	-0.740E-02	0.214E-02
7	0.0	0.0	0.0	0.0	0.0	0.0
8	0.0	0.0	0.0	0.0	0.0	0.0
9	0.0	0.0	0.0	0.0	0.0	0.0
10	0.0	0.0	0.0	0.0	0.0	0.0
11	-0.305E-02	-0.171E-02	-0.429E-04	0.942E-03	0.263E-03	0.360E-03
12	0.162E-03	-0.178E-02	0.188E-02	0.229E-02	0.264E-03	0.385E-03
13	0.106E-01	-0.186E-02	0.411E-02	0.367E-02	0.263E-03	0.402E-03
14	0.289E-01	-0.194E-02	0.660E-02	0.508E-02	0.262E-03	0.417E-03
15	0.543E-01	-0.200E-02	0.866E-02	0.647E-02	0.263E-03	0.426E-03
16	0.823E-01	-0.202E-02	0.952E-02	0.777E-02	0.263E-03	0.430E-03
17	0.0	0.0	0.0	0.0	0.0	0.0
18	0.0	0.0	0.0	0.0	0.0	0.0
19	0.0	0.0	0.0	0.0	0.0	0.0
20	0.0	0.0	0.0	0.0	0.0	0.0
21	0.403E-01	0.604E-03	-0.333E-02	-0.452E-02	-0.184E-03	0.423E-04
22	0.156E-01	0.196E-02	-0.722E-02	-0.437E-02	-0.182E-03	0.285E-04
23	-0.229E-01	0.372E-02	-0.114E-01	-0.430E-02	-0.184E-03	-0.290E-05
24	-0.750E-01	0.250E-02	-0.164E-01	-0.433E-02	-0.181E-03	-0.900E-05
25	-0.152E+00	0.577E-03	-0.209E-01	-0.439E-02	-0.181E-03	-0.195E-04
26	-0.236E+00	-0.171E-02	-0.220E-01	-0.449E-02	-0.184E-03	-0.351E-04
27	-0.307E+00	-0.426E-02	-0.179E-01	-0.464E-02	-0.182E-03	-0.534E-04
28	-0.352E+00	-0.707E-02	-0.700E-02	-0.486E-02	-0.182E-03	-0.762E-04
29	-0.352E+00	-0.860E-02	0.680E-02	-0.511E-02	-0.184E-03	-0.100E-03
30	-0.320E+00	-0.956E-02	0.203E-01	-0.539E-02	-0.181E-03	-0.124E-03
31	-0.249E+00	-0.103E-01	0.385E-01	-0.572E-02	-0.183E-03	-0.149E-03
32	-0.128E+00	-0.907E-02	0.615E-01	-0.611E-02	-0.181E-03	-0.175E-03
33	0.541E-01	-0.690E-02	0.882E-01	-0.657E-02	-0.183E-03	-0.203E-03
34	0.304E+00	-0.297E-02	0.117E+00	-0.710E-02	-0.181E-03	-0.232E-03
35	0.617E+00	0.159E-02	0.137E+00	-0.770E-02	-0.184E-03	-0.255E-03
36	0.100E+01	0.552E-02	0.144E+00	-0.841E-02	-0.182E-03	-0.263E-03
37	0.0	0.0	0.0	0.0	0.0	0.0
38	0.0	0.0	0.0	0.0	0.0	0.0
39	-0.682E-01	0.139E-01	-0.197E-01	0.146E-01	0.118E-01	0.105E-01
40	0.168E-02	0.0	-0.108E-02	0.0	0.366E-03	0.0
41	-0.489E-01	0.380E-02	0.0	-0.181E-02	0.0	0.0
42	-0.227E-01	0.367E-02	0.0	-0.181E-02	0.0	0.0
43	0.690E-02	0.318E-02	0.0	-0.181E-02	0.0	0.0
44	0.313E-01	0.232E-02	0.0	-0.181E-02	0.0	0.0
45	0.473E-01	0.105E-02	0.0	-0.181E-02	0.0	0.0
46	0.513E-01	-0.209E-03	0.0	-0.181E-02	0.0	0.0
47	0.471E-01	-0.621E-03	0.0	-0.181E-02	0.0	0.0
48	0.424E-01	-0.545E-03	0.0	-0.181E-02	0.0	0.0
49	0.341E-01	-0.700E-03	0.0	-0.181E-02	0.0	0.0
50	0.199E-01	-0.148E-02	0.0	-0.181E-02	0.0	0.0
51	-0.102E-01	-0.203E-02	0.0	0.201E-02	0.0	0.0
52	0.0	0.0	0.0	0.0	0.0	0.0
53	0.0	0.0	0.0	0.0	0.0	0.0
54	0.0	0.0	0.0	0.0	0.0	0.0
55	0.0	0.0	0.0	0.0	0.0	0.0
56	-0.189E-01	-0.217E-02	0.0	0.116E-01	-0.225E-14	-0.611E-15

TABLE C-12
SYMMETRIC MODE SHAPE –
10-PERCENT WING FUEL, NO TIP WEIGHT, 4.54 kg IN BAY 47

MODE NO. 2172 FREQ = 23.09 GENERALIZED MASS= 0.00

PAY	H	ALPH	THET	F	L	PSI
1	-0.483E-08	0.0	0.0	-0.162E-01	0.178E-01	-0.506E-03
2	-0.530E-08	0.0	0.0	-0.208E-01	0.177E-01	-0.599E-03
3	-0.546E-08	0.0	0.0	-0.224E-01	0.177E-01	-0.599E-03
4	-0.561E-08	0.0	0.0	-0.239E-01	0.177E-01	-0.599E-03
5	-0.575E-08	0.0	0.0	-0.255E-01	0.177E-01	-0.599E-03
6	-0.590E-08	0.0	0.0	-0.270E-01	0.177E-01	-0.599E-03
7	0.0	0.0	0.0	0.0	0.0	0.0
8	0.0	0.0	0.0	0.0	0.0	0.0
9	0.0	0.0	0.0	0.0	0.0	0.0
10	0.0	0.0	0.0	0.0	0.0	0.0
11	-0.363E-02	0.338E-03	0.190E-03	-0.184E-01	0.113E-01	-0.213E-03
12	-0.289E-02	0.367E-03	0.229E-03	-0.196E-01	0.113E-01	-0.429E-03
13	-0.192E-02	0.403E-03	0.337E-03	-0.213E-01	0.113E-01	-0.580E-03
14	-0.472E-03	0.439E-03	0.513E-03	-0.236E-01	0.113E-01	-0.703E-03
15	0.150E-02	0.464E-03	0.676E-03	-0.260E-01	0.113E-01	-0.784E-03
16	0.363E-02	0.474E-03	0.740E-03	-0.285E-01	0.113E-01	-0.814E-03
17	0.0	0.0	0.0	0.0	0.0	0.0
18	0.0	0.0	0.0	0.0	0.0	0.0
19	0.0	0.0	0.0	0.0	0.0	0.0
20	0.0	0.0	0.0	0.0	0.0	0.0
21	0.466E-02	-0.391E-03	-0.107E-04	-0.164E-01	0.117E-01	0.142E-02
22	0.518E-02	-0.606E-03	0.199E-03	-0.394E-02	0.117E-01	0.374E-02
23	0.644E-02	-0.912E-03	0.407E-03	0.157E-01	0.117E-01	0.578E-02
24	0.727E-02	-0.106E-02	0.556E-05	0.413E-01	0.117E-01	0.802E-02
25	0.602E-02	-0.130E-02	-0.661E-03	0.803E-01	0.117E-01	0.112E-01
26	0.198E-02	-0.167E-02	-0.145E-02	0.131E+00	0.117E-01	0.149E-01
27	-0.419E-02	-0.216E-02	-0.206E-02	0.189E+00	0.117E-01	0.187E-01
28	-0.117E-01	-0.276E-02	-0.219E-02	0.260E+00	0.117E-01	0.228E-01
29	-0.174E-01	-0.324E-02	-0.173E-02	0.331E+00	0.117E-01	0.267E-01
30	-0.208E-01	-0.365E-02	-0.926E-03	0.401E+00	0.117E-01	0.302E-01
31	-0.214E-01	-0.406E-02	0.511E-03	0.478E+00	0.117E-01	0.336E-01
32	-0.178E-01	-0.397E-02	0.259E-02	0.564E+00	0.117E-01	0.370E-01
33	-0.844E-02	-0.370E-02	0.511E-02	0.659E+00	0.117E-01	0.404E-01
34	0.738E-02	-0.311E-02	0.785E-02	0.762E+00	0.117E-01	0.439E-01
35	0.291E-01	-0.242E-02	0.974E-02	0.872E+00	0.117E-01	0.465E-01
36	0.567E-01	-0.191E-02	0.104E-01	0.100E+01	0.117E-01	0.474E-01
37	0.0	0.0	0.0	0.0	0.0	0.0
38	0.0	0.0	0.0	0.0	0.0	0.0
39	-0.213E-02	0.269E-02	0.611E-01	0.989E-02	-0.526E-01	-0.345E-01
40	-0.835E-04	0.0	0.540E-04	0.0	-0.183E-04	0.0
41	-0.701E-02	0.676E-03	0.0	-0.210E-01	0.0	0.0
42	-0.241E-02	0.637E-03	0.0	-0.210E-01	0.0	0.0
43	0.257E-02	0.513E-03	0.0	-0.210E-01	0.0	0.0
44	0.623E-02	0.312E-03	0.0	-0.210E-01	0.0	0.0
45	0.787E-02	0.323E-04	0.0	-0.210E-01	0.0	0.0
46	0.698E-02	-0.217E-03	0.0	-0.210E-01	0.0	0.0
47	0.473E-02	-0.385E-03	0.0	-0.210E-01	0.0	0.0
48	0.994E-03	-0.467E-03	0.0	-0.210E-01	0.0	0.0
49	-0.496E-02	-0.427E-03	0.0	-0.210E-01	0.0	0.0
50	-0.782E-02	0.620E-04	0.0	-0.210E-01	0.0	0.0
51	-0.203E-02	0.459E-03	0.0	-0.217E-01	0.0	0.0
52	0.0	0.0	0.0	0.0	0.0	0.0
53	0.0	0.0	0.0	0.0	0.0	0.0
54	0.0	0.0	0.0	0.0	0.0	0.0
55	0.0	0.0	0.0	0.0	0.0	0.0
56	0.207E-03	0.419E-03	0.0	-0.242E-01	-0.136E-13	-0.369E-14

TABLE C-13
SYMMETRIC MODE SHAPE –
10-PERCENT WING FUEL, NO TIP WEIGHT, 4.54 kg IN BAY 47

MODE NO. 2173 FREQ = 23.24 GENERALIZED MASS= 0.01

BAY	H	ALPH	THET	F	L	PSI
1	0.233E-08	0.0	0.0	-0.145E-01	0.181E-01	-0.775E-03
2	0.256E-08	0.0	0.0	-0.214E-01	0.180E-01	-0.890E-03
3	0.264E-08	0.0	0.0	-0.238E-01	0.180E-01	-0.890E-03
4	0.271E-08	0.0	0.0	-0.261E-01	0.180E-01	-0.890E-03
5	0.278E-08	0.0	0.0	-0.283E-01	0.180E-01	-0.890E-03
6	0.285E-08	0.0	0.0	-0.306E-01	0.180E-01	-0.890E-03
7	0.0	0.0	0.0	0.0	0.0	0.0
8	0.0	0.0	0.0	0.0	0.0	0.0
9	0.0	0.0	0.0	0.0	0.0	0.0
10	0.0	0.0	0.0	0.0	0.0	0.0
11	-0.401E-02	0.585E-03	0.295E-03	-0.163E-01	0.101E-01	-0.252E-03
12	-0.301E-02	0.635E-03	0.267E-03	-0.176E-01	0.101E-01	-0.453E-03
13	-0.204E-02	0.698E-03	0.299E-03	-0.194E-01	0.101E-01	-0.595E-03
14	-0.868E-03	0.762E-03	0.389E-03	-0.217E-01	0.101E-01	-0.710E-03
15	0.572E-03	0.806E-03	0.478E-03	-0.241E-01	0.101E-01	-0.785E-03
16	0.209E-02	0.824E-03	0.510E-03	-0.266E-01	0.101E-01	-0.813E-03
17	0.0	0.0	0.0	0.0	0.0	0.0
18	0.0	0.0	0.0	0.0	0.0	0.0
19	0.0	0.0	0.0	0.0	0.0	0.0
20	0.0	0.0	0.0	0.0	0.0	0.0
21	-0.708E-02	0.171E-02	-0.151E-02	-0.130E-01	0.999E-02	0.129E-02
22	-0.199E-01	0.469E-02	-0.326E-02	-0.169E-02	0.999E-02	0.341E-02
23	-0.335E-01	0.879E-02	-0.337E-02	0.162E-01	0.999E-02	0.524E-02
24	-0.438E-01	0.105E-01	-0.178E-02	0.397E-01	0.999E-02	0.745E-02
25	-0.428E-01	0.131E-01	0.280E-02	0.763E-01	0.999E-02	0.107E-01
26	-0.194E-01	0.174E-01	0.971E-02	0.125E+00	0.999E-02	0.144E-01
27	0.260E-01	0.229E-01	0.161E-01	0.181E+00	0.999E-02	0.182E-01
28	0.867E-01	0.293E-01	0.195E-01	0.250E+00	0.999E-02	0.225E-01
29	0.137E+00	0.341E-01	0.153E-01	0.321E+00	0.999E-02	0.265E-01
30	0.167E+00	0.380E-01	0.863E-02	0.390E+00	0.999E-02	0.302E-01
31	0.174E+00	0.417E-01	-0.379E-02	0.468E+00	0.999E-02	0.338E-01
32	0.144E+00	0.398E-01	-0.217E-01	0.555E+00	0.999E-02	0.374E-01
33	0.661E-01	0.354E-01	-0.425E-01	0.651E+00	0.999E-02	0.411E-01
34	-0.638E-01	0.270E-01	-0.637E-01	0.756E+00	0.999E-02	0.448E-01
35	-0.238E+00	0.182E-01	-0.771E-01	0.869E+00	0.999E-02	0.477E-01
36	-0.454E+00	0.125E-01	-0.812E-01	0.100E+01	0.999E-02	0.486E-01
37	0.0	0.0	0.0	0.0	0.0	0.0
38	0.0	0.0	0.0	0.0	0.0	0.0
39	0.307E-01	-0.208E-01	-0.633E+00	-0.182E-01	0.535E+00	0.328E+00
40	0.562E-03	0.0	-0.363E-03	0.0	0.123E-03	0.0
41	0.461E-02	-0.461E-03	0.0	-0.183E-01	0.0	0.0
42	0.146E-02	-0.435E-03	0.0	-0.183E-01	0.0	0.0
43	-0.195E-02	-0.354E-03	0.0	-0.183E-01	0.0	0.0
44	-0.453E-02	-0.226E-03	0.0	-0.183E-01	0.0	0.0
45	-0.584E-02	-0.511E-04	0.0	-0.183E-01	0.0	0.0
46	-0.560E-02	0.978E-04	0.0	-0.183E-01	0.0	0.0
47	-0.495E-02	-0.344E-04	0.0	-0.183E-01	0.0	0.0
48	-0.653E-02	-0.294E-03	0.0	-0.183E-01	0.0	0.0
49	-0.107E-01	-0.302E-03	0.0	-0.183E-01	0.0	0.0
50	-0.115E-01	0.267E-03	0.0	-0.183E-01	0.0	0.0
51	-0.176E-02	0.744E-03	0.0	-0.195E-01	0.0	0.0
52	0.0	0.0	0.0	0.0	0.0	0.0
53	0.0	0.0	0.0	0.0	0.0	0.0
54	0.0	0.0	0.0	0.0	0.0	0.0
55	0.0	0.0	0.0	0.0	0.0	0.0
56	0.182E-02	0.727E-03	0.0	-0.237E-01	-0.123E-13	-0.334E-14

TABLE C-14
SYMMETRIC MODE SHAPE –
10-PERCENT WING FUEL, NO TIP WEIGHT, 4.54 kg IN BAY 47

MODE NO. 2174 FREQ = 28.69 GENERALIZED MASS= 0.01

BAY	H	ALPH	THET	F	L	PSI
1	0.369E-06	0.0	0.0	0.279E-01	-0.306E+00	0.463E-01
2	0.404E-06	0.0	0.0	0.443E+00	-0.305E+00	0.538E-01
3	0.417E-06	0.0	0.0	0.591E+00	-0.305E+00	0.538E-01
4	0.428E-06	0.0	0.0	0.727E+00	-0.305E+00	0.538E-01
5	0.439E-06	0.0	0.0	0.863E+00	-0.305E+00	0.538E-01
6	0.451E-06	0.0	0.0	0.100E+01	-0.305E+00	0.538E-01
7	0.0	0.0	0.0	0.0	0.0	0.0
8	0.0	0.0	0.0	0.0	0.0	0.0
9	0.0	0.0	0.0	0.0	0.0	0.0
10	0.0	0.0	0.0	0.0	0.0	0.0
11	0.862E-01	-0.408E-01	-0.183E-01	-0.206E-02	-0.149E-01	0.910E-02
12	0.340E-01	-0.468E-01	-0.105E-01	0.343E-01	-0.149E-01	0.109E-01
13	0.122E-01	-0.544E-01	-0.183E-02	0.749E-01	-0.149E-01	0.122E-01
14	0.224E-01	-0.624E-01	0.800E-02	0.119E+00	-0.149E-01	0.132E-01
15	0.642E-01	-0.683E-01	0.170E-01	0.164E+00	-0.149E-01	0.139E-01
16	0.124E+00	-0.710E-01	0.212E-01	0.206E+00	-0.149E-01	0.142E-01
17	0.0	0.0	0.0	0.0	0.0	0.0
18	0.0	0.0	0.0	0.0	0.0	0.0
19	0.0	0.0	0.0	0.0	0.0	0.0
20	0.0	0.0	0.0	0.0	0.0	0.0
21	-0.711E-01	0.190E-01	0.143E-01	0.215E-01	-0.894E-02	-0.118E-02
22	-0.711E-02	0.173E-01	0.147E-01	0.173E-01	-0.906E-02	-0.887E-03
23	0.502E-01	0.146E-01	0.123E-01	0.141E-01	-0.894E-02	-0.665E-03
24	0.892E-01	0.158E-01	0.802E-02	0.124E-01	-0.902E-02	-0.361E-03
25	0.106E+00	0.172E-01	-0.217E-03	0.116E-01	-0.904E-02	-0.788E-05
26	0.852E-01	0.175E-01	-0.112E-01	0.122E-01	-0.894E-02	0.402E-03
27	0.273E-01	0.165E-01	-0.217E-01	0.144E-01	-0.898E-02	0.829E-03
28	-0.594E-01	0.138E-01	-0.282E-01	0.181E-01	-0.900E-02	0.130E-02
29	-0.143E+00	0.104E-01	-0.278E-01	0.224E-01	-0.895E-02	0.176E-02
30	-0.204E+00	0.722E-02	-0.222E-01	0.273E-01	-0.904E-02	0.216E-02
31	-0.245E+00	0.350E-02	-0.945E-02	0.330E-01	-0.897E-02	0.257E-02
32	-0.243E+00	0.394E-02	0.118E-01	0.398E-01	-0.903E-02	0.298E-02
33	-0.180E+00	0.515E-02	0.414E-01	0.475E-01	-0.896E-02	0.340E-02
34	-0.353E-01	0.860E-02	0.783E-01	0.564E-01	-0.902E-02	0.383E-02
35	0.195E+00	0.143E-01	0.108E+00	0.661E-01	-0.894E-02	0.415E-02
36	0.504E+00	0.200E-01	0.119E+00	0.778E-01	-0.899E-02	0.426E-02
37	0.0	0.0	0.0	0.0	0.0	0.0
38	0.0	0.0	0.0	0.0	0.0	0.0
39	0.410E-01	-0.192E-01	-0.328E-02	0.108E-01	0.336E-02	0.179E-02
40	-0.757E-03	0.0	0.490E-03	0.0	-0.166E-03	0.0
41	0.350E+00	-0.384E-01	0.0	-0.374E-01	0.0	0.0
42	0.910E-01	-0.353E-01	0.0	-0.374E-01	0.0	0.0
43	-0.177E+00	-0.264E-01	0.0	-0.374E-01	0.0	0.0
44	-0.352E+00	-0.129E-01	0.0	-0.374E-01	0.0	0.0
45	-0.391E+00	0.467E-02	0.0	-0.374E-01	0.0	0.0
46	-0.277E+00	0.190E-01	0.0	-0.374E-01	0.0	0.0
47	-0.104E+00	0.277E-01	0.0	-0.374E-01	0.0	0.0
48	0.147E+00	0.292E-01	0.0	-0.374E-01	0.0	0.0
49	0.484E+00	0.225E-01	0.0	-0.374E-01	0.0	0.0
50	0.553E+00	-0.156E-01	0.0	-0.374E-01	0.0	0.0
51	-0.108E+00	-0.547E-01	0.0	0.355E-01	0.0	0.0
52	0.0	0.0	0.0	0.0	0.0	0.0
53	0.0	0.0	0.0	0.0	0.0	0.0
54	0.0	0.0	0.0	0.0	0.0	0.0
55	0.0	0.0	0.0	0.0	0.0	0.0
56	-0.302E+00	-0.555E-01	0.0	0.210E+00	-0.129E-12	-0.349E-13

TABLE C-15
SYMMETRIC MODE SHAPE –
10-PERCENT WING FUEL, NO TIP WEIGHT, 4.54 kg IN BAY 47

MODE NO. 2175 FREQ = 32.39 GENERALIZED MASS= 0.00

BAY	H	ALPH	THET	F	L	PSI
1	0.496E-07	0.0	0.0	-0.255E-02	0.657E-01	-0.825E-02
2	0.544E-07	0.0	0.0	-0.781E-01	0.651E-01	-0.984E-02
3	0.560E-07	0.0	0.0	-0.105E+00	0.651E-01	-0.984E-02
4	0.576E-07	0.0	0.0	-0.130E+00	0.651E-01	-0.984E-02
5	0.591E-07	0.0	0.0	-0.155E+00	0.651E-01	-0.984E-02
6	0.606E-07	0.0	0.0	-0.180E+00	0.651E-01	-0.984E-02
7	0.0	0.0	0.0	0.0	0.0	0.0
8	0.0	0.0	0.0	0.0	0.0	0.0
9	0.0	0.0	0.0	0.0	0.0	0.0
10	0.0	0.0	0.0	0.0	0.0	0.0
11	-0.263E-01	0.709E-02	0.306E-02	-0.349E-02	0.712E-02	-0.172E-02
12	-0.178E-01	0.855E-02	0.199E-02	-0.108E-01	0.711E-02	-0.230E-02
13	-0.119E-01	0.105E-01	0.146E-02	-0.196E-01	0.712E-02	-0.270E-02
14	-0.706E-02	0.125E-01	0.142E-02	-0.295E-01	0.712E-02	-0.303E-02
15	-0.224E-02	0.141E-01	0.147E-02	-0.399E-01	0.712E-02	-0.325E-02
16	0.215E-02	0.149E-01	0.142E-02	-0.499E-01	0.712E-02	-0.332E-02
17	0.0	0.0	0.0	0.0	0.0	0.0
18	0.0	0.0	0.0	0.0	0.0	0.0
19	0.0	0.0	0.0	0.0	0.0	0.0
20	0.0	0.0	0.0	0.0	0.0	0.0
21	-0.251E-02	0.188E-02	0.937E-02	0.798E-02	-0.393E-02	-0.172E-03
22	0.621E-01	0.339E-02	0.178E-01	0.735E-02	-0.394E-02	-0.125E-03
23	0.149E+00	0.444E-02	0.234E-01	0.697E-02	-0.393E-02	-0.462E-04
24	0.236E+00	0.741E-02	0.221E-01	0.657E-02	-0.395E-02	-0.182E-03
25	0.308E+00	0.105E-01	0.109E-01	0.548E-02	-0.395E-02	-0.361E-03
26	0.310E+00	0.103E-01	-0.115E-01	0.371E-02	-0.393E-02	-0.543E-03
27	0.224E+00	0.620E-02	-0.386E-01	0.156E-02	-0.394E-02	-0.705E-03
28	0.498E-01	-0.223E-02	-0.619E-01	-0.110E-02	-0.394E-02	-0.852E-03
29	-0.147E+00	-0.134E-01	-0.702E-01	-0.375E-02	-0.394E-02	-0.963E-03
30	-0.313E+00	-0.245E-01	-0.643E-01	-0.618E-02	-0.395E-02	-0.104E-02
31	-0.446E+00	-0.378E-01	-0.413E-01	-0.880E-02	-0.394E-02	-0.109E-02
32	-0.497E+00	-0.401E-01	0.307E-02	-0.115E-01	-0.395E-02	-0.113E-02
33	-0.413E+00	-0.409E-01	0.689E-01	-0.143E-01	-0.394E-02	-0.114E-02
34	-0.142E+00	-0.368E-01	0.156E+00	-0.171E-01	-0.395E-02	-0.114E-02
35	0.334E+00	-0.250E-01	0.228E+00	-0.198E-01	-0.394E-02	-0.112E-02
36	0.100E+01	-0.116E-01	0.256E+00	-0.228E-01	-0.394E-02	-0.111E-02
37	0.0	0.0	0.0	0.0	0.0	0.0
38	0.0	0.0	0.0	0.0	0.0	0.0
39	0.413E-01	0.607E-02	-0.137E-01	0.390E-01	0.148E-01	0.785E-02
40	-0.432E-02	0.0	0.279E-02	0.0	-0.944E-03	0.0
41	0.509E-01	-0.614E-02	0.0	0.749E-03	0.0	0.0
42	0.974E-02	-0.555E-02	0.0	0.749E-03	0.0	0.0
43	-0.317E-01	-0.400E-02	0.0	0.749E-03	0.0	0.0
44	-0.575E-01	-0.181E-02	0.0	0.749E-03	0.0	0.0
45	-0.618E-01	0.857E-03	0.0	0.749E-03	0.0	0.0
46	-0.443E-01	0.271E-02	0.0	0.749E-03	0.0	0.0
47	-0.266E-01	0.608E-03	0.0	0.749E-03	0.0	0.0
48	-0.402E-01	-0.323E-02	0.0	0.749E-03	0.0	0.0
49	-0.900E-01	-0.372E-02	0.0	0.749E-03	0.0	0.0
50	-0.105E+00	0.233E-02	0.0	0.749E-03	0.0	0.0
51	0.143E-02	0.947E-02	0.0	-0.115E-01	0.0	0.0
52	0.0	0.0	0.0	0.0	0.0	0.0
53	0.0	0.0	0.0	0.0	0.0	0.0
54	0.0	0.0	0.0	0.0	0.0	0.0
55	0.0	0.0	0.0	0.0	0.0	0.0
56	0.436E-01	0.989E-02	0.0	-0.522E-01	0.328E-14	0.889E-15

TABLE C-16

SYMMETRIC MODE SHAPE –
10-PERCENT WING FUEL, NO TIP WEIGHT, 4.54 kg IN BAY 47

MODE NO. 2176 FREQ = 42.70 GENERALIZED MASS= 0.00

BAY	H	ALPH	THET	F	L	PSI
1	0.478E-07	0.0	0.0	-0.910E-03	0.312E-01	-0.629E-02
2	0.524E-07	0.0	0.0	-0.706E-01	0.300E-01	-0.949E-02
3	0.540E-07	0.0	0.0	-0.967E-01	0.300E-01	-0.949E-02
4	0.554E-07	0.0	0.0	-0.121E+00	0.300E-01	-0.949E-02
5	0.569E-07	0.0	0.0	-0.145E+00	0.300E-01	-0.949E-02
6	0.584E-07	0.0	0.0	-0.169E+00	0.300E-01	-0.949E-02
7	0.0	0.0	0.0	0.0	0.0	0.0
8	0.0	0.0	0.0	0.0	0.0	0.0
9	0.0	0.0	0.0	0.0	0.0	0.0
10	0.0	0.0	0.0	0.0	0.0	0.0
11	-0.334E-01	-0.326E-03	-0.190E-02	0.142E-02	0.572E-02	0.216E-03
12	-0.435E-01	-0.533E-03	-0.310E-02	0.267E-02	0.572E-02	0.459E-03
13	-0.505E-01	-0.818E-03	0.581E-05	0.459E-02	0.572E-02	0.630E-03
14	-0.372E-01	-0.116E-02	0.853E-02	0.700E-02	0.572E-02	0.769E-03
15	0.808E-02	-0.148E-02	0.187E-01	0.970E-02	0.572E-02	0.860E-03
16	0.742E-01	-0.165E-02	0.235E-01	0.124E-01	0.572E-02	0.894E-03
17	0.0	0.0	0.0	0.0	0.0	0.0
18	0.0	0.0	0.0	0.0	0.0	0.0
19	0.0	0.0	0.0	0.0	0.0	0.0
20	0.0	0.0	0.0	0.0	0.0	0.0
21	0.134E-01	0.112E-01	-0.119E-02	0.754E-02	-0.632E-02	-0.146E-03
22	-0.142E-02	0.278E-01	-0.510E-02	0.690E-02	-0.632E-02	-0.178E-03
23	-0.349E-01	0.497E-01	-0.117E-01	0.592E-02	-0.632E-02	-0.315E-03
24	-0.581E-01	0.828E-01	-0.168E-01	0.493E-02	-0.633E-02	-0.223E-03
25	-0.169E+00	0.131E+00	-0.221E-01	0.424E-02	-0.634E-02	-0.122E-03
26	-0.259E+00	0.190E+00	-0.245E-01	0.389E-02	-0.632E-02	-0.522E-04
27	-0.340E+00	0.257E+00	-0.213E-01	0.377E-02	-0.633E-02	-0.296E-04
28	-0.400E+00	0.331E+00	-0.135E-01	0.363E-02	-0.633E-02	-0.656E-04
29	-0.428E+00	0.396E+00	-0.603E-02	0.332E-02	-0.632E-02	-0.158E-03
30	-0.437E+00	0.461E+00	-0.160E-02	0.280E-02	-0.634E-02	-0.282E-03
31	-0.440E+00	0.539E+00	-0.268E-02	0.190E-02	-0.633E-02	-0.452E-03
32	-0.451E+00	0.611E+00	-0.426E-02	0.567E-03	-0.634E-02	-0.661E-03
33	-0.452E+00	0.698E+00	0.528E-02	-0.135E-02	-0.633E-02	-0.909E-03
34	-0.415E+00	0.824E+00	0.276E-01	-0.390E-02	-0.633E-02	-0.120E-02
35	-0.314E+00	0.937E+00	0.543E-01	-0.717E-02	-0.632E-02	-0.145E-02
36	-0.143E+00	0.100E+01	0.676E-01	-0.113E-01	-0.632E-02	-0.155E-02
37	0.0	0.0	0.0	0.0	0.0	0.0
38	0.0	0.0	0.0	0.0	0.0	0.0
39	-0.199E-01	-0.429E-01	0.931E-02	-0.141E-01	-0.142E-01	-0.736E-02
40	0.268E-02	0.0	-0.173E-02	0.0	0.586E-03	0.0
41	0.341E-01	-0.476E-02	0.0	0.196E-02	0.0	0.0
42	0.301E-02	-0.406E-02	0.0	0.196E-02	0.0	0.0
43	-0.251E-01	-0.241E-02	0.0	0.196E-02	0.0	0.0
44	-0.374E-01	-0.380E-03	0.0	0.196E-02	0.0	0.0
45	-0.305E-01	0.175E-02	0.0	0.196E-02	0.0	0.0
46	-0.769E-02	0.291E-02	0.0	0.196E-02	0.0	0.0
47	0.116E-01	0.146E-02	0.0	0.196E-02	0.0	0.0
48	0.105E-01	-0.148E-02	0.0	0.196E-02	0.0	0.0
49	-0.198E-01	-0.255E-02	0.0	0.196E-02	0.0	0.0
50	-0.420E-01	-0.615E-04	0.0	0.196E-02	0.0	0.0
51	-0.399E-01	-0.174E-02	0.0	-0.157E-02	0.0	0.0
52	0.0	0.0	0.0	0.0	0.0	0.0
53	0.0	0.0	0.0	0.0	0.0	0.0
54	0.0	0.0	0.0	0.0	0.0	0.0
55	0.0	0.0	0.0	0.0	0.0	0.0
56	0.687E-01	0.109E-01	0.0	-0.242E-01	0.104E-12	0.283E-13

TABLE C-17
SYMMETRIC MODE SHAPE –
10-PERCENT WING FUEL, NO TIP WEIGHT, 4.54 kg IN BAY 47

MODE NO. 2177 FREQ = 43.04 GENERALIZED MASS= 0.00

BAY	H	ALPH	THET	F	L	PSI
1	-0.167E-07	0.0	0.0	0.656E-01	-0.174E-01	0.303E-01
2	-0.184E-07	0.0	0.0	0.448E+00	-0.856E-02	0.533E-01
3	-0.189E-07	0.0	0.0	0.594E+00	-0.857E-02	0.533E-01
4	-0.194E-07	0.0	0.0	0.730E+00	-0.856E-02	0.533E-01
5	-0.199E-07	0.0	0.0	0.865E+00	-0.857E-02	0.533E-01
6	-0.205E-07	0.0	0.0	0.100E+01	-0.849E-02	0.533E-01
7	0.0	0.0	0.0	0.0	0.0	0.0
8	0.0	0.0	0.0	0.0	0.0	0.0
9	0.0	0.0	0.0	0.0	0.0	0.0
10	0.0	0.0	0.0	0.0	0.0	0.0
11	0.168E+00	0.384E-01	0.271E-01	-0.473E-02	-0.329E-01	-0.123E-01
12	0.281E+00	0.639E-01	0.316E-01	-0.674E-01	-0.329E-01	-0.218E-01
13	0.357E+00	0.993E-01	0.508E-02	-0.156E+00	-0.329E-01	-0.284E-01
14	0.271E+00	0.142E+00	-0.614E-01	-0.243E+00	-0.329E-01	-0.338E-01
15	-0.654E-01	0.182E+00	-0.141E+00	-0.381E+00	-0.329E-01	-0.373E-01
16	-0.567E+00	0.204E+00	-0.179E+00	-0.496E+00	-0.329E-01	-0.386E-01
17	0.0	0.0	0.0	0.0	0.0	0.0
18	0.0	0.0	0.0	0.0	0.0	0.0
19	0.0	0.0	0.0	0.0	0.0	0.0
20	0.0	0.0	0.0	0.0	0.0	0.0
21	-0.514E-02	0.225E-03	-0.796E-03	-0.410E-02	0.296E-02	0.341E-04
22	-0.871E-02	0.248E-02	-0.793E-03	-0.407E-02	0.296E-02	-0.978E-05
23	-0.118E-01	0.570E-02	-0.683E-03	-0.419E-02	0.296E-02	-0.464E-04
24	-0.133E-01	0.107E-01	-0.111E-03	-0.433E-02	0.296E-02	-0.264E-04
25	-0.129E-01	0.131E-01	0.139E-03	-0.436E-02	0.296E-02	0.171E-04
26	-0.135E-01	0.271E-01	-0.634E-03	-0.417E-02	0.296E-02	0.855E-04
27	-0.186E-01	0.369E-01	-0.250E-02	-0.373E-02	0.296E-02	0.174E-03
28	-0.314E-01	0.474E-01	-0.523E-02	-0.294E-02	0.296E-02	0.292E-03
29	-0.501E-01	0.555E-01	-0.725E-02	-0.191E-02	0.296E-02	0.422E-03
30	-0.638E-01	0.633E-01	-0.798E-02	-0.730E-03	0.296E-02	0.550E-03
31	-0.877E-01	0.726E-01	-0.747E-02	0.786E-03	0.296E-02	0.691E-03
32	-0.103E+00	0.825E-01	-0.454E-02	0.264E-02	0.296E-02	0.841E-03
33	-0.106E+00	0.951E-01	0.280E-02	0.490E-02	0.296E-02	0.100E-02
34	-0.853E-01	0.114E+00	0.151E-01	0.755E-02	0.296E-02	0.118E-02
35	-0.330E-01	0.133E+00	0.270E-01	0.106E-01	0.296E-02	0.132E-02
36	0.491E-01	0.144E+00	0.321E-01	0.142E-01	0.296E-02	0.137E-02
37	0.0	0.0	0.0	0.0	0.0	0.0
38	0.0	0.0	0.0	0.0	0.0	0.0
39	-0.615E-02	-0.622E-02	0.827E-03	-0.933E-02	-0.140E-02	-0.728E-03
40	0.302E-03	0.0	-0.195E-03	0.0	0.659E-04	0.0
41	-0.139E-01	0.197E-02	0.0	-0.229E-02	0.0	0.0
42	-0.107E-02	0.167E-02	0.0	-0.229E-02	0.0	0.0
43	0.105E-01	0.100E-02	0.0	-0.229E-02	0.0	0.0
44	0.157E-01	0.185E-03	0.0	-0.229E-02	0.0	0.0
45	0.134E-01	-0.651E-03	0.0	-0.229E-02	0.0	0.0
46	0.497E-02	-0.105E-02	0.0	-0.229E-02	0.0	0.0
47	-0.276E-02	-0.971E-03	0.0	-0.229E-02	0.0	0.0
48	-0.781E-02	-0.119E-03	0.0	-0.229E-02	0.0	0.0
49	-0.324E-02	0.526E-03	0.0	-0.229E-02	0.0	0.0
50	-0.341E-02	-0.122E-02	0.0	-0.229E-02	0.0	0.0
51	0.369E+00	0.675E-01	0.0	-0.549E-02	0.0	0.0
52	0.0	0.0	0.0	0.0	0.0	0.0
53	0.0	0.0	0.0	0.0	0.0	0.0
54	0.0	0.0	0.0	0.0	0.0	0.0
55	0.0	0.0	0.0	0.0	0.0	0.0
56	-0.563E+00	-0.679E-01	0.0	0.372E-01	-0.110E-11	-0.298E-12

TABLE C-18
SYMMETRIC MODE SHAPE –
10-PERCENT WING FUEL, NO TIP WEIGHT, 4.54 kg IN BAY 47

MODE NO. 2178 FREQ = 46.90 GENERALIZED MASS= 0.00

BAY	H	ALPH	THET	F	L	PSI
1	-0.336E-06	0.0	0.0	-0.253E-01	-0.14CE+00	0.136E-01
2	-0.368E-06	0.0	0.0	0.111E+00	-0.138E+00	0.181E-01
3	-0.379E-06	0.0	0.0	0.161E+00	-0.138E+00	0.181E-01
4	-0.390E-06	0.0	0.0	0.207E+00	-0.138E+00	0.181E-01
5	-0.400E-06	0.0	0.0	0.253E+00	-0.138E+00	0.181E-01
6	-0.410E-06	0.0	0.0	0.299E+00	-0.138E+00	0.181E-01
7	0.0	0.0	0.0	0.0	0.0	0.0
8	0.0	0.0	0.0	0.0	0.0	0.0
9	0.0	0.0	0.0	0.0	0.0	0.0
10	0.0	0.0	0.0	0.0	0.0	0.0
11	0.893E-01	-0.209E-01	0.117E-02	0.116E-01	-0.181E-01	0.118E-01
12	0.110E+00	-0.497E-01	0.854E-02	0.816E-01	-0.181E-01	0.260E-01
13	0.135E+00	-0.911E-01	0.279E-02	0.191E+00	-0.181E-01	0.360E-01
14	0.110E+00	-0.144E+00	-0.200E-01	0.329E+00	-0.181E-01	0.441E-01
15	-0.541E-02	-0.197E+00	-0.493E-01	0.484E+00	-0.181E-01	0.495E-01
16	-0.183E+00	-0.229E+00	-0.636E-01	0.638E+00	-0.181E-01	0.514E-01
17	0.0	0.0	0.0	0.0	0.0	0.0
18	0.0	0.0	0.0	0.0	0.0	0.0
19	0.0	0.0	0.0	0.0	0.0	0.0
20	0.0	0.0	0.0	0.0	0.0	0.0
21	-0.995E-01	-0.185E-01	-0.149E-01	-0.385E-01	0.31CE-01	0.775E-03
22	-0.163E+00	-0.203E-01	-0.123E-01	-0.370E-01	0.310E-01	0.162E-03
23	-0.190E+00	-0.171E-01	0.166E-02	-0.370E-01	0.31CE-01	-0.182E-03
24	-0.141E+00	-0.919E-02	0.254E-01	-0.377E-01	0.31CE-01	-0.135E-03
25	0.165E-01	0.625E-02	0.504E-01	-0.380E-01	0.311E-01	0.855E-04
26	0.230E+00	0.281E-01	0.552E-01	-0.367E-01	0.31CE-01	0.528E-03
27	0.382E+00	0.498E-01	0.263E-01	-0.339E-01	0.310E-01	0.117E-02
28	0.374E+00	0.664E-01	-0.355E-01	-0.285E-01	0.31CE-01	0.208E-02
29	0.181E+00	0.618E-01	-0.923E-01	-0.209E-01	0.310E-01	0.313E-02
30	-0.826E-01	0.516E-01	-0.121E+00	-0.121E-01	0.311E-01	0.418E-02
31	-0.388E+00	0.370E-01	-0.123E+00	-0.435E-03	0.310E-01	0.536E-02
32	-0.648E+00	0.447E-01	-0.827E-01	0.140E-01	0.311E-01	0.663E-02
33	-0.748E+00	0.614E-01	0.104E-01	0.320E-01	0.310E-01	0.8C1E-02
34	-0.545E+00	0.103E+00	0.165E+00	0.532E-01	0.310E-01	0.950E-02
35	0.499E-01	0.165E+00	0.311E+00	0.781E-01	0.31CE-01	0.107E-01
36	0.100E+01	0.217E+00	0.372E+00	0.108E+00	0.31CE-01	0.111E-01
37	0.0	0.0	0.0	0.0	0.0	0.0
38	0.0	0.0	0.0	0.0	0.0	0.0
39	-0.589E-01	-0.152E-01	-0.298E-02	-0.893E-01	0.311E-02	0.161E-02
40	0.244E-02	0.0	-0.158E-02	0.0	0.533E-03	0.0
41	-0.335E+00	0.499E-01	0.0	0.608E-02	0.0	0.0
42	-0.114E-01	0.414E-01	0.0	0.608E-02	0.0	0.0
43	0.268E+00	0.231E-01	0.0	0.608E-02	0.0	0.0
44	0.378E+00	0.234E-02	0.0	0.608E-02	0.0	0.0
45	0.303E+00	-0.169E-01	0.0	0.608E-02	0.0	0.0
46	0.103E+00	-0.232E-01	0.0	0.608E-02	0.0	0.0
47	-0.423E-01	-0.127E-01	0.0	0.608E-02	0.0	0.0
48	-0.738E-01	0.424E-02	0.0	0.608E-02	0.0	0.0
49	0.526E-01	0.116E-01	0.0	0.608E-02	0.0	0.0
50	0.177E+00	0.336E-02	0.0	0.608E-02	0.0	0.0
51	0.307E-01	-0.229E-01	0.0	0.195E-01	0.0	0.0
52	0.0	0.0	0.0	0.0	0.0	0.0
53	0.0	0.0	0.0	0.0	0.0	0.0
54	0.0	0.0	0.0	0.0	0.0	0.0
55	0.0	0.0	0.0	0.0	0.0	0.0
56	-0.394E-01	-0.168E-01	0.0	0.110E+00	0.103E-12	0.280E-13

TABLE C-19
SYMMETRIC MODE SHAPE –
10-PERCENT WING FUEL, NO TIP WEIGHT, 4.54 kg IN BAY 47

MODE NO. 2179 FREQ = 48.86 GENERALIZED MASS= 0.00

BAY	H	ALPH	THET	F	L	PSI
1	0.779E-08	0.0	0.0	-0.309E-02	0.672E-02	-0.43CE-03
2	0.855E-08	0.0	0.0	-0.827E-02	0.661E-02	-0.717E-03
3	0.881E-08	0.0	0.0	-0.102E-01	0.661E-02	-0.717E-03
4	0.905E-08	0.0	0.0	-0.121E-01	0.661E-02	-0.717E-03
5	0.928E-08	0.0	0.0	-0.139E-01	0.661E-02	-0.717E-03
6	0.952E-08	0.0	0.0	-0.157E-01	0.660E-02	-0.717E-03
7	0.0	0.0	0.0	0.0	0.C	0.0
8	0.0	0.0	0.0	0.0	0.0	0.0
9	0.0	0.0	0.0	0.0	0.0	0.0
10	0.0	0.0	0.0	0.0	0.C	0.0
11	0.127E-02	0.193E-01	0.804E-03	0.111E-01	0.238E-02	0.161E-01
12	0.488E-02	0.712E-01	0.109E-02	0.115E+00	0.238E-02	0.399E-01
13	0.807E-02	0.147E+00	0.550E-03	0.286E+00	0.238E-02	0.567E-01
14	0.735E-02	0.249E+00	-0.117E-02	0.505E+00	0.238E-02	0.7C3E-01
15	-0.280E-03	0.353E+00	-0.344E-02	0.753E+00	0.238E-02	0.793E-01
16	-0.130E-01	0.417E+00	-0.460E-02	0.100E+01	0.238E-02	0.826E-01
17	0.0	0.0	0.0	0.0	0.0	0.0
18	0.0	0.0	0.0	0.0	0.C	0.0
19	0.0	0.0	0.0	0.0	0.0	0.0
20	0.0	0.0	0.0	0.0	0.0	0.0
21	0.209E-02	0.467E-03	0.358E-03	-0.361E-02	0.220E-02	-0.637E-04
22	0.366E-02	0.585E-03	0.315E-03	-0.402E-02	0.22CE-02	-0.113E-03
23	0.441E-02	0.602E-03	-0.189E-04	-0.456E-02	0.22CE-02	-0.145E-03
24	0.358E-02	0.442E-03	-0.447E-03	-0.510E-02	0.220E-02	-0.140E-03
25	0.689E-03	0.104E-03	-0.958E-03	-0.561E-02	0.22CE-02	-0.105E-03
26	-0.353E-02	-0.429E-03	-0.114E-02	-0.589E-02	0.22CE-02	-0.259E-04
27	-0.636E-02	-0.103E-02	-0.662E-03	-0.578E-02	0.220E-02	0.959E-04
28	-0.727E-02	-0.161E-02	0.533E-03	-0.516E-02	0.22CE-02	0.276E-03
29	-0.386E-02	-0.174E-02	0.172E-02	-0.406E-02	0.22CE-02	0.491E-03
30	0.122E-02	-0.175E-02	0.239E-02	-0.260E-02	0.220E-02	0.712E-03
31	0.745E-02	-0.170E-02	0.260E-02	-0.566E-03	0.22CE-02	0.965E-03
32	0.132E-01	-0.200E-02	0.196E-02	0.212E-02	0.22CE-02	0.124E-02
33	0.160E-01	-0.250E-02	0.127E-03	0.553E-02	0.220E-02	0.155E-02
34	0.126E-01	-0.358E-02	-0.319E-02	0.972E-02	0.22CE-02	0.189E-02
35	0.480E-03	-0.515E-02	-0.648E-02	0.147E-01	0.22CE-02	0.217E-02
36	-0.196E-01	-0.641E-02	-0.791E-02	0.208E-01	0.22CE-02	0.227E-02
37	0.0	0.0	0.0	0.0	0.0	0.0
38	0.0	0.0	0.0	0.0	0.C	0.0
39	-0.221E-03	0.508E-03	0.128E-03	-0.357E-02	-0.810E-04	-0.332E-04
40	-0.496E-04	0.0	0.321E-04	0.0	-0.108E-04	0.0
41	0.905E-02	-0.139E-02	0.0	-0.545E-02	0.0	0.0
42	0.122E-03	-0.114E-02	0.0	-0.545E-02	0.0	0.0
43	-0.742E-02	-0.609E-03	0.0	-0.545E-02	0.0	0.0
44	-0.102E-01	-0.353E-04	0.0	-0.545E-02	0.0	0.0
45	-0.796E-02	0.466E-03	0.0	-0.545E-02	0.0	0.0
46	-0.271E-02	0.580E-03	0.0	-0.545E-02	0.0	0.0
47	0.900E-03	0.374E-03	0.0	-0.545E-02	0.0	0.0
48	0.262E-02	0.222E-04	0.0	-0.545E-02	0.0	0.0
49	0.665E-03	-0.231E-03	0.0	-0.545E-02	0.0	0.0
50	-0.338E-02	-0.251E-03	0.0	-0.545E-02	0.0	0.0
51	0.667E-02	0.205E-02	0.0	-0.566E-02	0.0	0.0
52	0.0	0.0	0.0	0.0	0.0	0.0
53	0.0	0.0	0.0	0.0	0.0	0.0
54	0.0	0.0	0.0	0.0	0.0	0.0
55	0.0	0.0	0.0	0.0	0.0	0.0
56	0.264E-02	0.553E-03	0.0	-0.794E-02	-0.124E-13	-0.337E-14

TABLE C-20
SYMMETRIC MODE SHAPE –
10-PERCENT WING FUEL, NO TIP WEIGHT, 4.54 kg IN BAY 47

MODE NO. 2180 FREQ = 49.48 GENERALIZED MASS= 0.00

BAY	H	ALPH	THET	F	L	PSI
1	0.359E-07	0.0	0.0	0.287E-02	0.317E-01	-0.516E-03
2	0.394E-07	0.0	0.0	0.811E-02	0.323E-01	0.101E-02
3	0.406E-07	0.0	0.0	0.109E-01	0.323E-01	0.101E-02
4	0.417E-07	0.0	0.0	0.135E-01	0.323E-01	0.101E-02
5	0.429E-07	0.0	0.0	0.160E-01	0.323E-01	0.101E-02
6	0.439E-07	0.0	0.0	0.186E-01	0.323E-01	0.101E-02
7	0.0	0.0	0.0	0.0	0.0	0.0
8	0.0	0.0	0.0	0.0	0.0	0.0
9	0.0	0.0	0.0	0.0	0.0	0.0
10	0.0	0.0	0.0	0.0	0.0	0.0
11	0.124E-01	-0.195E-01	0.773E-02	0.102E-01	0.153E-02	0.152E-01
12	0.481E-01	-0.936E-01	0.110E-01	0.112E+00	0.153E-02	0.396E-01
13	0.807E-01	-0.203E+00	0.581E-02	0.282E+00	0.153E-02	0.567E-01
14	0.746E-01	-0.351E+00	-0.114E-01	0.502E+00	0.153E-02	0.706E-01
15	-0.135E-02	-0.505E+00	-0.344E-01	0.751E+00	0.153E-02	0.798E-01
16	-0.129E+00	-0.599E+00	-0.463E-01	0.100E+01	0.153E-02	0.832E-01
17	0.0	0.0	0.0	0.0	0.0	0.0
18	0.0	0.0	0.0	0.0	0.0	0.0
19	0.0	0.0	0.0	0.0	0.0	0.0
20	0.0	0.0	0.0	0.0	0.0	0.0
21	0.129E-01	0.214E-02	0.225E-02	-0.363E-03	-0.464E-03	-0.112E-03
22	0.242E-01	0.292E-02	0.243E-02	-0.768E-03	-0.469E-03	-0.876E-04
23	0.314E-01	0.300E-02	0.643E-03	-0.111E-02	-0.463E-03	-0.768E-04
24	0.276E-01	0.260E-02	-0.290E-02	-0.141E-02	-0.472E-03	-0.874E-04
25	0.672E-02	0.131E-02	-0.723E-02	-0.177E-02	-0.473E-03	-0.884E-04
26	-0.261E-01	-0.108E-02	-0.906E-02	-0.209E-02	-0.463E-03	-0.690E-04
27	-0.534E-01	-0.361E-02	-0.581E-02	-0.226E-02	-0.467E-03	-0.261E-04
28	-0.598E-01	-0.551E-02	0.295E-02	-0.223E-02	-0.469E-03	0.493E-04
29	-0.375E-01	-0.429E-02	0.117E-01	-0.195E-02	-0.464E-03	0.149E-03
30	-0.239E-02	-0.213E-02	0.167E-01	-0.146E-02	-0.473E-03	0.257E-03
31	0.411E-01	0.924E-03	0.181E-01	-0.685E-03	-0.466E-03	0.387E-03
32	0.808E-01	0.110E-02	0.134E-01	0.444E-03	-0.472E-03	0.535E-03
33	0.998E-01	0.358E-03	0.767E-03	0.194E-02	-0.465E-03	0.704E-03
34	0.763E-01	-0.328E-02	-0.215E-01	0.390E-02	-0.471E-03	0.894E-03
35	-0.493E-02	-0.107E-01	-0.433E-01	0.628E-02	-0.464E-03	0.105E-02
36	-0.139E+00	-0.174E-01	-0.527E-01	0.926E-02	-0.468E-03	0.111E-02
37	0.0	0.0	0.0	0.0	0.0	0.0
38	0.0	0.0	0.0	0.0	0.0	0.0
39	0.724E-02	0.234E-02	0.348E-03	0.674E-02	-0.262E-03	-0.134E-03
40	-0.624E-03	0.0	0.404E-03	0.0	-0.136E-03	0.0
41	0.409E-01	-0.631E-02	0.0	-0.592E-02	0.0	0.0
42	0.381E-03	-0.514E-02	0.0	-0.592E-02	0.0	0.0
43	-0.336E-01	-0.271E-02	0.0	-0.592E-02	0.0	0.0
44	-0.455E-01	-0.843E-04	0.0	-0.592E-02	0.0	0.0
45	-0.347E-01	0.218E-02	0.0	-0.592E-02	0.0	0.0
46	-0.104E-01	0.268E-02	0.0	-0.592E-02	0.0	0.0
47	0.497E-02	0.103E-02	0.0	-0.592E-02	0.0	0.0
48	0.285E-02	-0.134E-02	0.0	-0.592E-02	0.0	0.0
49	-0.238E-01	-0.225E-02	0.0	-0.592E-02	0.0	0.0
50	-0.442E-01	-0.136E-03	0.0	-0.592E-02	0.0	0.0
51	0.520E-01	0.146E-01	0.0	-0.112E-01	0.0	0.0
52	0.0	0.0	0.0	0.0	0.0	0.0
53	0.0	0.0	0.0	0.0	0.0	0.0
54	0.0	0.0	0.0	0.0	0.0	0.0
55	0.0	0.0	0.0	0.0	0.0	0.0
56	-0.420E-01	-0.345E-02	0.0	-0.287E-01	-0.184E-12	-0.498E-13

TABLE C-21
SYMMETRIC MODE SHAPE –
10-PERCENT WING FUEL, NO TIP WEIGHT, 4.54 kg IN BAY 47

MODE NO. 1751 FREQ = 48.87 GENERALIZED MASS= 0.00

BAY	H	ALPH	THET	F	L	PSI
1	0.370E-08	0.0	0.0	-0.377E-02	0.519E-02	-0.216E-03
2	0.406E-08	0.0	0.0	-0.661E-02	0.512E-02	-0.400E-03
3	0.418E-08	0.0	0.0	-0.771E-02	0.512E-02	-0.400E-03
4	0.430E-08	0.0	0.0	-0.875E-02	0.512E-02	-0.400E-03
5	0.441E-08	0.0	0.0	-0.974E-02	0.512E-02	-0.400E-03
6	0.452E-08	0.0	0.0	-0.108E-01	0.512E-02	-0.400E-03
7	0.0	0.0	0.0	0.0	0.0	0.0
8	0.0	0.0	0.0	0.0	0.0	0.0
9	0.0	0.0	0.0	0.0	0.0	0.0
10	0.0	0.0	0.0	0.0	0.0	0.0
11	0.274E-02	0.185E-01	0.933E-03	0.107E-01	0.234E-02	0.101E-01
12	0.722E-02	0.683E-01	0.140E-02	0.115E+00	0.234E-02	0.400E-01
13	0.114E-01	0.142E+00	0.703E-03	0.235E+00	0.234E-02	0.508E-01
14	0.102E-01	0.239E+00	-0.104E-02	0.505E+00	0.234E-02	0.704E-01
15	-0.514E-03	0.339E+00	-0.472E-02	0.753E+00	0.234E-02	0.795E-01
16	-0.177E-01	0.401E+00	-0.836E-02	0.100E+01	0.234E-02	0.826E-01
17	0.0	0.0	0.0	0.0	0.0	0.0
18	0.0	0.0	0.0	0.0	0.0	0.0
19	0.0	0.0	0.0	0.0	0.0	0.0
20	0.0	0.0	0.0	0.0	0.0	0.0
21	0.334E-03	0.439E-03	0.216E-03	-0.439E-02	0.284E-02	-0.158E-03
22	0.105E-02	0.955E-03	0.445E-03	-0.587E-02	0.284E-02	-0.373E-03
23	0.208E-02	0.157E-02	-0.931E-04	-0.715E-02	0.284E-02	-0.532E-03
24	0.148E-02	0.255E-02	-0.204E-03	-0.989E-02	0.284E-02	-0.612E-03
25	-0.379E-03	0.391E-02	-0.892E-03	-0.123E-01	0.284E-02	-0.657E-03
26	-0.406E-02	0.532E-02	-0.121E-02	-0.150E-01	0.284E-02	-0.613E-03
27	-0.877E-02	0.666E-02	-0.145E-02	-0.139E-01	0.284E-02	-0.400E-03
28	-0.132E-01	0.788E-02	-0.100E-02	-0.180E-01	0.284E-02	-0.162E-03
29	-0.152E-01	0.859E-02	-0.258E-03	-0.179E-01	0.284E-02	0.257E-03
30	-0.148E-01	0.915E-02	0.608E-03	-0.107E-01	0.284E-02	0.747E-03
31	-0.120E-01	0.970E-02	0.185E-02	-0.141E-01	0.284E-02	0.136E-02
32	-0.578E-02	0.968E-02	0.266E-02	-0.933E-02	0.284E-02	0.218E-02
33	0.574E-03	0.905E-02	0.323E-02	-0.329E-02	0.284E-02	0.322E-02
34	0.767E-02	0.709E-02	0.245E-02	0.021E-02	0.284E-02	0.466E-02
35	0.115E-01	0.207E-02	0.282E-04	0.197E-01	0.284E-02	0.639E-02
36	0.757E-02	-0.320E-02	-0.255E-02	0.390E-01	0.284E-02	0.775E-02
37	0.0	0.0	0.0	0.0	0.0	0.0
38	0.0	0.0	0.0	0.0	0.0	0.0
39	-0.140E-02	-0.628E-03	0.134E-03	-0.757E-02	-0.581E-03	-0.240E-03
40	-0.718E-05	0.0	0.404E-05	0.0	-0.157E-05	0.0
41	0.491E-02	-0.753E-03	0.0	-0.582E-02	0.0	0.0
42	0.011E-04	-0.016E-03	0.0	-0.582E-02	0.0	0.0
43	-0.404E-02	-0.332E-03	0.0	-0.582E-02	0.0	0.0
44	-0.558E-02	-0.201E-04	0.0	-0.582E-02	0.0	0.0
45	-0.447E-02	0.238E-03	0.0	-0.582E-02	0.0	0.0
46	-0.181E-02	0.288E-03	0.0	-0.582E-02	0.0	0.0
47	0.590E-05	0.217E-03	0.0	-0.582E-02	0.0	0.0
48	0.135E-02	0.758E-04	0.0	-0.582E-02	0.0	0.0
49	0.102E-02	-0.795E-04	0.0	-0.582E-02	0.0	0.0
50	-0.129E-02	-0.190E-03	0.0	-0.582E-02	0.0	0.0
51	0.755E-02	0.183E-02	0.0	-0.209E-02	0.0	0.0
52	0.0	0.0	0.0	0.0	0.0	0.0
53	0.0	0.0	0.0	0.0	0.0	0.0
54	0.0	0.0	0.0	0.0	0.0	0.0
55	0.0	0.0	0.0	0.0	0.0	0.0
56	0.119E-02	0.197E-03	0.0	-0.714E-02	-0.155E-13	-0.415E-14

TABLE C-22
SYMMETRIC MODE SHAPE –
10-PERCENT WING FUEL, NO TIP WEIGHT, 4.54 kg IN BAY 47

MODE NO. 1752 FREQ = 49.39 GENERALIZED MASS= 0.00

BAY	H	ALPH	THET	F	L	PSI
1	0.767E-08	0.0	0.0	0.417E-03	0.190E-01	0.647E-03
2	0.841E-08	0.0	0.0	0.176E-01	0.206E-01	0.201E-02
3	0.867E-08	0.0	0.0	0.248E-01	0.206E-01	0.201E-02
4	0.890E-08	0.0	0.0	0.314E-01	0.206E-01	0.201E-02
5	0.914E-08	0.0	0.0	0.380E-01	0.206E-01	0.201E-02
6	0.937E-08	0.0	0.0	0.447E-01	0.206E-01	0.201E-02
7	0.0	0.0	0.0	0.0	0.0	0.0
8	0.0	0.0	0.0	0.0	0.0	0.0
9	0.0	0.0	0.0	0.0	0.0	0.0
10	0.0	0.0	0.0	0.0	0.0	0.0
11	0.203E-01	-0.215E-01	0.838E-02	0.103E-01	0.331E-04	0.155E-01
12	0.392E-01	-0.986E-01	0.122E-01	0.112E+00	0.302E-04	0.397E-01
13	0.958E-01	-0.213E+00	0.874E-02	0.283E+00	0.310E-04	0.367E-01
14	0.876E-01	-0.366E+00	-0.136E-01	0.502E+00	0.338E-04	0.736E-01
15	-0.142E-02	-0.525E+00	-0.402E-01	0.751E+00	0.324E-04	0.797E-01
16	-0.150E+00	-0.823E+00	-0.859E-01	0.100E+01	0.327E-04	0.851E-01
17	0.0	0.0	0.0	0.0	0.0	0.0
18	0.0	0.0	0.0	0.0	0.0	0.0
19	0.0	0.0	0.0	0.0	0.0	0.0
20	0.0	0.0	0.0	0.0	0.0	0.0
21	0.279E-02	0.146E-02	0.110E-02	-0.364E-02	0.219E-02	-0.152E-03
22	0.941E-02	0.393E-02	0.153E-02	-0.482E-02	0.219E-02	-0.342E-03
23	0.141E-01	0.678E-02	0.194E-03	-0.655E-02	0.219E-02	-0.492E-03
24	0.122E-01	0.120E-01	-0.153E-02	-0.834E-02	0.219E-02	-0.573E-03
25	-0.203E-03	0.192E-01	-0.477E-02	-0.110E-01	0.219E-02	-0.824E-03
26	-0.248E-01	0.267E-01	-0.782E-02	-0.134E-01	0.219E-02	-0.593E-03
27	-0.539E-01	0.342E-01	-0.838E-02	-0.152E-01	0.219E-02	-0.492E-03
28	-0.780E-01	0.412E-01	-0.908E-02	-0.164E-01	0.219E-02	-0.196E-03
29	-0.851E-01	0.464E-01	0.442E-03	-0.165E-01	0.219E-02	0.168E-03
30	-0.760E-01	0.505E-01	0.520E-02	-0.155E-01	0.219E-02	0.631E-03
31	-0.595E-01	0.546E-01	0.104E-01	-0.133E-01	0.219E-02	0.122E-02
32	-0.408E-01	0.555E-01	0.146E-01	-0.976E-02	0.219E-02	0.195E-02
33	0.957E-02	0.526E-01	0.168E-01	-0.338E-02	0.219E-02	0.291E-02
34	0.434E-01	0.429E-01	0.999E-02	0.503E-02	0.219E-02	0.424E-02
35	0.510E-01	0.202E-01	-0.377E-02	0.174E-01	0.219E-02	0.536E-02
36	0.214E-01	-0.100E-01	-0.175E-01	0.351E-01	0.219E-02	0.713E-02
37	0.0	0.0	0.0	0.0	0.0	0.0
38	0.0	0.0	0.0	0.0	0.0	0.0
39	0.228E-02	-0.387E-02	0.189E-02	-0.522E-02	-0.290E-02	-0.191E-02
40	-0.332E-03	0.0	0.215E-03	0.0	-0.726E-04	0.0
41	0.997E-02	-0.154E-02	0.0	-0.535E-02	0.0	0.0
42	0.815E-04	-0.125E-02	0.0	-0.535E-02	0.0	0.0
43	-0.823E-02	-0.668E-03	0.0	-0.535E-02	0.0	0.0
44	-0.113E-01	-0.374E-04	0.0	-0.535E-02	0.0	0.0
45	-0.684E-02	0.501E-03	0.0	-0.535E-02	0.0	0.0
46	-0.329E-02	0.598E-03	0.0	-0.535E-02	0.0	0.0
47	-0.523E-03	-0.758E-04	0.0	-0.535E-02	0.0	0.0
48	-0.550E-02	-0.100E-02	0.0	-0.535E-02	0.0	0.0
49	-0.213E-01	-0.122E-02	0.0	-0.535E-02	0.0	0.0
50	-0.298E-01	0.280E-03	0.0	-0.535E-02	0.0	0.0
51	0.540E-01	0.125E-01	0.0	-0.959E-02	0.0	0.0
52	0.0	0.0	0.0	0.0	0.0	0.0
53	0.0	0.0	0.0	0.0	0.0	0.0
54	0.0	0.0	0.0	0.0	0.0	0.0
55	0.0	0.0	0.0	0.0	0.0	0.0
56	-0.457E-01	-0.493E-02	0.0	-0.195E-01	-0.175E-12	-0.474E-13

TABLE C-23

SYMMETRIC MODE SHAPE –

10-PERCENT WING FUEL, 20-GRAM TIP WEIGHT, STIFF PYLON

MODE NO. 1735 FREQ = 0.0 GENERALIZED MASS= 0.06

DAY	H	ALPH	THET	F	L	PSI
1	0.0	0.0	0.0	-0.592E+00	-0.806E+00	0.0
2	0.0	0.0	0.0	-0.592E+00	-0.806E+00	0.0
3	0.0	0.0	0.0	-0.592E+00	-0.806E+00	0.0
4	0.0	0.0	0.0	-0.592E+00	-0.806E+00	0.0
5	0.0	0.0	0.0	-0.592E+00	-0.806E+00	0.0
6	0.0	0.0	0.0	-0.592E+00	-0.806E+00	0.0
7	0.0	0.0	0.0	0.0	0.0	0.0
8	0.0	0.0	0.0	0.0	0.0	0.0
9	0.0	0.0	0.0	0.0	0.0	0.0
10	0.0	0.0	0.0	0.0	0.0	0.0
11	0.985E+00	0.0	0.0	-0.869E-01	-0.150E+00	0.0
12	0.985E+00	0.0	0.0	-0.869E-01	-0.150E+00	0.0
13	0.985E+00	0.0	0.0	-0.869E-01	-0.150E+00	0.0
14	0.985E+00	0.0	0.0	-0.869E-01	-0.150E+00	0.0
15	0.985E+00	0.0	0.0	-0.869E-01	-0.150E+00	0.0
16	0.985E+00	0.0	0.0	-0.869E-01	-0.150E+00	0.0
17	0.0	0.0	0.0	0.0	0.0	0.0
18	0.0	0.0	0.0	0.0	0.0	0.0
19	0.0	0.0	0.0	0.0	0.0	0.0
20	0.0	0.0	0.0	0.0	0.0	0.0
21	0.998E+00	0.0	0.0	-0.309E-01	-0.472E-01	0.0
22	0.998E+00	0.0	0.0	-0.309E-01	-0.472E-01	0.0
23	0.998E+00	0.0	0.0	-0.309E-01	-0.472E-01	0.0
24	0.998E+00	0.0	0.0	-0.309E-01	-0.472E-01	0.0
25	0.998E+00	0.0	0.0	-0.309E-01	-0.472E-01	0.0
26	0.998E+00	0.0	0.0	-0.309E-01	-0.472E-01	0.0
27	0.998E+00	0.0	0.0	-0.309E-01	-0.472E-01	0.0
28	0.998E+00	0.0	0.0	-0.309E-01	-0.472E-01	0.0
29	0.998E+00	0.0	0.0	-0.309E-01	-0.472E-01	0.0
30	0.998E+00	0.0	0.0	-0.309E-01	-0.472E-01	0.0
31	0.998E+00	0.0	0.0	-0.309E-01	-0.472E-01	0.0
32	0.998E+00	0.0	0.0	-0.309E-01	-0.472E-01	0.0
33	0.998E+00	0.0	0.0	-0.309E-01	-0.472E-01	0.0
34	0.998E+00	0.0	0.0	-0.309E-01	-0.472E-01	0.0
35	0.998E+00	0.0	0.0	-0.309E-01	-0.472E-01	0.0
36	0.998E+00	0.0	0.0	-0.309E-01	-0.472E-01	0.0
37	0.0	0.0	0.0	0.0	0.0	0.0
38	0.0	0.0	0.0	0.0	0.0	0.0
39	0.100E+01	0.0	0.0	0.0	0.0	0.0
40	0.0	0.0	0.0	0.0	0.0	0.0
41	0.100E+01	0.0	0.0	0.0	0.0	0.0
42	0.100E+01	0.0	0.0	0.0	0.0	0.0
43	0.100E+01	0.0	0.0	0.0	0.0	0.0
44	0.100E+01	0.0	0.0	0.0	0.0	0.0
45	0.100E+01	0.0	0.0	0.0	0.0	0.0
46	0.100E+01	0.0	0.0	0.0	0.0	0.0
47	0.100E+01	0.0	0.0	0.0	0.0	0.0
48	0.100E+01	0.0	0.0	0.0	0.0	0.0
49	0.100E+01	0.0	0.0	0.0	0.0	0.0
50	0.100E+01	0.0	0.0	0.0	0.0	0.0
51	0.100E+01	0.0	0.0	0.0	0.0	0.0
52	0.0	0.0	0.0	0.0	0.0	0.0
53	0.0	0.0	0.0	0.0	0.0	0.0
54	0.0	0.0	0.0	0.0	0.0	0.0
55	0.0	0.0	0.0	0.0	0.0	0.0
56	0.100E+01	0.0	0.0	-0.262E-01	0.0	0.0

TABLE C-24

SYMMETRIC MODE SHAPE –

10-PERCENT WING FUEL, 20-GRAM TIP WEIGHT, STIFF PYLON

MODE NO. 1736 FREQ = 0.0 GENERALIZED MASS= 53.50

BAY	H	ALPH	THET	F	L	PSI
1	0.154E-04	0.0	0.0	-0.340E+02	-0.357E+02	-0.100E+01
2	0.168E-04	0.0	0.0	-0.420E+02	-0.357E+02	-0.100E+01
3	0.173E-04	0.0	0.0	-0.447E+02	-0.357E+02	-0.100E+01
4	0.178E-04	0.0	0.0	-0.473E+02	-0.357E+02	-0.100E+01
5	0.183E-04	0.0	0.0	-0.498E+02	-0.357E+02	-0.100E+01
6	0.188E-04	0.0	0.0	-0.523E+02	-0.357E+02	-0.100E+01
7	0.0	0.0	0.0	0.0	0.0	0.0
8	0.0	0.0	0.0	0.0	0.0	0.0
9	0.0	0.0	0.0	0.0	0.0	0.0
10	0.0	0.0	0.0	0.0	0.0	0.0
11	0.509E+02	0.853E+00	0.493E+00	-0.570E+01	-0.705E+01	-0.174E+00
12	0.527E+02	0.853E+00	0.493E+00	-0.638E+01	-0.705E+01	-0.174E+00
13	0.545E+02	0.853E+00	0.493E+00	-0.699E+01	-0.705E+01	-0.174E+00
14	0.562E+02	0.853E+00	0.493E+00	-0.759E+01	-0.705E+01	-0.174E+00
15	0.578E+02	0.853E+00	0.493E+00	-0.815E+01	-0.705E+01	-0.174E+00
16	0.593E+02	0.853E+00	0.493E+00	-0.869E+01	-0.705E+01	-0.174E+00
17	0.0	0.0	0.0	0.0	0.0	0.0
18	0.0	0.0	0.0	0.0	0.0	0.0
19	0.0	0.0	0.0	0.0	0.0	0.0
20	0.0	0.0	0.0	0.0	0.0	0.0
21	0.517E+01	0.835E+00	0.547E+00	0.193E+01	-0.101E+01	-0.504E-01
22	0.753E+01	0.835E+00	0.547E+00	0.169E+01	-0.102E+01	-0.504E-01
23	0.980E+01	0.835E+00	0.547E+00	0.145E+01	-0.151E+01	-0.504E-01
24	0.118E+02	0.835E+00	0.547E+00	0.125E+01	-0.102E+01	-0.504E-01
25	0.141E+02	0.835E+00	0.547E+00	0.102E+01	-0.152E+01	-0.504E-01
26	0.162E+02	0.835E+00	0.547E+00	0.796E+00	-0.101E+01	-0.504E-01
27	0.181E+02	0.835E+00	0.547E+00	0.604E+00	-0.152E+01	-0.504E-01
28	0.199E+02	0.835E+00	0.547E+00	0.412E+00	-0.152E+01	-0.504E-01
29	0.215E+02	0.835E+00	0.547E+00	0.240E+00	-0.101E+01	-0.504E-01
30	0.229E+02	0.835E+00	0.547E+00	0.112E+00	-0.152E+01	-0.504E-01
31	0.242E+02	0.835E+00	0.547E+00	-0.299E-01	-0.152E+01	-0.504E-01
32	0.255E+02	0.835E+00	0.547E+00	-0.153E+00	-0.152E+01	-0.504E-01
33	0.269E+02	0.835E+00	0.547E+00	-0.304E+00	-0.101E+01	-0.504E-01
34	0.282E+02	0.835E+00	0.547E+00	-0.438E+00	-0.152E+01	-0.504E-01
35	0.295E+02	0.835E+00	0.547E+00	-0.579E+00	-0.101E+01	-0.504E-01
36	0.309E+02	0.835E+00	0.547E+00	-0.724E+00	-0.152E+01	-0.504E-01
37	0.0	0.0	0.0	0.0	0.0	0.0
38	0.0	0.0	0.0	0.0	0.0	0.0
39	0.567E+00	0.100E+01	0.0	0.498E+01	0.0	0.0
40	0.0	0.0	0.0	0.0	0.0	0.0
41	-0.409E+02	0.100E+01	0.0	0.0	0.0	0.0
42	-0.399E+02	0.100E+01	0.0	0.0	0.0	0.0
43	-0.313E+02	0.100E+01	0.0	0.0	0.0	0.0
44	-0.220E+02	0.100E+01	0.0	0.0	0.0	0.0
45	-0.131E+02	0.100E+01	0.0	0.0	0.0	0.0
46	-0.306E+01	0.100E+01	0.0	0.0	0.0	0.0
47	0.362E+01	0.100E+01	0.0	0.0	0.0	0.0
48	0.122E+02	0.100E+01	0.0	0.0	0.0	0.0
49	0.254E+02	0.100E+01	0.0	0.0	0.0	0.0
50	0.380E+02	0.100E+01	0.0	0.0	0.0	0.0
51	0.544E+02	0.100E+01	0.0	-0.214E+01	0.0	0.0
52	0.0	0.0	0.0	0.0	0.0	0.0
53	0.0	0.0	0.0	0.0	0.0	0.0
54	0.0	0.0	0.0	0.0	0.0	0.0
55	0.0	0.0	0.0	0.0	0.0	0.0
56	0.585E+02	0.100E+01	0.0	-0.865E+01	0.0	0.0

TABLE C-25

SYMMETRIC MODE SHAPE –
10-PERCENT WING FUEL, 20-GRAM TIP WEIGHT, STIFF PYLON

MODE NO. 1737 FREQ = 0.0 GENERALIZED MASS= 0.06

BAY	H	ALPH	THET	F	L	PSI
1	0.0	0.0	0.0	0.806E+00	-0.592E+00	0.0
2	0.0	0.0	0.0	0.806E+00	-0.592E+00	0.0
3	0.0	0.0	0.0	0.806E+00	-0.592E+00	0.0
4	0.0	0.0	0.0	0.806E+00	-0.592E+00	0.0
5	0.0	0.0	0.0	0.806E+00	-0.592E+00	0.0
6	0.0	0.0	0.0	0.806E+00	-0.592E+00	0.0
7	0.0	0.0	0.0	0.0	0.0	0.0
8	0.0	0.0	0.0	0.0	0.0	0.0
9	0.0	0.0	0.0	0.0	0.0	0.0
10	0.0	0.0	0.0	0.0	0.0	0.0
11	0.0	0.0	0.0	0.866E+00	-0.500E+00	0.0
12	0.0	0.0	0.0	0.866E+00	-0.500E+00	0.0
13	0.0	0.0	0.0	0.866E+00	-0.500E+00	0.0
14	0.0	0.0	0.0	0.866E+00	-0.500E+00	0.0
15	0.0	0.0	0.0	0.866E+00	-0.500E+00	0.0
16	0.0	0.0	0.0	0.866E+00	-0.500E+00	0.0
17	0.0	0.0	0.0	0.0	0.0	0.0
18	0.0	0.0	0.0	0.0	0.0	0.0
19	0.0	0.0	0.0	0.0	0.0	0.0
20	0.0	0.0	0.0	0.0	0.0	0.0
21	0.0	0.0	0.0	0.837E+00	-0.548E+00	0.0
22	0.0	0.0	0.0	0.837E+00	-0.548E+00	0.0
23	0.0	0.0	0.0	0.837E+00	-0.548E+00	0.0
24	0.0	0.0	0.0	0.837E+00	-0.548E+00	0.0
25	0.0	0.0	0.0	0.837E+00	-0.548E+00	0.0
26	0.0	0.0	0.0	0.837E+00	-0.548E+00	0.0
27	0.0	0.0	0.0	0.837E+00	-0.548E+00	0.0
28	0.0	0.0	0.0	0.837E+00	-0.548E+00	0.0
29	0.0	0.0	0.0	0.837E+00	-0.548E+00	0.0
30	0.0	0.0	0.0	0.837E+00	-0.548E+00	0.0
31	0.0	0.0	0.0	0.837E+00	-0.548E+00	0.0
32	0.0	0.0	0.0	0.837E+00	-0.548E+00	0.0
33	0.0	0.0	0.0	0.837E+00	-0.548E+00	0.0
34	0.0	0.0	0.0	0.837E+00	-0.548E+00	0.0
35	0.0	0.0	0.0	0.837E+00	-0.548E+00	0.0
36	0.0	0.0	0.0	0.837E+00	-0.548E+00	0.0
37	0.0	0.0	0.0	0.0	0.0	0.0
38	0.0	0.0	0.0	0.0	0.0	0.0
39	0.0	0.0	0.0	0.100E+01	0.0	0.0
40	0.0	0.0	0.0	0.0	0.0	0.0
41	0.0	0.0	0.0	0.100E+01	0.0	0.0
42	0.0	0.0	0.0	0.100E+01	0.0	0.0
43	0.0	0.0	0.0	0.100E+01	0.0	0.0
44	0.0	0.0	0.0	0.100E+01	0.0	0.0
45	0.0	0.0	0.0	0.100E+01	0.0	0.0
46	0.0	0.0	0.0	0.100E+01	0.0	0.0
47	0.0	0.0	0.0	0.100E+01	0.0	0.0
48	0.0	0.0	0.0	0.100E+01	0.0	0.0
49	0.0	0.0	0.0	0.100E+01	0.0	0.0
50	0.0	0.0	0.0	0.100E+01	0.0	0.0
51	0.0	0.0	0.0	0.100E+01	0.0	0.0
52	0.0	0.0	0.0	0.0	0.0	0.0
53	0.0	0.0	0.0	0.0	0.0	0.0
54	0.0	0.0	0.0	0.0	0.0	0.0
55	0.0	0.0	0.0	0.0	0.0	0.0
56	0.262E-01	0.0	0.0	0.100E+01	0.0	0.0

TABLE C-26

SYMMETRIC MODE SHAPE – 10-PERCENT WING FUEL, 20-GRAM TIP WEIGHT, STIFF PYLON

MODE NO. 1738 FREQ = 4.78 GENERALIZED MASS= 3.00

BAY	H	ALPH	THET	F	L	PSI
1	0.000E-10	0.0	0.0	0.420E-01	0.441E-01	0.160E-02
2	0.878E-10	0.0	0.0	0.555E-01	0.441E-01	0.163E-02
3	0.903E-10	0.0	0.0	0.600E-01	0.441E-01	0.163E-02
4	0.930E-10	0.0	0.0	0.642E-01	0.441E-01	0.163E-02
5	0.954E-10	0.0	0.0	0.683E-01	0.441E-01	0.163E-02
6	0.979E-10	0.0	0.0	0.724E-01	0.441E-01	0.163E-02
7	0.0	0.0	0.0	0.0	0.0	0.0
8	0.0	0.0	0.0	0.0	0.0	0.0
9	0.0	0.0	0.0	0.0	0.0	0.0
10	0.0	0.0	0.0	0.0	0.0	0.0
11	-0.647E-01	-0.139E-02	-0.974E-03	0.620E-02	0.950E-02	0.284E-03
12	-0.688E-01	-0.139E-02	-0.153E-02	0.723E-02	0.950E-02	0.288E-03
13	-0.739E-01	-0.140E-02	-0.160E-02	0.823E-02	0.950E-02	0.291E-03
14	-0.799E-01	-0.140E-02	-0.188E-02	0.925E-02	0.950E-02	0.293E-03
15	-0.864E-01	-0.140E-02	-0.210E-02	0.102E-01	0.950E-02	0.294E-03
16	-0.930E-01	-0.140E-02	-0.219E-02	0.111E-01	0.950E-02	0.294E-03
17	0.0	0.0	0.0	0.0	0.0	0.0
18	0.0	0.0	0.0	0.0	0.0	0.0
19	0.0	0.0	0.0	0.0	0.0	0.0
20	0.0	0.0	0.0	0.0	0.0	0.0
21	-0.122E-01	-0.651E-04	0.630E-03	-0.913E-03	0.151E-02	0.503E-07
22	-0.683E-02	0.303E-04	0.170E-02	-0.912E-03	0.151E-02	0.350E-06
23	0.320E-02	0.170E-03	0.332E-02	-0.909E-03	0.151E-02	0.981E-06
24	0.190E-01	0.325E-03	0.555E-02	-0.905E-03	0.151E-02	0.974E-06
25	0.487E-01	0.556E-03	0.808E-02	-0.901E-03	0.151E-02	0.942E-06
26	0.930E-01	0.808E-03	0.139E-01	-0.897E-03	0.151E-02	0.874E-06
27	0.144E+00	0.123E-02	0.177E-01	-0.895E-03	0.151E-02	0.790E-06
28	0.213E+00	0.185E-02	0.223E-01	-0.892E-03	0.151E-02	0.697E-06
29	0.280E+00	0.240E-02	0.270E-01	-0.891E-03	0.151E-02	0.581E-06
30	0.355E+00	0.312E-02	0.305E-01	-0.890E-03	0.151E-02	0.139E-06
31	0.434E+00	0.400E-02	0.343E-01	-0.890E-03	0.151E-02	-0.165E-06
32	0.521E+00	0.501E-02	0.381E-01	-0.891E-03	0.151E-02	-0.541E-06
33	0.620E+00	0.602E-02	0.429E-01	-0.893E-03	0.151E-02	-0.103E-05
34	0.731E+00	0.942E-02	0.481E-01	-0.896E-03	0.151E-02	-0.169E-05
35	0.854E+00	0.132E-01	0.524E-01	-0.901E-03	0.151E-02	-0.250E-05
36	0.100E+01	0.176E-01	0.549E-01	-0.909E-03	0.151E-02	-0.313E-05
37	0.0	0.0	0.0	0.0	0.0	0.0
38	0.0	0.0	0.0	0.0	0.0	0.0
39	-0.157E-01	0.213E-02	0.286E-02	0.433E-02	-0.193E-01	0.587E-03
40	-0.326E-03	0.0	0.212E-03	0.0	-0.717E-04	0.0
41	-0.213E-01	0.263E-03	0.0	-0.101E-02	0.0	0.0
42	-0.200E-01	0.260E-03	0.0	-0.101E-02	0.0	0.0
43	-0.178E-01	0.239E-03	0.0	-0.101E-02	0.0	0.0
44	-0.159E-01	0.199E-03	0.0	-0.101E-02	0.0	0.0
45	-0.143E-01	0.131E-03	0.0	-0.101E-02	0.0	0.0
46	-0.135E-01	0.473E-04	0.0	-0.101E-02	0.0	0.0
47	-0.138E-01	-0.220E-03	0.0	-0.101E-02	0.0	0.0
48	-0.177E-01	-0.684E-03	0.0	-0.101E-02	0.0	0.0
49	-0.293E-01	-0.973E-03	0.0	-0.101E-02	0.0	0.0
50	-0.451E-01	-0.141E-02	0.0	-0.101E-02	0.0	0.0
51	-0.710E-01	-0.165E-02	0.0	0.169E-02	0.0	0.0
52	0.0	0.0	0.0	0.0	0.0	0.0
53	0.0	0.0	0.0	0.0	0.0	0.0
54	0.0	0.0	0.0	0.0	0.0	0.0
55	0.0	0.0	0.0	0.0	0.0	0.0
56	-0.769E-01	-0.165E-02	0.0	0.101E-01	-0.120E-14	-0.340E-15

TABLE C-27

SYMMETRIC MODE SHAPE –
10-PERCENT WING FUEL, 20-GRAM TIP WEIGHT, STIFF PYLON

MODE NO. 1739 FREQ = 8.47 GENERALIZED MASS= 0.01

BAY	H	ALPH	THET	F	L	PSI
1	-0.103E-06	0.0	0.0	-0.270E+00	-0.153E+00	-0.244E-01
2	-0.113E-06	0.0	0.0	-0.470E+00	-0.153E+00	-0.252E-01
3	-0.116E-06	0.0	0.0	-0.559E+00	-0.153E+00	-0.252E-01
4	-0.119E-06	0.0	0.0	-0.603E+00	-0.153E+00	-0.252E-01
5	-0.123E-06	0.0	0.0	-0.667E+00	-0.153E+00	-0.252E-01
6	-0.126E-06	0.0	0.0	-0.751E+00	-0.153E+00	-0.252E-01
7	0.0	0.0	0.0	0.0	0.0	0.0
8	0.0	0.0	0.0	0.0	0.0	0.0
9	0.0	0.0	0.0	0.0	0.0	0.0
10	0.0	0.0	0.0	0.0	0.0	0.0
11	0.357E+00	0.214E-01	0.171E-01	-0.414E-01	-0.479E-01	-0.441E-02
12	0.435E+00	0.218E-01	0.262E-01	-0.515E-01	-0.479E-01	-0.452E-02
13	0.543E+00	0.218E-01	0.354E-01	-0.733E-01	-0.479E-01	-0.460E-02
14	0.680E+00	0.221E-01	0.444E-01	-0.894E-01	-0.479E-01	-0.466E-02
15	0.858E+00	0.222E-01	0.513E-01	-0.105E+00	-0.479E-01	-0.471E-02
16	0.100E+01	0.223E-01	0.554E-01	-0.119E+00	-0.479E-01	-0.472E-02
17	0.0	0.0	0.0	0.0	0.0	0.0
18	0.0	0.0	0.0	0.0	0.0	0.0
19	0.0	0.0	0.0	0.0	0.0	0.0
20	0.0	0.0	0.0	0.0	0.0	0.0
21	-0.293E+00	-0.431E-02	-0.507E-02	0.120E-01	0.117E-01	0.384E-03
22	-0.319E+00	-0.287E-02	-0.318E-02	0.137E-01	0.117E-01	0.334E-03
23	-0.344E+00	-0.449E-03	-0.394E-02	0.153E-01	0.117E-01	0.372E-03
24	-0.300E+00	-0.632E-03	-0.519E-02	0.167E-01	0.117E-01	0.393E-03
25	-0.382E+00	-0.777E-03	-0.257E-02	0.183E-01	0.117E-01	0.423E-03
26	-0.394E+00	-0.377E-03	0.242E-02	0.201E-01	0.117E-01	0.455E-03
27	-0.383E+00	-0.049E-04	0.950E-02	0.217E-01	0.117E-01	0.487E-03
28	-0.310E+00	0.813E-03	0.187E-01	0.234E-01	0.117E-01	0.519E-03
29	-0.240E+00	0.203E-02	0.270E-01	0.249E-01	0.117E-01	0.547E-03
30	-0.172E+00	0.349E-02	0.353E-01	0.263E-01	0.117E-01	0.570E-03
31	-0.740E-01	0.503E-02	0.425E-01	0.277E-01	0.117E-01	0.589E-03
32	0.507E-01	0.930E-02	0.575E-01	0.291E-01	0.117E-01	0.606E-03
33	0.208E+00	0.153E-01	0.721E-01	0.307E-01	0.117E-01	0.620E-03
34	0.405E+00	0.262E-01	0.893E-01	0.322E-01	0.117E-01	0.629E-03
35	0.642E+00	0.412E-01	0.104E+00	0.337E-01	0.117E-01	0.630E-03
36	0.938E+00	0.582E-01	0.113E+00	0.354E-01	0.117E-01	0.622E-03
37	0.0	0.0	0.0	0.0	0.0	0.0
38	0.0	0.0	0.0	0.0	0.0	0.0
39	-0.333E+00	0.550E-02	-0.976E-02	0.130E-01	0.905E-01	-0.161E-01
40	0.962E-03	0.0	-0.523E-03	0.0	0.210E-03	0.0
41	0.711E+00	-0.278E-01	0.0	0.204E-01	0.0	0.0
42	0.517E+00	-0.274E-01	0.0	0.204E-01	0.0	0.0
43	0.290E+00	-0.255E-01	0.0	0.204E-01	0.0	0.0
44	0.801E-01	-0.220E-01	0.0	0.204E-01	0.0	0.0
45	-0.102E+00	-0.163E-01	0.0	0.204E-01	0.0	0.0
46	-0.226E+00	-0.980E-02	0.0	0.204E-01	0.0	0.0
47	-0.274E+00	-0.300E-02	0.0	0.204E-01	0.0	0.0
48	-0.264E+00	0.505E-02	0.0	0.204E-01	0.0	0.0
49	-0.150E+00	0.103E-01	0.0	0.204E-01	0.0	0.0
50	0.512E-01	0.199E-01	0.0	0.204E-01	0.0	0.0
51	0.448E+00	0.257E-01	0.0	-0.268E-01	0.0	0.0
52	0.0	0.0	0.0	0.0	0.0	0.0
53	0.0	0.0	0.0	0.0	0.0	0.0
54	0.0	0.0	0.0	0.0	0.0	0.0
55	0.0	0.0	0.0	0.0	0.0	0.0
56	0.534E+00	0.255E-01	0.0	-0.134E+00	0.255E-13	0.691E-14

TABLE C-28

SYMMETRIC MODE SHAPE –

10-PERCENT WING FUEL, 20-GRAM TIP WEIGHT, STIFF PYLON

MODE NO. 1740 FREQ = 8.84 GENERALIZED MASS= 0.01

BAY	H	ALPH	THET	F	L	PSI
1	0.981E-08	0.0	0.0	0.252E-01	0.109E-01	0.238E-02
2	0.108E-07	0.0	0.0	0.447E-01	0.109E-01	0.240E-02
3	0.111E-07	0.0	0.0	0.614E-01	0.109E-01	0.240E-02
4	0.114E-07	0.0	0.0	0.577E-01	0.109E-01	0.240E-02
5	0.117E-07	0.0	0.0	0.639E-01	0.109E-01	0.246E-02
6	0.120E-07	0.0	0.0	0.701E-01	0.109E-01	0.240E-02
7	0.0	0.0	0.0	0.0	0.0	0.0
8	0.0	0.0	0.0	0.0	0.0	0.0
9	0.0	0.0	0.0	0.0	0.0	0.0
10	0.0	0.0	0.0	0.0	0.0	0.0
11	-0.310E-01	-0.208E-02	-0.109E-02	0.498E-02	0.333E-02	0.431E-03
12	-0.387E-01	-0.210E-02	-0.262E-02	0.856E-02	0.333E-02	0.444E-03
13	-0.496E-01	-0.213E-02	-0.357E-02	0.814E-02	0.334E-02	0.454E-03
14	-0.634E-01	-0.216E-02	-0.459E-02	0.971E-02	0.333E-02	0.451E-03
15	-0.795E-01	-0.217E-02	-0.523E-02	0.112E-01	0.334E-02	0.406E-03
16	-0.980E-01	-0.218E-02	-0.533E-02	0.127E-01	0.333E-02	0.408E-03
17	0.0	0.0	0.0	0.0	0.0	0.0
18	0.0	0.0	0.0	0.0	0.0	0.0
19	0.0	0.0	0.0	0.0	0.0	0.0
20	0.0	0.0	0.0	0.0	0.0	0.0
21	0.305E-01	0.951E-03	-0.188E-03	-0.242E-03	-0.210E-02	-0.172E-03
22	0.277E-01	0.167E-02	-0.957E-03	-0.138E-02	-0.210E-02	-0.393E-03
23	0.222E-01	0.238E-02	-0.168E-02	-0.361E-02	-0.210E-02	-0.583E-03
24	0.149E-01	0.286E-02	-0.218E-02	-0.604E-02	-0.210E-02	-0.728E-03
25	0.554E-02	0.278E-02	-0.232E-02	-0.937E-02	-0.210E-02	-0.906E-03
26	-0.271E-02	0.306E-02	-0.184E-02	-0.132E-01	-0.210E-02	-0.107E-02
27	-0.752E-02	0.351E-02	-0.891E-03	-0.171E-01	-0.210E-02	-0.120E-02
28	-0.869E-02	0.410E-02	0.203E-03	-0.214E-01	-0.210E-02	-0.129E-02
29	-0.091E-02	0.457E-02	0.948E-03	-0.252E-01	-0.210E-02	-0.133E-02
30	-0.411E-02	0.497E-02	0.132E-02	-0.284E-01	-0.210E-02	-0.131E-02
31	-0.590E-03	0.534E-02	0.154E-02	-0.310E-01	-0.210E-02	-0.125E-02
32	0.345E-02	0.515E-02	0.164E-02	-0.329E-01	-0.210E-02	-0.113E-02
33	0.886E-02	0.476E-02	0.273E-02	-0.370E-01	-0.210E-02	-0.936E-03
34	0.177E-01	0.424E-02	0.471E-02	-0.390E-01	-0.210E-02	-0.822E-03
35	0.322E-01	0.443E-02	0.710E-02	-0.400E-01	-0.210E-02	-0.192E-03
36	0.536E-01	0.542E-02	0.850E-02	-0.399E-01	-0.210E-02	0.134E-03
37	0.0	0.0	0.0	0.0	0.0	0.0
38	0.0	0.0	0.0	0.0	0.0	0.0
39	0.117E-01	0.102E-02	-0.301E-01	0.140E-02	0.100E+01	-0.205E+00
40	0.225E-03	0.0	-0.145E-03	0.0	0.491E-04	0.0
41	-0.613E-01	0.258E-02	0.0	-0.487E-03	0.0	0.0
42	-0.432E-01	0.253E-02	0.0	-0.487E-03	0.0	0.0
43	-0.222E-01	0.235E-02	0.0	-0.487E-03	0.0	0.0
44	-0.294E-02	0.202E-02	0.0	-0.487E-03	0.0	0.0
45	0.138E-01	0.150E-02	0.0	-0.487E-03	0.0	0.0
46	0.253E-01	0.917E-03	0.0	-0.487E-03	0.0	0.0
47	0.299E-01	0.291E-03	0.0	-0.487E-03	0.0	0.0
48	0.290E-01	-0.472E-03	0.0	-0.487E-03	0.0	0.0
49	0.183E-01	-0.998E-03	0.0	-0.487E-03	0.0	0.0
50	-0.112E-02	-0.193E-02	0.0	-0.487E-03	0.0	0.0
51	-0.397E-01	-0.250E-02	0.0	0.429E-02	0.0	0.0
52	0.0	0.0	0.0	0.0	0.0	0.0
53	0.0	0.0	0.0	0.0	0.0	0.0
54	0.0	0.0	0.0	0.0	0.0	0.0
55	0.0	0.0	0.0	0.0	0.0	0.0
56	-0.480E-01	-0.249E-02	0.0	0.145E-01	-0.233E-14	-0.832E-15

TABLE C-29
SYMMETRIC MODE SHAPE –
10-PERCENT WING FUEL, 20-GRAM TIP WEIGHT, STIFF PYLON

MODE NO. 1741 FREQ = 13.23 GENERALIZED MASS= 0.00

BAY	H	ALPH	THET	F	L	PSI
1	-0.202E-07	0.0	0.0	0.949E-02	-0.182E-01	0.155E-02
2	-0.222E-07	0.0	0.0	0.221E-01	-0.181E-01	0.160E-02
3	-0.228E-07	0.0	0.0	0.265E-01	-0.181E-01	0.160E-02
4	-0.234E-07	0.0	0.0	0.306E-01	-0.181E-01	0.160E-02
5	-0.241E-07	0.0	0.0	0.346E-01	-0.181E-01	0.160E-02
6	-0.247E-07	0.0	0.0	0.387E-01	-0.181E-01	0.160E-02
7	0.0	0.0	0.0	0.0	0.0	0.0
8	0.0	0.0	0.0	0.0	0.0	0.0
9	0.0	0.0	0.0	0.0	0.0	0.0
10	0.0	0.0	0.0	0.0	0.0	0.0
11	0.390E-02	-0.134E-02	-0.123E-02	0.925E-02	-0.621E-02	0.297E-03
12	-0.220E-02	-0.138E-02	-0.217E-02	0.104E-01	-0.621E-02	0.336E-03
13	-0.117E-01	-0.142E-02	-0.324E-02	0.116E-01	-0.621E-02	0.363E-03
14	-0.246E-01	-0.146E-02	-0.440E-02	0.129E-01	-0.621E-02	0.385E-03
15	-0.409E-01	-0.148E-02	-0.534E-02	0.142E-01	-0.621E-02	0.399E-03
16	-0.579E-01	-0.149E-02	-0.572E-02	0.154E-01	-0.621E-02	0.404E-03
17	0.0	0.0	0.0	0.0	0.0	0.0
18	0.0	0.0	0.0	0.0	0.0	0.0
19	0.0	0.0	0.0	0.0	0.0	0.0
20	0.0	0.0	0.0	0.0	0.0	0.0
21	0.513E-01	-0.335E-02	-0.305E-02	0.302E-02	-0.584E-02	0.332E-04
22	0.218E-01	-0.910E-02	-0.935E-02	0.319E-02	-0.584E-02	0.391E-04
23	-0.343E-01	-0.106E-01	-0.187E-01	0.338E-02	-0.584E-02	0.548E-04
24	-0.119E+00	-0.175E-01	-0.270E-01	0.360E-02	-0.583E-02	0.693E-04
25	-0.248E+00	-0.182E-01	-0.327E-01	0.392E-02	-0.583E-02	0.888E-04
26	-0.397E+00	-0.184E-01	-0.411E-01	0.431E-02	-0.584E-02	0.110E-03
27	-0.541E+00	-0.178E-01	-0.405E-01	0.472E-02	-0.584E-02	0.130E-03
28	-0.667E+00	-0.159E-01	-0.319E-01	0.520E-02	-0.584E-02	0.149E-03
29	-0.748E+00	-0.120E-01	-0.180E-01	0.506E-02	-0.584E-02	0.166E-03
30	-0.760E+00	-0.724E-02	-0.227E-02	0.608E-02	-0.583E-02	0.180E-03
31	-0.744E+00	0.191E-03	0.216E-01	0.654E-02	-0.584E-02	0.192E-03
32	-0.651E+00	0.145E-01	0.361E-01	0.701E-02	-0.583E-02	0.203E-03
33	-0.481E+00	0.303E-01	0.102E+00	0.752E-02	-0.584E-02	0.212E-03
34	-0.140E+00	0.822E-01	0.164E+00	0.834E-02	-0.583E-02	0.218E-03
35	0.333E+00	0.148E+00	0.223E+00	0.858E-02	-0.584E-02	0.221E-03
36	0.100E+01	0.224E+00	0.263E+00	0.917E-02	-0.584E-02	0.218E-03
37	0.0	0.0	0.0	0.0	0.0	0.0
38	0.0	0.0	0.0	0.0	0.0	0.0
39	0.306E+00	-0.507E-01	-0.559E-02	-0.106E+00	-0.112E-01	0.714E-02
40	0.114E-02	0.0	-0.736E-03	0.0	0.250E-03	0.0
41	-0.135E+00	0.725E-02	0.0	0.904E-02	0.0	0.0
42	-0.840E-01	0.705E-02	0.0	0.904E-02	0.0	0.0
43	-0.274E-01	0.621E-02	0.0	0.904E-02	0.0	0.0
44	0.210E-01	0.472E-02	0.0	0.904E-02	0.0	0.0
45	0.549E-01	0.258E-02	0.0	0.904E-02	0.0	0.0
46	0.857E-01	-0.145E-03	0.0	0.904E-02	0.0	0.0
47	0.987E-01	-0.115E-02	0.0	0.904E-02	0.0	0.0
48	0.500E-01	-0.919E-03	0.0	0.904E-02	0.0	0.0
49	0.381E-01	-0.914E-03	0.0	0.904E-02	0.0	0.0
50	0.238E-01	-0.129E-02	0.0	0.904E-02	0.0	0.0
51	0.102E-04	-0.160E-02	0.0	0.122E-01	0.0	0.0
52	0.0	0.0	0.0	0.0	0.0	0.0
53	0.0	0.0	0.0	0.0	0.0	0.0
54	0.0	0.0	0.0	0.0	0.0	0.0
55	0.0	0.0	0.0	0.0	0.0	0.0
56	-0.611E-02	-0.157E-02	0.0	0.204E-01	0.253E-14	0.644E-15

TABLE C-30

SYMMETRIC MODE SHAPE –
10-PERCENT WING FUEL, 20-GRAM TIP WEIGHT, STIFF PYLON

MODE NO. 1742 FREQ = 14.7+ GENERALIZED MASS= 3.00

BAY	H	ALPH	THET	F	L	PSI
1	-0.730E-08	0.0	0.0	0.255E-01	0.203E-01	0.138E-03
2	-0.800E-08	0.0	0.0	0.325E-01	0.204E-01	0.919E-03
3	-0.825E-08	0.0	0.0	0.350E-01	0.204E-01	0.919E-03
4	-0.847E-08	0.0	0.0	0.374E-01	0.204E-01	0.919E-03
5	-0.869E-08	0.0	0.0	0.397E-01	0.204E-01	0.919E-03
6	-0.892E-08	0.0	0.0	0.420E-01	0.204E-01	0.919E-03
7	0.0	0.0	0.0	0.0	0.0	0.0
8	0.0	0.0	0.0	0.0	0.0	0.0
9	0.0	0.0	0.0	0.0	0.0	0.0
10	0.0	0.0	0.0	0.0	0.0	0.0
11	-0.266E-01	-0.176E-03	0.959E-02	0.509E-02	0.432E-02	0.300E-04
12	0.428E-01	-0.161E-03	0.294E-01	0.531E-02	0.432E-02	0.716E-04
13	0.184E+00	-0.168E-03	0.516E-01	0.559E-02	0.432E-02	0.868E-04
14	0.404E+00	-0.174E-03	0.764E-01	0.591E-02	0.432E-02	0.991E-04
15	0.691E+00	-0.198E-03	0.964E-01	0.629E-02	0.432E-02	0.107E-03
16	0.106E+01	-0.200E-03	0.105E+00	0.675E-02	0.432E-02	0.115E-03
17	0.0	0.0	0.0	0.0	0.0	0.0
18	0.0	0.0	0.0	0.0	0.0	0.0
19	0.0	0.0	0.0	0.0	0.0	0.0
20	0.0	0.0	0.0	0.0	0.0	0.0
21	-0.392E-02	-0.132E-02	0.446E-04	0.244E-03	0.151E-03	0.211E-04
22	-0.301E-02	-0.219E-02	0.200E-03	0.319E-03	0.152E-03	0.172E-04
23	-0.185E-02	-0.373E-02	0.421E-03	0.397E-03	0.151E-03	0.212E-04
24	-0.212E-03	-0.387E-02	0.675E-03	0.474E-03	0.152E-03	0.215E-04
25	0.376E-02	-0.402E-02	0.129E-02	0.502E-03	0.153E-03	0.223E-04
26	0.992E-02	-0.417E-02	0.191E-02	0.534E-03	0.151E-03	0.241E-04
27	0.174E-01	-0.433E-02	0.236E-02	0.740E-03	0.152E-03	0.266E-04
28	0.258E-01	-0.454E-02	0.249E-02	0.837E-03	0.152E-03	0.302E-04
29	0.326E-01	-0.483E-02	0.220E-02	0.932E-03	0.151E-03	0.346E-04
30	0.378E-01	-0.515E-02	0.181E-02	0.102E-02	0.153E-03	0.392E-04
31	0.413E-01	-0.565E-02	0.957E-03	0.112E-02	0.151E-03	0.446E-04
32	0.420E-01	-0.657E-02	-0.436E-03	0.124E-02	0.153E-03	0.514E-04
33	0.388E-01	-0.806E-02	-0.253E-02	0.138E-02	0.151E-03	0.595E-04
34	0.291E-01	-0.108E-01	-0.349E-02	0.153E-02	0.152E-03	0.702E-04
35	0.117E-01	-0.150E-01	-0.866E-02	0.172E-02	0.151E-03	0.825E-04
36	-0.152E-01	-0.198E-01	-0.110E-01	0.193E-02	0.152E-03	0.917E-04
37	0.0	0.0	0.0	0.0	0.0	0.0
38	0.0	0.0	0.0	0.0	0.0	0.0
39	0.469E-01	-0.827E-02	0.244E-02	-0.108E-01	0.102E-03	-0.153E-02
40	-0.253E-03	0.0	0.102E-03	0.0	-0.347E-04	0.0
41	-0.125E-01	0.588E-03	0.0	0.132E-02	0.0	0.0
42	-0.843E-02	0.566E-03	0.0	0.132E-02	0.0	0.0
43	-0.395E-02	0.490E-03	0.0	0.132E-02	0.0	0.0
44	-0.592E-03	0.280E-03	0.0	0.132E-02	0.0	0.0
45	0.817E-03	0.129E-03	0.0	0.132E-02	0.0	0.0
46	-0.044E-03	-0.321E-03	0.0	0.132E-02	0.0	0.0
47	-0.412E-02	-0.636E-03	0.0	0.132E-02	0.0	0.0
48	-0.108E-01	-0.852E-03	0.0	0.132E-02	0.0	0.0
49	-0.216E-01	-0.822E-03	0.0	0.132E-02	0.0	0.0
50	-0.309E-01	-0.578E-03	0.0	0.132E-02	0.0	0.0
51	-0.359E-01	-0.191E-04	0.0	0.237E-02	0.0	0.0
52	0.0	0.0	0.0	0.0	0.0	0.0
53	0.0	0.0	0.0	0.0	0.0	0.0
54	0.0	0.0	0.0	0.0	0.0	0.0
55	0.0	0.0	0.0	0.0	0.0	0.0
56	-0.453E-01	-0.101E-02	0.0	0.812E-02	-0.723E-14	-0.145E-14

TABLE C-31
SYMMETRIC MODE SHAPE –
10-PERCENT WING FUEL, 20-GRAM TIP WEIGHT, STIFF PYLON

MODE NO. 1743 FREQ = 15.71 GENERALIZED MASS= 0.00

BAY	H	ALPH	THET	F	L	PSI
1	0.304E-07	0.0	0.0	0.481E-01	0.126E-01	0.929E-02
2	0.399E-07	0.0	0.0	0.127E+00	0.131E-01	0.100E-01
3	0.412E-07	0.0	0.0	0.154E+00	0.131E-01	0.100E-01
4	0.423E-07	0.0	0.0	0.180E+00	0.131E-01	0.100E-01
5	0.434E-07	0.0	0.0	0.205E+00	0.131E-01	0.100E-01
6	0.445E-07	0.0	0.0	0.231E+00	0.131E-01	0.100E-01
7	0.0	0.0	0.0	0.0	0.0	0.0
8	0.0	0.0	0.0	0.0	0.0	0.0
9	0.0	0.0	0.0	0.0	0.0	0.0
10	0.0	0.0	0.0	0.0	0.0	0.0
11	-0.545E-01	-0.760E-02	0.602E-02	-0.397E-02	0.154E-01	0.126E-02
12	0.470E-02	-0.792E-02	0.274E-01	0.185E-02	0.154E-01	0.104E-02
13	0.143E+00	-0.826E-02	0.521E-01	0.770E-02	0.154E-01	0.109E-02
14	0.369E+00	-0.859E-02	0.779E-01	0.136E-01	0.154E-01	0.172E-02
15	0.671E+00	-0.880E-02	0.102E+00	0.193E-01	0.154E-01	0.175E-02
16	0.100E+01	-0.888E-02	0.112E+00	0.240E-01	0.154E-01	0.175E-02
17	0.0	0.0	0.0	0.0	0.0	0.0
18	0.0	0.0	0.0	0.0	0.0	0.0
19	0.0	0.0	0.0	0.0	0.0	0.0
20	0.0	0.0	0.0	0.0	0.0	0.0
21	0.110E+00	0.890E-02	-0.113E-02	-0.175E-01	0.318E-02	-0.107E-03
22	0.108E+00	0.221E-01	-0.250E-02	-0.181E-01	0.318E-02	-0.123E-03
23	0.983E-01	0.395E-01	-0.139E-02	-0.188E-01	0.318E-02	-0.219E-03
24	0.846E-01	0.416E-01	-0.628E-02	-0.197E-01	0.317E-02	-0.290E-03
25	0.445E-01	0.440E-01	-0.136E-01	-0.211E-01	0.317E-02	-0.394E-03
26	-0.248E-01	0.461E-01	-0.223E-01	-0.228E-01	0.318E-02	-0.514E-03
27	-0.115E+00	0.484E-01	-0.294E-01	-0.248E-01	0.318E-02	-0.640E-03
28	-0.223E+00	0.514E-01	-0.332E-01	-0.273E-01	0.318E-02	-0.779E-03
29	-0.320E+00	0.553E-01	-0.326E-01	-0.297E-01	0.318E-02	-0.914E-03
30	-0.395E+00	0.595E-01	-0.290E-01	-0.321E-01	0.317E-02	-0.104E-02
31	-0.457E+00	0.639E-01	-0.208E-01	-0.348E-01	0.318E-02	-0.110E-02
32	-0.491E+00	0.773E-01	-0.814E-02	-0.377E-01	0.317E-02	-0.129E-02
33	-0.480E+00	0.958E-01	0.109E-01	-0.411E-01	0.318E-02	-0.143E-02
34	-0.399E+00	0.130E+00	0.526E-01	-0.447E-01	0.317E-02	-0.158E-02
35	-0.223E+00	0.182E+00	0.950E-01	-0.488E-01	0.318E-02	-0.174E-02
36	0.800E-01	0.243E+00	0.120E+00	-0.530E-01	0.318E-02	-0.183E-02
37	0.0	0.0	0.0	0.0	0.0	0.0
38	0.0	0.0	0.0	0.0	0.0	0.0
39	-0.434E+00	0.905E-01	-0.201E-01	0.183E+00	0.283E-02	0.153E-01
40	0.221E-02	0.0	-0.143E-02	0.0	0.483E-03	0.0
41	-0.374E-01	0.392E-02	0.0	-0.225E-01	0.0	0.0
42	-0.104E-01	0.382E-02	0.0	-0.225E-01	0.0	0.0
43	0.212E-01	0.350E-02	0.0	-0.225E-01	0.0	0.0
44	0.500E-01	0.317E-02	0.0	-0.225E-01	0.0	0.0
45	0.785E-01	0.289E-02	0.0	-0.225E-01	0.0	0.0
46	0.102E+00	0.241E-02	0.0	-0.225E-01	0.0	0.0
47	0.116E+00	0.155E-02	0.0	-0.225E-01	0.0	0.0
48	0.123E+00	-0.550E-03	0.0	-0.225E-01	0.0	0.0
49	0.100E+00	-0.253E-02	0.0	-0.225E-01	0.0	0.0
50	0.425E-01	-0.695E-02	0.0	-0.225E-01	0.0	0.0
51	-0.969E-01	-0.913E-02	0.0	-0.514E-02	0.0	0.0
52	0.0	0.0	0.0	0.0	0.0	0.0
53	0.0	0.0	0.0	0.0	0.0	0.0
54	0.0	0.0	0.0	0.0	0.0	0.0
55	0.0	0.0	0.0	0.0	0.0	0.0
56	-0.137E+00	-0.104E-01	0.0	0.320E-01	-0.253E-13	-0.699E-14

TABLE C-32

SYMMETRIC MODE SHAPE –

10-PERCENT WING FUEL, 20-GRAM TIP WEIGHT, STIFF PYLON

MODE NO. 1744 FREQ = 21.53 GENERALIZED MASS= 0.00

BAY	H	ALPH	THET	F	L	PSI
1	-0.262E-08	0.0	0.0	-0.183E-01	0.191E-01	-0.332E-03
2	-0.288E-08	0.0	0.0	-0.214E-01	0.191E-01	-0.401E-03
3	-0.296E-08	0.0	0.0	-0.225E-01	0.191E-01	-0.401E-03
4	-0.304E-08	0.0	0.0	-0.235E-01	0.191E-01	-0.401E-03
5	-0.312E-08	0.0	0.0	-0.245E-01	0.191E-01	-0.401E-03
6	-0.321E-08	0.0	0.0	-0.255E-01	0.191E-01	-0.401E-03
7	0.0	0.0	0.0	0.0	0.0	0.0
8	0.0	0.0	0.0	0.0	0.0	0.0
9	0.0	0.0	0.0	0.0	0.0	0.0
10	0.0	0.0	0.0	0.0	0.0	0.0
11	-0.395E-02	0.191E-03	0.149E-03	-0.212E-01	0.130E-01	-0.177E-03
12	-0.321E-02	0.205E-03	0.270E-03	-0.222E-01	0.130E-01	-0.301E-03
13	-0.194E-02	0.222E-03	0.473E-03	-0.238E-01	0.130E-01	-0.525E-03
14	0.158E-03	0.239E-03	0.755E-03	-0.259E-01	0.130E-01	-0.641E-03
15	0.308E-02	0.251E-03	0.101E-02	-0.281E-01	0.130E-01	-0.718E-03
16	0.634E-02	0.256E-03	0.111E-02	-0.303E-01	0.130E-01	-0.746E-03
17	0.0	0.0	0.0	0.0	0.0	0.0
18	0.0	0.0	0.0	0.0	0.0	0.0
19	0.0	0.0	0.0	0.0	0.0	0.0
20	0.0	0.0	0.0	0.0	0.0	0.0
21	0.438E-02	-0.572E-04	0.196E-04	-0.192E-01	0.135E-01	0.122E-02
22	0.492E-02	0.183E-03	0.207E-03	-0.855E-02	0.135E-01	0.363E-02
23	0.536E-02	0.494E-03	0.537E-03	0.848E-02	0.135E-01	0.501E-02
24	0.525E-02	0.678E-03	0.453E-03	0.308E-01	0.135E-01	0.702E-02
25	0.975E-02	0.947E-03	0.262E-03	0.650E-01	0.135E-01	0.994E-02
26	0.102E-01	0.128E-02	-0.776E-04	0.110E+00	0.135E-01	0.134E-01
27	0.910E-02	0.168E-02	-0.572E-03	0.162E+00	0.135E-01	0.176E-01
28	0.608E-02	0.215E-02	-0.122E-02	0.227E+00	0.135E-01	0.211E-01
29	0.162E-02	0.256E-02	-0.180E-02	0.294E+00	0.135E-01	0.251E-01
30	-0.328E-02	0.297E-02	-0.221E-02	0.360E+00	0.135E-01	0.289E-01
31	-0.913E-02	0.348E-02	-0.257E-02	0.435E+00	0.135E-01	0.329E-01
32	-0.156E-01	0.413E-02	-0.270E-02	0.520E+00	0.135E-01	0.371E-01
33	-0.219E-01	0.514E-02	-0.232E-02	0.617E+00	0.135E-01	0.419E-01
34	-0.262E-01	0.704E-02	-0.102E-02	0.725E+00	0.135E-01	0.476E-01
35	-0.263E-01	0.101E-01	0.972E-03	0.849E+00	0.135E-01	0.535E-01
36	-0.210E-01	0.139E-01	0.272E-02	0.100E+01	0.135E-01	0.574E-01
37	0.0	0.0	0.0	0.0	0.0	0.0
38	0.0	0.0	0.0	0.0	0.0	0.0
39	-0.151E-02	0.112E-02	-0.102E-02	0.205E-02	0.356E-02	-0.257E-02
40	-0.737E-04	0.0	0.477E-04	0.0	-0.161E-04	0.0
41	-0.575E-02	0.490E-03	0.0	-0.245E-01	0.0	0.0
42	-0.234E-02	0.470E-03	0.0	-0.245E-01	0.0	0.0
43	0.136E-02	0.367E-03	0.0	-0.245E-01	0.0	0.0
44	0.420E-02	0.254E-03	0.0	-0.245E-01	0.0	0.0
45	0.573E-02	0.674E-04	0.0	-0.245E-01	0.0	0.0
46	0.556E-02	-0.103E-03	0.0	-0.245E-01	0.0	0.0
47	0.425E-02	-0.253E-03	0.0	-0.245E-01	0.0	0.0
48	0.153E-02	-0.371E-03	0.0	-0.245E-01	0.0	0.0
49	-0.348E-02	-0.370E-03	0.0	-0.245E-01	0.0	0.0
50	-0.658E-02	-0.108E-04	0.0	-0.245E-01	0.0	0.0
51	-0.312E-02	0.204E-03	0.0	-0.249E-01	0.0	0.0
52	0.0	0.0	0.0	0.0	0.0	0.0
53	0.0	0.0	0.0	0.0	0.0	0.0
54	0.0	0.0	0.0	0.0	0.0	0.0
55	0.0	0.0	0.0	0.0	0.0	0.0
56	-0.170E-02	0.213E-03	0.0	-0.208E-01	-0.141E-13	-0.383E-14

TABLE C-33

SYMMETRIC MODE SHAPE –

10-PERCENT WING FUEL, 20-GRAM TIP WEIGHT, STIFF PYLON

MODE NO. 1745 FREQ = 23.82 GENERALIZED MASS= 0.00

BAY	H	ALPH	THET	F	L	PSI
1	-0.325E-07	0.0	0.0	0.453E-02	-0.274E-01	0.422E-02
2	-0.357E-07	0.0	0.0	0.410E-01	-0.272E-01	0.408E-02
3	-0.366E-07	0.0	0.0	0.539E-01	-0.272E-01	0.408E-02
4	-0.378E-07	0.0	0.0	0.657E-01	-0.272E-01	0.468E-02
5	-0.388E-07	0.0	0.0	0.776E-01	-0.272E-01	0.468E-02
6	-0.398E-07	0.0	0.0	0.895E-01	-0.272E-01	0.408E-02
7	0.0	0.0	0.0	0.0	0.0	0.0
8	0.0	0.0	0.0	0.0	0.0	0.0
9	0.0	0.0	0.0	0.0	0.0	0.0
10	0.0	0.0	0.0	0.0	0.0	0.0
11	0.671E-02	-0.307E-02	-0.100E-02	0.350E-03	-0.144E-02	0.794E-03
12	0.251E-02	-0.400E-02	-0.699E-03	0.342E-02	-0.144E-02	0.900E-03
13	0.182E-02	-0.442E-02	0.331E-03	0.671E-02	-0.144E-02	0.975E-03
14	0.495E-02	-0.485E-02	0.151E-02	0.102E-01	-0.144E-02	0.103E-02
15	0.117E-01	-0.513E-02	0.233E-02	0.137E-01	-0.144E-02	0.107E-02
16	0.203E-01	-0.527E-02	0.299E-02	0.169E-01	-0.144E-02	0.109E-02
17	0.0	0.0	0.0	0.0	0.0	0.0
18	0.0	0.0	0.0	0.0	0.0	0.0
19	0.0	0.0	0.0	0.0	0.0	0.0
20	0.0	0.0	0.0	0.0	0.0	0.0
21	0.579E-01	0.828E-04	-0.672E-02	-0.956E-02	0.159E-02	0.182E-03
22	0.997E-02	0.161E-02	-0.136E-01	-0.857E-02	0.160E-02	0.249E-03
23	-0.593E-01	0.354E-02	-0.195E-01	-0.748E-02	0.159E-02	0.260E-03
24	-0.143E+00	-0.255E-02	-0.250E-01	-0.631E-02	0.160E-02	0.379E-03
25	-0.250E+00	-0.119E-01	-0.270E-01	-0.444E-02	0.160E-02	0.549E-03
26	-0.339E+00	-0.232E-01	-0.180E-01	-0.194E-02	0.159E-02	0.743E-03
27	-0.373E+00	-0.364E-01	0.201E-03	0.904E-03	0.159E-02	0.943E-03
28	-0.327E+00	-0.523E-01	0.279E-01	0.450E-02	0.160E-02	0.110E-02
29	-0.206E+00	-0.672E-01	0.338E-01	0.829E-02	0.159E-02	0.130E-02
30	-0.523E-01	-0.825E-01	0.729E-01	0.118E-01	0.160E-02	0.137E-02
31	0.149E+00	-0.105E+00	0.915E-01	0.159E-01	0.159E-02	0.177E-02
32	0.389E+00	-0.131E+00	0.105E+00	0.205E-01	0.160E-02	0.198E-02
33	0.648E+00	-0.177E+00	0.104E+00	0.250E-01	0.159E-02	0.220E-02
34	0.870E+00	-0.259E+00	0.770E-01	0.313E-01	0.160E-02	0.247E-02
35	0.100E+01	-0.385E+00	0.222E-01	0.370E-01	0.159E-02	0.274E-02
36	0.979E+00	-0.529E+00	-0.350E-01	0.453E-01	0.159E-02	0.291E-02
37	0.0	0.0	0.0	0.0	0.0	0.0
38	0.0	0.0	0.0	0.0	0.0	0.0
39	-0.831E-01	0.142E-01	-0.359E-01	0.558E-02	0.228E-01	0.190E-01
40	0.316E-02	0.0	-0.205E-02	0.0	0.892E-03	0.0
41	-0.751E-01	0.722E-02	0.0	-0.305E-02	0.0	0.0
42	-0.260E-01	0.677E-02	0.0	-0.305E-02	0.0	0.0
43	0.271E-01	0.550E-02	0.0	-0.305E-02	0.0	0.0
44	0.671E-01	0.354E-02	0.0	-0.305E-02	0.0	0.0
45	0.881E-01	0.888E-03	0.0	-0.305E-02	0.0	0.0
46	0.857E-01	-0.133E-02	0.0	-0.305E-02	0.0	0.0
47	0.734E-01	-0.124E-02	0.0	-0.305E-02	0.0	0.0
48	0.686E-01	-0.784E-04	0.0	-0.305E-02	0.0	0.0
49	0.685E-01	-0.986E-04	0.0	-0.305E-02	0.0	0.0
50	0.535E-01	-0.240E-02	0.0	-0.305E-02	0.0	0.0
51	-0.765E-02	-0.456E-02	0.0	0.380E-02	0.0	0.0
52	0.0	0.0	0.0	0.0	0.0	0.0
53	0.0	0.0	0.0	0.0	0.0	0.0
54	0.0	0.0	0.0	0.0	0.0	0.0
55	0.0	0.0	0.0	0.0	0.0	0.0
56	-0.261E-01	-0.472E-02	0.0	0.249E-01	-0.332E-14	-0.898E-15

TABLE C-34
SYMMETRIC MODE SHAPE –
10-PERCENT WING FUEL, 20-GRAM TIP WEIGHT, STIFF PYLON

MODE NO. 1746 FREQ = 29.50 GENERALIZED MASS= 0.01

BAY	H	ALPH	THET	F	L	PSI
1	0.349E-06	0.0	0.0	0.163E-01	-0.314E+00	0.466E-01
2	0.363E-06	0.0	0.0	0.436E+00	-0.311E+00	0.545E-01
3	0.394E-06	0.0	0.0	0.586E+00	-0.311E+00	0.545E-01
4	0.405E-06	0.0	0.0	0.724E+00	-0.311E+00	0.545E-01
5	0.416E-06	0.0	0.0	0.862E+00	-0.311E+00	0.545E-01
6	0.426E-06	0.0	0.0	0.100E+01	-0.311E+00	0.545E-01
7	0.0	0.0	0.0	0.0	0.0	0.0
8	0.0	0.0	0.0	0.0	0.0	0.0
9	0.0	0.0	0.0	0.0	0.0	0.0
10	0.0	0.0	0.0	0.0	0.0	0.0
11	0.900E-01	-0.413E-01	-0.165E-01	-0.825E-02	-0.133E-01	0.917E-02
12	0.427E-01	-0.477E-01	-0.109E-01	0.284E-01	-0.133E-01	0.110E-01
13	0.180E-01	-0.501E-01	-0.304E-02	0.695E-01	-0.133E-01	0.123E-01
14	0.223E-01	-0.649E-01	0.505E-02	0.114E+00	-0.133E-01	0.134E-01
15	0.545E-01	-0.715E-01	0.137E-01	0.159E+00	-0.133E-01	0.141E-01
16	0.103E+00	-0.744E-01	0.174E-01	0.202E+00	-0.133E-01	0.145E-01
17	0.0	0.0	0.0	0.0	0.0	0.0
18	0.0	0.0	0.0	0.0	0.0	0.0
19	0.0	0.0	0.0	0.0	0.0	0.0
20	0.0	0.0	0.0	0.0	0.0	0.0
21	-0.113E+00	0.164E-01	0.112E-01	0.132E-01	-0.243E-02	-0.119E-02
22	-0.702E-01	0.100E-01	0.388E-02	0.106E-01	-0.248E-02	-0.101E-02
23	-0.413E-01	0.316E-02	0.469E-02	0.670E-02	-0.242E-02	-0.815E-03
24	-0.275E-01	0.224E-02	0.270E-02	0.419E-02	-0.250E-02	-0.501E-03
25	-0.205E-01	0.128E-02	0.978E-03	0.254E-02	-0.252E-02	-0.234E-03
26	-0.189E-01	0.592E-03	-0.110E-03	0.227E-02	-0.243E-02	0.182E-03
27	-0.206E-01	-0.120E-03	-0.690E-03	0.372E-02	-0.240E-02	0.651E-03
28	-0.229E-01	-0.110E-02	-0.829E-03	0.670E-02	-0.248E-02	0.115E-02
29	-0.242E-01	-0.240E-02	0.107E-03	0.108E-01	-0.243E-02	0.167E-02
30	-0.220E-01	-0.385E-02	0.129E-02	0.155E-01	-0.252E-02	0.210E-02
31	-0.167E-01	-0.562E-02	0.335E-02	0.214E-01	-0.245E-02	0.269E-02
32	-0.542E-02	-0.718E-02	0.605E-02	0.287E-01	-0.251E-02	0.325E-02
33	0.124E-01	-0.956E-02	0.855E-02	0.373E-01	-0.244E-02	0.396E-02
34	0.348E-01	-0.139E-01	0.950E-02	0.479E-01	-0.253E-02	0.470E-02
35	0.560E-01	-0.213E-01	0.702E-02	0.603E-01	-0.243E-02	0.555E-02
36	0.709E-01	-0.302E-01	0.434E-02	0.763E-01	-0.247E-02	0.610E-02
37	0.0	0.0	0.0	0.0	0.0	0.0
38	0.0	0.0	0.0	0.0	0.0	0.0
39	0.438E-01	-0.253E-01	0.142E-01	-0.265E-01	-0.113E-01	-0.706E-02
40	0.490E-03	0.0	-0.322E-03	0.0	0.139E-03	0.0
41	0.383E+00	-0.410E-01	0.0	-0.429E-01	0.0	0.0
42	0.100E+00	-0.375E-01	0.0	-0.429E-01	0.0	0.0
43	-0.177E+00	-0.279E-01	0.0	-0.429E-01	0.0	0.0
44	-0.383E+00	-0.139E-01	0.0	-0.429E-01	0.0	0.0
45	-0.410E+00	0.397E-02	0.0	-0.429E-01	0.0	0.0
46	-0.303E+00	0.180E-01	0.0	-0.429E-01	0.0	0.0
47	-0.137E+00	0.273E-01	0.0	-0.429E-01	0.0	0.0
48	0.117E+00	0.303E-01	0.0	-0.429E-01	0.0	0.0
49	0.474E+00	0.241E-01	0.0	-0.429E-01	0.0	0.0
50	0.501E+00	-0.147E-01	0.0	-0.429E-01	0.0	0.0
51	-0.999E-01	-0.556E-01	0.0	0.295E-01	0.0	0.0
52	0.0	0.0	0.0	0.0	0.0	0.0
53	0.0	0.0	0.0	0.0	0.0	0.0
54	0.0	0.0	0.0	0.0	0.0	0.0
55	0.0	0.0	0.0	0.0	0.0	0.0
56	-0.297E+00	-0.563E-01	0.0	0.207E+00	-0.137E-12	-0.372E-13

TABLE C-35

SYMMETRIC MODE SHAPE –

10-PERCENT WING FUEL, 20-GRAM TIP WEIGHT, STIFF PYLON

MODE NO. 1747 FREQ = 31.00 GENERALIZED MASS= 0.31

BAY	H	ALPH	INCI	F	L	PSI
1	0.442E-08	0.0	0.0	-0.351E-02	0.159E-01	-0.173E-02
2	0.484E-08	0.0	0.0	-0.193E-01	0.158E-01	-0.205E-02
3	0.499E-08	0.0	0.0	-0.249E-01	0.158E-01	-0.205E-02
4	0.513E-08	0.0	0.0	-0.301E-01	0.158E-01	-0.205E-02
5	0.526E-08	0.0	0.0	-0.353E-01	0.158E-01	-0.205E-02
6	0.540E-08	0.0	0.0	-0.406E-01	0.158E-01	-0.205E-02
7	0.0	0.0	0.0	0.0	0.0	0.0
8	0.0	0.0	0.0	0.0	0.0	0.0
9	0.0	0.0	0.0	0.0	0.0	0.0
10	0.0	0.0	0.0	0.0	0.0	0.0
11	-0.572E-02	0.145E-02	0.84?E-05	-0.391E-02	0.332E-02	-0.4?5E-03
12	-0.382E-02	0.172E-02	0.425E-05	-0.572E-02	0.332E-02	-0.508E-03
13	-0.256E-02	0.206E-02	0.314E-03	-0.802E-02	0.332E-02	-0.719E-03
14	-0.152E-02	0.242E-02	0.299E-03	-0.107E-01	0.332E-02	-0.829E-03
15	-0.518E-03	0.270E-02	0.303E-03	-0.135E-01	0.332E-02	-0.895E-03
16	0.379E-03	0.283E-02	0.291E-03	-0.163E-01	0.332E-02	-0.921E-03
17	0.0	0.0	0.0	0.0	0.0	0.0
18	0.0	0.0	0.0	0.0	0.0	0.0
19	0.0	0.0	0.0	0.0	0.0	0.0
20	0.0	0.0	0.0	0.0	0.0	0.0
21	0.09?E-02	-0.?30E-02	0.486E-04	-0.204E-02	0.162E-02	0.974E-04
22	0.4?3E-01	-0.668E-02	0.105E-01	-0.130E-02	0.162E-02	0.?2?E-03
23	0.953E-01	-0.127E-01	0.139E-01	0.785E-03	0.162E-02	0.371E-03
24	0.143E+00	-0.184E-01	0.111E-01	0.279E-02	0.162E-02	0.493E-03
25	0.171E+00	-0.279E-01	0.104E-02	0.452E-02	0.162E-02	0.?49E-03
26	0.145E+00	-0.431E-01	-0.153E-01	0.?5?E-02	0.162E-02	0.143E-03
27	0.?36E-01	-0.?40E-01	-0.?12E-01	0.?5?E-02	0.162E-02	-0.139E-03
28	-0.59?E-01	-0.910E-01	-0.385E-01	0.463E-02	0.162E-02	-0.?30E-03
29	-0.165E+00	-0.116E+00	-0.?28E-01	0.?9?E-02	0.162E-02	-0.?80E-03
30	-0.?50E+00	-0.140E+00	-0.181E-01	0.628E-03	0.162E-02	-0.115E-02
31	-0.242E+00	-0.169E+00	0.109E-01	-0.?59E-02	0.162E-02	-0.152E-02
32	-0.167E+00	-0.189E+00	0.?22E-01	-0.?80E-02	0.162E-02	-0.192E-02
33	0.154E-01	-0.215E+00	0.907E-01	-0.122E-01	0.162E-02	-0.?40E-02
34	0.299E+00	-0.?55E+00	0.133E+00	-0.169E-01	0.162E-02	-0.310E-02
35	0.640E+00	-0.310E+00	0.141E+00	-0.?73E-01	0.162E-02	-0.?19E-02
36	0.100E+01	-0.384E+00	0.123E+00	-0.383E-01	0.162E-02	-0.4?7E-02
37	0.0	0.0	0.0	0.0	0.0	0.0
38	0.0	0.0	0.0	0.0	0.0	0.0
39	-0.?77E-01	0.316E-01	0.333E+00	0.459E-01	-0.448E+00	-0.?78E+00
40	-0.222E-02	0.0	0.144E-02	0.0	-0.?35E-03	0.0
41	0.485E-02	-0.542E-03	0.0	-0.344E-02	0.0	0.0
42	0.121E-02	-0.492E-03	0.0	-0.344E-02	0.0	0.0
43	-0.249E-02	-0.361E-03	0.0	-0.344E-02	0.0	0.0
44	-0.485E-02	-0.173E-03	0.0	-0.344E-02	0.0	0.0
45	-0.536E-02	0.610E-04	0.0	-0.344E-02	0.0	0.0
46	-0.394E-02	0.234E-03	0.0	-0.344E-02	0.0	0.0
47	-0.278E-02	-0.105E-03	0.0	-0.344E-02	0.0	0.0
48	-0.731E-02	-0.795E-03	0.0	-0.344E-02	0.0	0.0
49	-0.106E-01	-0.826E-03	0.0	-0.344E-02	0.0	0.0
50	-0.221E-01	0.485E-03	0.0	-0.344E-02	0.0	0.0
51	0.345E-03	0.192E-02	0.0	-0.602E-02	0.0	0.0
52	0.0	0.0	0.0	0.0	0.0	0.0
53	0.0	0.0	0.0	0.0	0.0	0.0
54	0.0	0.0	0.0	0.0	0.0	0.0
55	0.0	0.0	0.0	0.0	0.0	0.0
56	0.897E-02	0.201E-02	0.0	-0.143E-01	-0.52?E-14	-0.?88E-15

TABLE C-36

SYMMETRIC MODE SHAPE –

10-PERCENT WING FUEL, 20-GRAM TIP WEIGHT, STIFF PYLON

MODE NO. 1748 FREQ = 35.05 GENERALIZED MASS= 0.00

BAY	H	ALPH	THET	F	L	PSI
1	0.757E-07	0.0	0.0	-0.174E-02	0.398E-01	-0.460E-02
2	0.830E-07	0.0	0.0	-0.447E-01	0.394E-01	-0.563E-02
3	0.855E-07	0.0	0.0	-0.802E-01	0.394E-01	-0.563E-02
4	0.878E-07	0.0	0.0	-0.745E-01	0.394E-01	-0.563E-02
5	0.901E-07	0.0	0.0	-0.868E-01	0.394E-01	-0.563E-02
6	0.925E-07	0.0	0.0	-0.103E+00	0.394E-01	-0.563E-02
7	0.0	0.0	0.0	0.0	0.0	0.0
8	0.0	0.0	0.0	0.0	0.0	0.0
9	0.0	0.0	0.0	0.0	0.0	0.0
10	0.0	0.0	0.0	0.0	0.0	0.0
11	-0.188E-01	0.373E-02	0.140E-02	-0.407E-02	0.590E-02	-0.102E-02
12	-0.147E-01	0.472E-02	0.907E-03	-0.869E-02	0.589E-02	-0.151E-02
13	-0.115E-01	0.603E-02	0.103E-02	-0.140E-01	0.589E-02	-0.185E-02
14	-0.663E-02	0.748E-02	0.188E-02	-0.213E-01	0.590E-02	-0.213E-02
15	0.120E-02	0.864E-02	0.282E-02	-0.288E-01	0.593E-02	-0.232E-02
16	0.105E-01	0.923E-02	0.319E-02	-0.300E-01	0.590E-02	-0.238E-02
17	0.0	0.0	0.0	0.0	0.0	0.0
18	0.0	0.0	0.0	0.0	0.0	0.0
19	0.0	0.0	0.0	0.0	0.0	0.0
20	0.0	0.0	0.0	0.0	0.0	0.0
21	-0.995E-02	0.201E-02	0.886E-02	0.902E-02	-0.426E-02	-0.223E-03
22	0.474E-01	0.214E-02	0.155E-01	0.835E-02	-0.427E-02	-0.114E-03
23	0.121E+00	0.470E-03	0.190E-01	0.810E-02	-0.426E-02	0.001E-05
24	0.192E+00	-0.210E-02	0.175E-01	0.799E-02	-0.428E-02	-0.781E-04
25	0.240E+00	-0.745E-02	0.752E-02	0.746E-02	-0.428E-02	-0.194E-03
26	0.242E+00	-0.180E-01	-0.107E-01	0.644E-02	-0.426E-02	-0.319E-03
27	0.170E+00	-0.340E-01	-0.305E-01	0.515E-02	-0.427E-02	-0.437E-03
28	0.387E-01	-0.506E-01	-0.450E-01	0.346E-02	-0.427E-02	-0.552E-03
29	-0.980E-01	-0.807E-01	-0.468E-01	0.170E-02	-0.426E-02	-0.647E-03
30	-0.203E+00	-0.105E+00	-0.378E-01	0.504E-04	-0.428E-02	-0.718E-03
31	-0.270E+00	-0.136E+00	-0.157E-01	-0.173E-02	-0.427E-02	-0.772E-03
32	-0.256E+00	-0.162E+00	0.209E-01	-0.369E-02	-0.426E-02	-0.807E-03
33	-0.128E+00	-0.197E+00	0.798E-01	-0.570E-02	-0.427E-02	-0.821E-03
34	0.139E+00	-0.253E+00	0.139E+00	-0.767E-02	-0.426E-02	-0.801E-03
35	0.528E+00	-0.320E+00	0.173E+00	-0.957E-02	-0.426E-02	-0.733E-03
36	0.100E+01	-0.380E+00	0.170E+00	-0.114E-01	-0.427E-02	-0.640E-03
37	0.0	0.0	0.0	0.0	0.0	0.0
38	0.0	0.0	0.0	0.0	0.0	0.0
39	0.353E-01	0.718E-02	-0.525E-01	0.349E-01	0.437E-01	0.279E-01
40	-0.370E-02	0.0	0.240E-02	0.0	-0.810E-03	0.0
41	0.821E-01	-0.101E-01	0.0	-0.250E-02	0.0	0.0
42	0.150E-01	-0.696E-02	0.0	-0.250E-02	0.0	0.0
43	-0.509E-01	-0.624E-02	0.0	-0.250E-02	0.0	0.0
44	-0.898E-01	-0.258E-02	0.0	-0.250E-02	0.0	0.0
45	-0.937E-01	0.166E-02	0.0	-0.250E-02	0.0	0.0
46	-0.642E-01	0.433E-02	0.0	-0.250E-02	0.0	0.0
47	-0.335E-01	0.271E-02	0.0	-0.250E-02	0.0	0.0
48	-0.272E-01	-0.867E-03	0.0	-0.250E-02	0.0	0.0
49	-0.494E-01	-0.188E-02	0.0	-0.250E-02	0.0	0.0
50	-0.389E-01	0.106E-02	0.0	-0.250E-02	0.0	0.0
51	-0.629E-02	0.496E-02	0.0	-0.883E-02	0.0	0.0
52	0.0	0.0	0.0	0.0	0.0	0.0
53	0.0	0.0	0.0	0.0	0.0	0.0
54	0.0	0.0	0.0	0.0	0.0	0.0
55	0.0	0.0	0.0	0.0	0.0	0.0
56	0.222E-01	0.552E-02	0.0	-0.350E-01	-0.379E-14	-0.238E-14

TABLE C-37

SYMMETRIC MODE SHAPE –

10-PERCENT WING FUEL, 20-GRAM TIP WEIGHT, STIFF PYLON

MODE NO. 1749 FREQ = 43.02 GENERALIZED MASS= 0.00

BAY	H	ALPH	THET	F	L	PSI
1	-0.210E-07	0.0	0.0	0.637E-01	-0.215E-01	0.505E-01
2	-0.230E-07	0.0	0.0	0.447E+00	-0.126E-01	0.534E-01
3	-0.237E-07	0.0	0.0	0.594E+00	-0.127E-01	0.534E-01
4	-0.244E-07	0.0	0.0	0.729E+00	-0.126E-01	0.534E-01
5	-0.250E-07	0.0	0.0	0.864E+00	-0.127E-01	0.534E-01
6	-0.256E-07	0.0	0.0	0.100E+01	-0.126E-01	0.534E-01
7	0.0	0.0	0.0	0.0	0.0	0.0
8	0.0	0.0	0.0	0.0	0.0	0.0
9	0.0	0.0	0.0	0.0	0.0	0.0
10	0.0	0.0	0.0	0.0	0.0	0.0
11	0.169E+00	0.374E-01	0.207E-01	-0.528E-02	-0.327E-01	-0.121E-01
12	0.281E+00	0.622E-01	0.312E-01	-0.667E-01	-0.327E-01	-0.213E-01
13	0.356E+00	0.967E-01	0.493E-02	-0.153E+00	-0.327E-01	-0.279E-01
14	0.269E+00	0.138E+00	-0.511E-01	-0.259E+00	-0.327E-01	-0.331E-01
15	-0.650E-01	0.177E+00	-0.140E+00	-0.374E+00	-0.327E-01	-0.366E-01
16	-0.564E+00	0.199E+00	-0.173E+00	-0.488E+00	-0.327E-01	-0.379E-01
17	0.0	0.0	0.0	0.0	0.0	0.0
18	0.0	0.0	0.0	0.0	0.0	0.0
19	0.0	0.0	0.0	0.0	0.0	0.0
20	0.0	0.0	0.0	0.0	0.0	0.0
21	-0.653E-02	-0.143E-02	-0.531E-03	-0.521E-02	0.396E-02	0.191E-04
22	-0.949E-02	-0.194E-02	0.929E-04	-0.535E-02	0.396E-02	-0.593E-04
23	-0.672E-02	-0.235E-02	0.139E-02	-0.570E-02	0.396E-02	-0.105E-03
24	0.126E-02	-0.324E-02	0.288E-02	-0.614E-02	0.396E-02	-0.130E-03
25	0.156E-01	-0.442E-02	0.409E-02	-0.670E-02	0.397E-02	-0.138E-03
26	0.310E-01	-0.590E-02	0.376E-02	-0.719E-02	0.396E-02	-0.111E-03
27	0.411E-01	-0.792E-02	0.136E-02	-0.747E-02	0.396E-02	-0.410E-04
28	0.392E-01	-0.108E-01	-0.269E-02	-0.742E-02	0.396E-02	0.842E-04
29	0.260E-01	-0.140E-01	-0.604E-02	-0.694E-02	0.396E-02	0.255E-03
30	0.910E-02	-0.173E-01	-0.756E-02	-0.609E-02	0.397E-02	0.451E-03
31	-0.946E-02	-0.213E-01	-0.729E-02	-0.470E-02	0.396E-02	0.702E-03
32	-0.243E-01	-0.256E-01	-0.452E-02	-0.263E-02	0.397E-02	0.101E-02
33	-0.294E-01	-0.298E-01	0.844E-03	0.314E-03	0.396E-02	0.141E-02
34	-0.175E-01	-0.277E-01	0.926E-02	0.438E-02	0.396E-02	0.196E-02
35	0.154E-01	-0.270E-01	0.171E-01	0.998E-02	0.396E-02	0.262E-02
36	0.879E-01	-0.255E-01	0.207E-01	0.178E-01	0.396E-02	0.313E-02
37	0.0	0.0	0.0	0.0	0.0	0.0
38	0.0	0.0	0.0	0.0	0.0	0.0
39	-0.409E-02	0.733E-03	-0.213E-02	-0.732E-02	0.227E-02	0.124E-02
40	-0.109E-03	0.0	0.704E-04	0.0	-0.238E-04	0.0
41	-0.134E-01	0.211E-02	0.0	-0.304E-02	0.0	0.0
42	-0.156E-02	0.179E-02	0.0	-0.304E-02	0.0	0.0
43	0.108E-01	0.100E-02	0.0	-0.304E-02	0.0	0.0
44	0.162E-01	0.161E-03	0.0	-0.304E-02	0.0	0.0
45	0.131E-01	-0.776E-03	0.0	-0.304E-02	0.0	0.0
46	0.303E-02	-0.128E-02	0.0	-0.304E-02	0.0	0.0
47	-0.625E-02	-0.105E-02	0.0	-0.304E-02	0.0	0.0
48	-0.103E-01	0.161E-03	0.0	-0.304E-02	0.0	0.0
49	-0.695E-03	0.942E-03	0.0	-0.304E-02	0.0	0.0
50	0.309E-02	-0.115E-02	0.0	-0.304E-02	0.0	0.0
51	0.966E+00	0.660E-01	0.0	-0.961E-02	0.0	0.0
52	0.0	0.0	0.0	0.0	0.0	0.0
53	0.0	0.0	0.0	0.0	0.0	0.0
54	0.0	0.0	0.0	0.0	0.0	0.0
55	0.0	0.0	0.0	0.0	0.0	0.0
56	-0.359E+00	-0.678E-01	0.0	0.393E-01	-0.109E-11	-0.295E-12

TABLE C-38

SYMMETRIC MODE SHAPE –

10-PERCENT WING FUEL, 20-GRAM TIP WEIGHT, STIFF PYLON

MODE NO. 1750 FREQ = 46.12 GENERALIZED MASS= 0.01

BAY	H	ALPH	THET	F	L	PSI
1	-0.430E-06	0.0	0.0	-0.327E-01	-0.194E+00	0.181E-01
2	-0.471E-06	0.0	0.0	0.144E+00	-0.192E+00	0.234E-01
3	-0.483E-06	0.0	0.0	0.208E+00	-0.192E+00	0.234E-01
4	-0.498E-06	0.0	0.0	0.268E+00	-0.192E+00	0.234E-01
5	-0.512E-06	0.0	0.0	0.327E+00	-0.192E+00	0.234E-01
6	-0.525E-06	0.0	0.0	0.387E+00	-0.192E+00	0.234E-01
7	0.0	0.0	0.0	0.0	0.0	0.0
8	0.0	0.0	0.0	0.0	0.0	0.0
9	0.0	0.0	0.0	0.0	0.0	0.0
10	0.0	0.0	0.0	0.0	0.0	0.0
11	0.113E+00	-0.270E-01	-0.113E-02	0.154E-01	-0.247E-01	0.135E-01
12	0.128E+00	-0.579E-01	0.716E-02	0.928E-01	-0.247E-01	0.285E-01
13	0.146E+00	-0.102E+00	0.140E-02	0.212E+00	-0.247E-01	0.391E-01
14	0.117E+00	-0.156E+00	-0.222E-01	0.301E+00	-0.247E-01	0.476E-01
15	-0.702E-02	-0.213E+00	-0.522E-01	0.529E+00	-0.247E-01	0.533E-01
16	-0.194E+00	-0.245E+00	-0.808E-01	0.594E+00	-0.247E-01	0.553E-01
17	0.0	0.0	0.0	0.0	0.0	0.0
18	0.0	0.0	0.0	0.0	0.0	0.0
19	0.0	0.0	0.0	0.0	0.0	0.0
20	0.0	0.0	0.0	0.0	0.0	0.0
21	-0.143E+00	-0.320E-01	-0.192E-01	-0.470E-01	0.390E-01	0.719E-03
22	-0.223E+00	-0.514E-01	-0.143E-01	-0.475E-01	0.391E-01	-0.422E-03
23	-0.238E+00	-0.692E-01	0.116E-01	-0.504E-01	0.390E-01	-0.105E-02
24	-0.129E+00	-0.105E+00	0.484E-01	-0.551E-01	0.391E-01	-0.139E-02
25	0.156E+00	-0.152E+00	0.903E-01	-0.615E-01	0.392E-01	-0.159E-02
26	0.553E+00	-0.202E+00	0.130E+00	-0.671E-01	0.390E-01	-0.143E-02
27	0.877E+00	-0.260E+00	0.138E-01	-0.713E-01	0.391E-01	-0.851E-03
28	0.100E+01	-0.331E+00	-0.900E-02	-0.725E-01	0.391E-01	0.276E-03
29	0.844E+00	-0.401E+00	-0.920E-01	-0.692E-01	0.390E-01	0.185E-02
30	0.552E+00	-0.470E+00	-0.143E+00	-0.630E-01	0.392E-01	0.307E-02
31	0.159E+00	-0.551E+00	-0.170E+00	-0.512E-01	0.391E-01	0.401E-02
32	-0.239E+00	-0.588E+00	-0.150E+00	-0.333E-01	0.391E-01	0.392E-02
33	-0.527E+00	-0.610E+00	-0.748E-01	-0.701E-02	0.391E-01	0.147E-01
34	-0.528E+00	-0.595E+00	0.074E-01	0.297E-01	0.391E-01	0.178E-01
35	-0.703E-01	-0.489E+00	0.270E+00	0.808E-01	0.390E-01	0.239E-01
36	0.801E+00	-0.319E+00	0.397E+00	0.152E+00	0.391E-01	0.287E-01
37	0.0	0.0	0.0	0.0	0.0	0.0
38	0.0	0.0	0.0	0.0	0.0	0.0
39	-0.385E-01	0.233E-01	-0.911E-01	-0.931E-01	0.344E-01	0.185E-01
40	0.204E-02	0.0	-0.132E-02	0.0	0.440E-03	0.0
41	-0.401E+00	0.580E-01	0.0	0.102E-01	0.0	0.0
42	-0.214E-01	0.488E-01	0.0	0.102E-01	0.0	0.0
43	0.310E+00	0.275E-01	0.0	0.102E-01	0.0	0.0
44	0.443E+00	0.315E-02	0.0	0.102E-01	0.0	0.0
45	0.350E+00	-0.201E-01	0.0	0.102E-01	0.0	0.0
46	0.114E+00	-0.288E-01	0.0	0.102E-01	0.0	0.0
47	-0.390E-01	-0.157E-01	0.0	0.102E-01	0.0	0.0
48	-0.100E+00	0.682E-02	0.0	0.102E-01	0.0	0.0
49	0.805E-01	0.102E-01	0.0	0.102E-01	0.0	0.0
50	0.248E+00	0.404E-02	0.0	0.102E-01	0.0	0.0
51	0.264E-01	-0.336E-01	0.0	0.299E-01	0.0	0.0
52	0.0	0.0	0.0	0.0	0.0	0.0
53	0.0	0.0	0.0	0.0	0.0	0.0
54	0.0	0.0	0.0	0.0	0.0	0.0
55	0.0	0.0	0.0	0.0	0.0	0.0
56	-0.396E-01	-0.211E-01	0.0	0.153E+00	0.176E-12	0.477E-13

REFERENCES

1. Albano, E. and Rodden, W. P.: A Doublet Lattice Method for Calculating Lift Distributions on Oscillating Surfaces in Subsonic Flows. AIAA Paper 68-73. January 1978.

2. Abel, I., Newsom, J. R. and Dunn, H. J.: Application of Two Synthesis Methods for Active Flutter Suppression on an Aeroelastic Wind Tunnel Model. AIAA Paper 79-1633, August 1979.

3. Abel, I. and Newsom, J. R.: Wind Tunnel Evaluation of NASA-Developed Control Laws for Flutter Suppression on a DC-10 Derivative Wing. AIAA Paper 81-0639. Presented at the AIAA Dynamics Specialist Conference, Atlanta, Georgia, 9-10 April 1981.

4. Perry, B. III: Comparison of Calculated Turbulence Responses with Wind Tunnel Measurements for DC-10 Derivative Wing with an Active Control System. AIAA Paper 81-0567. Presented at the AIAA Dynamics Specialist Conference, Atlanta, Georgia, 9-10 April 1981.

5. Winther, B. A., Shirley, W. A., and Heimbaugh, R. M.: Wind Tunnel Investigation of Active Controls Technology Applied to a DC-10 Derivative. A Collection of Technical Papers — AIAA/ASME/ASCE/AHS 21st Structures, Structural Dynamics and Materials Conference, Part 2, May 1980, pp. 649-655. (Available as AIAA-80-0771.)

1. Report No.	2. Government Accession No.	3. Recipient's Catalog No.
NASA CR-3472		

4. Title and Subtitle	5. Report Date
EXPERIMENTAL INVESTIGATION OF ELASTIC MODE CONTROL ON A MODEL OF A TRANSPORT AIRCRAFT	November 1981
	6. Performing Organization Code
7. Author(s)	8. Performing Organization Report No.
Staff of Douglas Aircraft Company	ACEE-17-FR-0278
	10. Work Unit No.
9. Performing Organization Name and Address	11. Contract or Grant No.
Douglas Aircraft Company McDonnell Douglas Corporation 3855 Lakewood Boulevard Long Beach, California 90846	NAS1-15327 (TASK 2)
	13. Type of Report and Period Covered
12. Sponsoring Agency Name and Address	Contractor Report February 1979-March 1981
National Aeronautics and Space Administration Washington, D.C. 20546	14. Sponsoring Agency Code

15. Supplementary Notes

Langley Technical Monitor: Thomas G. Gainer
Final Report under TASK 2

16. Abstract

A 4.5 percent scale DC-10 derivative flexible model with active controls was fabricated, developed, and tested to investigate the ability to suppress flutter and reduce gust loads with active controlled surfaces. The model was analyzed and tested in both semispan and complete model configurations. Analytical methods were refined and control laws were developed and successfully tested on both versions of the model. A 15 to 25 percent increase in flutter speed due to the active system was demonstrated. The capability of an active control system to significantly reduce wing bending moments due to turbulence was demonstrated. In general, good correlation was obtained between test and analytical predictions. Areas requiring further investigation and development were identified.

17. Key Words (Suggested by Author(s))	18. Distribution Statement
Active controls Flutter suppression Gust load alleviation Wing load alleviation Flexible wind tunnel models	FEDD Distribution Subject Category 05

19. Security Classif. (of this report)	20. Security Classif. (of this page)	21. No. of Pages	22. Price
Unclassified	Unclassified	214	

Available: NASA's Industrial Applications Centers